TARGETED, LIPOIDAL NANOSYSTEM FOR THE TREATMENT OF SCHISTOSOMIASIS

TAYO ALEX ADEKIYA

A thesis submitted to the Faculty of Health Sciences, University of the Witwatersrand, in fulfilment of the requirements for the degree of

Doctor of Philosophy

Supervisor:

Professor Yahya Essop Choonara

Department of Pharmacy and Pharmacology, Faculty of Health Sciences, University of the Witwatersrand, South Africa

Co-Supervisors:

Associate Professor Pradeep Kumar

Associate Professor Pierre PD Kondiah

Department of Pharmacy and Pharmacology, Faculty of Health Sciences, University of the Witwatersrand, South Africa

Johannesburg

2021

DECLARATION

I**,** Tayo Alex Adekiya, declare that this thesis is my own work except where specifically indicated in the text for outsource analysis. It has been submitted for the degree of Doctor of Philosophy in the Faculty of Health Sciences at the University of the Witwatersrand, Johannesburg, South Africa. It has not been submitted before any degree or examination at this or any other University.

Signed this…29th..day of …December..2021

ANIMAL ETHICS DECLARATION

I, Tayo Alex Adekiya, hereby confirm the study entitled "*In vivo* toxicity evaluation of targeted, praziquantel lipoidal nanosystem in Sprague Dawley rats model" was approved by the animal Ethics Screening Committee (AESC) of the University of the Witwatersrand with Ethics Clearance Number 2021/02/02B.

APPENDIX A

Also, the ethics certificate for the *in vivo* parasitological cure rate evaluation according to the standard of the international ethics was provided by Theodor Bilharz Research Institute, Schistosome Biological Supply Center.

APPENDIX B

RESEARCH OUTPUTS

Publications articles from PhD research

1. Adekiya, T.A., Kumar, P., Kondiah, P.P., Pillay, V. and Choonara, Y.E., 2021. Synthesis and therapeutic delivery approaches for praziquantel: a patent review (2010-present). *Expert Opinion on Therapeutic Patents*, 2021;1-15.

APPENDIX C

2. Adekiya Tayo Alex, Pierre PD Kondiah, Yahya Essop Choonara, Pradeep Kumar, and Viness Pillay. A Review of Nanotechnology for Targeted Anti-Schistosomal Therapy. *Frontiers in Bioengineering and Biotechnology* 8 (2020): 32.

APPENDIX D

3. Tayo Alex Adekiya, Pierre P D Kondiah, Pradeep Kumar and Yahya E. Choonara. Nano-enabled treatments for Tropical Diseases affecting the CNS. In: Lalit Kumar and Yashwant Pathak, ed. Nanocarriers For Drug Targeting to Brain Tumors. Elsevier, USA 2021 Chapter 26 (Accepted for Publication).

APPENDIX E

Research presentation

1. Adekiya Tayo Alex, Pierre PD Kondiah, Yahya Essop Choonara, Pradeep Kumar, and Viness Pillay. Development and evaluation of praziquantel loaded lecithin-compritol nanoparticles with and without pluronic F127 surfactant. Wits Faculty of Health Sciences Research Day and Postgraduate Expo. Johannesburg Virtual, 15th October 2020.

APPENDIX F

ABSTRACT

Schistosomiasis, also known as snail fever, is tagged by the World Health Organization (WHO) as Neglected Tropical Diseases (NTDs). This NTDs, is a chronic and acute disease initiated by blood flukes (parasitic worms) which belongs to the class of trematode (flatworm) and Schistosoma as its genus. In the region where this disease is prevalent, the lifestyles of both pregnant women and school children encounter detrimental effects because of the parasitizing of the flukes. Likewise, the endemic of this disease has a great consequential impact on reducing the agricultural produces. Thus, retarding the socio-economics developments of the area(s) afflicted by the disease. Over the past four decades, the Schistosoma disease treatment has been based on an oral single dose of praziquantel (PZQ). This is due to the following factors: it is inexpensive and readily available; its effectiveness against all forms of Schistosomes and it is well tolerated by patients of all ages. Sadly, the use of praziquantel has been faced with several challenges with regard to the treatment of schistosome-based infections. Such challenges include low aqueous solubility, the short plasma half-life of about 1 to 2 hours and extensive hepatic first-pass metabolism. In addition to this, other challenges that are encountered in the treatment of the disease include the ineffectiveness of praziquantel against young schistosome worms, and drug tolerance and resistance in some parts of the world, which is attributed to poor treatment compliance, rate of mutation of the parasite, overall parasite load and the co-infection of different strains of *Schistosoma* parasites. This novel study employed nanotechnological techniques to designed and developed praziquantel nanoliposomal (NLP) nanosystem and surface-functionalized the NLP with anticalpain antibody (anticalpain-NLP) for targeted PZQ delivery in the treatment of Schistosomiasis. Anticalpain-NLP were prepared and validated for their physicochemical properties, *in vitro* and *in vivo* toxicity, drug loading capacity (DLC), drug entrapment efficiency (DEE), drug release and parasitological cure rate. The particle sizes for the formulated nanoliposomes ranged from 88.3 to 92.7 nm (PdI = 0.17-0.35), and zeta potential ranged from -20.2 to -31.9 mV. The DLC and DEE ranged from 9.03% to 14.16% and 92.07% to 94.63%, respectively. The surface functionalization of the nanoliposomes was stable, uniform, and spherical in shape. Fourier transform infrared (FTIR), thermal behaviour and X-ray powder diffraction (XRPD) analysis confirmed that anticalpain antibody and PZQ were incorporated into the surface and inner core of the nanoliposomes, respectively. The sustained drug release was showed to be 93.2 and 91.1% of PZQ within 24 h for NLP and anticalpain-NLP, respectively. In the *in vitro* analysis study, the concentrations range of 30 to 120 μg/ml employed revealed acceptable levels of cell viability, with no significant cytotoxic effects on RAW 264.7 murine macrophage cells and 3T3 human fibroblast cells. More so, the study developed and evaluated the long-term stability of drug-loaded solid lipid nanoparticles (SLNs) which can extend drug release and overcome the problem of bioavailability and solubility as well as investigated its toxicity and efficacy. Solvent injection-co-homogenization techniques was used to fabricated SLNs in which compritol ATO 888 and lecithin were used as lipids, and Pluronic F127 (PF127) was used as a stabilizer. The long-term stability effect of the PF127 as a stabilizer on the SLNs was evaluated thoroughly. The particle size, stability and polydispersity were determined by a dynamic light scattering (DLS) technique. The morphological analysis of the SLNs was investigated by Transmission and Scanning Electron Microscopy (TEM) and (SEM), respectively. The chemical properties, mechanical, thermal, and crystal behaviours of SLNs were evaluated using FTIR, ElastoSens Bio2, XRPD, DSC and TGA, respectively. SLNs with PF127 depicted an encapsulation efficiency of 71.63% and a drug loading capacity of 11.46%. The *in vitro* drug release study for SLNs with PF127 showed a cumulative release of 48.08% for the PZQ within 24 h, with a similar release profile for SLNs suspension after 120 days. DLS, ELS, and optical characterization and stability profiling data indicate that the addition of PF127 as the surfactants provided long-term stability for SLNs. RAW 264.7 macrophages showed acceptable, dose-dependent levels of viability following treatment with SLNs in an *in vitro* toxicity study. Biochemical markers and histopathological analysis showed that the formulated nanoliposomes and SLNs present no or minimal oxidative stress and confer hepatoprotective effects on the animals. The cure rate of the anticalpain-NLP, SLNs and PZQ was assessed by parasitological analysis. It was discovered that, with treatment using the 250 mg/kg anticalpain-NLP and PF127 stabilized SLNs showed greater activity on the total worm burden, ova count in both the intestine and the liver of juvenile and adult schistosomes. From the findings obtained, the study supports the ability of oral anticalpain-NLP and SLNs to target young and adult schistosomes in the liver and portomesenteric locations, resulting in improved the overall effectiveness of PZQ.

ACKNOWLEDGEMENTS

I am grateful to Almighty God who has been there for me since the beginning of my existence, His love has been more than sufficient to keep and sustain me.

I want to express my heartfelt gratitude to my late father, Elder S.A Adekiya and my lovely mother, Mrs. M. Adekiya, for their moral, financial, spiritual, and physical assistance in helping me realize this dream. Seun, Lanre, Moses, Funke, Wale, Tunmise, and Adura; my indefatigable siblings. I will say it again “you're fantastic group of individuals”.

My profound gratitude also goes to my great and wonderful supervisors, late Prof. V Pillay; Prof. YE Choonara; Prof. P Kumar and Prof. PPD Kondiah, for their selfless, unwavering assistance, mentoring and supervision from the beginning to the completion of this program; may Almighty God bless you beyond your wildest dreams (Amen).

I appreciate my dearest wife, Dr (Mrs). Abisola O. Adeniyi-Adekiya for her unwavering support. My beloved friends turned brother, Raphael Taiwo Aruleba, Dr. Daniel Kehinde Aruleba, Dr. and Dr. (Mrs) Babatunji Emmanuel Oyinloye, your support and assistance from the beginning of the journey till this moment is heartwarming, I say more feats in all your endeavours.

I will not cease to acknowledge my beautiful friends and loved ones, Dr. and Mrs Segun Oke, Mumuni Sumaila, Cuthbert Kibungu, Mrs. Onyinye Uwaezuoke, Mr. and Mrs. Obadeyi Adeola, Dr. Olaniran Sunday, Mr. and Mrs. Olowookere Ayodele, Dr. and Mrs. Uleanya Chinaza, Mr. and Mrs. Olugbode Ayomikun, Dr. Owolabi M. Bankole, and others that time does not permit me to name, I thank you all for your assistance, support before and during the course of my research.

I also extend gratitude and appreciation to Ms. Busi Nompumelelo, Mr. Ramarumo Sello, Mr. Kleinbooi Mohlabi, Mr. Bafana Temba, Dr. Philemon Ubanako and Ms. Tshidi Mosete for their technical, administrative assistance during the course of my laboratories journey. All members of the Wits Advanced Drug Delivery Platform (WADDP) and the members of the department of Pharmacy and Pharmacology most especially Dr. S Adeyemi, Yosra, Ahmed, Thope, Lindo, Dr. H Mndlovu, Dr. GD Mahumane, Michelle, and others are all appreciated for their support in one way or the other.

I cannot help but acknowledge this group of great families who are in one way or another the main players and actresses in the success of my study, as well as for their beautiful words of

support before, during, and after my study; Dr. and Mrs. Cyril-Mary Olatunji. Hon. and Mrs. Tunde Oduntan, Mr. James Ajulo (Ajusco), Mr. and Mrs. Ehinola Clement, Prophetess and Mr. V.T Folorunso, Deaconess Joy Oladapo, Dr. (Mrs.) Abike Adamson Shodehinde.

My unalloyed thanks goes to all the staff of University of the Witwatersrand Central Animal Services (CAS) and Schistosome Biological Supply Centre (SBSC) of Theodor Bilharz Research Institute (TBRI), Giza, Egypt for their expertise support during the *in vivo* experimentations.

Special thanks to all my funders; the National Research Foundation (NRF) Grantholder, Departmental Community Transformation Grant (CTG), and Postgraduate Merit Award (PMA), for their financial supports during this program.

God bless you all.

DEDICATION

This thesis is dedicated to my maker, the king of kings and the Lord of Lords. Also, to my late father, Elder Samuel A. Adekiya.

In memory of my late hero (Elder Samuel A. Adekiya), who gave me the best gifts any child could have ever wished for.

TABLE OF CONTENTS

CHAPTER ONE

INTRODUCTION AND BACKGROUND

CHAPTER TWO

THE PROMISE OF NANOTECHNOLOGY FOR TARGETED ANTI-SCHISTOSOMAL THERAPY

CHAPTER THREE

SYNTHESIS AND THERAPEUTIC DELIVERY APPROACHES FOR PRAZIQUANTEL: A PATENT REVIEW (2010-PRESENT)

CHAPTER FOUR

ANTI-CALPAIN ENGINEERED LIPOIDIAL NANOSYSTEMS: PREPARATION, CHARACTERIZATION AND APPLICATION IN PRAZIQUANTEL DELIVERY AS POTENTIAL FOR SCHISTOSOMIASIS TREATMENT

CHAPTER FIVE

SYNTHESIS AND EVALUATION OF PRAZIQUANTEL-LOADED COMPRITOL ATO 888-LECITHIN SOLID LIPID NANOPARTICLES AGAINST *S. mansoni* INFECTION IN PRECLINICAL MURINE MODELS

APPENDICES

LIST OF ABBREVIATIONS

ACh	Acetylcholine
AChE	acetylcholinesterase
ACS	American Cancer Society
AD	Alzheimer's Disease
ADME	Absorption, distribution, metabolism, and elimination
AFM	atomic force microscopy
AJs	Adherent junctions
ALT	Alanine aminotransferase
Anticalpain-NLP - anticalpain-functionalized PZQ-loaded nanoliposomes	
AST	Aspartate aminotransferase
AuNP	gold nanoparticle
BBB	Blood brain barrier
BBBD	Blood brain barrier disruption
BCS	Biopharmaceutical classification system
BCSFB	Blood cerebrospinal fluid barrier
CDs	Carbon dots
CHOL	Cholesterol
CLF-SLNs	Compritol-lecithin- solid lipid nanoparticles with pluronic F127
CLPF-SLNs	PZQ-loaded compritol-lecithin- solid lipid nanoparticles with pluronic F127
PF127	Pluronic F127
CM	Cerebral malaria
CNOs	Carbon nanoonions
CNS	Central nervous system
CNTs	Carbon nanotubes
CSF	Cerebrospinal fluid
CT	Computed tomography
CTDs	Cerebral tropical diseases
DCC	N,N′ -dicyclohexylcarbodiimide
DDSs	Drug delivery systems
DSC	Differential scanning calorimetry
DSPE-mPEG2000COOH - Phosphatidylethanolamine distearoyl methoxypolyethleneglycol conjugate	
EMA	European Medicines Agency
FDA	Food and Drug Administration

FTIR	Fourier transform infrared
GIT	Gastrointestinal tract
GJs	Gap junctions
HBO	Hyperbaric oxygen
IgGs	Immunoglobulins
IVM	Ivermectin
LBNPs	Lipid-based nanoparticles
LGIC	Ligand-gated ion channel
LNCs	Lipid nanocapsules
MB	Methylene blue
MWNTs	Multiwalled walled carbon nanotubes
NAC	N-acetyl-L-cysteine
nAChR	nicotinic acetylcholine receptor
NHS	N-hydroxysulfosuccinimide
NK	natural killer
NL	Nanoliposomes
NLCs	nano-lipid carriers
NLP	PZQ-loaded nanoliposome
NTDs	Neglected tropical diseases
PACA	Poly(alkylcyanoacylate)
PAMAM	Polyamidoamine
PBEC	Porcine brain endothelial cells
PBS	Phosphate buffered saline
PDI	polydispersity index
PEG	Poly(ethylene glycol)
PiB	Pittsburgh compound B
PLA	Poly(lactide)
PLGA	Poly(D,L-lactide-co-glycolic acid)
PMs	Polymeric micelles
PNs	Polymeric nanoparticles
PPI	Polypropylene imine
pRBCs	*Plasmodium*-infected red blood cells
PZQ	Praziquantel
RBCs	Red blood cells
RES	Reticuloendothelial system
RVG29	Rabies virus glycoprotein
SBSC	Schistosome Biological Supply Centre

SEM	Scanning electron microscopy
SGTP1	Schistosome glucose transporter 1
SGTP4	Schistosome glucose transporter 4
SLNs	Solid lipid nanoparticles
SWNTs	Single walled carbon nanotubes
TBRI	Theodor Bilharz Research Institute
TDs	Tropical diseases
TEM	Transmission Electron Microscope
TGA	Thermogravimetric analyser
Th1	T-helper 1 cells
Th2	T-helper 2 cells
TJs	Tight junctions
TSPs	Tetraspanins
WHO	World Health Organisation
XRPD	X-ray powder diffraction

LIST OF EQUATIONS

LIST OF FUGURES

LIST OF TABLES

CHAPTER ONE
INTRODUCTION AND BACKGROUND

1.1. BACKGROUND OF THIS STUDY

Schistosomiasis have been recognized as the second most prevalent among the group of Neglected Tropical Disease (NTD) in sub-Saharan Africa (SSA) following hookworm disease (Adekiya, 2018; Adekiya *et al.,* 2020). Schistosomiasis is a parasitic infection caused by flatworms which belongs to the group of trematode and genus of *Schistosoma* that results in chronic and acute disease (McManus *et al.,* 2018; McManus *et al.,* 2020). This disease poses a great consequential effect on agricultural produce and on the life and development of pregnant women and school children in afflicted areas. The disease-causing species of Schistosomiasis are *Schistosoma mansoni*, *Schistosoma intercalatum, Schistosoma haematobium*, *Schistosoma japonicum* and *Schistosoma mekongi* (Adekiya *et al.,* 2017; McManus *et al.,* 2018). The parasitizing of this infectious disease results in fever, abdominal pain, malaise, and skin rashes in an acute state, while intestinal, liver, urinary tract and lung diseases are the resultant diseases from the chronic state of the infection. The reappearance of the infection over time may result in the blockage of the urinary tract and pulmonary hypertension, which can ultimately generate additional complications and even death. In addition, schistosomes infection promotes the severity of other pathogenic infections such as; *Plasmodium falciparum, Staphylococcus aureus, Toxoplasma gondii, Leishmania spp., Mycobacteria, Salmonella* and *Entamoeba histolytica* (Abruzzi and Fried, 2011). Currently, over 200 million people have been affected by this disease, including 40 million women of reproductive age and approximately 600 to 779 million individuals are at risk of getting the infection, and the mortality has been estimated to be 280 000 deaths per year in Sub-Saharan countries (Cioli *et al.,* 2014).

In South Africa, *S. haematobium* and *S. mansoni* are the most prevalent *Schistosoma species*; which causes urogenital and intestinal schistosomiasis, respectively (Appleton and Miranda, 2015). The disease is mostly prevalent in the northern and eastern regions of the country with results shown that over 4.2 million people are suffering from this parasitic infection, with school-aged children having the highest prevalence (Mbabazi *et al.,* 2011). Consequently, over 25.7 million people are at risk of schistosomiasis as a result of poor socio-economic factors, climate change and other environmental factors (Appleton and Miranda, 2015). With the prevalence of schistosomiasis is sub-Saharan Africa, and the continual increase in infection rates praziquantel (PZQ) remains the only choice of drug and the best therapeutic agent against acute disease. This is due to the following factors: 1) its effectiveness against

all forms of Schistosomes, 2) it is inexpensive and readily available and 3) it possesses a lower side-effects profile which is well tolerated in patients of all ages. Unfortunately, the shortcomings of PZQ include; 1) resistance in some regions globally, 2) has poor patient compliance to treatment, 3) its ineffectiveness against the immature forms of the Schistosoma species and 4) its inability to prevent the re-infection of Schistosomiasis. Furthermore, there is an increase in parasite alteration and modification, the global parasite load and the co-infection of several strains of *Schistosoma* parasites (Doenhoff *et al.,* 2008). Recently, there are no alternative approaches to treat the infection since pharmaceutical companies jettison diseases that are not lucrative.

The design and development of new drugs for Schistosomiasis has been faced with major challenges, including poor financial support and motivation for pharmaceutical companies to develop new chemical entities (NCEs) in this area as well as the huge investment associated with the process of designing new drug molecules (Garcia-Salcedo *et al.,* 2016). It has been reported that over 40% of active pharmaceutical ingredients are less bioavailable and possess a poor therapeutic effect due to poor water insolubility (Qin *et al.,* 2018). Hence, nanotechnology is considered to have great impact on improving the solubility of drug molecules for improved drug delivery applications (Veerasamy *et al.,* 2011). Lipid-based formulations have drawn attention in enhancing the bioavailability and drugs, more so, to reduce some of the side-effects. In addition, nanoliposomes have gained significant interest in drug delivery due to their amphipathic nature, making them play a pivotal role in solubility modification, and the rate at which drugs can be released for the improvement and enhancement of drug absorption across biological barriers (Cheng *et el.,* 2017).

Since drugs repositioning approved for other diseases provide a shortcut to clinical trials, as it is expected that such drugs rapidly pass the regulatory authorities (Bergquist *et al.,* 2017). More so, with no additional candidates currently in the anti-schistosome drug clinical trial pipeline, a practical and necessary approach is to optimise the health benefits from praziquantel (Trainor-Moss and Mutapi, 2015), and due to lack of a protective vaccine for schistosomiasis. Therefore, this study is first to design a novel lipoidal nanosystem surface-engineered with an antibody (anti-calpain) for the targeted delivery PZQ in the treatment of Schistosomiasis. There are several target proteins and molecular receptors, which have been identified on the surface of the schistosome tegument such as; schistosome cysteine protease calpain which belongs to calpain family that are expressed in the Schistosoma tegument (Siddiqui *et al.,* 1992; Wang *et al.,* 2017). Schistosome glucose transporter 1 (SGTP1) and 4 (SGTP4) which are found in all types of schistosomes (Skelly *et al.,* 1994; Skelly *et al.,* 1998), acetylcholinesterase (AChE) and a nicotinic type of acetylcholine receptor (nAChR) which are

predominantly found on the surface of male schistosomes (Mansour and Mansour, 2002; MacDonald *et al.,* 2014). Other targeted protein found on the surface of the tegument is dynein (*Schistosoma mansoni*) (Mansour and Mansour, 2002). Calpain, a cysteine protease, was chosen as the target protein on the schistosomes for this work because its activities occur in extracellular cell-cell adhesion and cell-substrate adhesion sites. In schistosomes, calpain are part of the tegumental proteases which are expressed at the host-parasite interface. They are located in the cytoplasmic extensions of microtubular bundles that connect the surface syncytial epithelium to the schistosomes cell bodies underlying muscle of both the juvenile and adult schistosomes (Siddiqui *et al.,* 1992; Wang *et al.,* 2017). In that location, they perform similar functions with other calpains such as the transportation and delivery of membrane precursors that is, as a mediator in the synthesis of surface membranes. They are also found across the syncytial layer, where they function with the apical plasma membrane, causing membrane turnover (Siddiqui *et al.,* 1992). Based on the function of calpains in calcium-mediated signaling processes, surface membrane biogenesis and immunological evasion, they have been proposed as a potential candidate for chemotherapy targets and/or for a define-molecular vaccine (Siddiqui *et al.,* 1992; Wang *et al.,* 2017).

1. 2. RATIONAL AND MOTIVATION OF THE STUDY

Due to the bi-layered structure of nanoliposomes (NLs), this allows the maintenance of cell membrane fluidity. Conversely, the development of an amphiphilic drug-lipid complex or pharmacosomes improves drug permeability into the cell membranes without altering the lipid bilayer of the cell, thereby, improving the therapeutic efficacy and absorption of poorly soluble drugs (Cheng *et al.,* 2017). The uptake of PZQ through the human gut is prompt, with over 80% of the dose administered orally been absorbed in the GIT, reaching its highest plasma concentration between 1-2 hours (Chai, 2013). Several studies have revealed that PZQ-loaded liposomes improved the anti-schistosomal activity of PZQ and this can serve as a base for alternative administration routes for PZQ. Hence, this study developed lipoidal nanosystem for PZQ delivery as well as nanoliposomes surface-engineered antibody- anti-calpain as targeted delivery for the treatment of schistosomiasis. The NLs system improved the therapeutic efficacy of PZQ by disrupting the schistosomes' tegument in a targeted manner. More so, the surface functionalization of the NLs with anti-calpain stopped the schistosomes to undergo calcium-mediated signalling and inhibited the biogenesis of the membrane surface.

The successful incorporation of PZQ into the functionalized NLs could be a promising vehicle for the delivery of PZQ and this could enhance the therapeutic efficacy, reduce the dosage frequency and improve patient compliance. The nanosystem also improve the rate at which

PZQ causes spastic paralysis in the worm musculature since one of the proposed mechanisms by which PZQ acts on the *Schistosoma* parasite is the phenomenon associated with immediate alteration in the worm musculature (Pax *et al.,* 1978; Kohn *et al.,* 2001). This alteration in the worm musculature causes contractions probably due to the rapid influx of Ca^{2+} into the schistosome. Hence, the Ca^{2+}channels of schistosomes will be a probable molecular target for PZQ. The mechanism of action for PZQ has also been observed relating to Ca^{2+} homeostasis in the schistosomes, and the β-subunits of schistosomes channels, possessing a unique structure from other common β-subunits that inhibit the flow of current through the α_1 subunit of the schistosome with which they are associated. In addition, PZQ allows the opening of more channels or allows more current to flow through the individual channels and lead to the disruption of α1/β interaction in these channels, thereby resulting in normal Ca^{2+} homeostasis disruption (Kohn *et al.,* 2001).

Loading of PZQ into the NLs could also increase and improve the lipophilicity of PZQ and facilitate its interaction with the hydrophobic core of the worm tegument. Since PZQ causes morphological alterations in the schistosomes tegument which is indicated by vacuolization of parts of the tegument and blebbing at the surface. These morphological modifications resulting in an increase exposure of the schistosomes antigen present on the surface of the parasite. The tegument is covered by a double outer membrane which encloses the surface of the fluke, and this has been shown to be associated with the immune evasion system, rendering them undetectable by the host antibodies (Pearce and Freitas, 2008). Hence, functionalization of the NLs with the anti-calpain will specifically target and bind to the calpain protein on the schistosomes tegument. Calpains are calcium-dependent cysteine proteases which are generally expressed in nature (Siddiqui *et al.,* 1992; Wang *et al.,* 2017). They are part of the tegumental proteases which are expressed at the host-parasite interface of the schistosomes. They are located in the microtubular bundles of cytoplasmic extensions between the surface syncytial epithelium and the underlying musculature of the schistosomes cell bodies (Siddiqui *et al.,* 1992; Wang *et al.,* 2017).

Thus, functionalizing the surface of the nanoliposomes with antibody (anti-calpain) could suppress the activities of calpain protein. Thereby, impairing the ability of the schistosomes to undergo calcium-mediated signalling and stop the surface membrane biogenesis that is, the surface membrane synthetic process through the blockade of cell-cell adhesion or cell-substrate adhesion, which occur via the host-parasite interfaces. The calpain host-parasite is important for the schistosomes developmental processes, and failure in delivery and transportation of membrane precursors could lead to the rupture of the tegument, also, cause disruption in the ability of the worm to maintain solute balancing. Thus, the NLs designed in

this study have a significant effect on targeting adult and the juvenile schistosomes via anti-calpain functionalization, also, the NLs will clear all the traces of drug resistance and avert the reinfection of the disease by scavenging all the remnant of the parasite in the human host body. Figure 1 provides a schematic overview of this study.

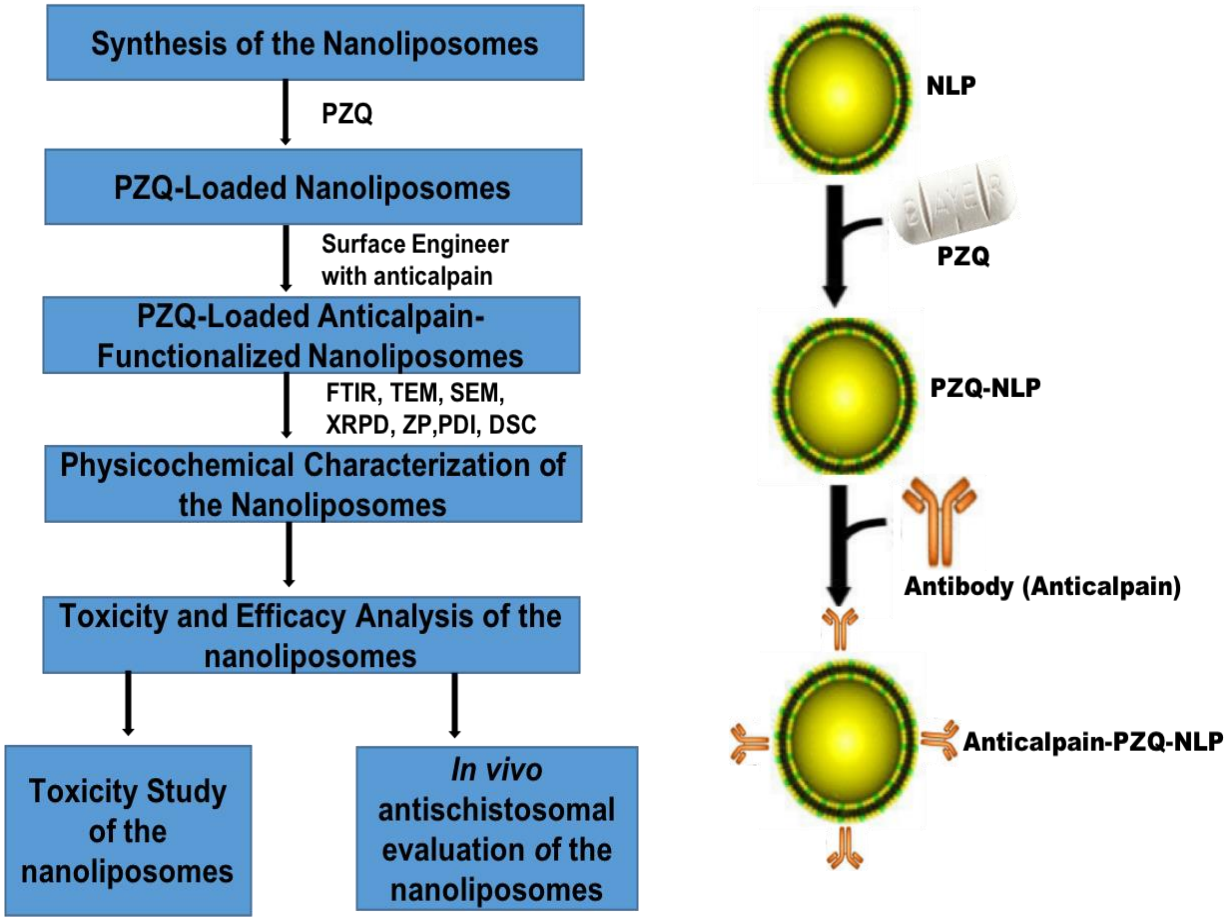

Figure 1.1: (a) Flowchart of experimental procedures (b) Scheme of surface functionalization of PZQ-loaded nanoliposome with antibody (Anticalpain) capable of targeting of cysteine protease calpain protein found on the surface of schistosomes, as well as disruption of the schistosomes tegument for the delivery of the PZQ.

1. 3. AIM AND OBJECTIVES

The aim of this study was to design and develop a surface-functionalized anti-calpain nanoliposome system for targeted PZQ delivery in the treatment of Schistosomiasis. The aim were attained with the following specific objectives:

1. Comprehensive patent review in the field of synthesis and therapeutic delivery approach for PZQ and critical literature review of nanotechnology for targeted antischistosomal therapy.

2. Development of the novel PZQ lipoidal nanosystems to increase the metabolic stability and therapeutic efficacy of PZQ.
3. Surface-engineering of the nanoliposomes with anti-calpain antibody to generate a PZQ anticalpain-functionalized nanoliposomes.
4. Determination of the physicochemical parameters of the native PZQ, PZQ-lipoidal nanosystems and PZQ-loaded anticalpain-functionalized nanoliposome. This was done to help in determining the thermal behaviour, particle size, molecular and morphological structure of the samples.
5. Investigation of the *in vitro* drug release of the PZQ loaded lipoidal nanosystems and PZQ-loaded anticalpain-functionalized nanoliposome as compared to the native PZQ.
6. Investigation of the *in vitro* cytotoxicity of the PZQ loaded lipoidal nanosystems and PZQ-loaded anticalpain-functionalized nanoliposome as compared to the native PZQ.
7. Evaluation of the *in vivo* toxicity, histopathological analysis and the *in vivo* antischistosomal evaluation of PZQ loaded lipoidal nanosystems and PZQ-loaded anticalpain-functionalized nanoliposome in order to investigate the *in vivo* safety and the efficacy of the nanosystems when compared with native PZQ.

1.4. NOVELTY OF THIS STUDY

1. This study is first to design a novel lipoidal nanosystem surface-engineered with an antibody (anticalpain) for the targeted delivery PZQ in the treatment of Schistosomiasis.
2. The NLs designed in this study have a significant effect on targeting adult and the juvenile schistosomes via anti-calpain functionalization, also, the NLs could clear all the traces of drug resistance and avert the reinfection of the disease by scavenging all the remnant of the parasite in the human host body.
3. This study has shown that the addition of Pluronic F127 as the surfactants provided long-term stability for compritol ATO 888-lecithin solid lipid nanoparticles nanosuspension over 120 days at room temperature.
4. This study reported that the formulated PZQ-loaded lipoidal nanosystems do not cause any oxidative stress damage to the rats, rather confer hepatoprotective effects on the rats and could have the ability to circumvent traces of toxicity associated with bioactive molecules.

1.5. OVERVIEW OF THE THESIS

CHAPTER 1: In this chapter, the introduction and background of this current study were provided. The rationale and motivation for the study is detailed, and the aims and objectives were presented in detail for undertaking this study. More so, the novelty of this study was

presented, and a schematic representation of the synthetic procedure employed for the preparation of NLs was presented for better understanding of the reaction procedure.

CHAPTER 2: This chapter provides a concise insight on the use of various advance approaches to achieve targeted anti-schistosomal therapy, mainly through the use of nano-enabled drug delivery systems. It also assimilates the molecular structure and function of the schistosome tegument and highlights the potential molecular targets found on the tegument, for effective specific interaction with receptors for more efficacious anti-schistosomal therapy.

Furthermore, the chapter gives an insight of cerebral tropical diseases, highlighted several current conventional drug delivery strategies into the CNS. More so, highlighting several potential nano-delivery systems that can be employed to bypass the blood brain barrier (BBB) as well as the blood cerebrospinal fluid barrier (BCSFB) so as to deliver bioactive molecules effectively to the brain with great and improved bioavailability.

CHAPTER 3: This chapter discussed several approaches used in the synthesis of praziquantel aimed at reducing the time and cost of production, the toxicity and experimental harsh conditions are discussed. Also, patented methods involved in the pharmaceutical reformulation of praziquantel in the treatment of diverse endoparasitic infestation are reported. Additionally, future perspectives in terms of nanomedicine approach in the formulation of praziquantel are highlighted.

CHAPTER 4: In this chapter nanotechnological techniques were employed to design and develop praziquantel nanoliposomal (NLP) nanosystem and surface-functionalized the NLP with anticalpain antibody (anticalpain-NLP) for targeted praziquantel (PZQ) delivery in the treatment of schistosomiasis. Anticalpain-NLP were prepared and validated for their physicochemical properties using fourier transform infrared (FTIR), thermal behaviour, X-ray powder diffraction (XRPD), scanning electron microscopy (SEM) and transmission electron microscopy (TEM) analysis. *In vitro* and *in vivo* toxicity, drug loading capacity (DLC), drug entrapment efficiency (DEE), drug release and parasitological cure rate were also validated.

CHAPTER 5: This chapter aimed to develop and evaluate the long-term stability of drug-loaded solid lipid nanoparticles (SLNs). The SLNs were designed to extend the release profile and overcome the problem of bioavailability and solubility, investigate its toxicity and improve the anti-schistosomal efficacy of praziquantel. The aim was pursued using solvent injection-co-homogenization techniques to fabricate SLNs in which compritol ATO 888 and lecithin were used as lipids, and Pluronic F127 (PF127) was used as a stabilizer. The long-term stability effect of the PF127 as a stabilizer on the SLNs was evaluated. The particle size, stability and

polydispersity were determined by a dynamic light scattering (DLS) technique. The morphological analysis of the SLNs was investigated by Transmission and Scanning Electron Microscopy (TEM) and (SEM). The chemical properties, mechanical, thermal, and crystal behaviours of SLNs were evaluated using FTIR, ElastoSens Bio2, XRPD, DSC and TGA, respectively.

CHAPTER 6: The developed anticalpain engineered lipoidal nanosystem and the stable compritol ATO 888 lecithin solid lipid nanoparticles resulted to be nanocarrier systems that fulfilled the aims and objectives of this study. The physicochemical parameters, *in vitro* and *in vivo* evaluations of the developed nanoliposomes and SLNs nanocarrier systems produced outstanding results. In this chapter, the concluding remark of the thesis was provided, also the recommendations and future perspectives in the field of lipoidal nanosystem technology application in the treatment of schistosomiasis.

1.6. REFERENCES

1. Abruzzi A., and Fried B. (2011). Coinfection of Schistosoma (Trematoda) with bacteria, protozoa and helminths. *In Advances in parasitology*, *77*:1-85.
2. Adekiya, T.A., 2018. *Theoretical modelling of temperature and rainfall inuence on Schistosoma species population dynamics* (Doctoral dissertation, University of Zululand).
3. Adekiya, T.A., Aruleba, R.T., Klein, A. and Fadaka, A.O., 2020. In silico inhibition of SGTP4 as a therapeutic target for the treatment of schistosomiasis. *Journal of Biomolecular Structure and Dynamics*, pp.1-9.
4. Adekiya, T.A., Kappo, A.P. and Okosun, K.O., 2017. Temperature and rainfall impact on schistosomiasis. *Global Journal of Pure and Applied Mathematics*, *13*(12), pp.8453-8469.
5. Amara, R.O., Ramadan, A.A., El-Moslemany, R.M., Eissa, M.M., El-Azzouni, M.Z. and El-Khordagui, L.K., 2018. Praziquantel–lipid nanocapsules: an oral nanotherapeutic with potential Schistosoma mansoni tegumental targeting. *International journal of nanomedicine*, *13*, p.4493.
6. Appleton, C.C. and Miranda, N.A.F., 2015. Two Asian freshwater snails newly introduced into South Africa and an analysis of alien species reported to date. *African Invertebrates*, *56*(1), pp.1-17.
7. Bergquist, R., Utzinger, J. and Keiser, J., 2017. Controlling schistosomiasis with praziquantel: how much longer without a viable alternative?. *Infectious diseases of poverty*, *6*(1), p.74.

8. Chai, J.Y., 2013. Praziquantel treatment in trematode and cestode infections: an update. *Infection & chemotherapy*, *45*(1), pp.32-43.

9. Cheng, W., Li, X., Zhang, C., Chen, W., Yuan, H. and Xu, S., 2017. Preparation and In Vivo-In Vitro Evaluation of Polydatin-Phospholipid Complex with Improved Dissolution and Bioavailability. *Int J Drug Dev Res*, *9*, pp.39-43.

10. Cioli, D.; Pica-Mattoccia, L.; Basso, A.; Guidi, A. Schistosomiasis control: praziquantel forever?. *Mol. Biochem. Parasitol*. 2014, *195*(1), 23-29.

11. Doenhoff M.J., Cioli D. and Utzinger J. (2008). Praziquantel: mechanisms of action, resistance and new derivatives for schistosomiasis. *Current opinion in infectious diseases,* 21(6):659-667.

12. Dora, C.P., Kushwah, V., Katiyar, S.S., Kumar, P., Pillay, V., Suresh, S. and Jain, S., 2017. Improved metabolic stability and therapeutic efficacy of a novel molecular gemcitabine phospholipid complex. *International journal of pharmaceutics*, *530*(1-2), pp.113-127

13. Frezza, T.F., Gremião, M.P.D., Zanotti-Magalhães, E.M., Magalhães, L.A., de Souza, A.L.R. and Allegretti, S.M., 2013. Liposomal-praziquantel: efficacy against Schistosoma mansoni in a preclinical assay. *Acta tropica*, *128*(1), pp.70-75.

14. Garcia-Salcedo, J.A., Unciti-Broceta, J.D., Valverde-Pozo, J. and Soriano, M., 2016. New approaches to overcome transport related drug resistance in trypanosomatid parasites. *Frontiers in pharmacology*, *7*, p.351.

15. Kohn, A.B., Anderson, P.A., Roberts-Misterly, J.M. and Greenberg, R.M., 2001. Schistosome calcium channel β subunits unusual modulatory effects and potential role in the action of the antischistosomal drug praziquantel. *Journal of Biological Chemistry*, *276*(40), pp.36873-36876.

16. Krautz-Peterson, G.; Simoes, M.; Faghiri, Z.; Ndegwa, D.; Oliveira, G.; Shoemaker, C.B.; Skelly, P.J. Suppressing glucose transporter gene expression in schistosomes impairs parasite feeding and decreases survival in the mammalian host. *PLoS Pathog.* 2010, *6*(6), e1000932

17. MacDonald, K.; Buxton, S.; Kimber, M.J.; Day, T.A.; Robertson, A.P.; Ribeiro, P. Functional characterization of a novel family of acetylcholine-gated chloride channels in Schistosoma mansoni. *PLoS Pathog.* 2014, *10*(6), e1004181.

18. Mansour, T. and Mansour, J. (2002). Targets in the Tegument of Flatworms. In *Chemotherapeutic Targets in Parasites: Contemporary Strategies* (pp. 189-214).

19. Mbabazi P, Andan O, Fitzgerald DW, Chitsulo L, Engels D, Downs JA (2011). Examining the relationship between urogenital schistosomiasis and HIV infection. *PLoS Neglected Tropical Diseases* **5**(12): e1396.

20. McManus, D.P., Bergquist, R., Cai, P., Ranasinghe, S., Tebeje, B.M. and You, H., 2020, June. Schistosomiasis—from immunopathology to vaccines. In *Seminars in immunopathology* (Vol. 42, No. 3, pp. 355-371). Springer Berlin Heidelberg.

21. McManus, D.P., Dunne, D.W., Sacko, M., Utzinger, J., Vennervald, B.J. and Zhou, X.N., Schistosomiasis. Nature reviews Disease primers. 2018; 4 (1): 13.

22. Pax, R., Bennett, J.L. and Fetterer, R., 1978. A benzodiazepine derivative and praziquantel: effects on musculature of Schistosoma mansoni and Schistosoma japonicum. *Naunyn-Schmiedeberg's archives of pharmacology*, *304*(3), pp.309-315.

23. Pearce, E.J. and Freitas, T.C., 2008. Reverse genetics and the study of the immune response to schistosomes. *Parasite immunology*, *30*(4), pp.215-221.

24. Qin, L., Niu, Y., Wang, Y. and Chen, X., 2018. Combination of phospholipid complex and submicron emulsion techniques for improving Oral bioavailability and therapeutic efficacy of water-insoluble drug. *Molecular pharmaceutics*, *15*(3), pp.1238-1247.

25. Siddiqui, A.A., Zhou, Y., Podesta, R.B., Karcz, S.R., Tognon, C.E., Strejan, G.H., Dekaban, G.A. and Clarke, M.W., 1993. Characterization of Ca2+-dependent neutral protease (calpain) from human blood flukes, *Schistosoma mansoni*. Biochimica et Biophysica Acta (BBA)-Molecular Basis of Disease, 1181(1), pp.37-44.

26. Skelly, P.J. and Shoemaker, C.B., 1996. Rapid appearance and asymmetric distribution of glucose transporter SGTP4 at the apical surface of intramammalian-stage Schistosoma mansoni. *Proceedings of the National Academy of Sciences*, *93*(8), pp.3642-3646.

27. Skelly, P.J. and Shoemaker, C.B., 2001. The Schistosoma mansoni host-interactive tegument forms from vesicle eruptions of a cyton network. *Parasitology*, *122*(1), pp.67-73.

28. Skelly, P.J.; Kim, J.W.; Cunningham, J.; Shoemaker, C.B. Cloning, characterization, and functional expression of cDNAs encoding glucose transporter proteins from the human parasite Schistosoma mansoni. *J. Biol. Chem.* 1994, *269*(6), 4247-4253.

29. Skelly, P.J.; Tielens, A.G.M.; Shoemaker, C.B. Glucose transport and metabolism in mammalian-stage schistosomes. *Parasitol. Today*, 1998, *14*(10), 402-406.

30. Song, S., Liu, D., Peng, J., Sun, Y., Li, Z., Gu, J.R. and Xu, Y., 2008. Peptide ligand-mediated liposome distribution and targeting to EGFR expressing tumor in vivo. *International journal of pharmaceutics*, *363*(1-2), pp.155-161.

31. Sun, Q., Mao, R., Wang, D., Hu, C., Zheng, Y. and Sun, D., 2016. The cytotoxicity study of praziquantel enantiomers. *Drug design, development and therapy*, *10*, p.2061.

32. Suzuki, R., Takizawa, T., Negishi, Y., Hagisawa, K., Tanaka, K., Sawamura, K., Utoguchi, N., Nishioka, T. and Maruyama, K., 2007. Gene delivery by combination of novel liposomal bubbles with perfluoropropane and ultrasound. *Journal of Controlled Release*, *117*(1), pp.130-136.

33. Trainor-Moss, S. and Mutapi, F., 2016. Schistosomiasis therapeutics: whats in the pipeline?.

34. Veerasamy R., Xin T. Z., Gunasagaran S., Xiang T. F. W., Yang E. F. C., Jeyakumar N. and Dhanaraj S. A. (2011). Biosynthesis of silver nanoparticles using mangosteen leaf extract and evaluation of their antimicrobial activities. *Journal of Saudi Chemical Society*. **15**(2): 113-120

35. Verma, D.D., Verma, S., Blume, G. and Fahr, A., 2003. Particle size of liposomes influences dermal delivery of substances into skin. *International journal of pharmaceutics*, *258*(1-2), pp.141-151.

36. Wang, Q., Da'dara, A.A. and Skelly, P.J., 2017. The human blood parasite Schistosoma mansoni expresses extracellular tegumental calpains that cleave the blood clotting protein fibronectin. Scientific reports, 7(1), pp.1-13.

CHAPTER TWO

THE PROMISE OF NANOTECHNOLOGY FOR TARGETED ANTI-SCHISTOSOMAL THERAPY

frontiers in Bioengineering and Biotechnology

REVIEW
published: 31 January 2020
doi: 10.3389/fbioe.2020.00032

A Review of Nanotechnology for Targeted Anti-schistosomal Therapy

*Tayo Alex Adekiya, Pierre P. D. Kondiah, Yahya E. Choonara, Pradeep Kumar and Viness Pillay**

Wits Advanced Drug Delivery Platform Research Unit, Department of Pharmacy and Pharmacology, School of Therapeutic Science, Faculty of Health Sciences, University of the Witwatersrand, Johannesburg, South Africa

Schistosomiasis is one of the major parasitic diseases and second most prevalent among the group of neglected diseases. The prevalence of schistosomiasis may be due to environmental and socio-economic factors, as well as the unavailability of vaccines for schistosomiasis. To date, current treatment; mainly the drug praziquantel (PZQ), has not been effective in treating the early forms of schistosome species. The development of drug resistance has been documented in several regions globally, due to the overuse of PZQ, rate of parasitic mutation, poor treatment compliance, co-infection with different strains of schistosomes and the overall parasite load. Hence, exploring the schistosome tegument may be a potential focus for the design and development of targeted anti-schistosomal therapy, with higher bioavailability as molecular targets using nanotechnology. This chapter aims to provide a concise incursion on the use of various advance approaches to achieve targeted anti-schistosomal therapy, mainly through the use of nano-enabled drug delivery systems. It also assimilates the molecular structure and function of the schistosome tegument and highlights the potential molecular targets found on the tegument, for effective specific interaction with receptors for more efficacious anti-schistosomal therapy.

2.1. Introduction

Schistosomiasis is recognized as the second most prevalent among the group of Neglected Tropical Diseases (NTDs) in sub-Saharan Africa, following hookworm infection (Adekiya *et al.,* 2017). Schistosomiasis is an infectious disease caused by parasitic worms that belong to the group of trematode and genus of *Schistosoma*, that results in chronic and acute disease (Adekiya *et al.,* 2017). It poses a significant challenge on agricultural productivity and the life, growth and development of pregnant women and school children in afflicted areas. The disease-causing species of *Schistosoma* are *Schistosoma mansoni*, *Schistosoma haematobium*, *Schistosoma japonicum*, *Schistosoma intercalatum* and *Schistosoma mekongi* (Adekiya *et al.,* 2017; da Paixão Siqueira *et al.,* 2017). For these worms to cause disease, the intermediate hosts (freshwater snails) need to be infected with the miracidia in freshwater where it develops into cercaria. Following human-water exposure, the cercaria penetrates the intact skin of humans.

Schistosomiasis affects the world's poorest countries where there is no safe water, basic sanitation and hygiene education (da Paixão Siqueira *et al.,* 2017). Currently, over 200 million people have been affected by schistosomiasis, including 40 million women of reproductive age and approximately 600-779 million individuals are at risk of becoming infected. The mortality rate has been estimated at 280 000 deaths annually in Sub-Saharan countries (Cioli *et al.,* 2014).

The parasitizing of this infectious disease results in fever, malaise, abdominal pain, and skin rashes in an acute state, while intestinal, liver, urinary tract and lung diseases are the result of chronic infection. Acute and chronic disease is solely reliant on the type of species that infects an individual. Reappearance of schistosomiasis over latent periods can result in blockage of the urinary tract and pulmonary hypertension that can lead to fatal complications. In addition, schistosome infection promotes the severity of infection with additional pathogens such as; *Plasmodium falciparum, Toxoplasma gondii, Leishmania spp., Mycobacteria, Staphylococcus aureus, Salmonella* and *Entamoeba histolytica* (Abruzzi and Fried, 2011).

The incidence of schistosomiasis is predominant in Sub-Saharan Africa, and with the increasing rate of infection, due to climate change and other socio-economic factors. To date, praziquantel (PZQ) remains the only drug for the treatment of this debilitating disease. PZQ has the following benefits: 1) its effective against all forms of Schistosomes, 2) it is inexpensive and readily available and 3) it has a low side-effect profile, well tolerated in patients of all ages. Unfortunately, the use of PZQ is limited by the following: 1) drug resistance, 2) poor patient compliance to treatment in certain populations, 3) its ineffective against immature forms of the

Schistosoma species and 4) it cannot prevent re-infection of Schistosomiasis. Furthermore, there is an increase in parasite alteration and modification, the global parasite load and co-infection with several strains of *Schistosoma* parasites (Doenhoff *et al.,* 2008; Caffrey, 2007; Fenwick *et al.,* 2009). Coupled with cases of cerebral schistosomiasis in some regions globally, there is an urgent need for an alternative anti-schistosomal drug molecule or to improve the delivery efficacy of PZQ using approaches such as nanotechnology to achieve targeted anti-schistosomal therapy, for example in the central nervous system (CNS).

There has not been a considerable impetus placed on developing novel and new drug treatments for schistosomiasis. However, based on the debilitating impact of the disease, researchers need to be alerted on exploring several essential target proteins found in the *Schistosoma species* and could play a significant role in ensuring the possibility of designing new drug molecules for schistosomiasis (Garcia-Salcedo *et al.,* 2016). In the absence of any meaningful drug discovery programs for identifying new drug targets and molecules for schistosomiasis, pharmaceutical researchers have turned to providing more efficacious delivery systems for the gold-standard drug PZQ. Hence, nanotechnology and the use of nano-enable drug delivery systems (Fig. 2.1), has been a major focus to potentially provide better treatment outcomes for schistosomiasis using PZQ (Veerasamy *et al.,* 2011). Nano-enabled drug delivery systems can enhance the bioavailability and therapeutic efficacy of PZQ (or other drugs) and reduce the side effect profile by having more targeted drug delivery.

Nanoparticulate systems currently in use involve, but are not limited to, lipid-based nanoparticles (liposomes, micelles, solid lipid nanoparticles, nanostructured lipid carriers and nanodiscs). Others include polymeric-based nanoparticles (nanospheres, nanocapsules, nanofibers/nanotubes, nanodiscs and micelles), metallic/inorganic-based nanoparticles (nanospheres, nanocapsules, nanodiscs and nanowires/nanotubes) and metal nanoparticles fabricated by green chemistry (gold, silver, copper, platinum, palladium and zinc nanoparticles).

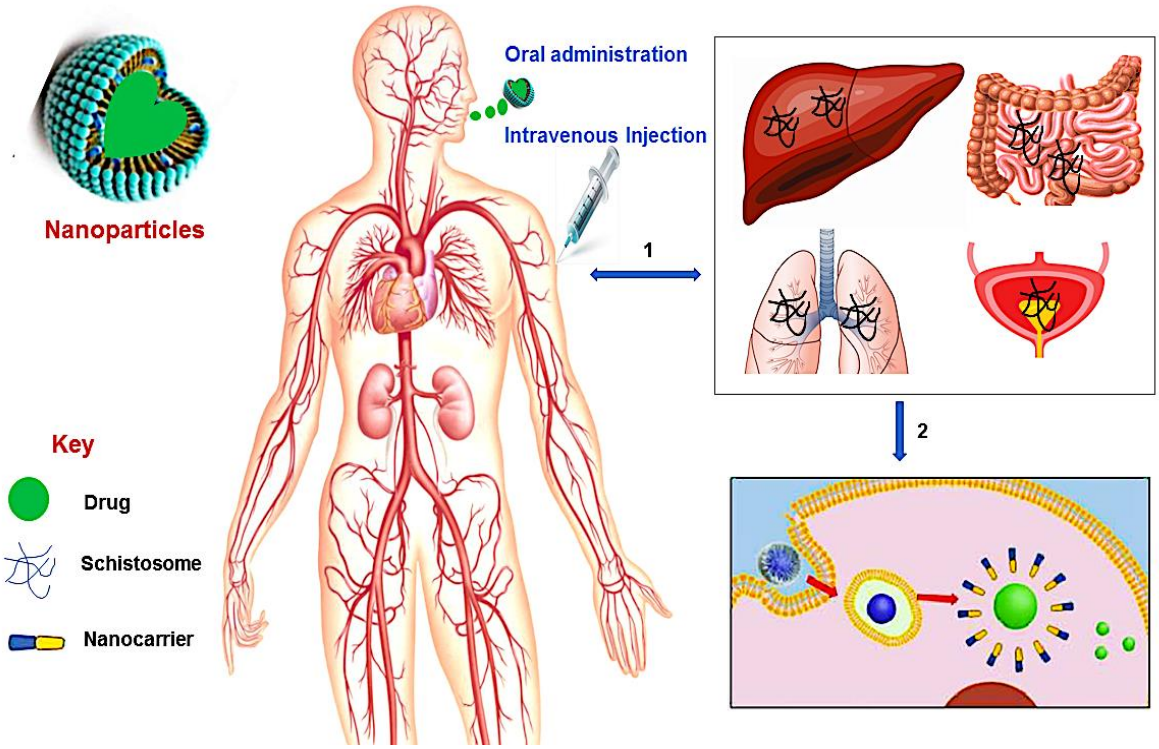

Figure 2.1: A schematic overview of nanotechnology in schistosomiasis treatment.1) The Schistosoma parasites penetrates the human skin and enter the bloodstream where they travel via the blood vessels of the liver and lungs, and then to the vein around the intestines and bladder, 2) the administration (oral or intravenous injection) of nanotechnological-based drug leads to the disruption of the membrane (tegument) of the worms thereby releasing the drug to kill the worms.

The advent of smart lipid-based nanoparticles (LBNPs) (Fig. 2.2) has provided secure platforms for the use of nano-biomaterials in medical applications such as therapeutic drug encapsulation for targeted drug delivery for disease therapy in biomedicine. Recently, the use of LBNPs has gained much interest, particularly in treating schistosomiasis because it can be better absorbed by the tegument of schistosomes, which has an affinity for phospholipids bilayer. LBNPs amphipathic nature allows them to play a pivotal role in the solubility modification and rate at which drugs such as PZQ can be targeted, for enhancing drug absorption across biological barriers (Cheng *et al.,* 2017). Furthermore, targeted LBNPs can improve the efficacy and specificity of drugs to cells or tissues by upregulating surface molecular receptors such as antigens, unregulated selectin and serpin enzyme complex-receptor (Cheng *et al.,* 2017). The *Schistosoma* parasite consists of different molecules that are found on the surface of the parasite tegument, which are needed for the parasite survival. This is a largely unexplored approach for targeted drug delivery in anti-schistosomal therapy. To this end, nanotechnology has played a central role in the design of systems intended to target the parasite tegument. Hence, this review aims to provide a concise incursion into the molecular structure and function of the schistosome tegument and assimilate the potential

targeting proteins/molecules on the tegument to identify new targets and targeting molecules in anti-schistosomiasis therapy.

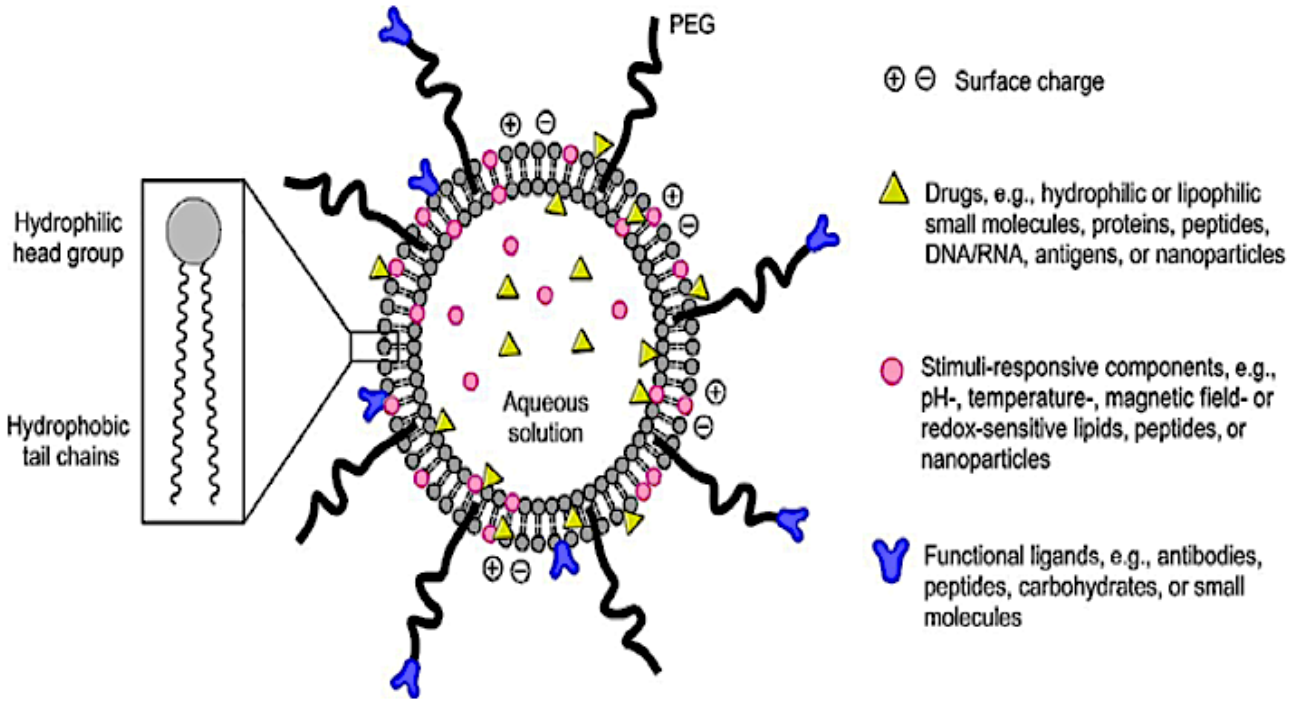

Figure 2.2: A schematic diagram of a smart lipid-based nanoparticles system as a nano-enabled drug delivery platform (reprinted with permission from Li and Takeoka, 2018).

2.2. Overview of the Past and Present Anti-Schistosomiasis Therapies

In 1984, the World Health Organisation (WHO) Expert Committee proposed chemotherapy as the best treatment approach to eliminate schistosomiasis (Conlon, 2005). Ever since, chemotherapy continues to be the only measure for the control of schistosomiasis and depends only on a single dose treatment with PZQ. Among other anti-schistosomal drugs that have been explored, PZQ is the most widely used. PZQ is active against all forms of *Schistosoma* species that cause schistosomiasis. It reduces the parasitic load and is able to reduce the severity of symptoms. It is also the most preferred drug because of its simple administration, efficacy and affordability. Although, the mechanism of action in treating schistosomiasis is not well understood, a widely proposed mechanism is the immediate alteration in the worm musculature. This was reported by Pax and co-workers (1978) when they noticed that the alteration in the worm musculature causes contraction probably due to rapid influx of Ca^{2+} into the schistosome. This assertion was corroborated by interesting work undertaken by Kohn and co-workers (2001) that drew attention to the voltage-gated calcium channels of schistosomes as the potential target for PZQ. In their study, the mechanism of action for PZQ was suggested to be consistent with the observed effects of PZQ on Ca^{2+}

homeostasis in schistosomes. It was noted that β-subunits of schistosome channels had a unique form of β-subunit structure that was different from other common β-subunits which inhibit flow of current through the α_1 subunit of schistosome with which they are associated. The study further hypothesised that PZQ facilitated the opening of more channels for current to flow leading to the disruption of α1/β interaction in these channels resulting in disruption of Ca^{2+} homeostasis (Kohn *et al.,* 2001). It has also been reported that PZQ causes morphological transitions in the schistosomes tegument. This was initially indicated by the formation of vacuoles within the tegument and blebbing at the surface (Becker *et al.,* 1980; Mehlhorn *et al.,* 1981; Cioli and Pica-Mattoccia, 2003). These morphological transitions cause increased exposure of antigens on the surface of the parasite (Harnett and Kusel, 1986). Harnett and Kusel suggested that the action of PZQ on the exposed antigens may be due to its lipophilicity that makes it easier to interact with hydrophobic cores of the tegument.

Due to the shortcomings of the drugs listed in Table 2.1, researchers have resorted to the use of drug delivery technologies such as nanotechnology to provide more targeted therapies to all stages of the Schistosoma parasite such that drugs can be more effective in treating the immature forms of the parasite. These novel approaches can also reduce drug resistance and avert re-infection by clearing the schistosomes in the human host.

Table 2.1: Drugs that have been used to treat schistosomiasis to date, with their shortcomings evaluated

Anti-schistosomal drugs	**Shortcomings**	**Reference**
Metrifonate	Metrifonate is selective to only *S. haematobium* and due to medical standards and economic operations, the drug has been withdrawn from the market.	Eissa *et al*., 2011; de Moraes, 2012; Aruleba *et al*., 2018
Oltripaz	Oltripaz is another anti-schistosomal drug which has been used in the past, but not in the market again and discontinued in treating schistosomes infection due to its photosensitivity induction and longer time in curing the infections; approximately two months.	Nare *et al*., 1992
Niridazole	Niridazole was jettisoned due to its unpleasant adverse effects which include	Urman *et al*., 1975; Katz, 1977; Nare *et al*.,

	non-specificity destruction to the T waves electrocardiogram (ECG), toxicity to the renal and central nervous system, it has also been revealed to be a carcinogenic material.	1992; Thetiot-Laurent *et al*., 2013
Oxamniquine	Oxamniquine has also been used in the past, but it is ineffective against all schistosomes type, only effective to *S. mansoni,* and due to cost effectiveness, drug resistance and some side effects, the drug has been replaced by praziquantel in treating schistosomiasis.	Saconato and Atallah, 2000; Morgan *et al*., 2001; Richter, 2003; El Ridi and Tallima, 2013; Aruleba *et al*., 2018

2.3. The Schistosome Tegument: Revisit of The Molecular Structure and Function for Targeted Drug Delivery

The outer-surface of the schistosome is enclosed with an uncommon structure known as the tegument where some probable receptors for targeted nanodelivery system are found. It is a rare double layered membrane structure that plays a pivotal role in protecting the worm from harsh conditions in the host system. There are several organelles present in the tegument (Fig. 2.3). The heptalaminate tegumental surface is enclosed by a typical plasma membrane structure that is superimposed by a secreted membranocalyx (generated by the multi-laminate vesicles found in the tegument cytoplasm) and fuses with lateral channels protruding out into the base of the surface from the cytoplasm which also host some potential proteins for nanodelivery systems. The membranocalyx can be active by interacting with proteins and glycans via the extracellular loops of the tetraspanins protein, this depicts tetraspanins as a probable target for nanodelivery systems.

The initiation of heptalaminate membrane surface alongside dyneins protein starts from the outer membrane of the cercarial trilaminate 30 minutes after invasion of cercarial into the host skin, and within three hours, the change in cercarial membrane from the trilaminate to the heptalaminate mature membrane structure is accomplished in an immature schistosome (schistosomulum) (Mansour and Mansour, 2002), with the help of several molecules which are potential target for nanodelivery systems. The surface spines of schistosomes are made-up of paracrystalline arrangements of filamentous actin, which are found outside the tegument

and basal membranes with protruding tip which is above the general level of the tegument. The dorsal surface spines protrude into the endothelial cells surface of the human host blood vessels with the help of different molecular proteins such as; dyneins, SGTP4 and tetraspanins (some of the potential targets for nano-enabled drug delivery systems), where it helps the schistosomes to hold fast against the blood flow when the schistosomes are living in the host mesenteric blood vessels (Kasny *et al.,* 2017).

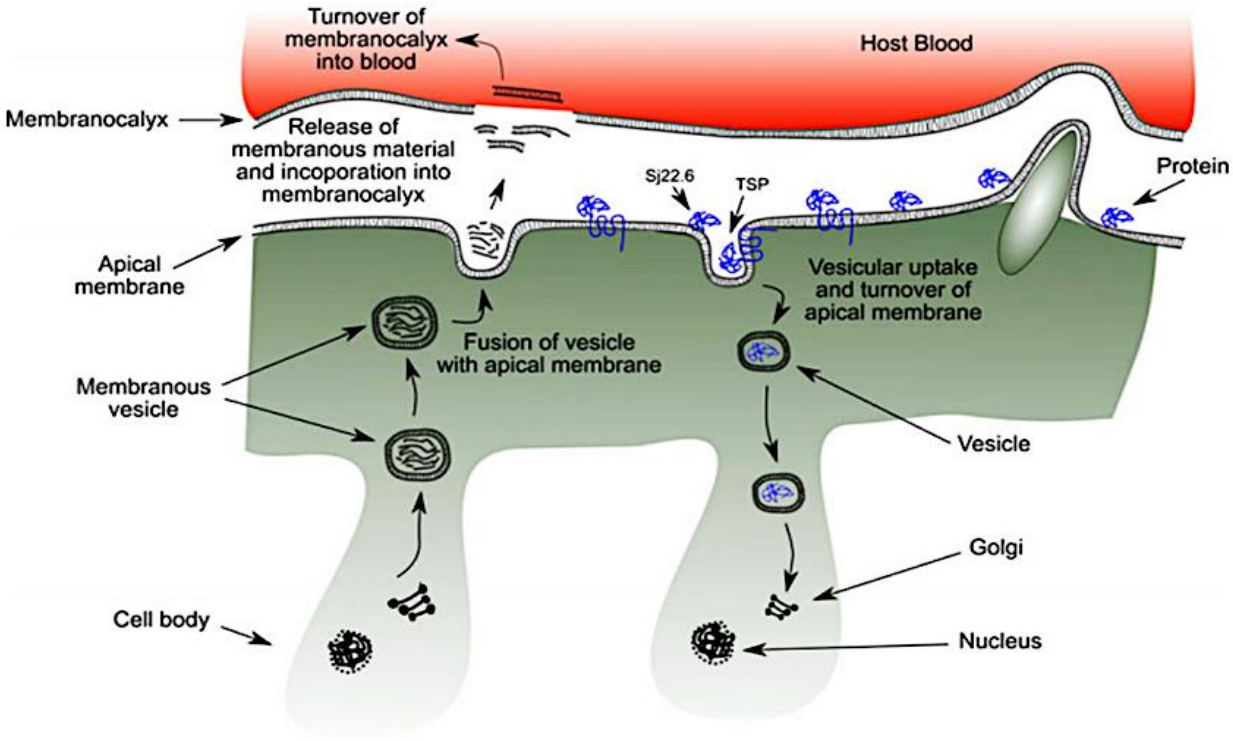

Figure 2.3: Schematic diagram of schistosome tegument structure with several organelles and the position of targeted proteins (as seen in blue) (reprinted with permission from Mulvenna *et al*., 2010).

The syncytium of the tegument consists of trilaminate vesicles that comprise membranous material, and they are either elongated or spherical in shape and are known as membranous bodies and elongate bodies. The syncytium is linked to nucleated cell bodies (cytons) by cytoplasmic tubes that are coated with microtubules. Although, cytons are not considered to be part of the tegument, they are found under the circular and longitudinal muscle fibers of the tegument where some potential targeted proteins and molecules are secreted. They consist of mitochondria, nuclei, Golgi complexes, ribosomes and glycogen particles (Mansour and Mansour, 2002). The biogenesis of new membrane material including tegumental proteins, and the maintenance of the schistosomes tegument are equipped inside the cytons, under the muscular layer and syncytium vesicles (El Ridi *et al.,* 2017). Though, the process has not been

well studied, both the elongated bodies and membranous bodies transport membranous material which are found to be scattered in the cytons in conjunction with Golgi complexes where they are possibly generated. These vesicles carry membranous material and some targeted proteins produced within the cytons and move them via the tubules of the cytoplasm to the syncytium, and thereafter, migrate to the outside of the surface tegument of the membrane (Kasny *et al.,* 2017; El Ridi *et al.,* 2017; Gobert *et al.,* 2017). More so, the incorporation of membrane vesicles content with other tegumental proteins (potential targeted molecules for nano-delivery systems) take place in the cytons where a fresh heptalaminate membrane is produced. This activity is not only restricted to schistosomula developments, also to adult schistosomes after the shedding or the rupture of the exterior schistosomes surface. Surface pits is another organelle found on the surface of the schistosomes tegument. The pits have an ability to increase the surface area of the worm not less than tenfold where it provides an avenue for the worm to absorb nutrients such as glucose and other molecules from the exterior milieu using its tegumental proteins and receptors.

Wendt and co-workers developed a new fluorescent schistosome tegument label technique. This proved that the schistosome parasite usually repairs and replaces the tegument continuously with a half-life of 5 days in order to survive harsh conditions in the host system (Wendt *et al.,* 2018). This corroborated with the work of Wilson and Barnes (1977), where they showed that there is a possibility for the membranocalyx of the schistosome tegument to replace itself at a variable rate and was dependent on the external environmental conditions in which the worm was found. This view was supported by Perez and Terry in (1973) where they observed that the surface of the schistosome was turning over more rapidly when schistosomes cultured in monkey anti-mouse serum were selected from the schistosome mice model.

This unique membrane structure allows the schistosome tegument to play a significant role in protecting the schistosome to survive in the host, some of which include; host response modulation that causes host immune response evasion (Elzoheiry *et al.,* 2018). This immune evasion occurs by rendering the infected host's antibody responses ineffective, hence fails to clear the established parasites (Han *et al.,* 2009). In addition, the tegument of the schistosomes has some other functions such as absorption of nutrients.

Trematodes have an incomplete digestive tract, and the *Schistosoma species* can survive under prolonged *in vitro* incubation in the absence of nutrient absorption within the intestine (Isseroff and Read, 1974; Popiel and Basch, 1984). Glucose absorption in trematodes is noticed during immature stages of the trematode's life cycle, which lacks a developed intestine

(Uglem and Lee, 1985). Both, immature and mature schistosomes rely mainly on plasma glucose from the host for energy. Physiological investigations demonstrated that the influx of glucose within the tegument occurred by a carrier-mediated process (Rogers and Bueding, 1975; Uglem and Read, 1975). Several enzymes function for the absorption of amino acids on the tegument (Skelly *et al*., 2014), and other enzymes, for instance, leucine aminopeptidase is absent in the gut. Cholesterol is also acquired by schistosomes from the host via the tegument where it is redistributed throughout the schistosomes body (Popiel and Basch, 1986; Haseeb *et al*., 1985).

In terms of parasite motility control, the mature *Schistosoma* species move based on several degrees of flow and confinement. Zhang and co-workers (2019) observed that movement mechanics of schistosomes may be an important factor for the specific morphological qualities of an adult male worm, some of which include tegument topography and the strength as well as the nature of its suckers. In addition, the regulation of osmotic and electrochemical gradients of the worms is also control by the tegument. Faghiri and Skelly (2009) revealed that the schistosomes tegument controlled the movement of drug molecules and water into the parasites. This highlighted the role of the tegument in the uptake of drugs and in the osmoregulatory control of the parasite. The tegument also controls the excretion of certain metabolic products like amino acids, lactate, NH_4^+ and H^+ (Skelly *et al.,* 2014; Faghiri *et al.,* 2010).

2.4. Potential Molecular Targets in The Schistosome Tegument

There are several targets which have been identified on the surface of the tegument (Table 2.2). These are essential for engineered drug-loaded nanoparticles to target schistosome glucose transporter 1 (SGTP1) and 4 (SGTP4) as well as acetylcholinesterase (AChE) and a nicotinic type of acetylcholine receptor (nAChR) that are predominantly found on the surface of the male schistosomes tegument. Other major surface proteins found on the tegument that can be targeted include dynein, aquaporins and tetraspanins among others. These molecules located on the surface of the tegument can serve as major molecular targets for the design and development of novel drug molecules and vaccines against the Schistosoma parasite.

Table 2.2: Different potential targets found on the schistosomes tegument for conjugated nanoparticles and their functions

Potential targets	**Functions**	**References**
Schistosome Glucose Transporters	Facilitate the uptake of glucose required for energy production in	Skelly et al., 1994; Skelly *et al.*, 1998; Skelly and

	schistosomes directly from the host bloodstream.	Shoemaker, 2000; Krautz-Peterson *et al.,* 2010; Skelly *et al.,* 2014
Acetylcholinesterase (AChE) and a nicotinic type of acetylcholine receptor (nAChR)	They maintain the schistosomes ion channels and nervous system, and they have glucose scavenging modulatory activity from the mammalian host blood.	[Camacho and Agnew, 1995; MacDonald *et al.,* 2014]
Microtubule liked-proteins (dyneins, actin, tubulin and paramyosin)	Microtube liked-proteins can play a role in schistosomes mobility. Dyneins helps in the attachment and detachment of the adjacent membranous organelles along microtubules. Also, they are implicated in the assembling of spindle which are used for chromosome movement in mitosis.	Braschi et al., 2006; Githui *et al*., 2009; Simanon *et al*., 2019
Aquaporins	They control the flow of water molecules in and out of the schistosomes. Some associates of aquaporins family also helps in metabolites (e.g lactate) diffusion in and out of the cell. In other words, aquaporins control the osmotic regulation of the schistosomes.	Tsukaguchi *et al*., 1998; Tsukaguchi *et al*., 1999; Braschi *et al*., 2006; Gonen and Walz, 2006; Faghiri and Skelly, 2009; Faghiri *et al*., 2010
Tetraspanins	They play an essential role in maintaining the plasma membrane structure of the schistosomes where they interact with one another. Also, interacts with many others, particularly associate proteins such as, integrins, MHC and co-stimulatory molecules to generate a huge signal transduction complexes	Braschi *et al*., 2006; Tran *et al*., 2010; Sotillo *et al*., 2015

	known as tetraspanin-enriched microdomains (TEMs).	
Molecular chaperone (heat shock proteins 70, 16 and 60)	They help the schistosomes to withstand stress by inducing heat shock responses. They may likely also be responsible for the dramatic changes in niche environments of the earlier stages of intra-mammalian schistosomula development.	Braschi *et al.*, 2006; Van Hellemond *et al*., 2006; Sotillo *et al*., 2015; Sotillo *et al*., 2016; Sotillo *et al.*, 2019
Enzymes (Esterases, c arbonic anhydrase, Pho sphodrolases, Thoredo xin peroxidase, Glyceralde hyde-3-phosphate dehydrogen ase, protein disulphide isomerase, Glutathione S-transferase etc.)	Carbonic anhydrase is responsible for the hydration of CO_2 released by schistosomes during respiration. Phosphodrolases facilitate the removal of phosphate groups from organic molecules so that both could enter into the schistosomes via the plasma membrane. All other enzymes found on schistosomes tegument contribute towards the survival of the schistosomes.	Braschi *et al.*, 2006; Van Hellemond *et al.,* 2006; Mulvenna *et al.*, 2010; Sotillo *et al.,* 2015; Sotillo *et al.,* 2016; Sotillo *et al.,* 2019;

2.4.1. Glucose Transporters as a potential molecular Target for nano-delivery systems

Several studies (Skelly *et al.*, 1994; Skelly *et al*., 1998; Skelly and Shoemaker, 2000; Krautz-Peterson *et al*., 2010; Skelly *et al*., 2014) have shown that *Schistosoma* parasites rely on energy (glucose) to survive. Energy (glucose) is consumed by the tegument first and not by the intestinal caecum. Uptake within the tegument is facilitated by the glucose transporters found on the tegument (Skelly *et al*., 1994; Skelly *et al*., 1998). Skelly and co-workers (1994) isolated and characterized three different cDNAs with predicted protein sequences that indicate a high degree of structural and sequence similarity to that of facilitated diffusion transporters in animals, bacteria and plants. It was discovered that two cDNAs encoded for two different glucose transporters in the tegument namely Schistosome Glucose Transporter 1 (SGTP1) and Schistosome Glucose Transporter 4 (SGTP4). In addition, the study described

that the SGTP 1 and 4 genes are expressed in adult and larval female and male schistosomes to facilitate the uptake of glucose from the host. In another related study by Cabezas-Cruz and co-workers (2015) four glucose transporters were encoded in the *Schistosoma mansoni* genome and only two out of the four facilitated glucose diffusion. Their results further proposed that *Schistosoma mansoni* class 1 glucose transporters failed to carry glucose and that this function developed independently in the schistosomes-specific glucose transporter.

There is a dynamic difference from the glucose transport of the platyhelminthes-specific transporters of the schistosomes when compared with humans (Cabezas-Cruz *et al*., 2015). It has been shown that the sequence of SGTP1 and 4 are 60% similar. Zhong and co-workers (1995) used electron microscopy to map the various locations of the transporters on the tegument. They observed that localization of SGTP1 was at the basal lamina and to a lesser extent under the muscle cells. This may help in transporting free glucose inside the tegument into the interstitial fluids that paddle the interior organs of the parasite. It was also demonstrated that SGTP4 was evenly distributed on the dorsal and ventral surfaces of female and male teguments with an extraordinary structure of a double lipid bilayer (Zhong *et al.*, 1995). The distinct location of SGTP4 on the outer tegumental membrane reveals that SGTP4 facilitated glucose transport into the parasite tegument from the host bloodstream (Skelly *et al*., 1998; Skelly and Shoemaker, 2001). In addition, SGTP4 is involved in the development of the free-living cercariae into schistosomula. Through maturation they satisfy the needs of the parasite for high glucose uptake as soon as they enter the host (schistosomula stage) and throughout adulthood (Skelly *et al.*, 1998; Skelly and Shoemaker, 1996).

Thus, proposing SGTP proteins as a potential target for nano-delivery systems, this postulation was supported by Krautz-Peterson and co-workers (2010) where RNAi was used to knock down the upregulation of SGTP4 and SGTP1 genes in schistosomula and in the life stages of adult worms. This study was undertaken to investigate the significance of these proteins to the parasite. Downregulation of either SGTP4 or SGTP1 displayed impairment in the ability of the protein to transport glucose when compared with the control. The study further showed that the simultaneous downregulation of both SGTP1 and SGTP4 reduced the ability of the parasite to transport glucose when compared with a single downregulated SGTP gene. It was also demonstrated that none of the parasites exhibited phenotypic distinction after prolonged incubation of all the suppressed parasites in enriched medium when compared to the control. Finally, it was suggested that SGTP1 and SGTP4 were important for transporting exogenous glucose from the mammalian host for normal parasite development. This was based on the observation that parasites with suppressed SGTPs showed decrease viability *in vivo* after infection of experimental animals (Krautz-Peterson *et al.,* 2010). This notion was

supported by a study performed by McKenzie and co-workers (2017), where the uptake of glucose was regulated in *Schistosoma mansoni* by Akt/Protein kinase B signalling. It was observed that Akt can be triggered by the host L-arginine, more so, insulin was shown to be effective in the layer of adult and schistosomula teguments. The inhibition of Akt decreased the upregulation and development of SGTP4 at the exterior of the host-invading larval stage of the parasite. The suppression of the SGTP4 upregulation at the tegument in adult worms was associated with a decrease in glucose uptake.

Hence, the functionalization of nanoparticles with targeted agents (antibodies, aptamers, antibody-like ligands, peptides and small molecules) with high specificity to SGTP proteins may be a superior alternative to anti-schistosomal treatment to nano-enabled the delivery of anti-schistosomal drugs. In achieving the desired selectivity of drug delivery, nanotechnology has allowed researchers to design nanoparticulate systems and incorporate therapeutic drugs to acts as nanocarriers. This is due to the overexpression of receptor molecules (SGTP proteins) which can serve as docking/interacting sites for targeting potential therapeutic drugs. Theoretically, the therapeutic drugs can be concentrated in a specific site in organ and tissues by functionalizing drug-containing nano-delivery systems with ligands against the receptors. Thus, nano-delivery systems with ligands specific to SGTPs as a receptor can be a potential target for designing, developing and delivering of anti-schistosomal drug.

2.4.2. Acetylcholine (nAChRs), Acetylcholinesterase (AChE) and nicotinic receptors; possible targets for nano-delivery systems

Acetylcholine (ACh) is an essential neurotransmitter, both in invertebrates and vertebrates. The neuromuscular consequences of ACh are normally mediated by postsynaptic nicotinic acetylcholine receptors (nAChRs) due to their high-affinity for nicotine. Based on the structure of nAChRs, they belong to the Cys-loop ligand-gated ion channel (LGIC) superfamily (Albuquerque *et al.*, 2009; MacDonald *et al.*, 2014). nAChRs generate hetero and homo-pentameric structures that are arranged in a barrel shape around a central ion-selective hole. nAChRs in invertebrates are anion and cation-selective (Cl_2) ACh-gated channels while in vertebrates nAChRs are cation-selective (Ca^{2+}, Na^{+}, K^{+}) and facilitate excitatory responses.

Both the nicotinic type of the acetylcholine receptor (nAChR) and acetylcholinesterase (AChE) are potential target for nano-enabled drug delivery system, because they are both found on the exterior surface of the tegument where they play an essential role in the schistosomes ion channels and nervous system (Mansour and Mansour, 2002; MacDonald *et al.*, 2014). AChE and nAChR are predominantly found on the surface of adult male schistosomes. The adult

female schistosomes usually lodges in the gynaecophoral canal of the male containing a lower number of these proteins. AChE has been shown to have glucose scavenging modulatory activity from the human host bloodstream. The uptake of glucose is controlled by the interaction of ACh with the nAChR and AChE on the surface of the tegument (Camacho and Agnew, 1995). It has also been discovered that the exposure of low concentrations of ACh to *S. haematobium* or *S. bovis* and not *S. mansoni* improved the uptake of the glucose by the parasites in the host blood. At higher concentrations of ACh, the uptake of glucose in the host by parasites was inhibited. This specificity between the nicotinic receptor and ACh was supported by showing the effect of α-bungarotoxin and d-tubocurarine as antagonists to ACh. Therefore, it is significant when instituting a nanotechnology approach to deliver antagonistic drug molecules to the binding sites of nAChR and AChE in order to inhibit their glucose scavenging activities from the host bloodstream.

2.4.3. Dyneins as a possible molecular Targets for nano-delivery systems

Dyneins is a protein that produces force and movement on microtubules for biological processes such as ciliary beating, intracellular transportation and cell division, it performs these functions through the help of ATP hydrolysis (Roberts *et al.*, 2013). Dyneins could serve as a possible target for nano-delivery system in the treatment of schistosomiasis owing to its biological function in the survival of the parasite. Several studies have employed immunostaining to identify various microtubule related proteins inside the schistosomes tegument such as actin, tubulin, paramyosin and dyneins. Studies have suggested that cytoplasmic dyneins may have a role to play in transporting of vesicles to the surface bilayers and tegument cytoplasm from the sub-tegumental cells. Dynein chains are part of a huge enzyme complex comprising heavy, intermediate and light chains. Dyneins are implicated in the assembly of spindles that are used for chromosome movement in mitosis. The upregulation of dyneins are involved in the developmental of *S. mansoni.* In addition, they are found in the schistosomula stage that occurs after the penetration of the intact skin of the host by the parasite and at the lung stage in adult worms. At this stage, early upregulation of the heptalaminate exterior membranes are exhibited. Meanwhile, dynein light chains are not found in the cercariae or ciliated miracidia (Hoffmann and Strand, 1996).

The dynein light chain protein discovered recently was shown to have high affinity to other proteins tegument with which they form highly complex associations. Another dynein light chain protein has been considered as a tegument antigen with the molecular weight of 20.8 kDa. In (2009), Githui *el al*., investigated the normal motor constituents of vesicular transport present in the schistosomes tegument. The NCBI database blast search analysis recognized

clones that are myosin and dynein light chains genes. After subjecting the genes of schistosome dynein to further analysis in the databases, they detected three dynein light chains families. They also observed that the Tctex family sequences of the dynein light chains are different significantly when compare to the mammalian homologs, Hence, could serve as probable drug/vaccine target against schistosomes infection. The three dynein light chains, *S. japonicum* dynein light chain-1*, S. mansoni* dynein light chain and SM10 studied via the immunolocalization of microtubule-related motor protein components show a specific and strong immunolocalization in the distal cytoplasm of the tegument (Kohlstädt *et al*., 1997; Yang *et al*., 1999). The tegument-associated protein of the *S. japonicum* which has 22.6 kDa displays similar localization arrangements (Li *et al*., 2000). In view of these aforementioned roles of dyneins in schistosomes survival, the delivery of targeted drug to localize and bind to dynein using nanotechnology approach will be a potential technique in eradicating schistosomiasis. Nanotechnology-based targeted delivery system functionalized with specific targeted molecules (antibodies, peptides, antibody-like molecule and aptamer) can recognise and selectively bind onto the dynein protein (receptors) on its active region thereby conferring targeted delivery.

2.4.4. Aquaporins as a potential molecular Targets for nano-delivery systems

Aquaporins is another promising target for the delivery of surface-engineered drug-loaded nanoparticles. They are small integral membrane proteins that are mostly upregulated in animal and plant kingdoms. Aquaporins consist of two short and six transmembrane helical segments that enclose cytoplasmic and extracellular vestibules linked by a narrow aqueous pore. They consist of several conserved motifs, and aquaporin monomers are assembled as tetramers in membranes, with every monomer working independently (Verkman, 2013). Aquaporins act as channels to selectively control the influx and efflux of water molecules within cells. Certain aquaporins allow the diffusion of metabolites in and out of the cell (Gonen and Walz, 2006; Tsukaguchi *et al*., 1998; Tsukaguchi *et al.*, 1999).

The nano-enabling drug delivery activity of aquaporins was corroborated by Braschi and co-workers (2006) where a proteomic study of the schistosome tegument was described. The presence of aquaporins was revealed on the surface of the tegument which indicated that aquaporins assisted with the influx of water and solutes within the plasma membrane of the schistosomes. The tegument (*S. mansoni*) as an excretory organ was investigated by Faghiri and co-workers (2010), where they observed that aquaporins on the surface of the tegument acted as a lactate transporter. In addition, it was also shown that the aquaporin found on the tegument was competent in transporting mannitol, water, alanine and fructose, but not

glucose. Their further analysis of the tegument using immunofluorescent and immune-EM suggested that the function of the tegument was far above the known ability as an organ of nutrient uptake, but rather, it also helped in excretion of waste metabolites (Faghiri *et al.*, 2010). The study supported the notion that the tegument controlled the osmoregulation and drug uptake in parasites (Faghiri and Skelly, 2009). It was also shown that the existence of aquaporins on the tegument controlled the movement of water following the suppression of *S. mansoni* aquaporins with iRNAs (Faghiri and Skelly, 2009).

It has also been shown that aquaporin-4 (a homologue of aquaporins) enhanced the granulomatous response with an increase in the accumulation of macrophages and eosinophils around the *S. japonicum* eggs in the liver of the mice model. Similarly, the study showed that aquaporin-4 mice enhanced T-helper 2 cells (Th2), but decreased T-helper 1 cells (Th1) and Treg cell formation in *S. japonicum.*, This accounts for the improvements of the liver granuloma formation (Zhang *et al*., 2015). These findings collectively indicate that aquaporins may be a desirable target for anti-schistosomal therapy using high precision delivery of drug-loaded nanostructures.

2.4.5. Tetraspanins as a potential molecular Target for nano-delivery systems

Tetraspanins (TSPs) is a family of integral membrane proteins expressed by schistosomes, found in the exterior surface of the membrane of the schistosomes tegument. Braschi and co-workers (2006) identified five tetraspanins in the schistosomes membrane surface, and the abundant components of these proteins are found in the tegument periphery. They speculated that the schistosome tetraspanins play an important role in the structure of the schistosomes plasma membrane, based on their analogy with other organisms (Braschi *et al*., 2006). They also showed that, some tetraspanins are recognized more readily than others, and the concentrations and locations of only three biotinylated are suggested to vary within the surface of schistosomes tegument. The capacity of tetraspanins homologous interaction to generate a tetraspanin web may help scaffold organisation in the lipid bilayer upon which there are assemblage of other proteins within the tegument. More so, the extracellular loops of the tetraspanins may provide platforms for gylcans and proteins which interact with the membranocalyx (Braschi *et al*., 2006).

The functions of tetraspanins in the tegument of *S. mansoni* was investigated with the inhibition of the upregulation of Sm-tsp-1 and Sm-tsp-2 mRNAs using RNA. The ultrastructural morphology of mature schistosomes treated with Sm-tsp-2 dsRNA, show a thinner tegument and there is a visible formation of vacuoles on the schistosomes tegument. More so,

schistosomula exposed to Sm-tsp-2 dsRNA showed a drastic thinner and extensive vacuolated tegument, and this morphological observation depends on failure of tegumentary invaginations (Tran *et al*., 2010). In another related study by Sotillo *et al* (2015), it was reported that tetraspanins were found in biotinylated and unbound tegument tissues. It was also reported that tetraspanin-2 found in *S. mansoni* is essential for the formation of the schistosomes tegument and is a target of protective immunity in naturally resistant human and vaccinated mice. On the other hand, *S. mansoni* tetraspanin-1 are detected on the apical membrane of schistosomula. Tetraspanin-2 was found only in the unbound sample, which corroborates with other findings, which shows that the localisation of tetraspanin-2 within the inner compartments of the schistosomes; relates with the exterior invaginations and vesicles in the tegument (Sotillo *et al.*, 2015). Targeted nanocarriers has three main components that is; as a targeting moiety-penetration enhancer, an apoptosis-inducing agent and also, as a carrier. Therefore, the inhibition of tetraspanin by the means of nanotechnology-based approach will stop the interaction of glycans and proteins to the schistosomes membranocalyx, because, nanomaterials can preferentially accumulate in the parasite via tetraspanin in an active targeting mechanism thereby, release the encapsulated drugs in a regulated manner. This will provide the benefits of increasing the anti-schistosomal drug concentration and its therapeutic efficacy.

2.4.6. Other Potential Molecular Targets for nano-delivery systems

Several studies have used proteomic in identifying constituents found within the tegument of schistosomes which potential targets for nano-delivery systems are. Braschi and co-workers (2006) used proteomics to detect molecules found within the S. mansoni tegument. In their study, they identified transporters for sugars, inorganic ions, amino acids and water, which indicated that the tegument plasma membrane was crucial for schistosomes to acquire nutrients from the host and help maintain solute levels. They also identified enzymes such as esterases, phosphohydrolases and carbonic anhydrase with their catalytic domains found in the outer core of the plasma membrane, more so, annexin, five tetraspanins and dysferlin were shown to play a pivotal role in the architecture of the membrane. The study was corroborated by another proteomic analysis of S. mansoni proteins that was performed in the same year by Braschi and co-workers (2006) not less than fifty-one (51) proteins were identified based on homology with known proteins in other organisms. Some of the identified proteins were enolase which involves energy metabolism; several cytoskeletal and molecular motor proteins such as severin, actin and dynein light chains. Others include molecular chaperone heat shock proteins 17, 19 and 20, calmodulin; vesicle proteins, and plasma membrane transporters; mitochondrial proteins for example ATP synthase; structural

molecules and enzymes such as glucose transporter protein, calcium ATPase, annexin, alkaline phosphatase and tetraspanins A, B, and C (Braschi *et al.*, 2006).

As shown in figure 2.4, Sotillo and co-workers (2015) used the same approach to detect novel therapeutic targets for nanocarriers in S. mansoni schistosomula. Over 450 proteins were detected on the apical membrane of S. mansoni schistosomula, in which the expression of 200 have significant controlled profiles at diverse stages of schistosomula development in vitro which are potential targets for nano-delivery systems, such as glucose transporters, heat shock proteins, sterols, antioxidant enzymes and peptidases. In addition, current vaccine antigens were also detected on the apical membrane such as calpain, Sm-TSP-1 or Sm-TSP-2, Sm29 found on sub-tegumental fractions of the schistosomula showing localization patterns that differ in some instances from those found on the adult stage of the worm. Another study used S. mansoni genome project, concurrently with proteomic and lipidomic approaches, which allowed the study to characterize the lipids and proteins within the tegument plasma membrane in details. This study detected some tegumental targeted proteins and lipids, which depicts the role of the tegument in the uptake of nutrients from the host, and in the evasion of immune response. Furthermore, the study demonstrated that the tegument of the worm is enriched in lipids which are not found in the host. Similarly, the schistosome tegument possess proteins which have no sequence similarity with any other sequence found in databases of species excepts in schistosomes (Van Hellemond *et al*., 2006). Several other studies (Pérez-Sánchez *et al*., 2006; Liu *et al*., 2006; Mulvenna *et al*., 2010; Castro-Borges *et al*., 2011; Sotillo *et al*., 2016; Sotillo *et al*., 2019) have employed proteomics technique in identification of several molecular receptors which are druggable and vaccine candidates for schistosomiasis treatment.

Up to date, there are no effective vaccine for schistosomiasis. Although, several potential promising vaccine candidates for *S. mansoni* and, to a lesser extent, *S. haematobium* have been discovered and published in literatures, only one vaccine, namely, BILHVAX, or the 28-kDa GST from *S. haematobium*, has entered clinical trials (Capron *et al.,* 2005). Unfortunately, published data are not available on the clinical efficacy of this vaccine, but nonetheless, it is disappointing that other vaccines have not progressed to this stage. More so, there are several nanotechnology approaches in developing vaccine for schistosomiasis published in the literature, but have not entered clinical trials, some of which include oral vaccination with chitosan nanoparticles loaded with plasmid DNA encoding a Rho1-CTPase protein of *S. mansoni* (Oliveira *et al*., 2012). Another approach includes a novel nanoparticle formulation of the Sj26GST DNA vaccine; although there was no significant reduction in worm burden, a

highly significant decline in tissue egg burden and the fecundity of female adult worms was reported (Mbanefo *et al.,* 2015).

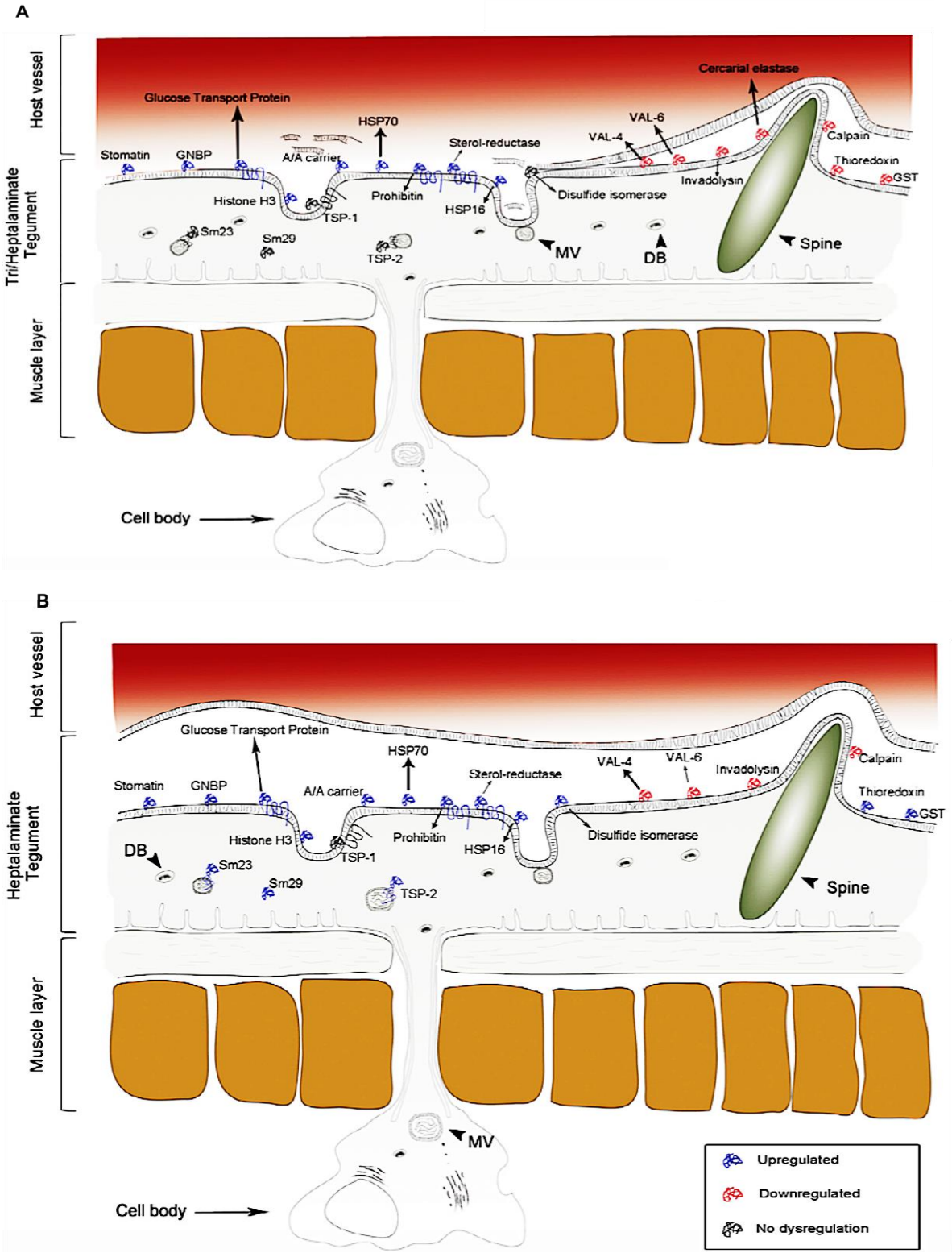

Figure 2.4: Proteome identification of upregulated, downregulated and no dysregulation proteins found on the tegument of S. mansoni (schistosomula). The dysregulation of these

proteins changes over time. (a) 3 hours of infection and (b) 5 days of infection (reprinted with permission from Sotillo *et al*., 2015).

2.5. An overview of nano-delivery system

Nanomedicine is the application of nanotechnology for treatment, prevention, monitoring, and control of biological diseases. In applying nanomedicine in the treatment of diseases, the precise targets (cells and/or receptors) specific to the clinical disease is identified and the suitable nanoparticles for delivery system to minimize the side effects and improve the efficacy of the original drug is selected. One of these precise targets are macrophages, endothelial, proteins, dendritic cells as well as tumour cells. Some typical examples of nano-delivery systems (Fig. 2.5) used over the years in the treatment of diseases includes; liposomes, micelles, dendrimer, polymeric nanoparticles, polymeric micelles, metallic nanoparticles, nanotubes and nanocrystals.

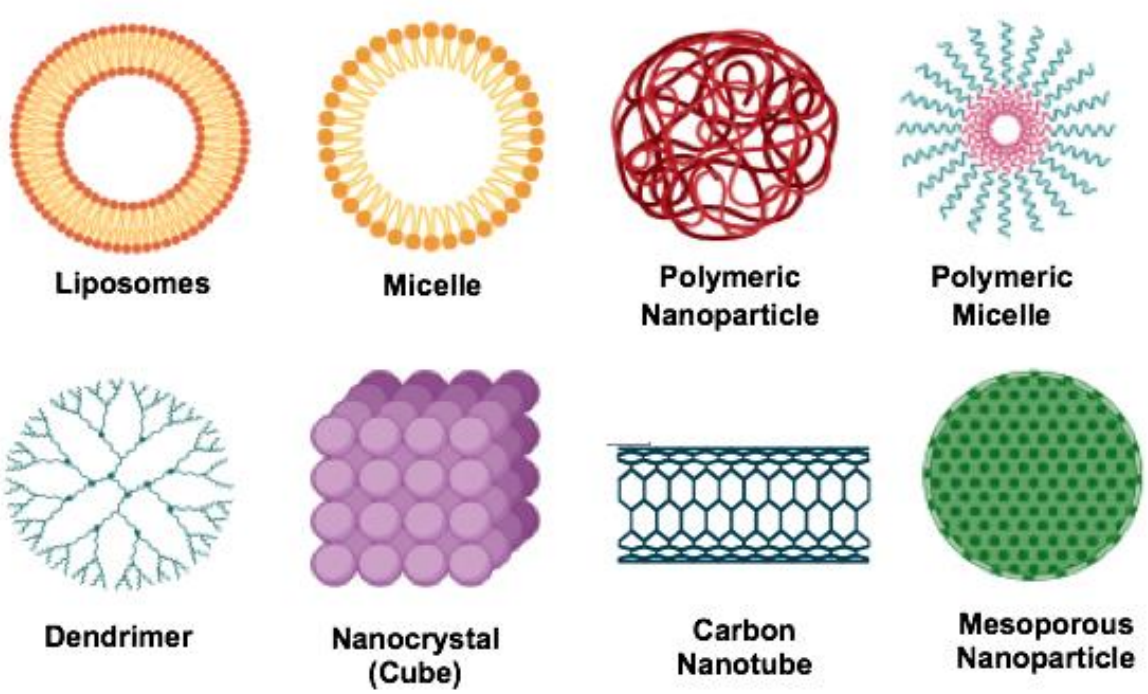

Figure 2.5: Types of nanocarriers for drug delivery

Morphological characteristics such as rigidity, size and aspect ratio play a vital role in, and affect the impact and fate of nanocarrier properties *in vivo* (Wang *et al*., 2017). The properties of nano-delivery systems are critically dependent on the morphological characteristics of the particle, and it is of importance to deliver drug into a specific site during the treatment of disease such as the delivery of antitumour drug into the site of solid tumour (Wang *et al.*,

2017). The characterization of the nanoparticles morphology and dimensions can be determined using scanning electron microscopy (SEM), transmission electron microscopy (TEM), and atomic force microscopy (AFM). Although, the most appropriate technique depends on the sample type and the desired information to be measured and in some cases, researchers usually adopt techniques which are available and well-known to them in characterize the dimensions of nanoparticles. A typical example of TEM, SEM and AFM of nanoparticle are shown in figure 2.6.

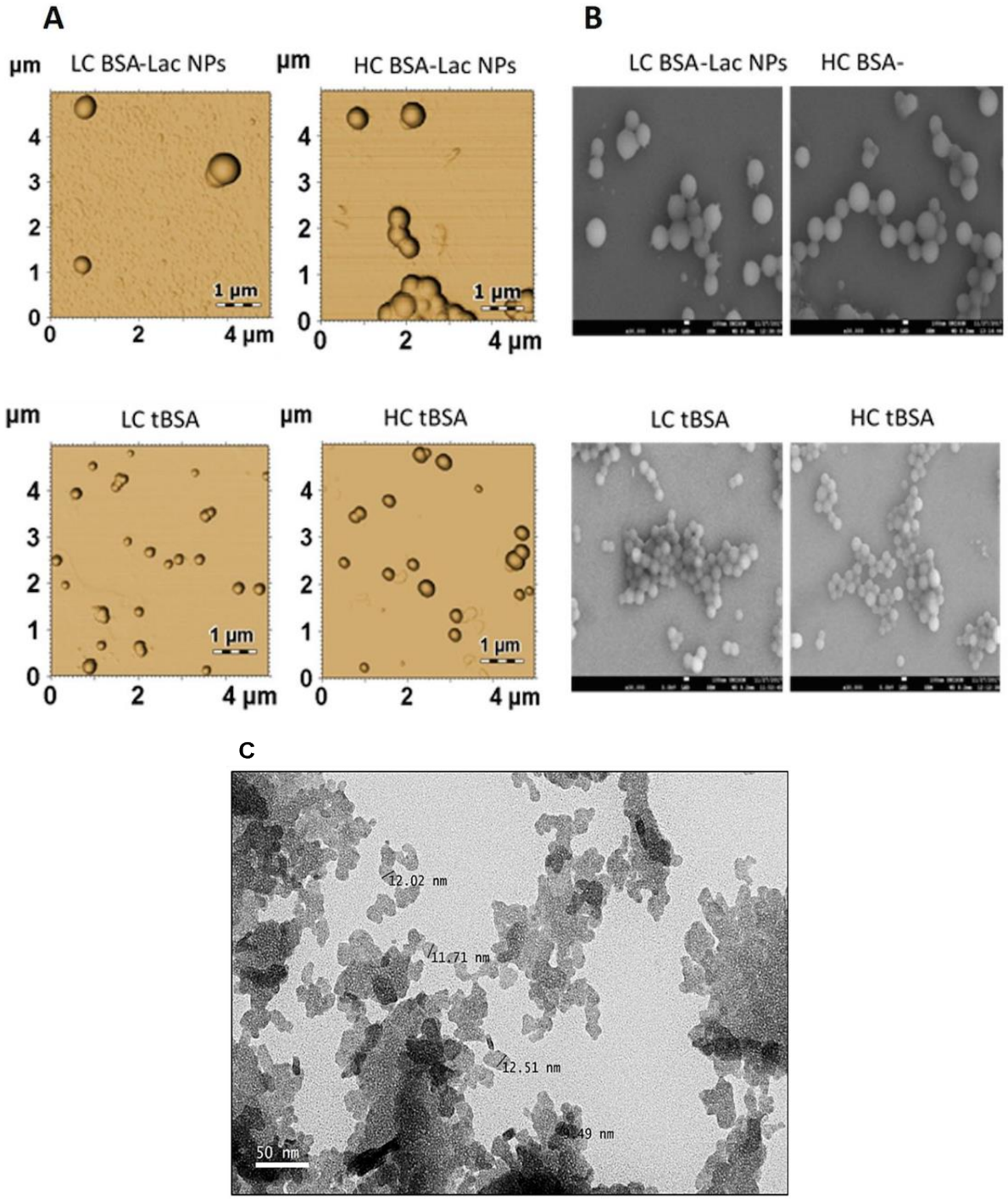

Figure 2.6: Morphology of HC and LC BSA-Lac and tBSA NPs (A) atomic force microscopy (AFM) and (B) scanning electron microscopy (SEM). (C) Transmission electron microscopy (TEM) image of Citral-loaded self nano-emulsifying drug delivery system (CIT-SNEDDS). Adapted from Teran-Saavedra *et al*., 2019; Izham *et al.,* 2019.

Several studies have explored the use of nano-delivery system in improving the therapeutic efficacy of different drug molecules in the treatment of diseases. Mehrizi and co-workers (2018), carried out the synthesis of a novel nanosized chitosan-betulinic acid against resistant Leishmania major, the first clinical observation of this parasite in the kidney. It was discovered that chitosan nanoparticle synthezised using phase separation and drug loading by phase separation improved the therapeutic dose of betulinic acid to 20 mg/kg. More so, the successful improvement in the use of nanosystem loaded betulinic acid in the treatment of leishmania major both in *in vitro* and *in vivo* studies was observed (Mehrizi *et al*., 2018). The effectiveness of ivermectin (IVM) was investigated using nanostructured lipid carriers in the treatment of hydatidosis, and some limitations and resistance associated with the drug was overcome by the carriers in an *in vitro* experiment. It was observed that NLCs-loaded IVM induced higher mRNA caspase-3 expression which suggested a more potent apoptotic effect on the parasite (Ahmadpour *et al.,* 2019). In another related study, nucleoside-lipid-based nanocarriers was used to encapsulated methylene blue (MB); a positively charged tricyclic phenothiazine molecule used in malaria treatment. This approach showed that the nanoparticles partially protected MB from oxido-reduction reactions, thereby preventing early degradation during storage, and the carrier also prolonged pharmacokinetics in plasma. It was concluded that this approach is an interesting technique in improving MB stability and delivery in malaria treatment (Kowouvi *et al*., 2019).

Hence, utilization of lipid nanoparticle-based drugs in the treatment of schistosomiasis will be beneficiary in terms of cost since solid lipid nanoparticles are easy to scale-up and involve low cost of production, relative nontoxic nature, biodegradable composition and stability against aggregation. More so, lipid-based formulations have the ability to enhance the bioavailability of drugs through solubility modification and the rate at which drugs can be released for the improvement and enhancement of drug absorption across biological barriers (Cheng *et el.,* 2017), and to reduce side-effects associated with drugs. This type of approach will be potent and effective in treating all forms of schistosomes (both mature and immature) by functionalizing the nanoparticles with targeted molecules which has ability to recognize and bind to molecular receptors present in all forms of schistosomes. Thus, preventing reinfection by specifically target all overexpressed schistosomes antigens present in the human host, and it has also been reported that nanoparticles have ability to induce heightened T cell immunity, which can prevent disease reactivation and reinfection (Tousif *et al*., 2017). The list of some

nano-delivery systems used in improving the therapeutic efficacy of PZQ in the treatment of *Schistosoma* infection reported in the literature is shown in Table 2.3.

Table 2.3: List of some nano-delivery systems which have been used in improving the therapeutic efficacy of PZQ in treating Schistosoma infection

S/N	Test Nanoparticles	Test *Schistosoma* species	Efficacy	References
1	PZQ-Liposomes	*S. mansoni*	Lip.PZQ causes a great significant reduction in the number of worm count, eggs/gram liver tissue and intestine. The nanosystem also reduced the number and diameter of hepatic granuloma in the histopathological studies.	Labib El Gendy *et al*., 2019
2	SLN-PZQ	*S. mansoni*	SLN-PZQ enhanced the bioavailability and antischistosomal efficacy against *S. mansoni* and reduced both the hepatic and intestinal tissue egg loads. In addition, the SLN-PZQ approximately cause complete disappearance on immature deposited eggs.	Radwan *et al*., 2019
3	Lipid nanocapsules (LNCs)-PZQ	*S. mansoni*	Oral LNCs-PZQ enhanced the efficacy of PZQ by targeting the distal postabsorption sites	Amara *et al.*, 2018
4	Gold nanoparticles	*S. mansoni*	Gold NP showed to regulate gene expression impaired by *S. mansoni* infection	Dkhil *et al.,* 2016
5	PZQ-Liposomes combined with	*S. mansoni*	100 mg/kg concentration of lip.PZQ + HBO was more effective (48.0% reduction of	Frezza *et al.,* 2015

	hyperbaric oxygen therapy (HBO)		worms, 83.3% reduction of eggs/gram of feces) and 100% of the mice had altered of oograms; indicating interruption of oviposition. Additionally, HBO was able to stimulate the immune system, hence, HBO can work as an adjuvant in the treatment of the infection.	
6	PZQ-Liposomes	*S. mansoni*	There is improvement in the efficacy of the treatment with lip.PZQ, especially when administered 45 days following infection. More so, lip.PZQ is better absorbed by the tegument of *S. mansoni*, which has an affinity for phospholipids	Frezza *et al.,* 2013
7	PZQ-Liposomes	*S. mansoni*	PZQ-liposomes caused a decrease in amounts of eggs and parasites. Liposomes improve the antischistosomal activity of praziquantel.	Mourão *et al.,* 2005

2.6. Targeted Nano-Enabled Drug Delivery

Targeted nano-enabled therapies are able to recognize or detect molecules that are highly expressed on the surface of specific cells. This approach has gained popularity in treating various cancers due to the overexpression of specific receptors on the membrane surface of cancer cells. In the field of cancer, targeted nanotherapies inhibit particular cell surface proteins or genes which are responsible for cancer growth and metastasis. It has been hypothesized that targeted nanotherapies may be desirable over other forms of treatment (Joo *et al.,* 2013; Camidge, 2014). According to a 2018 review published by the American Cancer Society (ACS), targeted nanotherapies have been approved for various anti-cancer therapies. Thus, employing a nanotherapeutic approach to target overexpressed proteins or genes on

the surface of the schistosome tegument will assist in overcoming PZQ resistant, reduce the burden of immature schistosomes (schistosomula), and finally, put an end to the morbidity and mortality of schistosomiasis (Fig. 2.7)**.** More so, this approach and can be employed in the treatment of various parasitic infections. Although, there are no report of targeted nano-enabled drug delivery against Schistosoma species yet. Nevertheless, there are few reports of this type of approach on other similar parasite such as; the preparation of the primaquine-containing liposomes functionalized with covalently bound heparin for the targeted delivery of antimalarial drugs to *Plasmodium*-infected red blood cells (pRBCs). Heparin covalently linked with targeted nano-enabled drug delivery to pRBCs was carried out to reduce anticoagulation risks. The study showed that heparin-based targeting can be predictably more long-lasting than pRBC recognition relying on antibodies, which typically are raised against highly variable exposed antigens whose expression is constantly modified by successive generations of the parasite (Marques *et al.,* 2017). Also, targeted nano-enabled drug delivery of a 19-amino peptide from the circumsporozoite protein of *Plasmodium berghei* which contained a conserved region I as well as a consensus heparin sulfate proteoglycan-binding sequence attached to the distal end of a lipid-polyethylene glycol bioconjugated, was prepared by incorporation into phosphatidylcholine liposomes (Longmuir *et al.,* 2006). Jain and co-workers (2014) developed chitosan-assisted immunotherapy for the intervention of experimental leishmaniasis via amphotericin B -SLPs to activate the macrophages in order to impart a specific immune response by improving the production of TNF-α and IL-12 (Jain *et al*., 2014).

2.6.1. Antibody-functionalized drug delivery systems for targeted therapy in schistosomes infection

Antibodies are mostly immunoglobulins (IgGs) or their fragments and have ability to recognize and interact virtually with any molecular target with high affinity and high specificity. Antibodies have gained special interest in targeted therapies due to their nanosized. They are biological materials which are part of the specific immune system, and they are toxin or pathogens neutralizers in nature. They help in recruitments of immune elements such as; improving phagocytosis, complement, cytotoxicity antibody dependent by natural killer (NK) cells. They can also help in carrying several elements such as; toxins, nanoparticles, drugs and fluorochroms to where they can be used in therapy to destroy a specific target, and for several other diagnostic procedures (Arruebo *et al*., 2009). Antibody-functionalized nanoparticulate systems are more site-specific, causing higher accumulation on the target region and subsequently, reducing dosage requirements.

The bioconjugation of antibodies with nanoparticles to generate a unique product which is composed of both the properties of the antibodies and nanoparticles can take place by

adsorption process that is, at the isoelectrical point of the antibody through electrostatic interaction (Arruebo *et al.,* 2009; Greene *et al.,* 2018). More so, the conjugation can take place by direct covalent bonding between the surface of the antibody and the nanoparticles (that is, coupling of the antibodies to nanoparticles by free carboxyl or amine functionalities on aspartic/glutamic acid or lysine residues or by thio-maleimide reaction) (Arruebo *et al.,* 2009). Another means by which the bioconjugation of the antibodies to the nanoparticles can be achieved is through the use of adapter molecules that is, bio-recognitions like streptavidin and biotin, which usually involves the formation of the complex. Greene and co-workers (2018), developed a novel approach for the site-specific conjugation of nanoparticulate systems which promotes the uniform and outward projection of paratopes for utmost target interaction. They demonstrated a successful re-bridging of the inter-chain disulphide linkage with a heterobifunctional linker and successive coupling to nanoparticles bearing complementary azide moieties in TRAZ F(ab) model. The administration of the antimalarial drug (chloroquine) loaded liposomes targeted to infected RBCs with a tagged antibody against infected erythrocytes surface antigens on the chloroquine liposomes against drug-resistant *Plasmodium berghei*, presented a cure rate of 75% to 90% on days 4 to 6 post infection in mice (Mohammad *et al*., 1995).

Secret and co-workers (2013), described the preparation of antibody-functionalized biodegradable porous silicon nanoparticles loaded with the hydrophobic anticancer drug camptothecin. Using a novel semicarbazide based bioconjugation technique in chemistry, the specific orientation of the immobilized antibody on the nanoparticles was achieved. Three antibodies mAb528 a monoclonal antibody to EGFR; MLR2 a monoclonal antibody to p75NTR and Rituximab a monoclonal antibody to CD20 were used to target glioblastoma, neuroblastoma and B lymphoma cells, respectively in an *in vitro* study. The successful targeting was demonstrated by means of immunocytochemistry and flow cytometry both with cell lines and primary cells. The incubation of the antibody-functionalized nanoparticles with the cell lines for cell viability, showed selective killing of cells expressing the receptor, which correspond to the antibody coupled on the porous silicon nanoparticles. Also, the incorporation of camptothecin an anticancer drug into a nanoparticle functionalized with the antibodies showed to be very effective and efficient in targeting and killing cancer cells (Secret *et al.*, 2013). In another recent study by Li and colleagues in (2019), they developed an antibody-functionalized gold nanoparticle (cetuximab-AuNP) to selectively target cancer cells and probe for their potential radiosensitizing impacts under proton irradiation. It was discovered that cetuximab-AuNP interacts and bound specifically and accumulate in EGRF-overexpressing A431 cells when compared with EGFR-negative MDA-MB-453 cells. It was further shown that, cetuximab-AuNP improved the influence of proton irradiation in A431 cells but not in MDA-

MB453 cells (Li *et al*., 2019). There are several other studies (Day *et al.,* 2010; Dai *et al*., 2015; Korkmaz *et al*., 2016) which have employed antibody-functionalized nanoparticles to selectively target some specific receptors on the cancer cells either for treatments or imaging (diagnostics).

2.6.2. Aptamer-functionalized drug delivery system for targeted therapy in schistosomes infection

Aptamers are short single-stranded oligonucleotide (RNA or DNA ligands) or peptides that bind to their target molecules; either small chemicals, large molecular cell-surface or transmembrane proteins with high specificity, affinity and versatility. They have been developed for over two decades against several targets and for different applications. Aptamers have emerged as promising molecules to target specific cancer antigens in therapy and clinical diagnosis (Cerchia and De Franciscis, 2010; Catuogno *et al*., 2016). Nucleic acid aptamers have gained attention as an attractive molecular vehicle because of their ability to bind to specific ligands with high affinity, they have high ability to penetrate cells, tissues and organs, and they also possess high chemical flexibility (Catuogno *et al*., 2016). Whereas, peptide aptamers, otherwise known as affimers are small stable proteins that are selected to interact and attach with high binding affinity to specific sites (surface) on their target molecules. They contain short amino acid of about 5 to 20 residues long sequences which are normally embedded as a loop inside a stable protein scaffold (Reverdatto *et al*., 2015). Aptamer based sensing platforms for the recognition of peptides, small molecules, proteins and cells have gained a huge interest due to their high sensitivity and selectivity. In general, aptamers are molecules that can generate unique 3-dimentional structure and has the ability to bind almost any molecular targets with higher binding affinity in the nanomolar level compared to monoclonal or polyclonal antibody.

Due to aptamers properties such as; high affinity, chemical stability, small size, ease of synthesis, low-immunogenicity and controllable chemical modification. Owing to these multiple attributes, aptamer conjugated nanoparticles are well qualified nanosystems for the development of biomedical devices for imaging, analytical, drug delivery and some other medical applications. The bioconjugation of the aptamers onto the nanoparticulate systems can be attained via noncovalent (affinities interaction e.g streptavidin-biotin or metal ion co-ordination). Also, the bioconjugation can be achieved through covalent (1-ethyl-3-carbodiimide or succinimdyl ester-amine chemistry and N-hydroxysuccinimide activation chemistry which cross link the carboxylic acid group on the surface of the nanoparticles and the amino group of the ligands) interactions. The covalent interaction strategies can also be

achieved by maleimide-thiol chemistry that is, the cross linking of the thiol group on the targeting moiety and the maleimide functional group on the surface of the nanoparticulate systems.

Yu and co-workers (2011), developed a novel aptamer bioconjugated nanoparticles in order to enhance the delivery of paclitaxel anticancer drug to MUC1-positive cancer cells. The aptamer was engineered into the surface of the nanoparticles via a DNA spacer. The flow cytometry analysis shown the higher uptake of the nanoparticulate systems conjugated with MUC1 specific aptamer into the target cells via the overexpression of MUC1. The results further showed that, paclitaxel loaded aptamer functionalized nanoparticles improved the *in vitro* drug delivery and cytotoxicity to MUC1 cancerous cells when compared to non-targeted nanoparticulate systems which lack the MUC1 aptamer. In (2013), Yang and co-workers developed a DNA aptamer envelope protein for the inhibition of hepatitis C virus. In their study, it was shown that selected aptamers for E1E2 particularly recognized the recombinant E1E2 protein and E1E2 protein from hepatitis C virus-infected cells. The aptamers exert antiviral properties via the inhibition of the virus binding to the host cell (Yang *et al*., 2013). Several other studies (Mathieu *et al*., 2016; Corda *et al*., 2018; Dou *et al*., 2018; Tan *et al*., 2019) have employed aptamer-conjugate as a targeted delivery system for therapeutics and diagnostics.

2.6.3. Other functionalized drug delivery systems for targeted therapy in schistosomes infection

Other small molecules or peptides that are highly specific for certain molecular receptors with high affinity, can also be screened or developed in order to localize and bind with the molecular receptors found on the tegument of the schistosomes. Lei and co-workers (2019), designed a novel alendronate-modified nanoparticle loaded with paclitaxel and coated with polydopamine for osteosarcoma-targeted therapy. In this study, it was reported that the polymerization of dopamine in a versatile modification method was not limited by the absence of functional groups on the surfaces of the compound and do not affect the chemical properties. The successful bioconjugation of the polydopamine with nanoparticles with a surface modifier which consist of a precise affinity for osteosarcoma cells was attained. They posit further that, the targeting nano-delivery systems exhibited a higher *in vitro* cytotoxicity on K7M2 of osteosarcoma cells when compared with the native nanosystems. Furthermore, the *in vivo* study showed that the targeting nano-delivery systems could accumulate within the tumour to a greater extent with remarkable decrease in the adverse effects of paclitaxel when compared with nontargeted nanosystems (Lei *et al*., 2019).

Saalik *et al* (2019), investigated the effect of a novel penetrating peptide-guided nanoparticles that targets cell surface LinTT1, p32 for glioblastoma targeting. In this study, the coupling of LinTT1 to albumin-paclitaxel nano-delivery systems was achieved by sulfosuccinimidyl 4-(N-maleimidomethyl) cyclohexane-1-carboxylate as a linker. They demonstrated that the novel p32 targeting peptide, LinTT1 promotes the targeted accumulation of nanoparticles to tumours across a panel of high-grade glioma mouse model effectively. They further showed that the treatment of mice with LinTT1-guided nanoparticles extend the survival rate of mice with the tumour; due to the ability of LinTT1-nanopaticles to recognise the upregulation of p32 on glioblastoma (Saalik *et al.*, 2019).

Ahlschwede and co-workers (2019), employed targeted nano-delivery approach in treating cerebral amyloid angiopathy and detecting cerebrovascular amyloid observed in Alzheimer's disease. A targeted nano-delivery system was developed by a cationic blood brain barrier penetrating peptide using a covalent bioconjugation technique. The results from the targeted nanosystem depicted a higher significant brain uptake due to the high binding affinity of the peptide (K16ApoE)-nano-delivery system to amyloid plaques. In another study carried out by Colombo and co-workers (2019) where the targeted biodegradable nano-delivery system for CD34+ endothelial precursors in the treatment of rheumatoid arthritis was achieved. The bioconjugation of the targeting molecule was activated by N-hydroxysuccinimide in order to exploit its primary amino groups. The results in this study showed that, the targeted nano-delivery system possess a greater advantage in delivery the drug to inflamed synovia via the synovium-homing peptide as a targeting molecular receptor.

Silva and colleague (2015) carried out mannose-functionalized polymeric nanoparticles to target the mannose receptors on antigen-presenting cells and therapeutic anti-tumor immune responses in a melanoma model. It was discovered that mannose-functionalized nanoparticles potentiated the Th1 immune activity, and the nanoparticulated vaccines reduced the rate of murine B16F10 melanoma tumors growth in prophylactic and therapeutic settings Silva *et al*., 2015). Also, Mufamadi and co-workers (2013) carried out a ligand-functionalized nanoliposomes for targeted delivery of galantamine in Alzheimer's Disease (AD). It was shown that ligand-functionalized nanoliposomes enhanced the uptake of galantamine into PC12 neuronal cells through the receptor of Serpin Enzyme Complex (Mufamadi *et al.*, 2013). Ruff *et al* (2017) investigated the effect of gold nanoparticles surface engineered with amyloidogenic β-amyloid specific peptides in a Blood-Brain Barrier (BBB) in an *in vitro* model. This study was carried out in order to increase the BBB permeability, as well as the nanoparticle concentration in the brain by the peptides. It was discovered that, the multivalent peptides bind selectively to Aβ-amyloid fibrils, thereby posing a strongly effect on the integrity

of BBB, thus, actively cause the transport of the gold nanoparticle conjugates via the Blood-Brain Barrier.

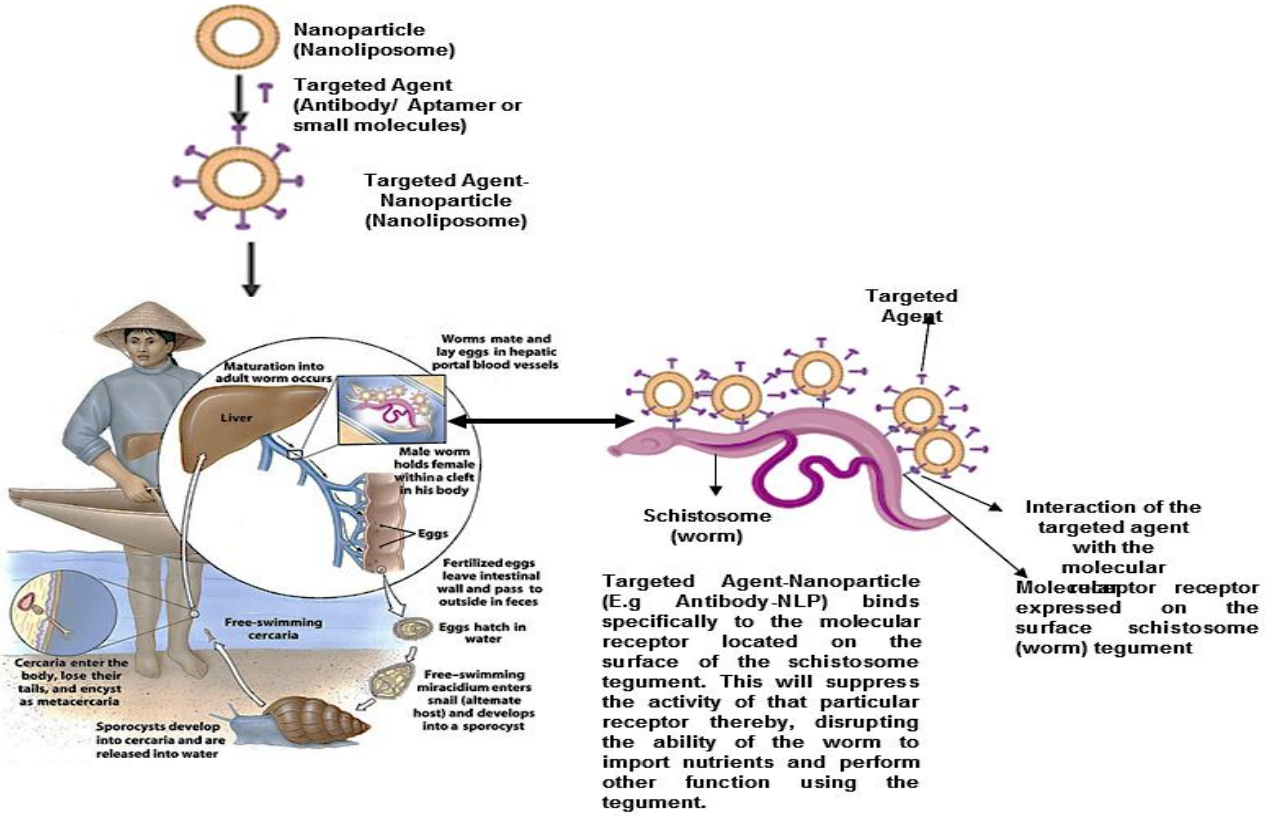

Figure 2.7: Proposed schematic for nanoparticle (nanoliposome) surface engineered (functionalized) with targeted agents (Antibodies, aptamers, antibody-like ligands or small molecules). This targeted nanoparticle localized/ detected as molecular receptors, located within the exterior of the schistosome tegument, and specifically binds to it. Thus, suppressing the activity of the receptor, as well as disrupt the ability of the worm to import nutrients from the host, and perform other activities.

2.7. NANO-ENABLED TREATMENTS FOR TROPICAL DISEASES AFFECTING THE CNS

2.7.1. Introduction

Tropical diseases (TDs) are groups of diseases that are prevalent or indigenous to tropical or subtropical regions of the world. Examples of such diseases are malaria, schistosomiasis, dengue, trypanosomiasis (African sleeping sickness), tuberculosis, Chagas (American sleeping sickness), leishmaniasis, neurocysticercosis among others. Cerebral tropical diseases (CTDs) or neuro-tropical diseases, occur due to central nervous system (CNS) involvement the diseases, which have been documented in several clinical reported cases where they cause various direct or indirect neurological manifestations or neuropsychiatric

symptoms (Morys *et al.,* 2015) . CTDs prevalent could be due to misdiagnosis, which lead to poor case ascertainment, global warming, increase in human migration, tourism in tropical regions, lack of potable water and sanitation systems that may result in the re-emergence of the diseases in endemic regions, population growth among other factors.

However, the treatments of CNS-tropical diseases are very challenging due to the existence of a diversity of formidable barriers that hinder the delivery of drug molecules into the CNS. The physiological or biological barrier for examples, the blood brain barrier (BBB) with the blood cerebrospinal fluid barrier (BCSFB) and some certain efflux transporter proteins (e.g. P-glycoprotein) (Figure 2.8). In particular, BBB (Figure 2.9) (Engelhardt and Sorokin, 2003; Stamatovic *et al.,* 2016) make the penetration of therapeutic agents or molecules into the CNS very complicated, thereby leading to the low bioavailability of therapeutic agents in the brain. Due to the fragile nature of the brain, the brain microvascular endothelial cells of the BBB shield the organ from exogenous materials. Additionally, the BBB works primarily by ensuring the proper environment for neuron functioning and interaction, which is imperative for the influx and efflux regulation, homeostasis maintenance and brain protection from pathogenic agents (Engelhardt and Sorokin, 2003; Stamatovic *et al.*, 2016).

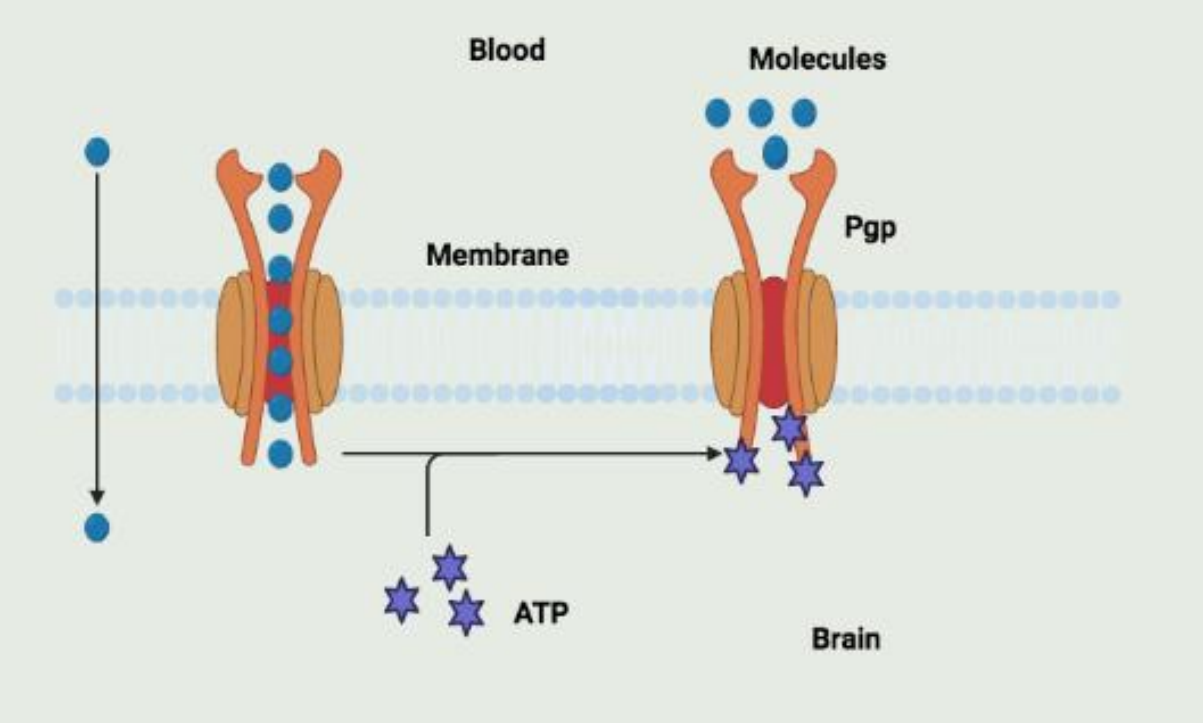

Figure 2.8: Schematic image of the P-glycoprotein; an ATP-binding transporter protein which helps with the efflux of drug molecules at the BBB

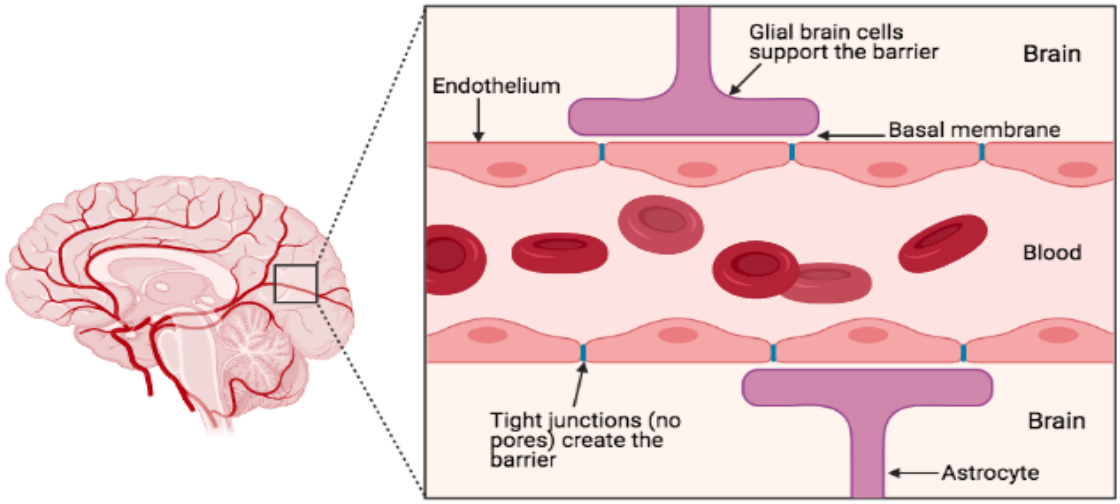

Figure 2.9: Schematic image of the BBB presenting the tight junctions, basement/basal membrane, capillary endothelial cells, glial brain cells which support the barrier, and glial podocytes (astrocytes)

The BBB is made up of continuous endothelial cell layers, which are joined via tight junctions (TJs), gap junctions (GJs) and adherent junctions (AJs). Amongst these groups of junctions, TJs act as the major composition element of the BBB, and they serves as a trans-endothelial resistance enhancer in the BBB (Ahlawat *et al.,* 2020). Furthermore, they control the movement of bioactive molecules across the BBB through the joining of the adjacent cells firmly, which leads to the blockade of the intercellular gap between them (Ahlawat *et al.,* 2020; Stamatovic *et al.,* 2016).

Several conventional strategies which have been employed over the years for CNS-diseases treatment was highlighted in this chapter, such as; prodrugs, ultrasound and microbubble, lipophilic analogs, carrier-mediated drug delivery systems, viral vectors, chemical drug delivery systems among others. Nanomedicine (advanced drug delivery systems (DDS) and targeted approach) which uses nanotechnological-based approach for the treatment, control, monitor and prevent diseases. Also, it has been a promising strategy that can be employed to improve the safety and effectiveness of drugs for the treatments of several diseases and disorders (Adekiya *et al.,* 2020). More so, nanomedicine approach can be utilized to target bioactive molecules to a precise location in the body so as to overcome off target and toxicity, it could also help to enhance the pharmacokinetic behavior of drugs by sustaining the release profile of drug without posing any adverse effect (Adekiya *et al.,* 2020; Adekiya *et al.,* 2021). In the area of neuro disorder, nanomedicine which is gaining recognition for the treatment, management and diagnostic of diseases such as cancer is quite green technique for the treatment of CNS-diseases when compared to conventional approaches. It is a potent and promising strategy for bioactive molecule delivery into the CNS, because nanocarriers have

been shown to traverse the BBB and/or BCSFB successfully and delivers drug molecules efficiently inside the CNS which is the target site (Ahlawat *et al.,* 2021; Lu *et al.,* 2014). The appropriate selection of the nanocarrier system is important for bioactive molecule delivery into the CNS. More so, the size, surface charge (zeta potential), surface area and morphology of nanocarriers also has great importance in the penetration of drugs across the BBB (Ahlawat *et al.,* 2020). In this chapter, several potential nanocarrier systems that can be used to circumvent the BBB so as to efficiently deliver drug molecules into the CNS with great and improve bioavailability are highlighted.

2.7.2. Insight overview of cerebral tropical diseases

Sometimes, neuropsychiatric symptoms such as; attention and cognitive deficit disorders, seizures, psychosis, migraine headaches, depressive mood, anxiety, uncontrolled anger, palsies, addictions among others may be presented as clinical symptoms of different systemic and CNS-diseases. These neuropsychiatric severe disturbances of cerebral function are sometimes directly caused by some tropical diseases, whilst others only alter the finer cerebral systems that control personality traits, anxiety and fears. Morys and co-workers (2015) documented that the mechanisms through which these neuropsychiatric manifestations are formed in tropical diseases are not in any way differ from any physical disorders related mechanisms. In (2015) Berkowitz et al., stated that out of over 17 neglected tropical diseases (NTDs) which were recognized by the World Health Organization (WHO), all were reported to be associated with neurologic manifestations except from yaws. Thus, in this section, the insight overview of all the major tropical diseases associated with neuropsychiatric symptoms is reported.

2.7.2.1. Cerebral malaria

Cerebral malaria (CM) is an acute nontraumatic encephalopathy, and the most severe neuropsychiatric complication of *Plasmodium falciparum* infection, which affect over 575,000 individuals per year, with the major prevalence in sub-Saharan Africa among the children (Idro *et al.,* 2010; Hoffmann and Wassmer, 2018). The neuro-disability is caused by the long-term risk posed to surviving patients as a result of cognitive and neurological deficits, epilepsy and behavioural difficulties, although the pathogenetic mechanisms causing CM are still being debated. The clinical symptoms of CM are impaired consciousness, which could cause seizures and coma as a severe manifestation. This believed is due to the parasitized red blood cells (pRBCs), which sequestered in the micro-circulation of cerebral, although this could also be attributed to impaired consciousness to inflammatory mediators and metabolic factors.

It was reported recently that CM could cause death in adult patients by triggering oxygen-deprivation in the brain (Sahu *et al.,* 2020). Some commonly observable hallmarks of CM include headache, fever, body ache, intracranial hypertension, brain swelling, changes in the retinal (macular and peripheral whitening, hemorrhages, papilledema and or vessel discoloration). More so, signs of brain stem (pupil size and reaction, abnormalities in posture, abnormal respiratory patterns and/or ocular movements), metabolic acidosis, hypoglycemia or hyperpyrexia, anemia, electrolyte imbalance and shock are some commonly presented systemic complications of CM. While repeated seizures, severe metabolic acidosis, hypoglycemia and shock are the grave prognosis in an unconscious patient (Idro *et al.,* 2010).

Parenteral antimalarials that is, cinchonoids or artemisinin derivatives are indicated as the treatment for CM in children, even though with this treatment, about 15 to 20% still lost their lives. While in the adult patients, the mortality was low when intravenous artesunate were administered to patients, and this treatment is currently undergoing investigation in the children with CM in African. Despite this treatment, it has been reported that many of the fully recovered surviving children sustain significant brain injury, and about 11% with gross neurological deficits 20 years after being discharged. Though, some of the major deficits, especially central hypotonia, blindness and ataxia improve with time, about 10% develop epilepsy with 25% having long-term cognitive impairments especially, behavioral impairments or motor function (Idro *et al.,* 2010). Thus, in African children, CM has been considered as a major neuro-disability initiator, and the pattern of neurological deficits in adults is different when compared to children.

2.7.2.2. Cerebral schistosomiasis

Schistosomiasis, happens to be one of the major groups of NTDs and tropical diseases and the second most prevalent after soil transmitted helminths and malaria respectively (Adekiya *et al.,* 2017; Aruleba *et al.,* 2019). The infection is caused by trematodes which belongs to *Schistosoma spp.,* and the blood flukes which live in the human host causes energy and protein malnutrition due to blood loss and tissue damage. Other consequential effects of this Schistosoma infection include anaemia caused as a result of iron deficit, and cognitive impairments (Adekiya *et al.,* 2017; Aruleba *et al.,* 2019). Neurological manifestations, tagged encephalic cerebral schistosomiasis and first illustrated by Yamagiwa in (1890) to be associated with *S. japonicum* infection; the prevalent *Schistosoma spp.* in East Asia. The neurological manifestations may occur as an acute toxaemia schistosomiasis in person which previously exposed to the infection, and present symptoms such as malaise, headache and muscle aches, weeks after the exposure, and the symptoms progress drastically as the trematodes continue to lay eggs (Yamagiwa, 1890). Encephalopathy in schistosomiasis is

associated with toxaemia in the clinical picture. The neurological manifestation may occur in an individual with the chronic infection where the eggs migrate to the CNS and induces granulomatous lesion, which causes severe symptoms of an increase in intracranial pressure (papilloedema, nausea, headache and visual changes), as well as focal neurological manifestations (Morys *et al.,* 2015).

In (2005), Betting and co-workers reported that CNS symptoms are usually noticed in the infection of *S. japonicum*, which are generally present in the form of focal deficiency and generalized or focal tonic-clonic seizures. *S. mansoni* infection usually comes in the form of myelitis transverse as the major neurological symptoms, which seldom affects the brain. Tumor-like in *S. mansoni* infection are common in young and male patients, and the usual manifestations normally display by the patients include focal neurologic deficiency, headache, and seizures. In a recent case study carried out by Zaqout and colleagues (2019) in Qatar on three males young adult patients who showed tumour-like lesions in their brain and presented with seizures. Necrosis granulomas, which contains Schistosoma eggs was revealed through the magnetic resonance imaging (MRI) image analysis. Furthermore, the frontal gyrus regions of high-signal foci on T2/FLAIR and left anterior temporal lobe, with linear pattern and a nodular of improvement in the post-contrast analysis was revealed by cerebral MRI. More so, the parenchyma of the brain subverted by necrotizing granulomas that harbour *Schistosoma* eggs are revealed by histopathological analysis.

Several other studies have reported cerebral and seizures schistosomiasis in different case reported either by MRI (Zaqout *et al.,* 2019; Roberts *et al.,* 2006; Liu *et al.,* 2008; Rave *et al.,* 2013; Rose *et al.,* 2014), PCR (Imai *et al.,* 2011) and computed tomography (CT) (Wan *et al.,* 2009) analysis in different *Schistosoma spp.* For example, the unusual reported case of primary cerebral schistosomiasis, which was described by magnetic resonance imagining in a healthy 21 year old man who showed symptoms of constant headache for 3 days (Rave *et al.,* 2013). Rose and co-workers (2014) reported a case study carried out on a 25 year old healthy woman of the United States origin who showed a specific general tonic-clonic seizure with no any other neurological manifestations after four years of swimming once in a river in Ghana during her one year semester stay in the country. The case report from the brain MRI examinations carried out on the woman showed that there were signal abnormalities areas and mottled nodular linear improvement in the right posterior temporal/partial and left temporal lobes also with right cerebellum with no mass impact. It was further reported by biopsy of left temporal lesions that there was pronounced granulomas and dense mixed with inflammatory infiltration made up of plasma cells, eosinophils. Also, lymphocytes, which surrounded the

refractive egg shell consisting the features of von Lichtenberg's envelope and embryonal cells and showed the pathognomic of *S. mansoni* spine shape.

2.7.2.3. Cerebral Dengue

Dengue is a vector-borne infection, which virtually exist in all the southern hemisphere countries. Flavivirus which is transmitted by the *Aedes albipictus* or *Aedes aegypti* mosquitoes bite is the disease is causing agent, and usually develop symptoms four to seven days following the mosquito bite to cause a severe flu-like illness. Most time, the presentation of dengue fever varies from mild to severe with different manifestations which include dengue shock syndrome, thrombocytopenia, and hemorrhagic diathesis and dengue hemorrhagic fever. Neurological hallmarks are common during dengue, but sometimes attributed to encephalopathy instead of direct CNS infection (Puccioni-Sohler *et al.,* 2013; Calderon-Pelaez *et al.,* 2019). This virus can be identified in the cerebrospinal fluid (CSF) and brain with the help of PCR, immunohistochemistry and immunoglobin examinations consistent with direct CNS infection. The symptom manifestations can be acute, nonspecific neurological symptoms (headache, sleeplessness, retrobulbar pain, dizziness, mood change, restlessness among others). Acute, encephalitic or focal neurological is characterized by seizures, mononeuropathy or polyneuropathy, spastic pararesis, encephalitis, Bell's palsy and/or Guillain-Barre syndrome. The symptoms can also manifest in the form of post-infectious neurological complications which can be characterized by transverse myelitis or palsy (long thoracic, facial, peroneal, ulnar and palatine). In dengue, acute liver failure can be considered as one of the factors that cause CNS manifestations, and the manifestations initiated are multifactorial, but majorly discovered to be linked with metabolic acidosis, persisted shock and serious disseminated intravascular coagulopathy that may lead to brain and hepatic dysfunction (Morys *et al.,* 2015; Han *et al.,* 2006) .

Several reported cases have documented the cerebral dengue in several parts of the world from different patients. In (2014), Madi et al described dengue encephalitis case of a 49 year old man who showed 6 days history of headache, fever sensorium and seizures in Southern India. In this case study it was reported that tested antigen of dengue NS-1 was reactive, and IgM of dengue was also tested positive, meanwhile the herpes simplex 1 and 2 was tested negative to CSF PCR. It was summarised in their report that it would be very imperative to consider dengue encephalitis in the different fever diagnosis due to alteration in sensorium in a country like India where the endemic of dengue are well pronounced. In another case report by Jayasinghe and co-workers (2016) where diffuse cerebral haemorrhages of dengue fever with cranial diabetes insipidus and subdural hematoma in a 24 year healthy lady who was previously on third day admission of fever and thrombocytopenia. Sub arachnoid

haemorrhages and diffuse intracranial haemorrhages in the occipital lobes, right frontal, cerebral oedema, parietal and brainstem, and an acute subdural hematoma in the area of right temporoparietal was revealed by non-contrast CT brain carried out at tertiary care level. Another similar case report by Weerasinghe and Medagama (2019) where dengue haemorrhage was presented to be encephalitis in a Sri Lankan Sinhalese boy of 18 year old who showed a history of fever for one day with an occurrence of seizure accompanied by hemiparesis of the left-side. Another case report conducted by Calderon-Miranda et al (2017) where they reported the case of a patient who showed neurological complications as a result of dengue virus infection, and it was revealed that the patient developed intracerebral haemorrhage with fatal outcome as dengue neurological complications.

2.7.2.4. Cerebral African trypanosomiasis

African trypanosomiasis, otherwise called sleeping sickness is a vector-borne infection of humans and animals. It is caused by a protozoan parasite infection that belongs to the genus; *Trypanosoma,* which are transmitted as a result of the infected tsetse fly (*Glossina genus*) bites, which is harbouring the pathogenic parasites to humans. Both the *T. brucei gambiense* as well as *T. brucei rhodesiense* are prominently found in several parts of Africa causes chronic and acute infections respectively, which are associated with progressive behavioural deficiency. The disease develops quickly and attacks the CNS, weeks or months after the infection, where it causes complex underlying CNS pathology (Frevert *et al.,* 2012). Initial meningitis, which could occur in the early stage of the infection, have been reported in an extensive studied in man and experimental animals. This observation may be followed by a choroid plexus breakdown, parasite movement into certain localized brain regions, and consequent encephalitis (Pentreath *et al.,* 1994). The encephalitis involve chronic, spread of inflammation with perivascular infiltrations of plasma cells, B-cells, inactivated macrophages and T-cells. Other manifestations include the damage of the BBB, which lead to a vasogenic oedema, microglia and astrocytes become reactive and the mediator/cytokine network is perturbed. More so, alterations in some signalling substances such as prostaglandins and hypersomnia, the elevation levels of active substances in the CSF due to the parasite could also lead to immunopathology in the CNS (Pentreath *et al.,* 1994).

The case reports have been documented by several researchers one of which include a case of a woman of 88-year-old that exhibited mental status alteration, slurred speech and right-sided weakness (Kaushal *et al.,* 2019). Cerebral trypanosomiasis and AIDS reported in a 36 year old female with consistence headache for a month, coupled with short memory problems, vomiting, nausea, somnolence, weight loss (Antunes *et al.,* 2002). Other includes the early brain parenchyma invasion by African Trypanosomes (Frevert *et al.,* 2012).

2.7.2.5. Some other cerebral tropical diseases

The involvements of other several tropical diseases have also been associated with CNS. In Chagas disease, otherwise called American trypanosomiasis that is caused in America by *Trypanosoma cruzi*, the involvement of the CNS are unusual, but most neurological manifestations are found in immunosuppressed patients. In a reported case by Lury and Castillo (2005), brain MRI revealed the largest multiple ring-enhancing lesions in the corpus callosum in a Hispanic male of 56-year-old residing in the United States who showed general malaise and difficulty voiding for 3day. The appearance of all lesions is shown to be nonspecific and in addition to those in deep white matter, the corpus callosum and the subcortical regions, periventricular white matter, and cerebellum were also involved. The appropriate laboratory examinations revealed that the man was HIV positive with a CD4+ count of 50. Yoo and co-workers (2004) also reported a similar case study of concurrent cerebral Chagas and toxoplasmosis in a 22-year-old El Salvadoran AIDS patient (Yoo *et al.,* 2004). More so, a morphological characteristic of an organism which corresponded to the amastigote of Trypanosoma was revealed by electron microscopy, and the biopsy specimen of the lesion showed the granulomatous abscess presence with necrosis in a 40-year-old man in Manitoba. Further analysis revealed that the man has a low CD4+ count as a result of HIV infection after he died despite treatment with benzonidazole within a week (Nijjar *et al.,* 2007). Other tropical diseases where neurological manifestations have been reported include tuberculosis (Hwang *et al.,* 2017), leishmaniasis (Peterson and Greenlee, 2011; Melo *et al.,* 2017), neurocysticercosis (Forlenza *et al.,* 1997; Saenz *et al.,* 2006; Shah and Chakrabarti, 2013), filariasis (Shrivastava *et al.,* 2016; Bhalla *et al.,* 2013), ascariasis (Sharma *et al.,* 1974; Zaki and Lad, 2011) among others.

2.7.3. Mechanism of therapeutic agents target into the CNS

Bioactive molecules or therapeutic agents targeting into the CNS cross the BBB via paracellular carrier connecting the endothelial cells, and via the transcellular transporter. These could be achieved either through the active and passive mechanisms, through the luminal region of the endothelial cells, across the cytoplasm subsequently transverse the abluminal region, into the interstitial of the brain (Teleanu *et al.,* 2018). Passive diffusion, a ubiquitous mechanism of transporting most vital nutrients (such as hormones, amino acids, neurotransmitters, etc.), as well as small lipophilic therapeutic agents into the brain through the circulatory system (Alexander *et al.,* 2019). The transfer of drugs or endogenous molecules to the brain from the blood via the mechanism of passive diffusion requires a concentration gradient, and the transfer depends on the physicochemical properties and the size of the drug molecules. In the passive diffusion mechanism, the therapeutic agents are

dissolved primarily into the lipid-bilayer of the endothelial cell microcapillary of the brain, and thereafter delivered within the brain. This type of transportation of drugs across the BBB is only suitable for small size, lipophilic, neutral and compound with low molecular weight (Alexander *et al.,* 2019). Active targeting happens to be a non-invasive technique that involves the transportation of drugs or therapeutic agents to target organs or tissues or cells through the use of site-specific ligands (Beduneau *et al.,* 2019). In oncology, nanocarriers loaded with drugs have ability to identify or recognize endothelial cells capillary of the brain as well as the cerebral tumour cells, and this has shown potential promise in the brain or cerebral tumour. Endogenous and chimeric ligands, which are cell-specific and have a high affinity to bind to BBB receptors can be conjugated indirectly or directly to nanocarriers (Beduneau *et al.,* 2019). Table 2.4 shows different targeting moieties used for the active targeting of several receptors in the BBB for CNS or cerebral diseases and disorders treatment. In the section below, several conventional drug delivery strategies that have been employed or that can be used for the CNS disease treatment through the drug molecules structure modification were highlighted.

Table 2.4: Different targeting moieties that can be employed as active targeting for therapeutic agent delivery into the brain

Targeting moiety	**Nanocarriers systems investigated to date**	**Reference**
Transferrin	Liposomes, micelle, dendrimers, Carbon dots	(Hatakeyama *et al.,* 2004; Huang *et al.,* 2007; Zhang *et al.,* 2012; Li *et al.,* 2016)
Glucose (GLU1000)	Liposomes	(Xie *et al.,* 2012)
TAT	Liposomes	(Rao *et al.,* 2008)
Chlorotoxin	Niosomes	(De *et al.,* 2018)
N-palmitoylglucosamine	Niosomes	(Bragagni *et al.,* 2014)
Cannabinoids	LNCs	(Aparicio-Blanco *et al.,* 2019)
Lactoferrin	PEG-PLA nanoparticles	(Hu *et al.,* 2009)
RVG29 peptide (rabies virus glycoprotein) and Chitosan	Polymeric micelles	(Kim *et al.,* 2013)
Apolipoprotein E	SLNs,	(Neves *et al.,* 2016; Topal *et al.,* 2021)
Pittsburgh compound B (PiB)-derivative Gd^{3+}	Carbon nanotubes	(Costa *et a.,* 2018)

9-Amino-minocycline	Dendrimers	(Sharma *et al.,* 2017)

2.7.4. Conventional drug delivery strategies for CNS

The presence of two major barrier systems: BBB and BSCFB shielded the CNS against harmful and toxic substances. Unfortunately, the same mechanisms pose as the major challenges for bioactive agent delivery into the CNS thereby frustrating the therapeutic interventions of CNS complications like encephalitis, stroke, Alzheimer's disease, epilepsy, Huntington's disease, brain tumors, Parkinson's disease and multiple sclerosis. The conventional CNS disease treatment is considered difficult since the drugs have to move into the CNS through the blood circulatory system in order to attain highly efficient concentrations of drug at the sites of CNS disease. Thus, the raise in the systemic drugs concentration levels by substantially extend administration and improve dose concentrations which sometimes pose serious toxicity effects on the patients (Warren, 2018; Misra *et al.,* 2003). In view of this, scientists have derived several ways of transferring or delivering therapeutic agents into the CNS through either active and/or passive targeting mechanisms. This section discussed several conventional drug delivery strategies into the CNS.

2.7.4.1. Ultrasound and microbubble-assisted drug delivery strategies for CNS

Ultrasound uses pressure waves that have 20 kHz or larger frequencies. Through a medium such as audio or optical waves, ultrasonic waves can be refracted, focused, and reflected. The ultrasonic sound waves can be used for drugs or therapeutic agent delivery to the CNS by disrupting or forcibly breaking down the BBB (Pitt *et al.,* 2004). This forced opening could lead to the damage of the BBB structure, thereby allowing the uncontrolled passing of drugs. In recent technology, development that uses focused ultrasound have been employed as a carrier for numerous therapeutic agents successfully. This focusing ultrasound allows the use of less intensity only to the desired sites, and it also paves-way to reverse the BBB disruption and it is only restricted to the target site (Chen *et al.,* 2019; Kovacs *et al.,* 2017; Karakatsani *et al.,* 2019). The combination of focused ultrasound with microbubbles has appeared as a helpful approach to quickly and locally open the BBB so as to deliver drug molecules to the brain. In this approach the perfluorocarbon or air is entrapped in a carrier which is made up of albumin or lipid, and thereby injected intravenously, which is then followed by the application of low frequency of ultrasound through transcranial route. This leads to the oscillation of the injected air bubbles. The resultant interaction between the bubbles and cerebral capillaries results in the reversible disruption of BBB (Chen *et al.,* 2019; Konofagou *et al.,* 2012). Although, the air bubbles injection is not absolutely essential, but its usage reduces the need

for high ultrasound intensity. It has been reported that the disruption could last for about 4 to 24h (Chen *et al.,* 2019).

2.7.4.2. Prodrug approaches for CNS delivery

Prodrugs happen to be one of the best approaches used in achieving therapeutic concentration of drugs in the circulation, and this is done by suitably modified drugs such that they are biologically inactive, but at their target site, they are converted back to their active forms (Stella *et al.,* 1985). Prodrugs are produced by covalent attachment of an unrelated chemical moiety to the parent drugs so as to enhance and improve the pharmacokinetic properties. When prodrugs reach their target tissues after administration, they are converted into their active forms so as to carry out their therapeutic action (Stella *et al.,* 1985). The conversion of the prodrugs back to their active forms in an *in vivo* occurs by the cleavage of the attached chemical moieties through physical and chemical modification such as chemical change, change in pH or enzymatic action modification (Karaman *et al.,* 2013; Pavan *et al.,* 2008). In order to improve the permeation of drug through the BBB, the prodrugs have to be lipophilic, and this can be achieved by chemical modification of the parent drug via the chemical moieties attachment that improve the drug lipophilicity (Pavan *et al.,* 2008). Afterward, the drug in its active form is released upon crossing the BBB, which thereafter prevents the drug from exiting the brain. Morphine is a typical example of a drug that cannot easily and readily cross the BBB to the CNS, but after latentiation through the hydroxyl groups acetylation to produce the heroin with hallucinogenic properties as a prodrug, which can easily traverse the BBB. Subsequently, the cleavage of the acetyl groups via the hydrolytic process results in an effective concentration of morphine stuck in the brain because of its hydrophilicity. In using this prodrug method in the delivery of drug across the BBB, care should be taken since certain prodrug molecules could modify the initial tissue distribution, as well as the toxicity and efficacy of the native drug (Pavan *et al.,* 2008).

2.7.4.3. Lipophilic analogs as drug delivery strategies for CNS

The permeation of drug molecules through the BBB is favoured by lipid solubility of the drug, through which the lipophilic drug undergoes passive diffusion into the CNS, due to its strong and better cerebrovascular permeability when compared to its native drug. It has been reported that the lipophilic analogs of drug molecule must possess an optimal log P number (octanol-water partition coefficient) of about 1.5 - 2.5 in order to have good CNS permeability when delivered through the circulatory system (Dwibhashyam and Nagappa, 2008). Although, some major shortcomings with the use of this approach have been reported which include poor tissue distribution and low selectivity of drug molecules. More so, this approach could

affect the oxidative metabolism rate through cytochrome P450 enzymes alongside with other related enzymes (Lu *et al.,* 2014; Misra *et al.,* 2003).

2.7.4.4. Viral vectors-mediated drug delivery strategies for CNS

Several approaches have been utilized to enhance the dispersion and delivery of genes into the brain over the years, and viral vectors have been one of the valuable tool to deliver genes to specific sites (Choudhary *et al.,* 2017). One of the strategies through which this can be achieved is via the injection of viral vectors directly into the lateral ventricles of cerebral through which virus would be delivered in the CNS. Another method through which the viral vectors can be delivered is through several sites injections for large volume covering. Other agents have also been examined to enhance the vector distribution for instance, mannitol and heparin (Gray *et al.,* 2010; Choudhary *et al.,* 2017; Davidson *et al.,* 2003). Herpes simplex virus (HSV), helper-dependent adenovirus, recombinant adeno-associated virus (AAV), simian virus, retrovirus, as well as lentivirus are some of the virus types that have been employed as vectors for gene delivery into the CNS. Various hybrid viral vectors have been formed to combine various viral components with specific characteristics so as to attain consistent and reproducible gene delivery into the brain. (Choudhary *et al.,* 2017; Davidson *et al.,* 2003; Mandel *et al.,* 2006;). HSV/EBV/retrovirus hybrid amplicon vectors, adenovirus/AAV hybrid vectors, HSV/Epstein-Barr virus (EBV), adenovirus/retrovirus hybrid vectors and HSV/AAV hybrid amplicon vectors are examples of hybrid viral vectors created by combining two or more viral components or gene sources. Although, the used of this approach in the delivery of genes into the CNS has been effective, but several problems associated with the approach have been reported which include mutagenesis, which could result in oncogenesis; endogenous recombination which could change the properties of virus delivery; and unwanted destruction in immune response (Gray *et al.,* 2010; Choudhary *et al.,* 2017).

2.7.4.5. Other conventional drug delivery strategies for CNS

Other conventional current strategies which have been employed for drugs and other bioactive molecule delivery into the CNS include molecular packaging, which is used for peptide delivery; carrier-facilitated drug delivery, which exploits the advantage of the facilitating system of transportation found in the endothelial of the brain to deliver drugs. Chemical drug delivery systems which requires only a single activation step to carry drugs across the BBB through the smuggling of drug molecules across as their lipophilic precursors, and this strategy is one of the created retro metabolic drug technique. Receptor/vector-mediated drug delivery, which can be used to transport insulin, insulin-like growth factor and transferring. This is achieved by exploiting several transcytosis processes which are required for signaling molecules and essential nutrients extravasation that are unable to diffuse across the cerebromicrovasculature

for CNS disease treatment. BBB disruption through the osmotic and biochemical blood brain barrier disruption (BBBD) are other invasive methods used to enhance drug molecule delivery into the CNS (Lu *et al.,* 2014; Upadhyay, 2014).

2.7.5. Nanocarrier strategies for CNS drug delivery

Nanomedicine (advanced drug delivery systems (DDS) and targeted approach) which uses nanotechnology application for treatment, control, monitor and prevent biological diseases has been a potential method that could be employed to improve and enhance the safety and effectiveness of drugs in the treatments of several diseases and disorders. More so, nanomedicine approach could be used sites specific target for drugs so as to decrease off target and limit toxicity, it could also help to increase the pharmacokinetic behavior of drugs via the sustained release profile of drug with a great safety outcome (Adekiya *et al.,* 2020; Adekiya *et al.,* 2021). In the field of neurodisorder, nanomedicine is a still very new approach compared to conventional approaches and it is a potent and promising approach for the therapeutic agents supply into the CNS, because nanoparticulate systems have been shown to be successfully bypassed the BBB and/or BCSFB thereby releasing drugs inside the CNS; the target site efficiently (Ahlawat *et al.,* 2020; Lu *et al.,* 2014). Figure 2.10 showed several types of potential nanocarriers which could be employed as a carrier for therapeutic agents into the CNS. The human cells are about 10-20 μm in size, while blood capillaries are about 6-9 μm in diameter. Thus, nanomaterials can be easily transported and internalized, due to their nanosize in ranges through the capillaries of the brain endothelial cells through transcytosis as well as the endocytosis mechanism of transport (Naqvi *et al.,* 2020).

The proper selection of the nanocarrier system is critical for bioactive molecule transport through the BBB and into the CNS. The size, surface charge (zeta potential), surface area and the shape of nanocarriers has a great impact on the CNS permeability barriers (Ahlawat *et al.,* 2020). Hence, the nanocarriers system employed in the delivery of drug into the CNS should have optimum size, surface charge, and surface area, non-toxic, biodegradable, site-specific, biocompatible and cost-effective. In this section, several nanocarriers with particle sizes in the nano range that have the capability as transporters for drug molecule into the CNS for neurological condition treatment were discussed.

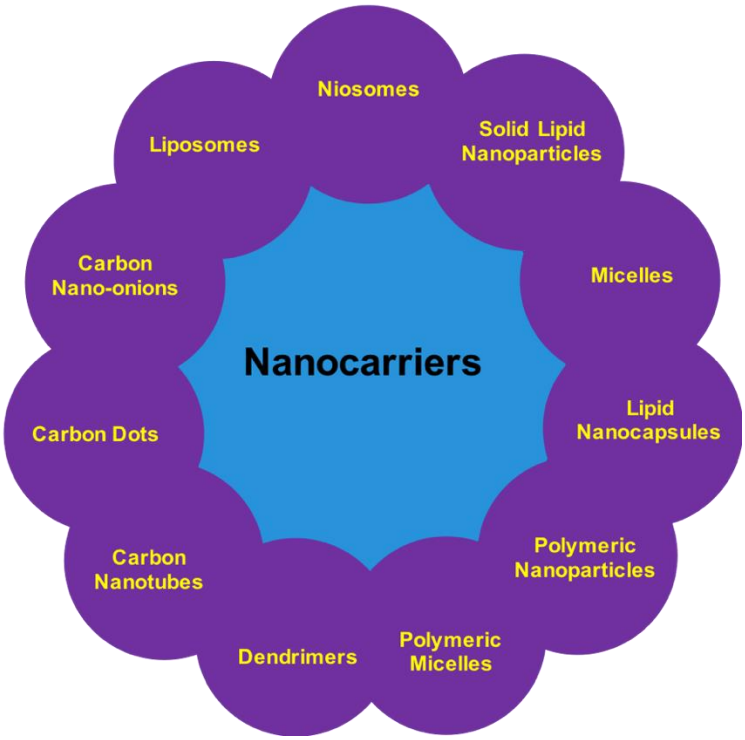

Figure 2.10: Several types of potential nanocarriers which could be utilized for therapeutic agent delivery into the CNS

2.7.5.1. Lipid-based nanocarriers

2.7.5.1.1. Liposomes

Liposomes are lipid spheres with one or more phospholipid bilayers that can store a variety of medicinal compounds such drugs, proteins, vaccines, and nucleic acids. The aqueous core of liposomes has ability to entrap hydrophilic drugs, whereas lipophilic and amphiphilic drugs can dissolve inside the phospholipid bilayer. The ease of surface modification with PEG (stealth liposomes), amphiphilic nature, biocompatibility, decreased plasma circulation periods due to removal through the system of reticuloendothelial. Also, the ability to extend the circulation period because of the reduction in the particle size (<100nm) makes liposomes an efficient nanocarrier system for bioactive molecule delivery.

The pharmacological features of docetaxel restricted the passage across the BBB. Thus, Shaw and co-workers (2017) designed nanoliposomes loaded docetaxel using a lipid hydration technique to treat brain solid tumors. In their study, the *in vitro* analysis showed that C6 glioma cells easily take up the nanoformulation. More so, the nanoformulation depicted better pharmacokinetics results when compared to native docetaxel, and the formulation increased drug uptake in the rat brain, which revealed that nanoliposomes could serve as an efficient carrier for docetaxel in the treatment of gliomas. Similarly, Rehman et al., (2017) created thermoresponsive liposomes for paclitaxel delivery. It was revealed in their study that

the formulation, improved drug permeability across the BBB and effective in targeting glioblastoma cells.

The surface modification techniques are shown to increase the distribution of loaded liposomes into the brain. The receptors of transferrin are overexpressed on the brain surface of the endothelial cell luminal membrane, and these receptors facilitate transferrin endocytosis into brain cells. Hatakeyama et al., (2004) designed transferrin-modified liposome, which was less than 80nm in size, and it was further revealed that modified liposomes have ability to target the brain. For the brain to function effectively, glucose is an important nutritional requirement that cannot be produced by the brain but is transported mainly by glucose transporters found on the brain capillary endothelial cells. In (2012), Xie and co-workers developed glucose-engineered liposomes GLU1000-LIP to target this transported and it was revealed that the liposomes surface modified with glucose had a high capacity for brain delivery. TAT peptide showed ability to improve drug delivery into the CNS. Rao et al., (2008) modified the surface of nanoformulation with TAT, and BBB absorption was improved by TAT conjugation, which was facilitated through transporter mechanisms other than transcytosis, and the developed TAT-conjugated formulation has the capability to circumvent the efflux mechanism of several BBB transport proteins. When compared to the free drug, the dual-targeting liposomes loaded doxorubicin was shown to enhance the therapeutic efficiency of doxorubicin in brain glioma with less toxicity. This was revealed in the study conducted by Gao et al., (2013) where dual-targeting liposomes loaded doxorubicin was conjugated with folate and transferrin, with the goal of improving selectivity for cancer cells in the brain and the to enhance the BBB transcytosis.

2.7.5.1.2. Niosomes

Niosomes, which are related to liposomal systems in that they can penetrate the BBB and deliver drugs to the brain, have the potential to treat cerebral tropical diseases. Although, they are nonionic surfactant vesicles, which are believed to be novel drug delivery systems with the ability to improve pharmaceutical molecule stability and solubility (Gharbavi *et al.,* 2018). Also, they are easy to surface modify due to the presence of functional groups on their hydrophilic heads, easy to produce and large-scale production requires simple methods, they have ability to enhance the stability of the encapsulated drug (Gharbavi *et al.,* 2018; Ag Seleci *et al.,* 2016). They are biocompatible, biodegradable, nonimmunogenic and less or no toxicity, they release drugs in a steady, sustained and organized manner and they also improve the oral bioavailability of therapeutic agents among other important advantage. They are made up of two major components which are lipid compounds (cholesterol or L-α-soya

phosphatidycholine) which provides the niosomes with appropriate shape, unbending nature and adaptation, while the nonionic surfactants (spans, tweens or Brij) assume the main part of the niosomes which help in the arrangement of the niosomes (Gharbavi *et al.,* 2018; Ag Seleci *et al.,* 2016; Kumar *et al.,* 2011; Ge *et al.,* 2019). The use of niosomes in the delivery of bioactive molecules into the brain has been reported in studies, for instance, De et al., (2018) developed temozolomide-loaded niosomes which were surface functionalized with chlorotoxin, a small 36 amino acid peptide found in scorpion venom. In their study, it was discovered that the active targeting of the surface modification nanosized particles facilitates and improve the accumulation of the drug in the cerebri by 3.04-folds. In another study by Bragagni et al., (2014) the hot plate test was used to evaluate the use of niosomes to functionalize N-palmitoylglucosamine for targeted delivery of dynorphin-B into the brain. It was discovered in the *in vivo* study that the developed niosomal formulation improves the delivery of dynorphin-B in mice, after intravenous administration and the drug was absorbed into the brain.

2.7.5.1.3. Solid lipid nanoparticles (SLNs)

Solid lipid nanoparticles (SLNs) are nanospheres that serve as a colloidal carrier system for therapeutic molecules. SLNs are made up of a solid lipid matrix, which includes fatty acids, waxes, and glycerides, and are stabilized with physiologically acceptable emulsifiers like bile salts, phospholipids, polyxyethylene ethers, Tween, or polyvinyl alcohol. The spherical particle size of SLNs is about 50-1000nm in the nanometer range when they are in aqueous surfactant solution or water (Claudio *et al.,* 2016). SLNs consists of solid hydrophobic core, which is conjugated with a phospholipid monolayer; the solid core may include the drug dispersed or dissolved within the solid high melting fat matrix, with the hydrophobic tails of the phospholipid chains incorporated inside the lipid matrix. (Puri *et al.,* 2009; Mukherjee *et al.,* 2009). Thus, they have the capability to deliver or integrate both hydrophilic and lipophilic drugs. They have the capacity to manage the release profile of the integrated drug for many weeks, extending the system's circulation duration, and may be utilized to broaden the breadth of drug targeting by ligand attachment or functionalization. They are very stable and have high drug payload, they are highly reproducible and cost effective. The carrier lipids are biodegradable and biocompatible, which makes the SLNs safe and less toxic when compared with polymeric nanoparticles, they are large scale production and sterilization is feasible (Puri *et al.,* 2009; Mukherjee *et al.,* 2009).

Owing to the unique advantages of SLNs among bioactive molecule carriers, they can be utilized to deliver drugs into the CNS across the BBB. They have served as a targeted and delivery mechanism for several therapeutics such as docetaxel, doxorubicin, atazanavir,

quercetin, quinine, resveratrol (Neves *et al.,* 2016), donepezil (Topal *et al.,* 2021), endorem (Peira *et al.,* 2003), and riluzole (Bondi *et al.,* 2010) to the brain. PEGylated SLNs have been extensively studied for drug delivery to the brain. SLNs and PEGylated SLNs are easily and readily absorbed by brain tissues due to their lipidic composition (Wong *et al.,* 2007; Brioschi *et al.,* 2007).

2.7.5.1.4. Micelles

Micelles are unilayered amphiphilic nanocarriers vesicles, which are composed of an aggregation of amphiphilic surfactants which help the controlled release of encapsulated drugs. Micelles improve the flow of hydrophobic drugs across the BBB for brain-associated disease treatments. They have been shown has potential nanocarrier for several bioactive molecules such as peptides and small molecules for the treatment of several cerebral disorders as well as offers MRI for brain inflammation as well as stroke imaging for diagnosis (Ahlawat *et al.,* 2020). The versatility and small size of micelles make this type of nanocarrier system a promising choice for the delivery of bioactive molecules into the brain. Shiraishi and co-workers in (2017) prepared gadolinium-micelles as an MRI contrast agent for clinical diagnostic. Clear contrast images of the ischemic hemisphere were observed in their study after about 30 mins of intravenous injection into a rat, which is an indication that the carrier improved the BBB permeation as well as the distribution area of the nanoformulation in the ischemic hemisphere. Numerous attempts have been made to improve the concentration of loaded drug across the BBB into the CNS. This is by modifying the micelles by directly conjugating the drug molecule as well as targeting the moiety to the amphiphilic portion of the micelles. Zhang et al., (2012) developed micelle functionalized with modified transferrin by cyclo-(Arg-Gly-Asp-d-Phe-Lys) for paclitaxel delivery. *In vitro* increased absorption by brain microvascular endothelial cells was found, and in addition extended in the drug retention times in the glioma tumor *in vivo*, with no significant toxicity was shown. Although, several shortcomings have been associated with this type of nanocarrier for the delivery of bioactive molecules which ranges from proneness to disassembly and deformation, high cost of production, high instability and inability to be stored for future use.

2.7.5.1.5. Lipid nanocapsules (LNCs)

Lipid nanocapsules (LNCs) are particles that consist of lipid liquid or semiliquid core at room temperature, coated with solid lipid film at room temperature, and this is opposite of nanosphere that are matrix particles, that is, the entire mass of nanosphere particles is made up of solid lipids. The pharmaceutically active molecules are finely dispersed within the solid matrix of nanosphere when they are composed of the active molecules (Battaglia *et al.,* 2012).

LNCs could emerge as a very prominent nanocarrier to transport bioactive compounds over the BBB and into the CNS due to their numerous features which ranges from easy to formulate, small particle size (20-100 nm) as well as the high entrapment efficacy of amphiphilic or hydrophobic drugs. In addition, LNCs are remarkably stable, and the simple, phase-inversion method used in producing the nanocarriers does not require organic solvents, and the excipients for making LNCs are FDA approved for parenteral administration. The method used in the production of LNCs can me optimized so as to encapsulate the hydrophilic drugs at the aqueous core of the nanocarrier (Hureaux *et al.,* 2009; Saliou *et al.,* 2013). More so, the surface modification of LNCs can further improve and enhance their bioavailability in the CNS (Moura *et al.,* 2020).

Studies have used this approach to deliver active molecules across the BBB, for instance, the neuroprotective efficacy of curcumin encapsulated with LNC in an Alzheimer's disease mouse model was demonstrated by Giacomeli et al., (2019). In that study, it was revealed that LNC increase the bioavailability of curcumin in the CNS and showed a very high neuroprotective potency in the CNS against a pro-inflammatory environment. LNCs functionalized with nonpsychotropic cannabinoids were created by Aparicio-Blanco and colleagues (2019) as pioneering non-immunogenic brain-targeting compounds. The permeability tests across the hCMEC/D3 cell-based *in vitro* BBB model as well as the biodistribution analysis in mice revealed that the smallest-sized cannabinoid-functionalized LNCs had a high significant brain-targeting potential. It was further revealed in their study that the enhancement of cannabinoid conjugated with LNCs for brain targeting outperforms was noticed 6-fold improvement in the G-technology; the major brain approach which is currently in the clinical trial for CNS diseases treatment (Aparicio-Blanco *et al.,* 2019). This is an indication that small cannabinoid-conjugated LNCs could be auspicious and promising platforms for the delivery of therapies into the CNS.

2.7.5.2. Polymeric-based nanoparticles

2.7.5.2.1. Polymeric nanoparticles

Polymeric nanoparticles (PN) are biodegradable and biocompatible, and non-soluble polymers like poly(alkylcyanoacylate) (PACA), polyesters like poly(D,L-lactide-co-glycolic acid) PLGA, poly(lactide) (PLA), as well as other natural proteins and polysaccharides with particle sizes ranging from 10 to 100 nanometers. The lipophilic medicines are encapsulated in their dense polymer matrix core, while the hydrophilic head offers steric stability to the nanoparticles. The bioactive molecules can be absorbed, encapsulated, and/or chemically attached to the nanoparticle surface when using this form of nanocarrier for drug delivery

(Sanchez *et al.,* 2020; Patra *et al.,* 2018). Polymeric nanoparticles formulated from PLGA and polylactic acid offer a number advantages for therapeutic drug delivery into the CNS, because these polymers are biocompatible, biodegradable, and unable elicit any type of inflammatory reaction following particle injection (Calzoni *et al.,* 2019; Lu *et al.,* 2009). More so, their breakdown products, lactic acid and glycolic acid, are removed from the body via their conversion in the Kreb's cycle to form carbon dioxide and water (Su and Kang, 2020; Deb, 2009; Elmowaft *et al.,* 2019). In addition, the entrapped hydrophobic and hydrophilic drug molecules inside the matrix of this type of nanoparticles can be released in a consistent manner over a period of time for many weeks.

Although polymeric nanoparticles can cross the BBB, their transport effectiveness is insufficient to provide therapeutic concentrations in the CNS. Thus, surface modification of the nanoparticles either by covalent binding or physical adsorption of hydrophilic polymers (polysaccharides and PEG) (Pathak, 2019). Also, the functionalization of tissue-specific ligands (small molecules, antibodies peptides, etc.) have been utilized to deliver therapeutic agents to the brain that are specifically targeted as well as increase their concentration. When compared to unconjugated nanoparticles, poly(butylcyanoacrylate) nanoparticles conjugated with polysorbate 80 loaded with both gemcitabine and doxorubicin demonstrate improved specificity and effectiveness in the brain (Ambruosi *et al.,* 2005).

Poloxamer 188 (F68) has also shown the capacity to improve the permeability of therapeutic agents into the brain, this was reported in the drug-loaded polybutylcyanoacrylate and PLGA nanoparticles into the rat brain. Interestingly, Kulkarni and co-workers have demonstrated in their comparative study that F68-modified PLGA nanoparticles are more effective in terms of drug delivery into the brain compared to poloxamer 407 (F127) and polysorbate 80-conjugated nanoparticles (Kulkarni and Feng, 2011). Other studies that have used this strategy to deliver therapeutic agents to the brain include poly(n-butylcyanoacrylate) nanoparticles conjugated with polysorbate 80 for rivastigmine delivery (Wilson *et al.,* 2008); double-coated of poly (butylcynanoacrylate) nanoparticles (Das, 2005); functionalized venlafaxine-PLGA nanoparticles (Cayero-Otero, 2019). In addition, transporters protein receptors found on the BBB have been explored as an example of drug transportation to the brain of such study is an *in vivo* and *in vitro* investigation of lactoferrin-conjugated PEG-PLA nanoparticles carried out by Hu et al., (2009).

The functionalization or conjugation of surfactants improves the permeability of therapeutic drugs into the brain by inhibiting the efflux activity of P-glycoprotein and solubilizing the lipid cell membrane of brain endothelial cells, allowing the therapeutic agents to permeate. More

specifically, the surface modification of nanoparticles with polysorbate 80 and F68 polymerizes both apolipoprotein E and/or apolipoprotein B and mimics low-density lipoproteins, allowing them to reach the brain via receptor-mediated endocytosis.

2.7.5.2.2. Polymeric micelles

Polymeric micelles (PMs) are vesicles composed of amphiphilic copolymers that accumulate and aggregate in an aqueous environment to generate spherical structures with a hydrophobic core and a hydrophilic shell that range in size from 10-100 nm (Ambruosi *et al.,* 2005). Recently, polymeric micelles as become most fascinated drug carrier systems across the BBB in the CNS. They are thought to be more stable than non-polymeric micelles, with a longer duration of action and biodistribution (Naqvi *et al.,* 2020). The inner hydrophobic core of PMs is synthesized using molecules like phospholipids, poly(D,L-lactide), polycaprolactone, fatty acids and poly(propylene glycols), which enable hydrophobic drugs to be loaded, while the hydrophilic environment are mostly composed of poly(ethylene glycol) (PEG) (Batrakova *et al.,* 2006; Croy and Kwon, 2006; Kumari *et al.,* 2014). The outer hydrophilic shell gives a high level of stability of the micelles in an aqueous atmosphere and increases their distribution time in the bloodstream, preventing the carrier from the reticulo-endothelial system (RES) and enhancing their concentration in specific areas with leaky vasculature (Batrakova *et al.,* 2006; Croy and Kwon, 2006; Kumari *et al.,* 2014; Hanafy *et al.,* 2018). The self-assembly approach is the most often utilized approach to making PMs. The choice of Pluronic class for block copolymer micelles is of particular interest in that drug efflux transporters are inhibited (for example, P-glycoprotein efflux transporter inhibition, which are abundant on the BBB) and improve drug transport into the CNS with no toxicity to the BBB. Additionally, it has been shown that Pluronic block copolymers facilitate the transportation of low molecular weight drugs integrated in them into the brain by increasing the stability and solubility of the drugs in plasma (Kabanov and Batrakova, 2004). However, PMs can deliver therapeutic agents by both active and passive mechanisms.

The delivery of therapeutic agents using this type of nanocarrier system was described by Kim et al., (2013) where Chitosan- and RVG29 peptide (rabies virus glycoprotein)-conjugated, Pluronic-based nanoparticles were used as targeted delivery of protein in the brain. Following the intravenous injection into the mice, it was revealed that the nanoparticle which was synthesized with Pluronic and conjugated with both the peptide and Chitosan has an effective brain accumulation of the protein and was remarkably better than peptide conjugated to the nanoparticle only.

2.7.5.2.3. Dendrimers

Dendrimers are promising polymeric structures recognized for their distinct structure and usefulness in drug delivery, they are tree-shaped synthetic molecules with 3-dimentional molecule and multiple branching monomers around the core. They are formulated through a nanoscale, multiple fabrication process (Madaan *et al.,* 2014). Their excellent properties such as the availability of several reactive functional groups that made surface modification easy, rigidity, high aqueous solubility, being nanosized and has a predictable molecular weight that allows for targeted drug delivery (Abedi-Gaballu *et al.,* 2018; Mitchell *et al.,* 2020; Sandoval-Yanez and Castro Rodriguez, 2020; Santos *et al.,* 2020; Mittal *et al.,* 2021). More so, biocompatibility, as well as a low polydispersity index makes them a versatile and potentially desirable nanocarriers over traditional polymers for therapeutic agent delivery (nucleic acids, drugs, contrast agents, proteins and peptides) for the treatment of CNS diseases, diagnosis, and imaging (Nanjwade *et al.,* 2009; Prajapati *et al.,* 2016). Depending on the generations, building block materials and complexity, polypropylene imine (PPI), polyamidoamine (PAMAM), and polylysine are well-known molecules used for the synthesis of dendrimers for both the delivery of hydrophilic and hydrophobic drug molecules (Abedi-Gaballu *et al.,* 2018; Mitchell *et al.,* 2020; Sandoval-Yanez and Castro Rodriguez, 2020; Santos *et al.,* 2020; Mittal *et al.,* 2021). To form a complex of drug-dendrimer, the high molecular mass hydrophobic or hydrophilic entities are either physically entrap or covalently linked to dendrimer functional groups on the periphery or conjugated by host-guest interactions to the dendrimer (Choudhary *et al.,* 2017; Madaan *et al.,* 2014). Although, dendrimers have broad application in drug delivery, there are concerns about the safety of cationic dendrimers, as well as their high toxicity and complex synthesis procedures has limited their use in biological systems (Madaan *et al.,* 2014; Noriega-Luna *et al.,* 2014).

Albertazzi and co-workers (2013) shown that conjugating PAMAMs dendrimers has a significant impact on their capacity to pass CNS tissue in vivo and enter live neurons, as indicated by intraventricular or intraparenchymal injections. Aso et al., 2019, revealed the high ability of synthesized dendrimers from poly(propylene imine) using a histidine-maltose shell to traverse the BBB and shown memory preservation in a transgenic mouse model of Alzheimer's disease via synapse protection with significant biocompatibility. Kannan et al., (2012) demonstrated that systemic administration of dendrimers synthesized from polyamidoamine activates microglia and astrocytes in the brains of neonatal rabbits with cerebral palsy. Also, discovered that N-acetyl-L-cysteine (NAC) based on dendrimers for brain injury therapy decreased neuroinflammation and resulted in a significant improvement in motor function in cerebral palsy kits. Some other studies that have been carried out in this area include the effective targeted delivery of genes to the brain using polyamidoamine

dendrimer modified with polyethyleneglycol functionalized with transferrin (Huang *et al.,* 2007). Synthesis of active microglia targeting dendrimer-minocycline conjugates as possible neuroinflammation therapies (Sharma *et al.,* 2017). The improvement of CNS penetration in animal with large brain injury through the intravenous administration of generation-6 hydroxyl PAMAM dendrimers was reported in a study carried out by (Zhang *et al.,* 2017).

2.7.5.3. Carbon-based nanoparticles

2.7.5.3.1. Carbon nanotubes (CNTs)

Iijima originally defined carbon nanotubes (CNTs) in the early 1990s as needle-like tubes made up of layers of nanoscaled cylinders of graphitic sheets (Karimi *et al.,* 2015). Carbon nanotubes (MWNTs or SWNTs) are multiwalled or single walled carbon nanotubes (MWNTs or SWNTs) are composed of one or more layers of graphene and have mostly been employed in the industry due to their features such as good electronic and thermal properties and high mechanical strength (Karimi *et al.,* 2015; Eatemadi *et al.,* 2014). Although, CNTs have been primarily used in cancer treatment, but it has shown promise as a nanocarrier system and therapeutic agent for a variety of brain-specific therapeutics due to many distinct properties such as the large surface area (Cheng *et al.,* 2017). Also, surface modification with particular chemical substances or molecules is simple, contributing to differences in biological and physical attributes, is one of the prominent properties (Aqel *et al.,* 2012; Kim *et al.,* 2012; Liu *et al.,* 2009).

Various research, for example, has demonstrated *in vitro* and *in vivo* experimental models of drug-loaded CNTs for brain delivery. Chemically functionalized multiwalled carbon nanotubes and polymer-coated carbon nanodots are able to quickly penetrate the BBB and create a connection with neurons by inducting hypotension through the regulation of the CNS (Wang *et al.,* 2017; Kafa *et al.,* 2016). Lohan et al., (2017) demonstrated in a preclinical study that surface modification of multiwalled carbon nanotubes with berberine has the potential to reduce β-amyloid induced AD and improve memory performance. This was due to an improvement in the uptake of the formulation in SH-SY5Y cell lines, and an *in vivo* investigation demonstrated that there is an improvement in the increase in drug uptake in the plasma and brain tissues when compared to the pure drug. It was also revealed in behavioral evaluation through Morris Maze test showed an improvement in performance efficiency (Lohan *et al.,* 2017). Kafa et al., (2015)] demonstrated that MWNTs-NH_3^+ was able to layer porcine brain endothelial cells (PBEC) in an *in vitro* analysis, and the accumulation of the formulation was noticed in the brain after intravenous injection in an *in vivo* assessment. The existence of MWNTs-NH_3^+ in both parenchyma fraction and brain capillaries was confirmed by the capillary depletion (Kafa *et al.,* 2015). Other investigations, both *in vitro* and *in vivo*,

have employed this method to deliver therapeutic molecules into the brain for treatments, imaging, and diagnostics include*;* multiwalled carbon nanotube functionalized with fluorescein isothiocyanate as a potential BBB-permeable CNS-targeting drug delivery mechanism. The functionalization of carbon nanotubes with Pittsburgh compound B (PiB)-derivative Gd^{3+} in order to enhance brain delivery through the target of amyloid (Costa *et al.,* 2018). Although, some drawbacks associated the CNTs has been reported such as toxicity, polydispersity in CNT type, batch-to-batch variation, high cost of production and the length and chirality of the CNT are uncontrollable (Ahlawat *et al.,* 2020; Fukushima *et al.,* 2017). More specifically, pulmonary inflammation, mesothelioma induction, and complement system activation have all been linked to nanocarriers. Also, high dose concentration of about 3mg/mouse has been observed to have carcinogenic effects in a mouse model (Ahlawat *et al.,* 2020; Fukushima *et al.,* 2017).

2.7.5.3.2. Carbon dots (CDs)

Carbon dots (CDs) are a novel form of nanoparticle and one of the most promising nanocarriers for drug delivery that have recently surfaced and piqued the interest of researchers due to their unique optical properties (Liu *et al.,* 2020; Das *et al.,* 2021). CDs are nanoparticles made of carbon with a reduced diameter (less than 100 nm) compared to liposomes, which also have high biocompatibility and relatively no toxicity (Liu *et al.,* 2020; Das *et al.,* 2021; Khan *et al.,* 2019). CDs are easy to synthesis compared to CNTs and they have a high ratio of surface area to volume, which increase drug loading capacity for drug delivery. As a result of uniqueness in the optical/photoluminescence properties of CDs, it has been widely applied in bioimaging and sensing (Guerrero *et al.,* 2021). Additionally, CDs have also been discovered to prevent amyloid beta peptides from fibrillating, thereby showing a great potential for AD and PD treatment, because the peptides and proteins have a same molecular mechanism for the formation of fibrils, a process linked to CNS disease disorders. (Guerrero *et al.,* 2021; Han *et al.,* 2017). However, few reports have been published that show that CDs have the capacity to penetrate the BBB without the use of surface transferrin or transporter proteins like GLUT1 and LAT1 (Zhou *et al.,* 2019). An example of such study includes the self-targeting fluorescent CDs for brain cancer diagnosis (Zheng *et al.,* 2015). Recently, Seven and co-workers designed saccharide-based CDs that can penetrate the BBB either through the help of passive diffusion or glucose transporter protein, due to the amphiphilic structure of the CDs with surface groups that is similar to the saccharide precursor. Zhou et al., (2019) developed amphiphilic yellow-emissive CDs with an ultrasonication-mediated method, and it was revealed by confocal image analyses that the yellow-emissive CDs penetrated the BBB of 5day old wild-type zebrafish, which could be as a result of passive diffusion because of the amphiphilicity of yellow-emissive CDs. It was further observed that

the CDs enter the cells and suppressed the upregulation of human β-amyloid and amyloid precursor protein. This approach can be employed to transport bioactive compounds into the CNS for cerebral tropical disease treatment. Li et al., (2016) covalently conjugated human transferrin to CDs and the formulation was injected into the vasculature of zebrafish, where it was revealed that the formulation conjugated with transferrin penetrate the BBB into the CNS through transferrin receptor-mediated endocytosis, while unconjugated CDs did not.

2.7.5.3.3. Carbon nanoonions

Carbon nanoonions (CNOs) is another type of carbon nanomaterial which has been used in biomedical applications, due to its unique structural and electronic properties. A wide surface area to volume ratio, a broad absorbance band, the capacity to reversibly accept multiple electrons, thermal stability, and biocompatibility are some of the other distinctive qualities that distinguish them as an excellent choice for biomedical applications (Ahlawat *et al.,* 2021; Baldrighi *et al.,* 2016; d'Amora *et al.,* 2016; Borgohain *et al.,* 2012). Onion-like nanocarbons are created by thermal annealing nanodiamonds under high pressure in an inert environment at a very high temperature and consist of 6 to 8 graphene shells on average (Bartelmess *et al.,* 2014). Although, they cannot be used in their pristine due to their poor solubility, but, aggregate in inorganic and organic solvents because of intermolecular interactions within the pristine nanostructures of CNOs can be avoided through surface modification (Bartelmess *et al.,* 2014; Plonska-Brzezinska, 2019). However, their biomedical applications have been faced with different limitations such as variation in batch size (number of graphitic shells) and size are dependent on the synthesis approach used). Because of their hydrophobic nature, failure to produce well-dissolved CNOs in aqueous solution might lead to bioaccumulation and thereby result in the toxicity of the nanocarriers (Ahlawat *et al.,* 2021; Bartelmess *et al.,* 2014; Plonska-Brzezinska, 2019). More so, unable to cross the BBB due to their large molecular mass that could hamper the integrity of the barrier via disruption process (Ahlawat *et al.,* 2021; Pakhira *et al*., 2016).

Meanwhile, Pakhira et al., (2016) developed fluorescent carbon nano onion (wsCNO) which is water soluble. They explored wsCNO due to their uniqueness such as water solubility and inability to stay within for a long time when compared to other dispersed but non-soluble nanoparticulate systems. In their study, it was discovered that the synthesized wsCNO has negative and very low zeta potential number, which has ability to internalize and penetrate the BBB, most likely via paracellular gaps, as seen in CADASIL mice. Furthermore, it was shown that the BBB tight-junction proteins are significantly downregulated, and that wsCNO does not accumulate in the brain but rather freely and swiftly exits under normal conditions. This was

observed in fluorescence spectroscopy monitoring, which revealed the clearance sixth day after the administration of the formulation similar to the results obtained in untreated mice.

2.8.6. Conclusions

Incidences of schistosomiasis continue to increase globally across sub-Saharan Africa and other tropical regions. However, the development of resistance against the only drug PZQ necessitates the design of more effective drug molecules to tackle the continual increase in Schistosomiasis cases. In this review, the molecular structure and function of the schistosomal tegument was described and several molecular targets have been identified to potentially target the schistosomes tegument as a site for enhanced PZQ delivery in anti- schistosomal therapy. In addition, potential agents that could target the molecular receptors identified have been highlighted. In general, surface functionalization of nanoparticles with antibodies, aptamers, antibody-like ligands, peptides and small molecules to specifically target and bind to the schistosomes tegument receptor genes and proteins presents a viable option for researchers to explore. This approach will suppress the activity of receptor genes/proteins, thereby impairing the ability of schistosomes to import nutrients from the host as well as disrupt the ability of the parasite to maintain solute balancing and evasion of the host immune response. Hence, exploration of the schistosomes tegument may be a possible and potential focus for designing and developing anti-schistosomal drug which can target receptors and proteins present on the worm tegument.

Furthermore, there is an alarming increase in reported cases of tropical disease's effect on the central nervous system (CNS) across the globe majorly in tropical and subtropical regions, which may be due to global warming, an increase in human migration, tourism in tropical regions, poor case ascertainment and/or inadequate reporting. More so, urbanization, population growth and lack of potable water sources and sanitation systems, could result in the re-emergence of the diseases in endemic countries. This involvement of tropical diseases in the CNS leads to direct or indirect neurologically manifestations. Thus, this chapter gives an insight overview of some tropical diseases and their involvement in the CNS, as well as highlighted some strategies of delivery bioactive molecules or therapeutic agents for the treatment of CNS diseases across the BBB. Additionally, the chapter discusses nanocarrier techniques for drug delivery into the CNS, which might be a promising and viable therapy option for cerebral tropical illnesses.

2.9.6. Reference

1. Abedi-Gaballu, F., Dehghan, G., Ghaffari, M., Yekta, R., Abbaspour-Ravasjani, S., Baradaran, B., Dolatabadi, J.E.N. and Hamblin, M.R., 2018. PAMAM dendrimers as efficient drug and gene delivery nanosystems for cancer therapy. *Applied materials today*, *12*, pp.177-190.
2. Abruzzi, A. and Fried, B., 2011. Coinfection of Schistosoma (Trematoda) with bacteria, protozoa and helminths. *Advances in parasitology*, *77*, pp.1-85.
3. Adekiya, T.A., Kappo, A.P. and Okosun, K.O., 2017. Temperature and rainfall impact on schistosomiasis. *Glob. J. Pure Appl. Math*, *13*, pp.8453-8469.
4. Adekiya, T.A., Kondiah, P.P., Choonara, Y.E., Kumar, P. and Pillay, V., 2020. A review of nanotechnology for targeted anti-schistosomal therapy. *Frontiers in bioengineering and biotechnology*, *8*, p.32.
5. Adekiya, T.A., Kumar, P., Kondiah, P.P., Pillay, V. and Choonara, Y.E., 2021. Synthesis and therapeutic delivery approaches for praziquantel: a patent review (2010-present). *Expert Opinion on Therapeutic Patents*, pp.1-15.
6. Ag Seleci D, Seleci M, Walter J-G, Stahl F, Scheper T. Niosomes as nanoparticular drug carriers: fundamentals and recent applications. J Nanomater. 2016.
7. Ahlawat, J., Asil, S.M., Barroso, G.G., Nurunnabi, M. and Narayan, M., 2021. Application of carbon nano onions in the biomedical field: Recent advances and challenges. *Biomaterials Science*.
8. Ahlawat, J., Guillama Barroso, G., Masoudi Asil, S., Alvarado, M., Armendariz, I., Bernal, J., Carabaza, X., Chavez, S., Cruz, P., Escalante, V. and Estorga, S., 2020. Nanocarriers as potential drug delivery candidates for overcoming the blood–brain barrier: challenges and possibilities. *ACS omega*, *5*(22), pp.12583-12595.
9. Ahlschwede, K.M., Curran, G.L., Rosenberg, J.T., Grant, S.C., Sarkar, G., Jenkins, R.B., et al. (2019). Cationic carrier peptide enhances cerebrovascular targeting of nanoparticles in Alzheimer's disease brain. Nanomed-Nanotechnol. Bio.l Med. 16, 258-266. doi: 10.1016/j.nano.2018.09.010.
10. Ahmadpour, E., Godrati-Azar, Z., Spotin, A., Norouzi, R., Hamishehkar, H., Nami, S., et al. (2019). Nanostructured lipid carriers of ivermectin as a novel drug delivery system in hydatidosis. Parasites vectors. 12(1), 1-9. doi: 10.1186/s13071-019-3719-x.
11. Albertazzi, L., Gherardini, L., Brondi, M., Sulis Sato, S., Bifone, A., Pizzorusso, T., Ratto, G.M. and Bardi, G., 2013. In vivo distribution and toxicity of PAMAM dendrimers in the central nervous system depend on their surface chemistry. *Molecular pharmaceutics*, *10*(1), pp.249-260.
12. Albuquerque, E.X., Pereira, E.F., Alkondon, M., Rogers, S.W. (2009). Mammalian nicotinic acetylcholine receptors: from structure to function. Physiol. Rev. 89(1), 73-120. doi: 10.1152/physrev.00015.2008

13. Alexander, A., Agrawal, M., Uddin, A., Siddique, S., Shehata, A.M., Shaker, M.A., Rahman, S.A.U., Abdul, M.I.M. and Shaker, M.A., 2019. Recent expansions of novel strategies towards the drug targeting into the brain. *International journal of nanomedicine*, *14*, p.5895.
14. Ambruosi, A., Yamamoto, H. and Kreuter, J., 2005. Body distribution of polysorbate-80 and doxorubicin-loaded [14C] poly (butyl cyanoacrylate) nanoparticles after iv administration in rats. *Journal of drug targeting*, *13*(10), pp.535-542.
15. Antunes, A.C.M., Cecchini, F.M.D.L., Bolli, F.V.B., Oliveira, P.P.D., Rebouças, R.G., Monte, T.L. and Fricke, D., 2002. Cerebral trypanosomiasis and AIDS. *Arquivos de neuro-psiquiatria*, *60*, pp.730-733.
16. Aparicio-Blanco, J., Romero, I.A., Male, D.K., Slowing, K., García-García, L. and Torres-Suarez, A.I., 2019. Cannabidiol enhances the passage of lipid nanocapsules across the blood–brain barrier both in vitro and in vivo. *Molecular pharmaceutics*, *16*(5), pp.1999-2010.
17. Aqel, A., Abou El-Nour, K.M., Ammar, R.A. and Al-Warthan, A., 2012. Carbon nanotubes, science and technology part (I) structure, synthesis and characterisation. *Arabian Journal of Chemistry*, *5*(1), pp.1-23.
18. Arruebo, M., Valladares, M., González-Fernández, Á. (2009). Antibody-conjugated nanoparticles for biomedical applications. J. Nanomaterials :37. http://dx.doi.org/10.1155/2009/439389.
19. Aruleba, R.T., Adekiya, T.A., Oyinloye, B.E., Masamba, P., Mbatha, L.S., Pretorius, A., Kappo, A.P. (2018). PZQ therapy: how close are we in the development of effective alternative anti-schistosomal drugs?. Infect. Disord. Drug Targets. doi: 10.2174/1871526519666181231153139
20. Baldrighi, M., Trusel, M., Tonini, R. and Giordani, S., 2016. Carbon nanomaterials interfacing with neurons: an in vivo perspective. *Frontiers in neuroscience*, *10*, p.250
21. Bartelmess, J. and Giordani, S., 2014. Carbon nano-onions (multi-layer fullerenes): chemistry and applications. *Beilstein journal of nanotechnology*, *5*(1), pp.1980-1998.
22. Batrakova, E.V., Bronich, T.K., Vetro, J.A. and Kabanov, A.V., 2006. Polymer micelles as drug carriers. *Nanoparticulates as drug carriers*, pp.57-93.
23. Battaglia, L. and Gallarate, M., 2012. Lipid nanoparticles: state of the art, new preparation methods and challenges in drug delivery. *Expert opinion on drug delivery*, *9*(5), pp.497-508.
24. Becker, B., Mehlhorn, H., Andrews, P., Thomas, H., Eckert, J. (1980). Light and electron microscopic studies on the effect of praziquantel on Schistosoma mansoni, Dicrocoelium dendriticum, andFasciola hepatica (Trematoda) in vitro. Zeitschrift für Parasitenkunde 63(2), 113-128. DOI: 10.1007/bf00927527

25. Béduneau, A., Saulnier, P. and Benoit, J.P., 2007. Active targeting of brain tumors using nanocarriers. *Biomaterials*, *28*(33), pp.4947-4967.
26. Berkowitz, A.L., Raibagkar, P., Pritt, B.S. and Mateen, F.J., 2015. Neurologic manifestations of the neglected tropical diseases. *Journal of the neurological sciences*, *349*(1-2), pp.20-32.
27. Betting, L.E., Pirani, C., de Souza Queiroz, L., Damasceno, B.P. and Cendes, F., 2005. Seizures and cerebral schistosomiasis. *Archives of neurology*, *62*(6), pp.1008-1010.
28. Bhalla D, Dumas M, Preux P-M., 2013. Neurological manifestations of filarial infections. Handbook Clin Neurol. (114), 235-242.
29. Bondì, M.L., Craparo, E.F., Giammona, G. and Drago, F., 2010. Brain-targeted solid lipid nanoparticles containing riluzole: preparation, characterization and biodistribution. *Nanomedicine*, *5*(1), pp.25-32.
30. Borgohain, R., Li, J., Selegue, J.P. and Cheng, Y.T., 2012. Electrochemical study of functionalized carbon nano-onions for high-performance supercapacitor electrodes. *The Journal of Physical Chemistry C*, *116*(28), pp.15068-15075.
31. Bragagni, M., Mennini, N., Furlanetto, S., Orlandini, S., Ghelardini, C. and Mura, P., 2014. Development and characterization of functionalized niosomes for brain targeting of dynorphin-B. *European Journal of Pharmaceutics and Biopharmaceutics*, *87*(1), pp.73-79.
32. Braschi, S., Borges, W.C., Wilson, R.A. (2006). Proteomic analysis of the shistosome tegument and its surface membranes. Memorias do Instituto Oswaldo Cruz 101, 205-212. doi: 10.1590/s0074-02762006000900032
33. Braschi, S., Curwen, R.S., Ashton, P.D., Verjovski-Almeida, S., Wilson, A. (2006). The tegument surface membranes of the human blood parasite Schistosoma mansoni: a proteomic analysis after differential extraction. Proteomics 6(5), 1471-1482. doi: 10.1002/pmic.200500368
34. Brioschi, A., Zenga, F., Zara, G.P., Gasco, M.R., Ducati, A. and Mauro, A., 2007. Solid lipid nanoparticles: could they help to improve the efficacy of pharmacologic treatments for brain tumors?. *Neurological research*, *29*(3), pp.324-330.
35. Cabezas-Cruz, A., Valdés, J.J., Lancelot, J., Pierce, R.J. (2015). Fast evolutionary rates associated with functional loss in class I glucose transporters of Schistosoma mansoni. BMC Genomics 16(1), 980. doi: 10.1186/s12864-015-2144-6.
36. Caffrey, C.R. (2007). Chemotherapy of schistosomiasis: present and future. Curr. Opin. Chem. Biol. 11, 433-439. DOI: 10.1016/j.cbpa.2007.05.031
37. Calderón-Miranda, W., Rojas-Martínez, J.A., Cabeza-Morales, M. and Moscote-Salazar, L.R., 2017. Hemorragia Intracerebral como complicación de dengue grave: reporte de Caso. *Revista Mexicana de Neurociencia*, *18*(2), pp.122-127.

38. Calderón-Peláez, M.A., Velandia-Romero, M.L., Bastidas-Legarda, L.Y., Beltrán, E.O., Camacho-Ortega, S.J. and Castellanos, J.E., 2019. Dengue virus infection of blood–brain barrier cells: Consequences of severe disease. *Frontiers in microbiology*, *10*, p.1435.
39. Calzoni, E., Cesaretti, A., Polchi, A., Di Michele, A., Tancini, B. and Emiliani, C., 2019. Biocompatible polymer nanoparticles for drug delivery applications in cancer and neurodegenerative disorder therapies. *Journal of functional biomaterials*, *10*(1), p.4.
40. Camacho, M., Agnew, A. (1995). Schistosoma: rate of glucose import is altered by acetylcholine interaction with tegumental acetylcholine receptors and acetylcholinesterase. Exp. Parasitol. 81(4), 584-591. doi: 10.1006/expr.1995.1152
41. Camidge, D.R. (2014). Targeted therapy vs chemotherapy: which has had more impact on survival in lung cancer? Does targeted therapy make patients live longer? Hard to prove, but impossible to ignore. Clin. Adv. Hematol. Oncol. H&O 12(11), 763-766.
42. Capron, A., Riveau, G., Capron, M., Trottein, F. **(**2005). Schistosomes: the road from host-parasite interactions to vaccines in clinical trials. Trends Parasitol. 21**,** 143-149. DOI: 10.1016/j.pt.2005.01.003
43. Castro-Borges, W., Dowle, A., Curwen, R.S., Thomas-Oates, J., Wilson, R.A. (2011). Enzymatic shaving of the tegument surface of live schistosomes for proteomic analysis: a rational approach to select vaccine candidates. PLoS Neg. Trop. Dis. 5(3), e993. doi: 10.1371/journal.pntd.0000993.
44. Catuogno, S., Esposito, C., de Franciscis, V. (2016). Aptamer-mediated targeted delivery of therapeutics: An update. Pharmaceut. 9(4), 69. DOI: 10.3390/ph9040069
45. Cayero-Otero, M.D., Gomes, M.J., Martins, C., Álvarez-Fuentes, J., Fernández-Arévalo, M., Sarmento, B. and Martín-Banderas, L., 2019. In vivo biodistribution of venlafaxine-PLGA nanoparticles for brain delivery: plain vs. functionalized nanoparticles. *Expert opinion on drug delivery*, *16*(12), pp.1413-1427.
46. Cerchia, L., De Franciscis, V. (2010). Targeting cancer cells with nucleic acid aptamers. Trends Biotechnol. 28(10), 517-525. doi: 10.1016/j.tibtech.2010.07.005
47. Chen, K.T., Wei, K.C. and Liu, H.L., 2019. Theranostic strategy of focused ultrasound induced blood-brain barrier opening for CNS disease treatment. *Frontiers in pharmacology*, *10*, p.86.
48. Chen, Z., Zhang, A., Wang, X., Zhu, J., Fan, Y., Yu, H. and Yang, Z., 2017. The advances of carbon nanotubes in cancer diagnostics and therapeutics. *Journal of Nanomaterials*, *2017*.
49. Cheng, W., Li, X., Zhang, C., Chen, W., Yuan, H., Xu, S. (2017). Preparation and In Vivo-In Vitro Evaluation of Polydatin-Phospholipid Complex with Improved Dissolution and Bioavailability. Int. J. Drug Dev. Res. 9, 39-43.

50. Choudhary, S., Gupta, L., Rani, S., Dave, K. and Gupta, U., 2017. Impact of dendrimers on solubility of hydrophobic drug molecules. *Frontiers in pharmacology*, *8*, p.261.
51. Choudhury, S.R., Hudry, E., Maguire, C.A., Sena-Esteves, M., Breakefield, X.O. and Grandi, P., 2017. Viral vectors for therapy of neurologic diseases. *Neuropharmacology*, *120*, pp.63-80.
52. Cioli, D., Pica-Mattoccia, L. (2003). Praziquantel. Parasitol. Res. 90(1), S3-S9. doi: https://doi.org/10.1007/s00436-002-0751-z
53. Cioli, D., Pica-Mattoccia, L., Basso, A., Guidi, A. (2014). Schistosomiasis control: praziquantel forever?. Mol. Biochem. Parasitol .195(1), 23-29. doi: 10.1016/j.molbiopara.2014.06.002
54. Claudio, P., Reatul, K., Brigitte, E. and Geraldine, P., 2016. Drug-delivery nanocarriers to cross the blood–brain barrier. In *Nanobiomaterials in Drug Delivery* (pp. 333-370). William Andrew Publishing.
55. Colombo, F., Durigutto, P., De Maso, L., Biffi, S., Belmonte, B., Tripodo, C., et al. (2019). Targeting CD34+ cells of the inflamed synovial endothelium by guided nanoparticles for the treatment of rheumatoid arthritis. J. Autoimmun. 03:102288. doi: 10.1016/j.jaut.2019.05.016
56. Conlon, C.P. (2005). Schistosomiasis. Med. 33, 64-67.
57. Corda, E., Du, X., Shim, S.Y., Klein, A.N., Siltberg-Liberles, J., Gilch, S. (2018). Interaction of peptide aptamers with prion protein central domain promotes α-cleavage of PrP C. Mol. Neurobiol. 1-17. doi: 10.1007/s12035-018-0944-9
58. Costa, P.M., Wang, J.T.W., Morfin, J.F., Khanum, T., To, W., Sosabowski, J., Tóth, E. and Al-Jamal, K.T., 2018. Functionalised carbon nanotubes enhance brain delivery of amyloid-targeting pittsburgh compound B (PiB)-derived ligands. *Nanotheranostics*, *2*(2), p.168.
59. Croy, S.R. and Kwon, G.S., 2006. Polymeric micelles for drug delivery. *Current pharmaceutical design*, *12*(36), pp.4669-4684.
60. d'Amora, M., Rodio, M., Bartelmess, J., Sancataldo, G., Brescia, R., Zanacchi, F.C., Diaspro, A. and Giordani, S., 2016. Biocompatibility and biodistribution of functionalized carbon nano-onions (f-CNOs) in a vertebrate model. *Scientific reports*, *6*(1), pp.1-9.
61. da Paixão Siqueira, L., Fontes, D.A.F., Aguilera, C.S.B., Timóteo, T.R.R., Ângelos. M.A., Silva, L.C.P.B.B., et al. (2017). Schistosomiasis: drugs used and treatment strategies. Acta trop. 176,179-187. doi: 10.1016/j.actatropica.2017.08.002
62. Dai, Q., Yan, Y., Ang, C.S., Kempe, K., Kamphuis, M.M., Dodds, S.J., et al. (2015). Monoclonal antibody-functionalized multilayered particles: targeting cancer cells in the presence of protein coronas. ACS Nano. 9(3), 2876-2885. doi: 10.1021/nn506929e
63. Das D, Lin S. Double-coated poly (butylcynanoacrylate) nanoparticulate delivery systems for brain targeting of dalargin via oral administration. J Pharm Sci. 2005;94:1343-1353.

64. Das S, Ngashangva L, Goswami P. Carbon Dots: An Emerging Smart Material for Analytical Applications. Micromachines. 2021;12:84.
65. Davidson BL, Breakefield XO. Viral vectors for gene delivery to the nervous system. N Rev Neurosci. 2003;4:353-364.
66. Day, E.S., Bickford, L.R., Slater, J.H., Riggall, N.S., Drezek, R.A., West, J.L. (2010). Antibody-conjugated gold-gold sulfide nanoparticles as multifunctional agents for imaging and therapy of breast cancer. Int. J. Nanomed. 5, 445.
67. De, A., Venkatesh, N., Senthil, M., Sanapalli, B.K.R., Shanmugham, R. and Karri, V.V.S.R., 2018. Smart niosomes of temozolomide for enhancement of brain targeting. *Nanobiomedicine*, *5*, p.1849543518805355.
68. de Moraes, J. (2012). Antischistosomal natural compounds: present challenges for new drug screens. In Current topics in tropical medicine IntechOpen.
69. Deb S. 2009. Degradable polymers and polymer composites for tissue engineering. Cellular Response Biomater. 28-60.
70. Doenhoff, M.J., Cioli, D., Utzinger, J. (2008). Praziquantel: mechanisms of action, resistance and new derivatives for schistosomiasis. Curr. Opin. Infect. Dis. 21(6), 659-667. doi: 10.1097/QCO.0b013e328318978f.
71. Dou, X.Q., Wang, H., Zhang, J., Wang, F., Xu, G.L., Xu, C.C., et al. (2018). Aptamer–drug conjugate: targeted delivery of doxorubicin in a her3 aptamer-functionalized liposomal delivery system reduces cardiotoxicity. Int. J. Nanomed. 13, 763. doi: 10.2147/IJN.S149887
72. Dwibhashyam V, Nagappa A. 2008. Strategies for enhanced drug delivery to the central nervous system. Indian J Pharm Sci. 70:145.
73. E Konofagou, E., Tunga, Y.S., Choia, J., Deffieuxa, T., Baseria, B. and Vlachosa, F., 2012. Ultrasound-induced blood-brain barrier opening. *Current pharmaceutical biotechnology*, *13*(7), pp.1332-1345.
74. Eatemadi, A., Daraee, H., Karimkhanloo, H., Kouhi, M., Zarghami, N., Akbarzadeh, A., Abasi, M., Hanifehpour, Y. and Joo, S.W., 2014. Carbon nanotubes: properties, synthesis, purification, and medical applications. *Nanoscale research letters*, *9*(1), pp.1-13.
75. Eissa, M.M., El Bardicy, S., Tadros, M. (2011). Bioactivity of miltefosine against aquatic stages of Schistosoma mansoni, Schistosoma haematobium and their snail hosts, supported by scanning electron microscopy. Parasit. Vectors 4(1), 73. doi: 10.1186/1756-3305-4-73
76. El Ridi, R., Tallima, H., Migliardo, F. (2017). Biochemical and biophysical methodologies open the road for effective schistosomiasis therapy and vaccination. Biochimica et Biophysica Acta (BBA)-General Subjects 1861(1), 3613-3620. doi: 10.1016/j.bbagen.2016.03.036

77. El Ridi, R.A.F., Tallima, H.A.M. (2013). Novel Therapeutic and Prevention Approaches for Schistosomiasis: Review. J. Adv. Res. 4(5), 467–478. doi: 10.1016/j.jare.2012.05.002
78. Elmowafy EM, Tiboni M, Soliman ME. 2019. Biocompatibility, biodegradation and biomedical applications of poly (lactic acid)/poly (lactic-co-glycolic acid) micro and nanoparticles. J Pharm Invest. 2019;49:347-380.
79. Elzoheiry, M., Da'dara, A.A., Bhardwaj, R., Wang, Q., Azab, M.S., El-Kholy, E.S.I., et al. (2018). Intravascular Schistosoma mansoni cleave the host immune and hemostatic signaling molecule sphingosine-1-phosphate via tegumental alkaline phosphatase. Front. Immunol. 9, 1746. doi: 10.3389/fimmu.2018.01746
80. Engelhardt B, Sorokin L. The blood-brain and the blood-cerebrospinal fluid barriers: function and dysfunction. Springer Semin Immunopathol. 2009;31(4):497-511.
81 Faghiri. Z., Skelly, P.J. (2009). The role of tegumental aquaporin from the human parasitic worm, Schistosoma mansoni, in osmoregulation and drug uptake. FASEB J. 23(8), 2780-2789. doi: 10.1096/fj.09-130757
82 Fenwick, A., Webster, J.P., Bosque-Oliva, E., Blair, L., Fleming, F.M., Zhang, Y., et al. (2009). The Schistosomiasis Control Initiative (SCI): rationale, development and implementation from 2002–2008. Parasitol. 136(13), 1719-1730. doi: 10.1017/S0031182009990400
83 Forlenza OV, Nobrega J, dos Ramos Machado L, et al. Psychiatric manifestations of neurocysticercosis: a study of 38 patients from a neurology clinic in Brazil. J Neurol Neurosurg Psych. 1997;62:612-616.
84 Frevert U, Movila A, Nikolskaia OV, et al. Early invasion of brain parenchyma by African trypanosomes. PloS One. 2012;7:e43913.
85 Fukushima S, Kasai T, Umeda Y, et al. Carcinogenicity of multi-walled carbon nanotubes: challenging issue on hazard assessment. J Occupat Health. 2017;17-0102-RA.
86 Gao J-Q, Lv Q, Li L-M, et al. Glioma targeting and blood–brain barrier penetration by dual-targeting doxorubincin liposomes. Biomater. 2013;34:5628-5639.
87 Garcia-Salcedo, J.A., Unciti-Broceta, J.D., Valverde-Pozo, J., Soriano, M. (2016). New approaches to overcome transport related drug resistance in trypanosomatid parasites. Front. Pharmacol. *7*, 351. DOI: 10.3389/fphar.2016.00351
88 Gayen B, Palchoudhury S, Chowdhury J. Carbon dots: A mystic star in the world of nanoscience. J Nanomater. 2019.
89 Ge X, Wei M, He S, Yuan W-E. Advances of non-ionic surfactant vesicles (niosomes) and their application in drug delivery. Pharm. 2019;11: 55.
90 Gharbavi M, Amani J, Kheiri-Manjili H, Danafar H, Sharafi A. Niosome: a promising nanocarrier for natural drug delivery through blood-brain barrier. Adv Parmacol Sci. 2018.

91 Giacomeli R, Izoton JC, Dos Santos RB, et al. Neuroprotective effects of curcumin lipid-core nanocapsules in a model Alzheimer's disease induced by β-amyloid 1-42 peptide in aged female mice. Brain Res. 2019;1721:146325.

92 Githui, E.K., Damian, R.T., Aman, R.A., Ali, M.A., Kamau, J.M. (2009). Schistosoma spp.: Isolation of microtubule associated proteins in the tegument and the definition of dynein light chains components. Exp. Parasitol, 121(1), 96-104. doi: 10.1016/j.exppara.2008.10.007.

93 Gobert, G.N., Schulte, L., KJones, M. (2017). Tegument and external features of Schistosoma (with particular reference to ultrastructure). Schistosoma. Biol. Pathol. Control 213. https://doi.org/10.1201/9781315368900-11.

94 Gonen, T., Walz, T. (2006). The structure of aquaporins. Quarterly Rev. Biophy. 39(4), 361-396. doi: 10.1017/S0033583506004458

95 Gray SJ, Woodard KT, Samulski RJ. Viral vectors and delivery strategies for CNS gene therapy. Therapeut Deliv. 2010;1:517-534.

96 Greene, M.K., Richards, D.A., Nogueira, J.C., Campbell, K., Smyth, P., Fernández, M., et al. (2018). Forming next-generation antibody–nanoparticle conjugates through the oriented installation of non-engineered antibody fragments. Chem. Sci. 9(1), 79-87. doi: 10.1039/c7sc02747h.

97 Guerrero ED, Lopez-Velazquez AM, Ahlawat J, Narayan M. Carbon Quantum Dots for Treatment of Amyloid Disorders. ACS Appl Nano Mater. 2021;4:2423-2433.

98 Han MH, Walker M, Zunt JR. Neurological infections in the returning international traveler. Continuum (Minneapolis, Minn) 2006;12:133.

99 Han X, Jing Z, Wu W, et al. Biocompatible and blood–brain barrier permeable carbon dots for inhibition of Aβ fibrillation and toxicity, and BACE1 activity. Nanoscale 2017;9:12862-12866.

100 Han, Z.G., Brindley, P.J., Wang, S.Y., Chen, Z. (2009). Schistosoma genomics: new perspectives on schistosome biology and host-parasite interaction. Ann Rev Genomics Hum. Genet. 10, 211-240. doi: 10.1146/annurev-genom-082908-150036.

101 Hanafy NA, El-Kemary M, Leporatti S. Micelles structure development as a strategy to improve smart cancer therapy. Cancers. 2018;10:238.

102 Harnett, W., Kusel, J.R. (1986). Increased exposure of parasite antigens at the surface of adult male Schistosoma mansoni exposed to praziquantel in vitro. Parasitol. 93(2), 401-405. doi: https://doi.org/10.1017/S0031182000051568

103 Haseeb, M.A., Eveland, L.K., Fried, B. (1985). The uptake, localization and transfer of [4-14C] cholesterol in Schistosoma mansoni males and females maintained in vitro. Comp. Biochem. Physiol. A Comp. Physiol. 82(2), 421-423. doi: 10.1016/0300-9629(85)90877-1

104 Hatakeyama H, Akita H, Maruyama K, Suhara T, Harashima H. Factors governing the in vivo tissue uptake of transferrin-coupled polyethylene glycol liposomes in vivo. Int J pharm 2004;281:25-33.

105 Hoffmann A, Wassmer SC. New syndromes identified by neuroimaging during cerebral malaria. Am J Trop Med Hygiene. 2018;98:349.

106 Hoffmann, K.F., Strand, M. (1996). Molecular identification of a Schistosoma mansoni tegumental protein with similarity to cytoplasmic dynein light chains. J. Biol. Chem. 271(42), 26117-26123. doi: 10.1074/jbc.271.42.26117

107 Hu K, Li J, Shen Y, et al. Lactoferrin-conjugated PEG–PLA nanoparticles with improved brain delivery: in vitro and in vivo evaluations. J Contr Release. 2009;134:55-61.

108 Huang R-Q, Qu Y-H, Ke W-L, et al. Efficient gene delivery targeted to the brain using a transferrin-conjugated polyethyleneglycol-modified polyamidoamine dendrimer. FASEB J. 2007;21:1117-1125.

109 Hureaux J, Lagarce F, Gagnadoux F, et al. The adaptation of lipid nanocapsule formulations for blood administration in animals. Int J Pharm. 2009;379:266-269.

110 Hwang JH, Lee KM, Park JE, et al. Atypical cerebral manifestations of disseminated Mycobacterium tuberculosis. Front Neurol. 2017;8:462.

111 Idro R, Kakooza-Mwesige A, Balyejjussa S, et al. Severe neurological sequelae and behaviour problems after cerebral malaria in Ugandan children. BMC Res Notes. 2010;3:1-6.

112 Imai K, Koibuchi T, Kumagai T, et al. Cerebral schistosomiasis due to Schistosoma haematobium confirmed by PCR analysis of brain specimen. J Clin Microbiol. 2011;49:3703.

113 Isseroff, H., Read, C.P. (1974). Studies on membrane transport—VIII. Absorption of monosaccharides by Fasciola hepatica. Comparative Biochemistry and Physiology Part A: Physiol. 47(1), 141-152. https://doi.org/10.1016/0300-9629(74)90060-7.

114 Izham, M., Nadiah, M., Hussin, Y., Aziz, M.N.M., Yeap, S.K., Rahman, H.S., et al., (2019). Preparation and Characterization of Self Nano-Emulsifying Drug Delivery System Loaded with Citraland Its Antiproliferative Effect on Colorectal Cells In Vitro. Nanomaterials. 9(7), 1028.

115 Jain, V., Gupta, A., Pawar, V.K., Asthana, S., Jaiswal, A.K., Dube, A., et al., (2014). Chitosan-assisted immunotherapy for intervention of experimental leishmaniasis via amphotericin B-loaded solid lipid nanoparticles. Appl. biochem. biotechnol. 174(4), 1309-1330. doi: 10.1007/s12010-014-1084-y

116 Jayasinghe NS, Thalagala E, Wattegama M, Thirumavalavan K. Dengue fever with diffuse cerebral hemorrhages, subdural hematoma and cranial diabetes insipidus. BMC Res Notes. 2016; 9:1-4.

117 Joo, W.D., Visintin, I., Mor, G. (2013). Targeted cancer therapy–are the days of systemic chemotherapy numbered?. Maturitas 76(4), 308-314. doi: 10.1016/j.maturitas.2013.09.008.

118 Kabanov A, Batrakova E. New technologies for drug delivery across the blood brain barrier. Curr Pharm Des. 2004;10:1355-1363.

119 Kafa H, Wang JT-W, Rubio N, et al. The interaction of carbon nanotubes with an in vitro blood-brain barrier model and mouse brain in vivo. Biomater. 2015;53:437-452.

120 Kafa H, Wang JT-W, Rubio N, et al. Translocation of LRP1 targeted carbon nanotubes of different diameters across the blood–brain barrier in vitro and in vivo. J Contr Rel. 2016;225:217-229.

121 Kannan S, Dai H, Navath RS, Balakrishnan B, Jyoti A, et al. (2012) Dendrimer-based postnatal therapy for neuroinflammation and cerebral palsy in a rabbit model. Science translational medicine 4: 130ra146-130ra146.

122 Karakatsani ME, Blesa J, Konofagou EE. Blood–brain barrier opening with focused ultrasound in experimental models of Parkinson's disease. Mov Disord. 2019;34:1252-1261.

123 Karaman R. Prodrugs Design Based on Inter-and Intramolecular Chemical Processes. Chem Biol Drug Des. 2013;82:643-668.

124 Karimi M, Solati N, Amiri M, et al. Carbon nanotubes part I: preparation of a novel and versatile drug-delivery vehicle. Expert Opin Drug Deliv. 2015;12:1071-1087.

125 Kašný, M., Haas, W., Jamieson, B.G., Horák, P. (2017). Cercaria of Schistosoma. Schistosoma: Biology. Pathol. Control 149.

126 Katz, M. (1977). Antihelmintics. Drugs 13(2),124-136.

127 Kaushal M, Shabani S, Cochran EJ, Samra H, Zwagerman NT. Cerebral Trypanosomiasis in an Immunocompromised Patient: Case Report and Review of the Literature. World Neurosurg. 2019;129:225-231.

128 Khan I, Saeed K, Khan I. Nanoparticles: Properties, applications and toxicities. Arabian J Chem. 2019;12:908-931.

129 Kim J-Y, Choi WI, Kim YH, Tae G. Brain-targeted delivery of protein using chitosan- and RVG peptide-conjugated, pluronic-based nano-carrier. Biomater. 2013;34:1170-1178.

130 Kim SW, Kim T, Kim YS, et al. Surface modifications for the effective dispersion of carbon nanotubes in solvents and polymers. Carbon 2012;50:3-33.

131 Kohlstädt, S., Couissinier-Paris, P., Bourgois, A., Bouchon, B., Piper, K., Kolbe, H., et al. (1997). Characterization of a schistosome T cell-stimulating antigen (Sm10) associated

with protective immunity in humans. Mol. Biochem. Parasitol. 84(2), 155-165. https://doi.org/10.1016/S0166-6851(96)02787-9.

132 Kohn, A.B., Anderson, P.A., Roberts-Misterly, J.M Greenberg, R.M. (2001). Schistosome calcium channel β subunits unusual modulatory effects and potential role in the action of the antischistosomal drug praziquantel. J. Biol. Chem. 276(40), 36873-36876. DOI: 10.1074/jbc.C100273200

133 Korkmaz, E., Friedrich, E.E., Ramadan, M.H., Erdos, G., Mathers, A.R., Ozdoganlar, O.B., et al. (2016). Tip-loaded dissolvable microneedle arrays effectively deliver polymer-conjugated antibody inhibitors of tumor-necrosis-factor-alpha into human skin. J. Pharm. Sci. 105(11), 3453-7. doi: 10.1016/j.xphs.2016.07.008

134 Kovacs ZI, Kim S, Jikaria N, et al. Disrupting the blood–brain barrier by focused ultrasound induces sterile inflammation. Proc Natl Acad Sci. 2017;114:E75-E84.

135 Kowouvi, K., Alies, B., Gendrot, M., Gaubert, A., Vacher, G., Gaudin, K., et al., (2019). Nucleoside-lipid-based nanocarriers for methylene blue delivery: potential application as anti-malarial drug. RSC Advances. 9(33), 18844-18852.

136 Krautz-Peterson, G., Simoes, M., Faghiri, Z., Ndegwa, D., Oliveira, G., Shoemaker, C.B., et al. (2010). Suppressing glucose transporter gene expression in schistosomes impairs parasite feeding and decreases survival in the mammalian host. PLoS Pathog. 6(6), e1000932. doi: 10.1371/journal.ppat.1000932.

137 Kulkarni SA, Feng S-S. Effects of surface modification on delivery efficiency of biodegradable nanoparticles across the blood–brain barrier. Nanomed. 2011;6:377-394.

138 Kumar GP, Rajeshwarrao P. Nonionic surfactant vesicular systems for effective drug delivery—an overview. Acta Pharm Sinica B 2011;1:208-219.

139 Kumari A, Singla R, Guliani A, Yadav SK. Nanoencapsulation for drug delivery. EXCLI J. 2014;13:265.

140 Lei, Z., Mengying, Z., Dongdong, B., Xiaoyu, Q., Yifei, G., Xiangtao, W., et al. (2019). Alendronate-modified polydopamine-coated paclitaxel nanoparticles for osteosarcoma-targeted therapy. J. Drug Deliv. Sci. Technol. 101133. https://doi.org/10.1016/j.jddst.2019.101133.

141 Li S, Peng Z, Dallman J, et al. Crossing the blood–brain–barrier with transferrin conjugated carbon dots: A zebrafish model study. Colloids and Surfaces B: Biointerfaces 2016;145:251-256.

142 Li, S., Bouchy, S., Penninckx, S., Marega, R., Fichera, O., Gallez, B., et al. 2019. Antibody-functionalized gold nanoparticles as tumor-targeting radiosensitizers for proton therapy. Nanomed. 14(3), 317-333. doi: 10.2217/nnm-2018-0161.

143 Li, T., Takeoka, S. (2018). 3 - Smart Liposomes for Drug Delivery. Smart Nanoparticles for Biomedicine. 31-47. https://doi.org/10.1016/B978-0-12-814156-4.00003-3.

144 Li, Y., Auliff, A., Jones, M.K., Yi, X., McManus, D.P. (2000). Immunogenicity and immunolocalization of the 22.6 kDa antigen of Schistosoma japonicum. Parasite Immunol. 22(8), 415-424. doi: 10.1046/j.1365-3024.2000.00319.x

145 Liu H, Lim CT, Feng X, et al. MRI in cerebral schistosomiasis: characteristic nodular enhancement in 33 patients. Am J Roentgenol. 2008;191:582-588.

146 Liu J, Li R, Yang B. Carbon Dots: A New Type of Carbon-Based Nanomaterial with Wide Applications. ACS Central Science. 2020

147 Liu Z, Tabakman S, Welsher K, Dai H. Carbon nanotubes in biology and medicine: in vitro and in vivo detection, imaging and drug delivery. Nano Res. 2009;2:85-120.

148 Liu, F., Lu, J., Hu, W., Wang, S.Y., Cui, S.J., Chi, M., et al. (2006). New perspectives on host-parasite interplay by comparative transcriptomic and proteomic analyses of Schistosoma japonicum. PLoS Pathog. 2(4), e29. doi: 10.1371/journal.ppat.0020029

149 Lohan S, Raza K, Mehta S, et al. Anti-Alzheimer's potential of berberine using surface decorated multi-walled carbon nanotubes: a preclinical evidence. Int J Pharm. 2017;530:263-278.

150 Longmuir, K.J., Robertson, R.T., Haynes, S.M., Baratta, J.L., Waring, A.J., (2006). Effective targeting of liposomes to liver and hepatocytes in vivo by incorporation of a Plasmodium amino acid sequence. Pharm. res. 23(4), 759-769. DOI: 10.1007/s11095-006-9609-x

151 Lu C-T, Zhao Y-Z, Wong HL, et al. Current approaches to enhance CNS delivery of drugs across the brain barriers. Int J Nanomed. 2014;9:2241.

152 Lü J-M, Wang X, Marin-Muller C, et al. Current advances in research and clinical applications of PLGA-based nanotechnology. Expert Rev Mol Diagnostics 2009;9:325-341.

153 Lury KM, Castillo M. Chagas' disease involving the brain and spinal cord: MRI findings. Am J Roentgenol. 2005;185:550-552.

154 MacDonald, K., Buxton, S., Kimber, M.J., Day, T.A., Robertson, A.P., Ribeiro, P. (2014). Functional characterization of a novel family of acetylcholine-gated chloride channels in Schistosoma mansoni. PLoS Pathog. 10(6), e1004181. doi: 10.1371/journal.ppat.1004181

155 Madaan K, Kumar S, Poonia N, Lather V, Pandita D. Dendrimers in drug delivery and targeting: Drug-dendrimer interactions and toxicity issues. J Pharm Bioallied Sci. 2014;6:139.

156 Madi D, Achappa B, Ramapuram JT, et al. Dengue encephalitis–A rare manifestation of dengue fever. Asian Pacific J Trop Biomed. 2014;4:S70-S72.

157 Mandel RJ, Manfredsson FP, Foust KD, et al. Recombinant adeno-associated viral vectors as therapeutic agents to treat neurological disorders. Mol Ther. 2006;13:463-483.

158 Mansour, T., Mansour, J. (2002). Targets in the Tegument of Flatworms. In Chemotherapeutic Targets in Parasites: Contemporary Strategies 189-214.

159 Marques, J., Valle-Delgado, J.J., Urbán, P., Baró, E., Prohens, R., Mayor, A., et al., (2017). Adaptation of targeted nanocarriers to changing requirements in antimalarial drug delivery. Nanomed. Nanotechnol. Biol. Med. 13(2), 515-525. doi: 10.1016/j.nano.2016.09.010

160 Mathieu, S., Cisse, C., Vitale, S., Ahmadova, A., Degardin, M., Perard, J., et al. (2016). From peptide aptamers to inhibitors of FUR, bacterial transcriptional regulator of iron homeostasis and virulence. ACS Chem. Bol. 11(9), 2519-2528. doi: 10.1021/acschembio.6b00360

161 Mbanefo, E.C., Takashi, K., Yukinobu, K., Tomoaki, K., Rieko, F., Mahamoud, S.C., et al., (2015). Immunogenicity and anti-fecundity effect of nanoparticle coated glutathione S-transferase (SjGST) DNA vaccine against murine Schistosoma japonicum infection. Parasitol. Int. 64 (4), 24-31. doi: 10.1016/j.parint.2015.01.005.

162 McKenzie, M., Kirk, R.S., Walker, A.J. (2017). Glucose Uptake in the Human Pathogen Schistosoma mansoni Is Regulated Through Akt/Protein Kinase B Signaling. J. Inf. Dis. 218(1), 152-164. doi: 10.1093/infdis/jix654

163 Mehlhorn, H., Becker, B., Andrews, P., Thomas, H., Frenkel, J.K. (1981). In vivo and in vitro experiments on the effects of praziquantel on Schistosoma mansoni. A light and electron microscopic study. Arzneimittel-forschung 31(3a), 544-554.

164 Mehrizi, T.Z., Ardestani, M.S., Hoseini, M.H.M., Khamesipour, A., Mosaffa, N. and Ramezani, A. (2018). Novel Nanosized Chitosan-Betulinic Acid Against Resistant Leishmania Major and First Clinical Observation of such parasite in Kidney. Scientific reports. 8(1), 11759.

165 Melo GD, Goyard S, Fiette L, et al. Unveiling Cerebral Leishmaniasis: parasites and brain inflammation in Leishmania donovani infected mice. Sci Rep. 2017;7:1-13.

166 Misra A, Ganesh S, Shahiwala A, Shah SP. Drug delivery to the central nervous system: a review. J Pharm Pharm Sci 2003;6:252-273.

167 Mitchell MJ, Billingsley MM, Haley RM, et al. Engineering precision nanoparticles for drug delivery. Nat Rev Drug Discov. 2020;1-24.

168 Mittal P, Saharan A, Verma R, et al. Dendrimers: A New Race of Pharmaceutical Nanocarriers. BioMed Res Int. 2021.

169 Mohammad, O., Varshney, G.C., Subhash Chandra, A.C., Gupta, C.M. (1995). Chloroquine encapsulated in malaria-infected erythrocyte-specific antibody-bearing liposomes effectively controls chloroquine-resistant Plasmodium berghei infections in mice. Antimicrobial agents. chemother. 39 (1), 80-184. DOI: 10.1128/aac.39.1.180

170 Morgan, J.A., de Jong, R.J., Snyder, S.D., Mkoji, G.M., Loker, E.S. (2001). *Schistosoma mansoni* and *Biomphalaria*: past history and future trends. Parasitol. 123, S211–S228. doi: 10.1017/s0031182001007703

171 Moryś JM, Jeżewska M, Korzeniewski K. Neuropsychiatric manifestations of some tropical diseases. Int Marit Health. 2015;66:30-35.

172 Moura RP, Pacheco C, Pêgo AP, des Rieux A, Sarmento B. Lipid nanocapsules to enhance drug bioavailability to the central nervous system. J Contr Rel 2020;322:390-400.

173 Mufamadi, M.S., Choonara, Y.E., Kumar, P., Modi, G., Naidoo, D., Vuuren, S., et al. (2013). Ligand-functionalized nanoliposomes for targeted delivery of galantamine, Int. J. Pharm. 448(1), 267-281. doi: 10.1016/j.ijpharm.2013.03.037

174 Mukherjee S, Ray S, Thakur R. Solid lipid nanoparticles: a modern formulation approach in drug delivery system. Indian J Pharm Sci. 2009;71:349.

175 Mulvenna, J., Moertel, L., Jones, M.K., Nawaratna, S., Lovas, E.M., Gobert, G.N., et al. (2010). Exposed proteins of the Schistosoma japonicum tegument. Intl. J. Parasitol. 40(5), 543-554. doi: 10.1016/j.ijpara.2009.10.002

176 Mulvenna, J., Moertel, L., Jones, M.K., Nawaratna, S., Lovas, E.M., Gobert, G.N., et al. (2010). Exposed proteins of the Schistosoma japonicum tegument. Int. J. Parasitol. 40(5), 543-554. doi: 10.1016/j.ijpara.2009.10.002.

177 Nanjwade BK, Bechra HM, Derkar GK, Manvi F, Nanjwade VK (2009) Dendrimers: emerging polymers for drug-delivery systems. European Journal of Pharmaceutical Sciences 38: 185-196.

178 Naqvi S, Panghal A, Flora S. Nanotechnology: a promising approach for delivery of neuroprotective drugs. Front Neurosci. 2020;14.

179 Nare. B., Smith, J.M., Prichard, R.K. (1992). Mechanisms of inactivation of and mammalian glutathione -transferase activity by the anti- schistosomal drug oltipraz. Biochem. Pharmaco. 43(6), 1345- 1351.

180 Neves AR, Queiroz JF, Reis S. Brain-targeted delivery of resveratrol using solid lipid nanoparticles functionalized with apolipoprotein E. J Nanobiotechnol. 2016;14:1-11.

181 Nijjar SS, Del Bigio MR. Cerebral trypanosomiasis in an incarcerated man. Cmaj 2007;176:448-448.

182 Noriega-Luna B, Godínez LA, Rodríguez FJ, et al. Applications of dendrimers in drug delivery agents, diagnosis, therapy, and detection. J Nanomater. 2014.

183 Oliveira, C.R., Rezende, C.M., Silva, M.R., Borges, O.M., Pêgo, A.P., Goes, A.M., 2012. Oral vaccination based on DNA-chitosan nanoparticles against Schistosoma mansoni infection. Scientific World Journal, 2012. doi: 10.1100/2012/938457.

184 Pakhira B, Ghosh M, Allam A, Sarkar S. Carbon nano onions cross the blood brain barrier. RSC Adv. 2016;6:29779-29782.

185 Pathak YV. Surface modification of nanoparticles for targeted drug delivery: Springer. 2019

186 Patra JK, Das G, Fraceto LF, et al. Nano based drug delivery systems: recent developments and future prospects. J Nanobiotechnol. 2018;16:1-33.

187 Pavan B, Dalpiaz A, Ciliberti N, et al. Progress in drug delivery to the central nervous system by the prodrug approach. Mol. 2008;13:1035-1065.

188 Pax, R., Bennett, J.L., Fetterer, R. (1978). A benzodiazepine derivative and praziquantel: effects on musculature of Schistosoma mansoni and Schistosoma japonicum. Naunyn-Schmiedebergs Arch. Pharmacol. 304(3), 309-315. doi: 10.1007/bf00507974

189 Peira E, Marzola P, Podio V, et al. In vitro and in vivo study of solid lipid nanoparticles loaded with superparamagnetic iron oxide. J Drug Tar. 2003;11:19-24.

190 Pentreath V, Baugh P, Lavin D. Sleeping sickness and the central nervous system. 1994.

191 Pérez-Sánchez, R., Ramajo-Hernández, A., Ramajo-Martín, V., Oleaga, A. (2006). Proteomic analysis of the tegument and excretory-secretory products of adult Schistosoma bovis worms. Proteomics 6(S1), S226-S236. doi: 10.1002/pmic.200500420

192 Perez, H., Terry, R.J. (1973). The killing of adult Schistosoma mansoni in vitro in the presence of antisera to host antigenic determinants and peritoneal cells. Int. J. Parasitol. 3(4), 499-503. doi: 10.1016/0020-7519(73)90046-5

193 Petersen CA, Greenlee MHW. Neurologic manifestations of Leishmania spp. infection. J Neuroparasitol. 2011;2.

194 Pitt WG, Husseini GA, Staples BJ. Ultrasonic drug delivery–a general review. Exert Opin Drug Deliv. 2004;1:37-56.

195 Plonska-Brzezinska ME. Carbon Nano-Onions: A Review of Recent Progress in Synthesis and Applications. Chem Nano Mat. 2019;5:568-580.

196 Popiel, I., Basch, P.F. (1984). Reproductive development of female Schistosoma mansoni (Digenea: Schistosomatidae) following bisexual pairing of worms and worm segments. J. Exp. Zool. 232(1), 141-150. doi: 10.1002/jez.1402320117

197 Popiel, I., Basch, P.F. (1986). Schistosoma mansoni: cholesterol uptake by paired and unpaired worms. Exp. Parasitol. 61(3), 343-347. doi: 10.1016/0014-4894(86)90189-x

198 Prajapati SK, Maurya SD, Das MK, et al. Dendrimers in drug delivery, diagnosis and therapy: basics and potential applications. J Drug Deliv Thera 2016;6:67-92.

199 Puccioni-Sohler M, Rosadas C, Cabral-Castro MJ. Neurological complications in dengue infection: a review for clinical practice. Arq Neuropsiquiatr. 2013;71:667-671.

200 Puri A, Loomis K, Smith B, et al. Lipid-based nanoparticles as pharmaceutical drug carriers: from concepts to clinic. Crit Rev Therapeut Drug Carrier Systems. 2009;26.

201 Rao KS, Reddy MK, Horning JL, Labhasetwar V. TAT-conjugated nanoparticles for the CNS delivery of anti-HIV drugs. Biomater. 2008;29:4429-4438.

202 Ravi N, Yi W, Yu L, Ping H, Hao C. Cerebral schistosomiasis. SA J Radiol. 2013;17.

203 Rehman M, Madni A, Shi D, et al. Enhanced blood brain barrier permeability and glioblastoma cell targeting via thermoresponsive lipid nanoparticles. Nanoscale 2017;9:15434-15440.

204 Reverdatto, S., Burz, D.S., Shekhtman, A. (2015). Peptide aptamers: development and applications. Curr. Topics Med. Chem. 15(12), 1082. DOI: 10.2174/1568026615666150413153143

205 Richter, J. (2003). The impact of chemotherapy on morbidity due to schis- tosomiasis, Acta Trop. 86(2–3), 161-183. doi: 10.1016/s0001-706x(03)00032-9

206 Roberts M, Cross J, Pohl U, Lucas S, Dean A. Cerebral schistosomiasis. Lancet Infect Dis. 2006;6:820.

207 Roberts, A.J., Kon, T., Knight, P.J., Sutoh, K., Burgess, S.A. (2013). Functions and mechanics of dynein motor proteins. Nat. Rev. Mol. Cell Biol. *14*(11), 713. doi: 10.1038/nrm3667

208 Rogers, S.H., Bueding, E. (1975). Anatomical localization of glucose uptake by Schistosoma mansoni adults. Int. J. Parasitol. 5(3), 369-371. doi: 10.1016/0020-7519(75)90086-7

209 Rose MF, Zimmerman EE, Hsu L, et al. Atypical presentation of cerebral schistosomiasis four years after exposure to Schistosoma mansoni. Epilepsy Behav Case Rep. 2014;2:80-85.

210 Ruff, J., Hüwel, S., Kogan, M.J., Simon, U., Galla, H.J. (2017). The effects of gold nanoparticles functionalized with ß-amyloid specific peptides on an in vitro model of blood–brain barrier. Nanomedicine: Nanotechnol. Biol. Med. 13(5), 1645-1652. doi: 10.1016/j.nano.2017.02.013.

211 Säälik, P., Lingasamy, P., Toome, K., Mastandrea, I., Rousso-Noori, L., Tobi, A., et al. (2019). Peptide-guided nanoparticles for glioblastoma targeting. J. Control Release. 308:109-118. doi: 10.1016/j.jconrel.2019.06.018

212 Saconato, H., Atallah, A. (2000). Interventions for treating *Schistosomiasi mansoni*. Cochrane Data System Review. https://doi.org/10.1002/14651858.CD000528

213 Sáenz B, Ruíz-Garcia M, Jiménez E, et al. Neurocysticercosis: clinical, radiologic, and inflammatory differences between children and adults. Pediatric Infect Dis J. 2006;25:801-803.

214 Sahu PK, Hoffmann A, Majhi M, et al. Brain Magnetic Resonance Imaging Reveals Different Courses of Disease in Pediatric and Adult Cerebral Malaria. Clin Infect Dis. 2020

215 Saliou B, Thomas O, Lautram N, et al. Development and in vitro evaluation of a novel lipid nanocapsule formulation of etoposide. Eur J Pharm Sci 2013;50:172-180.

216 Sánchez A, Mejía SP, Orozco J. Recent Advances in Polymeric Nanoparticle-Encapsulated Drugs against Intracellular Infections. Mol. 2020;25:3760.

217 Sandoval-Yañez C, Castro Rodriguez C. Dendrimers: Amazing platforms for bioactive molecule delivery systems. Mater. 2020;13:570.

218 Santos A, Veiga F, Figueiras A. Dendrimers as pharmaceutical excipients: Synthesis, properties, toxicity and biomedical applications. Mater. 2020;13:65.

219 Secret, E., Smith, K., Dubljevic, V., Moore, E., Macardle, P., Delalat, B., et al. (2013). Antibody-functionalized porous silicon nanoparticles for vectorization of hydrophobic drugs. Adv. Healthcare Materials 2(5), 718-727. doi: 10.1002/adhm.201200335.

220 Shah R, Chakrabarti S. Neuropsychiatric manifestations and treatment of disseminated neurocysticercosis: a compilation of three cases. Asian J Psychiatr. 2013;6:344-346.

221 Sharma R, Kim S-Y, Sharma A, et al. Activated microglia targeting dendrimer–minocycline conjugate as therapeutics for neuroinflammation. Bioconjug Chem. 2017;28:2874-2886.

222 Sharma U, Saxena S, Kanchan S. Cerebral (encephalopathy) associated with ascariasis. Indian J Pediatr. 1974;41:356-361.

223 Shaw TK, Mandal D, Dey G, et al. Successful delivery of docetaxel to rat brain using experimentally developed nanoliposome: a treatment strategy for brain tumor. Drug Deliv. 2017;24:346-357.

224 Shiraishi K, Wang Z, Kokuryo D, Aoki I, Yokoyama M. A polymeric micelle magnetic resonance imaging (MRI) contrast agent reveals blood–brain barrier (BBB) permeability for macromolecules in cerebral ischemia-reperfusion injury. J Contr Rel 2017;253:165-171.

225 Shrivastava A, Arora P, Khare A, Goel G, Kapoor N. Central nervous system filariasis masquerading as a glioma: case report. J Neurosurg. 2016;127:691-693.

226 Silva, J.M., Eva, Z., Gaëlle, V., Vanessa, G.O., Ana, S., Mafalda, V., Manuela, G., et al. (2015). "In vivo delivery of peptides and Toll-like receptor ligands by mannose-

functionalized polymeric nanoparticles induces prophylactic and therapeutic anti-tumor immune responses in a melanoma model." J. Contr. Release 198, 91-103. doi: 10.1016/j.jconrel.2014.11.033

227 Simanon, N., Adisakwattana, P., Thiangtrongjit, T., Limpanont, Y., Chusongsang, P., Chusongsang, Y., et al. (2019). Phosphoproteomics analysis of male and female Schistosoma mekongi adult worms. Scientific Reports. 9(1), 10012. doi: 10.1038/s41598-019-46456-6.

228 Skelly PJ, Shoemaker CB. (2000). Induction cues for tegument formation during the transformation of Schistosoma mansoni cercariae. Int. J. Parasitol. 30(5):625-631. doi: 10.1016/s0020-7519(00)00031-x

229 Skelly, P.J., Da'dara, A.A., Li, X.H., Castro-Borges, W., Wilson, R.A. (2014). Schistosome feeding and regurgitation. PLoS Pathog. 10(8), e1004246. doi: 10.1371/journal.ppat.1004246

230 Skelly, P.J., Da'dara, A.A., Li, X.H., Castro-Borges, W., Wilson, R.A. (2014). Schistosome feeding and regurgitation. PLoS pathog. 10(8), e1004246. doi: 10.1371/journal.ppat.1004246

231 Skelly, P.J., Kim, J.W., Cunningham, J., Shoemaker, C.B. (1994). Cloning, characterization, and functional expression of cDNAs encoding glucose transporter proteins from the human parasite Schistosoma mansoni. J. Biol. Chem. 269(6), 4247-4253.

232 Skelly, P.J., Shoemaker, C.B. (1996). Rapid appearance and asymmetric distribution of glucose transporter SGTP4 at the apical surface of intramammalian-stage Schistosoma mansoni. Pro. Nat. Aca. Sci. 93(8), 3642-3646. doi: 10.1073/pnas.93.8.3642

233 Skelly, P.J., Shoemaker, C.B. (2001). The Schistosoma mansoni host-interactive tegument forms from vesicle eruptions of a cyton network. Parasitol. 122(1), 67-73. doi: 10.1017/s0031182000007071

234 Skelly, P.J., Tielens, A.G.M., Shoemaker, C.B. (1998). Glucose transport and metabolism in mammalian-stage schistosomes. Parasitol. Today 14(10), 402-406. doi: 10.1016/s0169-4758(98)01319-2

235 Sotillo, J., Pearson, M., Becker, L., Mulvenna, J., Loukas, A. (2015). A quantitative proteomic analysis of the tegumental proteins from Schistosoma mansoni schistosomula reveals novel potential therapeutic targets. Int. J. Parasitol. 45(8), 505-516. doi: 10.1016/j.ijpara.2015.03.004.

236 Sotillo, J., Pearson, M., Potriquet, J., Becker, L., Pickering, D., Mulvenna, J., et al. (2016). Extracellular vesicles secreted by Schistosoma mansoni contain protein vaccine candidates. Int. J. Parasitol. 46(1),1-5. doi: 10.1016/j.ijpara.2015.09.002

237 Sotillo, J., Pearson, M.S., Becker, L., Mekonnen, G., Amoah, A.S., van Dam, G., et al. (2019). In-depth proteomic characterization of Schistosoma haematobium: Towards the development of new tools for elimination. PLoS Neg. Trop. Dis. 13(5), e0007362. doi: 10.1371/journal.pntd.0007362.

238 Stamatovic SM, Johnson AM, Keep RF, Andjelkovic AV. Junctional proteins of the blood-brain barrier: new insights into function and dysfunction. Tissue barriers. 2016;4:e1154641.

239 Stella VJ, Charman W, Naringrekar VH. Prodrugs. Drugs. 1985;29:455-473.

240 Su S, Kang PM. Systemic review of biodegradable nanomaterials in nanomedicine. Nanomater. 2020;10:656.

241 Tan, K.X., Danquah, M.K., Pan, S., Yon, L.S. (2019). Binding Characterization of Aptamer-Drug Layered Microformulations and In Vitro Release Assessment. J. Pharm. Sci. doi: 10.1016/j.xphs.2019.03.037

242 Teleanu DM, Chircov C, Grumezescu AM, Volceanov A, Teleanu RI (2018) Blood-brain delivery methods using nanotechnology. Pharmaceutics 10: 269.

243 Teran-Saavedra, N.G., Sarabia-Sainz, J.A.I., Silva-Campa, E., Burgara-Estrella, A.J., Guzmán-Partida, A.M., Ramos-Clamont Montfort, G., et al., (2019). Lactosylated albumin nanoparticles: Potential drug nanovehicles with selective targeting toward an in vitro model of hepatocellular carcinoma. Molecules. 24(7), 1382.

244 Thetiot-Laurent, S.A.L., Boissier, J., Robert, A., Meunier, B. (2013). Schistosomiasis Chemotherapy. Angewandte Chemie International Edition 52, 7936–7956. doi: 10.1002/anie.201208390.

245 Topal GR, Mészáros M, Porkoláb G, et al. ApoE-Targeting Increases the Transfer of Solid Lipid Nanoparticles with Donepezil Cargo across a Culture Model of the Blood–Brain Barrier. Pharma. 2021;13:38.

246 Tousif, S., Singh, D.K., Mukherjee, S., Ahmad, S., Arya, R., Nanda, R., et al., (2017). nanoparticle-Formulated curcumin Prevents Posttherapeutic Disease reactivation and reinfection with Mycobacterium tuberculosis following isoniazid Therapy. Front. immunol. 8, 739. doi: 10.3389/fimmu.2017.00739

247 Tran, M.H., Freitas, T.C., Cooper, L., Gaze, S., Gatton, M.L., Jones, M.K., et al. (2010). Suppression of mRNAs encoding tegument tetraspanins from Schistosoma mansoni results in impaired tegument turnover. PLoS Pathog. 6(4), e1000840. doi: 10.1371/journal.ppat.1000840

248 Tsukaguchi, H., Shayakul, C., Berger, U.V., Mackenzie, B., Devidas, S., Guggino, W.B., et al. (1998). Molecular characterization of a broad selectivity neutral solute channel. J. Biol. Chem. 273(38), 24737-24743. doi: 10.1074/jbc.273.38.24737

249 Tsukaguchi, H., Weremowicz, S., Morton, C.C., Hediger, M.A. (1999). Functional and molecular characterization of the human neutral solute channel aquaporin-9. Am. J. Physiol-Renal Physiol. 277(5), F685-F696.

250 Uglem, G.L Read, C.P. (1975). Sugar transport and metabolism in Schistosoma mansoni. J. Parasitol. 61(3), 390-397.

251 Uglem, G.L., Lee, K.J. (1985). Proterometra macrostoma (Trematoda: Azygiidae): Functional morphology of the tegument of the redia. Int. J. Parasitol. 15(1), 61-64. https://doi.org/10.1016/0020-7519(85)90102-X.

252 Upadhyay RK. Drug delivery systems, CNS protection, and the blood brain barrier. BioMed Res Int. 2014.

253 Urman, H.K., Bniay, O., Clayson, B.D., Shubik, P. (1975). Carcinogenic effects of niridazole. Cancer Letters 1, 69-74. doi: 10.1016/s0304-3835(75)95362-8

254 Van Hellemond, J.J., Retra, K., Brouwers, J.F., van Balkom, B.W., Yazdanbakhsh, M., Shoemaker, C.B., et al. (2006). Functions of the tegument of schistosomes: clues from the proteome and lipidome. Int. J. Parasitol. 36(6), 691-699. doi: 10.1016/j.ijpara.2006.01.007

255 Veerasamy, R., Xin, T.Z., Gunasagaran, S., Xiang, T.F.W., Yang, E.F.C., Jeyakumar, N., et al. (2011). Biosynthesis of silver nanoparticles using mangosteen leaf extract and evaluation of their antimicrobial activities. J. Saudi Chem. Soc. 15(2), 113-120. https://doi.org/10.1016/j.jscs.2010.06.004.

256 Verkman, A.S., 2013. Aquaporins. Curr. Biol. 23(2), R52-R55. doi: 10.1016/j.cub.2012.11.025

257 Wan H, Lei D, Mao Q. Cerebellar schistosomiasis: a case report with clinical analysis. Korean J Parasitol. 2009;47:53.

258 Wang S, Li C, Qian M, et al. Augmented glioma-targeted theranostics using multifunctional polymer-coated carbon nanodots. Biomater. 2017;141:29-39.

259 Wang, Z., Wu, Z., Liu, J. and Zhang, W. (2018). Particle morphology: an important factor affecting drug delivery by nanocarriers into solid tumors. Expert opin. drug deliv. 15(4), 379-395. doi: 10.1080/17425247.2018.1420051

260 Warren KE. Beyond the blood: brain barrier: the importance of central nervous system (CNS) pharmacokinetics for the treatment of CNS tumors, including diffuse intrinsic pontine glioma. Front Oncol. 2018;8:239.

261 Weerasinghe W, Medagama A. Dengue hemorrhagic fever presenting as encephalitis: a case report. J Med Case Rep. 2019;13:1-6.

262 Wendt, G.R., Collins, J.N., Pei, J., Pearson, M.S., Bennett, H.M., Loukas, A., et al. (2018). Flatworm-specific transcriptional regulators promote the specification of tegumental progenitors in Schistosoma mansoni. Elife 7, e33221. doi: 10.7554/eLife.33221

263 Wilson B, Samanta MK, Santhi K, et al. Poly (n-butylcyanoacrylate) nanoparticles coated with polysorbate 80 for the targeted delivery of rivastigmine into the brain to treat Alzheimer's disease. Brain Res. 2008;1200:159-168.

264 Wilson, R.A., Barnes, P.E. (1977). The formation and turnover of the membranocalyx on the tegument of Schistosoma mansoni. Parasitol. 74(1), 61-71. doi: 10.1017/s0031182000047533

265 Wong HL, Bendayan R, Rauth AM, Li Y, Wu XY. Chemotherapy with anticancer drugs encapsulated in solid lipid nanoparticles. Adv Drug Deliv Rev. 2007;59:491-504.

266 Xie F, Yao N, Qin Y, et al. Investigation of glucose-modified liposomes using polyethylene glycols with different chain lengths as the linkers for brain targeting. Int J Nanomed. 2012;7:163.

267 Yamagiwa K. XXIV. Beitrag zur Aetiologie der Jackson'schen Epilepsie. Band 119: De Gruyter. 1890;447-460.

268 Yang, D., Meng, X., Yu, Q., Xu, L., Long, Y., Liu, B., et al. (2013). Inhibition of hepatitis C virus infection by DNA aptamer against envelope protein. Antimicro. Agents Chemother. 57(10), 4937-4944. doi: 10.1128/AAC.00897-13

269 Yang, W., Jones, M.K., Fan, J., Hughes-Stamm, S.R., McManus, D.P. (1999). Characterisation of a family of Schistosoma japonicum proteins related to dynein light chains. Biochimica et Biophysica Acta (BBA)-Protein Struct. Mol. Enzymol.1432(1), 13-26. doi: 10.1016/s0167-4838(99)00089-8

270 Yoo TW, Mlikotic A, Cornford ME, Beck CK. Concurrent cerebral American trypanosomiasis and toxoplasmosis in a patient with AIDS. Clin Infect Dis. 2004;39:e30-e34.

271 Yu, C., Hu, Y., Duan, J., Yuan, W., Wang, C., Xu, H., et al. (2011). Novel aptamer-nanoparticle bioconjugates enhances delivery of anticancer drug to MUC1-positive cancer cells in vitro. PloS One 6(9), p.e24077. doi: 10.1371/journal.pone.0024077.

272 Zaki S, Lad V. Encephalopathy as a presenting feature of ascariasis in a child. Indian J Critic Care Med. 2011;15:63.

273 Zaqout A, Abid FB, Murshed K, et al. Cerebral schistosomiasis: Case series from Qatar. Int J Infect Dis. 2019;86:167-170.

274 Zhang F, Magruder JT, Lin Y-A, et al. Generation-6 hydroxyl PAMAM dendrimers improve CNS penetration from intravenous administration in a large animal brain injury model. J Contr Rel. 2017;249:173-182.

275 Zhang P, Hu L, Yin Q, Feng L, Li Y. Transferrin-modified c [RGDfK]-paclitaxel loaded hybrid micelle for sequential blood-brain barrier penetration and glioma targeting therapy. Mol Pharm. 2012;9:1590-1598.

276 Zhang, S., Skinner, D., Joshi, P., Criado-Hidalgo, E., Yeh, Y.T., Lasheras, J.C., et al. (2019). Quantifying the mechanics of locomotion of the schistosome pathogen with respect to changes in its physical environment. J. Royal Soc. Interf. 16(150), 2018-0675. https://doi.org/10.1098/rsif.2018.0675.

277 Zhang, W., Zhu, J., Song, X., Xu, Z., Xue, X., Chen, X., et al. (2015). An association of Aquaporin-4 with the immunoregulation of liver pathology in mice infected with Schistosoma japonicum. Parasites Vectors 8(1), 37. doi: 10.1186/s13071-015-0650-7

278 Zheng M, Ruan S, Liu S, et al. Self-targeting fluorescent carbon dots for diagnosis of brain cancer cells. ACS Nano 2015;9:11455-11461.

279 Zhong, C., Skelly, P.J., Leaffer, D., Cohn., R.G., Caulfield, J.P., Shoemaker, C.B. (1995). Immunolocalization of a Schistosoma mansoni facilitated diffusion glucose transporter to the basal, but not the apical, membranes of the surface syncytium. Parasitol

280 Zhou Y, Liyanage PY, Devadoss D, et al. Nontoxic amphiphilic carbon dots as promising drug nanocarriers across the blood–brain barrier and inhibitors of β-amyloid. Nanoscale 2019;11:22387-22397.

CHAPTER THREE

SYNTHESIS AND THERAPEUTIC DELIVERY APPROACHES FOR PRAZIQUANTEL: A PATENT REVIEW (2010-PRESENT)

Taylor & Francis

Expert Opinion on Therapeutic Patents

ISSN: (Print) (Online) Journal homepage: https://www.tandfonline.com/loi/ietp20

Synthesis and therapeutic delivery approaches for praziquantel: a patent review (2010-present)

Tayo A. Adekiya, Pradeep Kumar, Pierre P.D. Kondiah, Viness Pillay & Yahya E. Choonara

To cite this article: Tayo A. Adekiya, Pradeep Kumar, Pierre P.D. Kondiah, Viness Pillay & Yahya E. Choonara (2021): Synthesis and therapeutic delivery approaches for praziquantel: a patent review (2010-present), Expert Opinion on Therapeutic Patents, DOI: 10.1080/13543776.2021.1915292

To link to this article: https://doi.org/10.1080/13543776.2021.1915292

Among all the anti-schistosomal drugs that have been used over the years, praziquantel has been the most widely used. Although, some major challenges have been faced using the drug in the treatment of schistosome infections. Several approaches used in the synthesis of praziquantel aimed at reducing the time and cost of production, the toxicity and experimental harsh conditions are discussed. Also, patented methods involved in the pharmaceutical reformulation of praziquantel in the treatment of diverse endoparasitic infestation are reported. Additionally, future perspectives in terms of nanomedicine approach in the formulation of praziquantel are highlighted. Lipid-based nanosystems (LBNSs) formulations can be used to overcome the shortcomings associated with the used of praziquantel in the schistosomiasis treatment due to their amphiphatic nature. This could be a promising vehicle for the delivery of praziquantel, which could in turn improve the bioavailability, as well as reduce the frequent dose of the drug and improve patient compliance. This may sustain release of the drug and improve the rapid conversion of the drug into inactive metabolite due to rapid metabolism. Additionally, LBNSs approach could increase and improve the lipophilicity of the drug, which could make it easier to interact with the hydrophobic cores of the worm tegument.

3.1. INTRODUCTION

Praziquantel (PZQ), happens to be a compound which belongs to the class of organic compounds derived from tetrahydrogenated isoquinoline, otherwise known as tetrahydroisoquinoline. Chemically, praziquantel is known as 2-cyclohexanecarbonyl-1,2,3,4,6,7,11b-piperazino[2,1-a]isoquinolin-4-one (figure 3.1) with average molecular mass of 312.4061 g/mol. In biopharmaceutical classification system (BCS), PZQ is classified into group II, and the drug is easily soluble in dimethylsulfoxide and chloroform, soluble in ethanol and slightly soluble in water, with octanol-water partition coefficient at pH 7, 20^{o}C. It is usually available commercially in 600 mg tablet for oral administration with a dose recommendation of 20 mg/kg body weight for three times daily as a one day treatment for schistosomiasis. Although, the World Health Organisation (WHO) has recommended a single dose of 40 mg/kg of PZQ for the treatment of all forms of schistosomiasis, higher dose of 60 mg/kg has also been deployed for the treatment of the disease in some cases worldwide.

Over the years, this anthelmintic agent (Praziquantel) has been the drug of choice used in the treatment of schistosomiasis and many cestode infestations, due to its effectiveness against all forms of schistosomes both in adults and children, its availability, cost effectiveness, and lesser adverse effects which are well tolerated in patients of all ages [1,2]. Its cure rates against the three major schistosomes are; 63-85% cure rates for *S. mansoni*, 75-85% for *S. haematobium* and for the co-infections with *S. haematobium* and *S. mansoni* is 60-80% at the recommended dose of 40 mg/kg while the cure rates for *S. japonicum* is 80-90% for a higher dose of 60 mg/kg [1,3]. Although, several limitations associated with the used of this drug for the treatment of schistosomiasis have been reported, which includes the resistance that has described in the strains developed in the laboratory. Also, the resistance in an endemic region, due to failures that occurred in mass treatment of schistosomiasis although, this resistance has been recorded to be tolerant strains [4]. The insufficient long lasting of praziquantel therapy has also been reported, which ensue due to low bioavailability of the drug since the drug has low water solubility and rapid metabolism. This may also be attributed to the ability of the drug to quickly convert into an inactive or significantly less potent or weak compound following an oral administration. The bitter taste (racemic-PZQ) and high dose require for the treatment of schistosomiasis are other major administration drawbacks [5]. The ineffectiveness of the drug against young schistosome worm may be an evidence of the rapid metabolism of the drug, which caused the inability in the exposure of the younger form of the parasites in systemic circulation to praziquantel [6-8].

In addition, despite the poor solubility of praziquantel [9-11], it shows to be well absorbed across the gastrointestinal tract (GIT), but requires large doses of the drug to achieve

adequate concentration at the sites of target and to overcome first pass metabolism [5]. Although, parental formulations may serve as an alternative delivery route for praziquantel in order to achieve direct systemic delivery that will avoid first pass hepatic metabolism as well as reduces the required dose. Meanwhile, the preferred route of choice for the treatment of an infection by patients is an oral drug delivery, when compared to parental or any other administration routes. All the same, the oral administration required a large dose of praziquantel to achieve its adequate concentration at the sites of the target, which in turn results in the frequent administration of the tablet dosage [5]. The frequent administration of the praziquantel may result in poor patient compliance to treatment, which leads to the aggravation of underlying infection especially in the pediatric and geriatric patients. In recent times, no approach has been made to develop new drugs for this grave disease, and there are no anti-schistosome drug candidates currently in the clinical trial pipeline, a practical and necessary approach is to optimize the health benefits from praziquantel [12], and due to lack of a protective vaccine for schistosomiasis. Although, in recent times, different alternative approaches for novel anti-schistosomal agents have been reported, some of which include, molecular modelling, drugs repurposing or repositioning, as well as filtering for a most promising chemotherapeutic agent that possess anti-schistosomal activities [13-15]. Mafud et al [15] has recommended molecular modeling approaches and their integration with experimental techniques to hasten and improve the schistosomiasis drug discovery pipeline. In the field of drug discovery in recent years, these computational approaches have grown at a pace with the increasing amount of information that has become available. In [14], Bergquist and co-workers summarised several recent approaches that have been explored over the years in the area of designing novel schistosomiasis chemotherapy. In their article, emphasis was placed on repositioning of existing drugs against schistosomiasis, since this strategy might advance existing drugs more rapidly into clinical use for a typical disease of poverty with a deficient market. In a similar report by Lago et al [13] where about 100 compounds were gathered and information about their therapeutic action, which covered at least the *in vitro* and *in vivo* in animal models that described the pharmacokinetics and toxicity profiles of anti-schistosomal agents was documented. The preclinical examinations show a handful of promising future anti-schistosomal candidate drugs. All these aforementioned approaches could be considered as time consuming and expensive when compared to drug delivery systems (DDSs) approach. Thus, researchers in the past have devised several methods (DDSs) of improving and optimizing the existing active pharmaceutical ingredients with lesser bioavailability and poor therapeutic efficacy due to poor water insolubility, as well as reduce the dose frequency to improve patient compliance. Hence, this review is focused on several patent in the area of praziquantel formulation and optimization between the periods of 2010 to 2020.

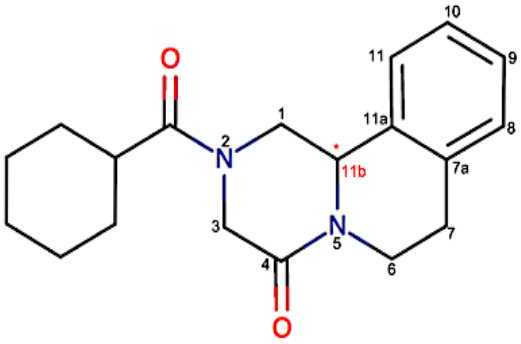

Figure 3.1: The structure of praziquantel showing the position of its chemical name

3.2. Mechanism of action of Praziquantel

The mechanism of action of praziquantel (PZQ) on the schistosomes remains unclear, but studies have proposed some mechanisms in which this drug can act on the *Schistosoma* parasites, and a few phenomenon associated with its effects is well understood (figure 3.2). The most observable and immediate alteration that can be noticed in schistosomes exposed to PZQ both in an *in vivo* or *in vitro* study is a spastic paralysis of the worm musculature, Pax and co-workers [16] stated that this contraction is probably caused by a rapid influx of Ca^{2+} into the schistosome. This assertion was corroborated by an interesting work carried out by Kohn et al [17] which drew attention to schistosome calcium channels as the possible molecular target for praziquantel. In their study, the mode of action for PZQ was suggested to be consistent with the observable effects of PZQ on Ca^{2+} homeostasis in schistosomes, it was noticed that β-subunits of schistosomes channels possesses a unique structure from other common β-subunits which probably inhibits the flow of currents through the α_1 subunits of schistosome with which they are associated. They further showed that PZQ allows the opening of more channels or allow more current to flow through the individual channels which lead to the disruption of α1/β interaction in these channels, thereby resulting in normal Ca^{2+} homeostasis disruption [17].

Other studies have reported and attributed the morphological alteration observed in the worm tegument to the effect of PZQ, this was initially represented by vacuolization of parts of the tegument and blebbing at the surface [18,19]. These morphological modifications result in an increased exposure of the schistosomes antigen presentation on the surface of the parasite, and in [20], Harnett and Kusel suggested that the actions of PZQ on the exposed worm-antigen may be due to its lipophilicity which makes it easier to interact with hydrophobic cores of the tegument. More so, the exposure of antigens has been identified and shown to be

associated with the host immune response which is required for the complete activity of PZQ [19,21].

The pharmacokinetics, which described the movement of PZQ, comprising the absorption, distribution, metabolism, and elimination (ADME) parameters of the drug. The drug is well absorbed by the gastrointestinal tract (GIT) with about 80%, although due to rapid first-pass metabolism, only a relatively small quantity enters systemic circulation. In the adults with normal liver and renal function, the drug has a serum half-life of 0.8 to 1.5 hours. While the metabolites of the drug have a half-life of 4 to 5 hours, the serum halt-life increases to about 3 to 8 hours in patients with significant liver function impairments [2,17]. Approximately, 70 to 80% of a single oral dose of PZQ is found in urine within the 24 hours of administration, but less than 0.1% as the unchanged drug. The drug and its metabolites are majorly excreted via the renal route of elimination. PZQ is metabolized via the pathway of cytochrome P450 through the CYP3A4, any bioactive molecules or compounds that inhibit or induce CYP3A4 could influence the PZQ metabolism [17,18].

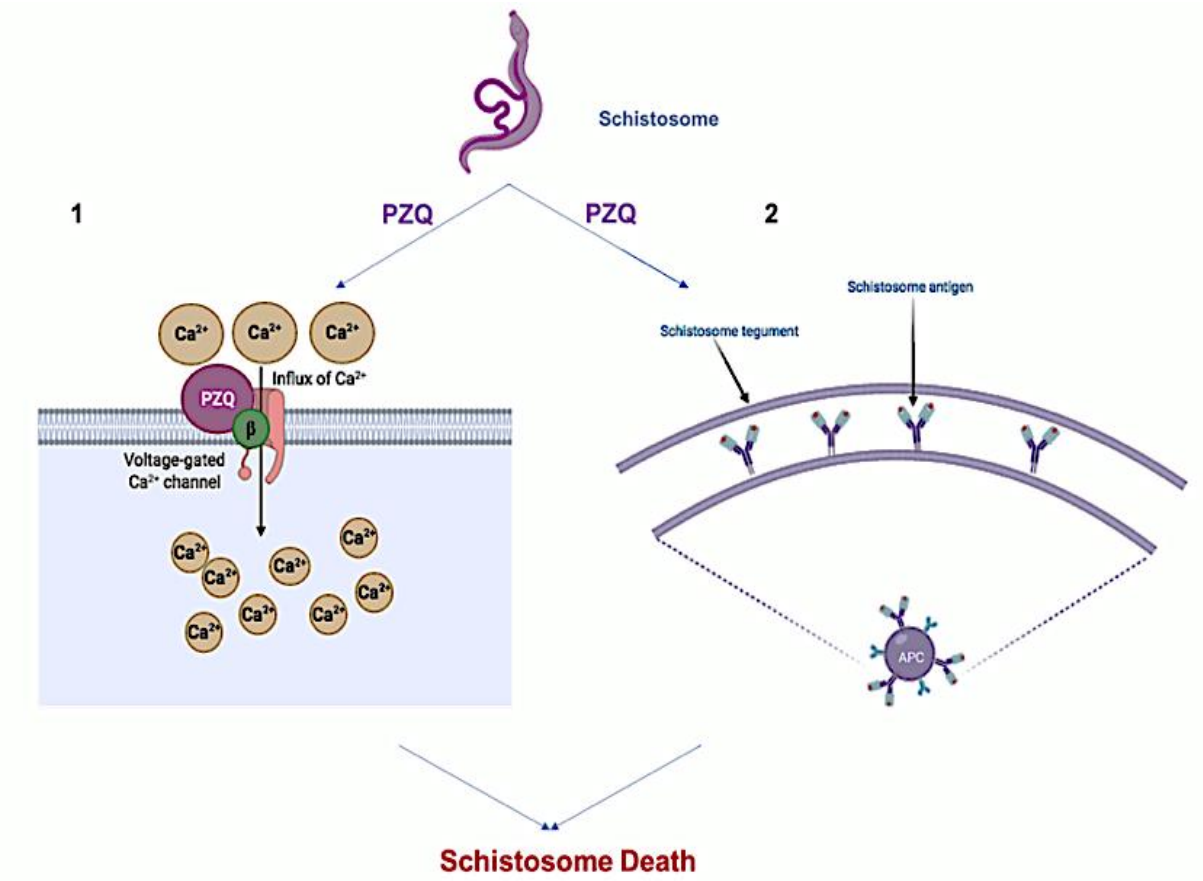

Figure 3.2: The mechanisms of action of praziquantel. (1) Disruption of Ca^{2+} homeostasis through the opening of voltage-gated channel, which allow the influx of current into the worm due to the disruption in the interaction of α1/β. (2) The alteration in the tegument of the worm,

which exposes the schistosome antigens presented by the antigen presenting cells (e.g. dendritic cells and macrophages) on the surface of the worm for the host immune response.

3.3. Recent patents on praziquantel synthesis and formulation

A comprehensive review of published patents in the period covered on praziquantel-related inventions show significant trends in the topics of a bulk of inventions as summarized hereafter. Although, the majority of the patented inventions cover a wide range of praziquantel synthesis and pharmaceutical composition, we attempt to classify them based on their invention types. The summary of the recent patents on praziquantel synthesis and formulation is shown in Table 3.1.

Table 3.1: Summary of the recent patents on praziquantel synthesis and formulation

S/N	Patents	Pharmaceutical composition	References
1	Pharmaceutical compositions	praziquantel	[5]
2	Process for the preparation of praziquantel	β-phenylethylamine, chloroacetyl chloride, benzylamine and chloroacetaldehyde dimethylacetal	[22]
3	Method for preparing (R)-praziquantel	Nitroacetate, cyclohexanoyl chloride, lipase (enzyme), chloroacetyl chloride, (R)-tetrahydroisoquinoline formate, 1R)-2-[(tert-butyl) oxycarbonyl]-1,2,3,4-tetrahydroisoquinoline-1-carboxylic acid	[23,24,25,26, 38,39]
4	Praziquantel crystal B substance, its preparation method and its applications in medicines and healthcare products	Crystal-praziquantel	[27,28]
6	Preparation method for praziquantel and intermediate compounds thereof	β-phenethylamine, chloroacetyl chloride	[29,30,31]
7	Method for the production of praziquantel and precursors thereof	Praziquanamine and other optically active compound	[32,33,34,35]
8	Method for the production of praziquantel	alkali alkoxide,	[36,37]

9	Taste masking compositions of praziquantel	Praziquantel, lipid and mixture of lipids	[40]
10	Oral gel composition	praziquantel, gelifyer, moxidectin, benzyl alcohol, colloidal silicon dioxide, surfactant, oil	[41,42,43]
11	Palatable ductile chewable veterinary composition	milbemycin oxime, natural meat flavouring, partially gelatinized starch, softener	[44]
12	Praziquantel emulsion injection and preparation technology thereof	Praziquantel, sucrose palmitate, pluronics F87, hydroxypropyl emthylcellulose	[45]
13	Praziquantel long-circulating nanoparticle injection and preparation method thereof	poloxamers, soybean phospholipids, sodium stearate, PHOSPHATIDYL ethanolamine-Macrogol 2000, praziquantel, Glyceryl Behenate, glyceryl monostearate, butyl acetate	[46]
14	Preparation method of praziquantel lipid lyophilized preparation	lecithin, cholesterol, praziquantel	[47]
15	Praziquantel-mebendazole nanoemulsion oral liquid and preparation method thereof	Surfactant, cosurfactant, ethyl acetate, N, N-dimethyl acetylamide, praziquantel, mebendazole	[48]
16	Praziquantel nanoemulsion in situ gel for preventing and treating bilharziasis and preparation method and application thereof	Praziquantel, Capryol 90, emulsifying agent (polyoxyethylene hydrogenated Oleum Ricini RH40 and tween 20), co-emulsifier (PEG-4000)	[49]
17	Compound ivermectin praziquantel bi-continuous phase emulsion and preparation method thereof	Ivermectin, praziquantel, Arecoline hydrobromide, solvent naphtha, hydrotropy Agent, emulsifying agent, co-emulsifier	[50]

3.3.1. Patented methods for R-praziquantel synthesis

In the conventional process of praziquantel synthesis and production, some drawback has been observed such as; the expensiveness of the raw material (aminoacetaldhyde dimethylacetal), harmfulness and the toxicity of the compounds involve in the process (cyclohexanoyl sulphoxide chloride, potassium cyanide, cyclohexamethylene chloride and so forth). More so, the long process required, and harsh experimental conditions involved in the production of praziquantel has given birth to several novel approaches for the preparation of praziquantel. All these novel praziquantel preparation approaches are developed to reduce

the overall cost of production, reduce the toxicity and experimental harsh conditions involve in the process of the production, as well as reduce the elongated time require in the production process.

In [2014], Balaya and co-workers patented (U.S. Patent 8,754,215) a novel, cost-effective methods of preparing a 4-oxo-1,2,3,6,7,11b-hexahydro-4H-pyrazino-[2,1-a]isoquinoline derivatives through the use of a novel compound (2-[(2,2-dimethoxyethyl)benzyl amino]-N-phenethylacetamide) as an intermediate with good yield and good purity for a commercial scale. In their patent, they also disclosed and described a novel crystalline form of 4-oxo-1,2,3,6,7,11b-hexahydro-4H-pyrazino[2,1-a]isoquinoline as shown in figure 3.3.

In their patent, it was recorded that the condensation of β-phenylethylamine with chloroacetyl chloride in the presence of a solvent lead to the production of 2-chloro-N-phenethylacetamide as showed in formula V. Subsequently, compound VI (N-benzyl-2,2-dimethoxyethanamine) was reported to be generated by the condensation of benzylamine with chloroacetaldehyde dimethylacetal in the presence of water. Hence, both the products formed in compounds V and VI were condensed to form 2-[(2,2-dimethoxyethyl) benzylamino]-N-phenethylacetamide of compound IV in the presence of water. Thereafter, the reduction of compound IV (2-[2,2-dimethoxyethyl) benzylamino]-N-phenethylacetamide) with the help of reducing agent and a solvent in the presence of hydrogen produced 2-[(2,2-dimethoxyethyl) amino]-N-(2-phenylethyl) acetamide showed in compound III. It was stated that the cyclisation of compound III (2-[(2,2-dimethoxyethyl) amino]-N-(2-phenylethyl) acetamide) produce compound II (4-oxo-1,2,3,6,7,11b-hexahydro-4H-pyrazino[2,1-a] isoquinoline) using an acid in the presence of solvent. The end product, which is praziquantel (compound I) was produced through the acylation of compound II with cyclohexanoylchloride in the presence of base and solvent [22].

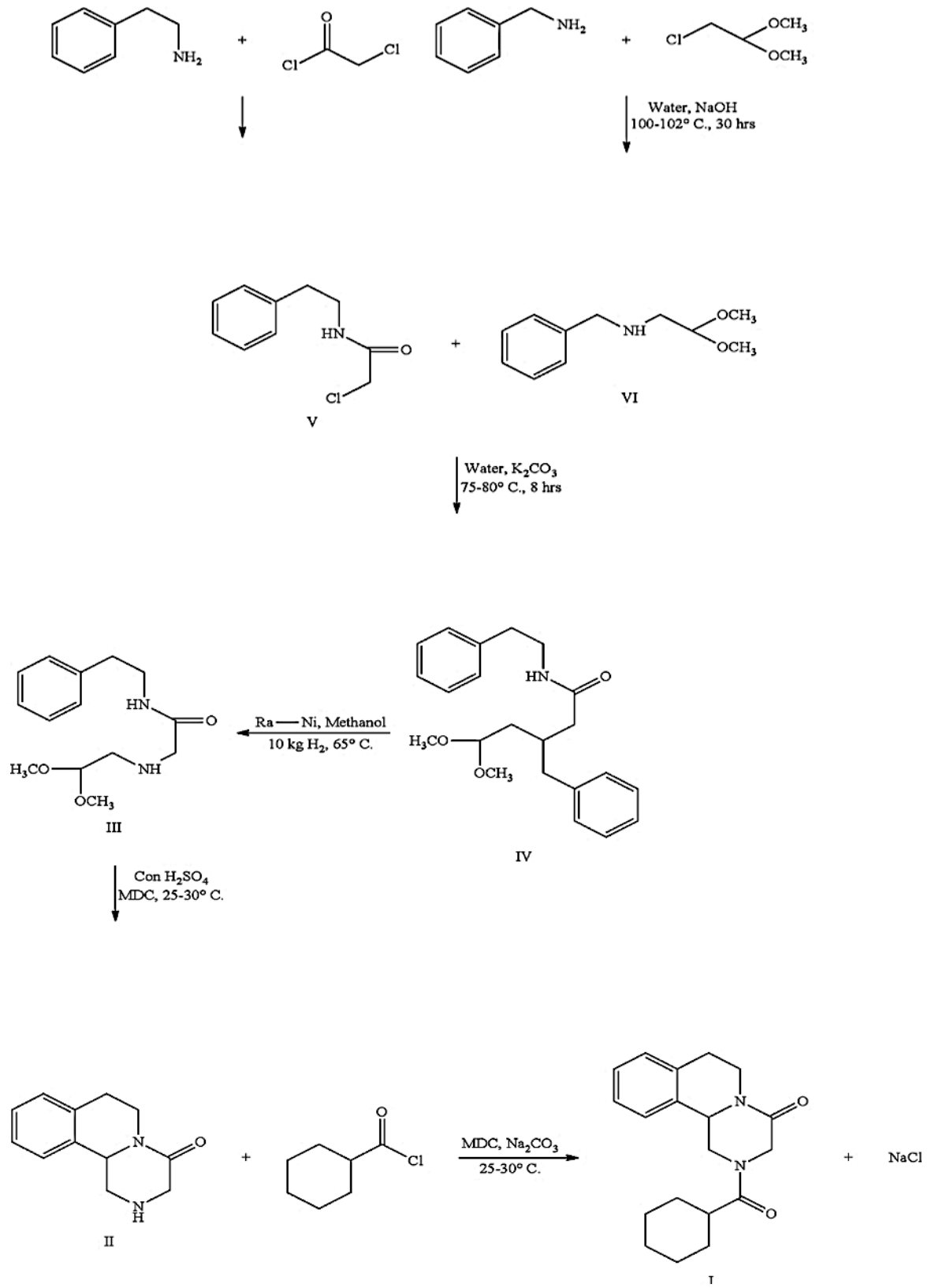

Figure 3.3: The schematic illustration of praziquantel preparation process from β-phenylethylamine with chloroacetyl chloride and benzylamine with chloroacetaldehyde dimethylacetal as precursors (U.S. Patent 8,754,215) [18].

In [2015], Qian and Suzhou Tongli Biomedical Co., LTD patented (U.S. Patent 9,175,321) the preparation of the R-praziquantel; an active component of praziquantel against schistosomes worm, which has also been proven to provide better clinical efficacy when compared to praziquantel at the same dose. In this patent, the features of biological enzyme (microbial lipase) used in the preparation of the R-praziquantel are; strong stereoselectivity, of high-resolution efficiency, site-selectivity, and regioselectivity, of simple operations to catalyze the hydrolysis of a specific enantiomer in a derivative or a chemically synthesized, and mild reaction conditions. It was further averred in the patent that the prepared R-praziquantel using the technique has above 98% purity.

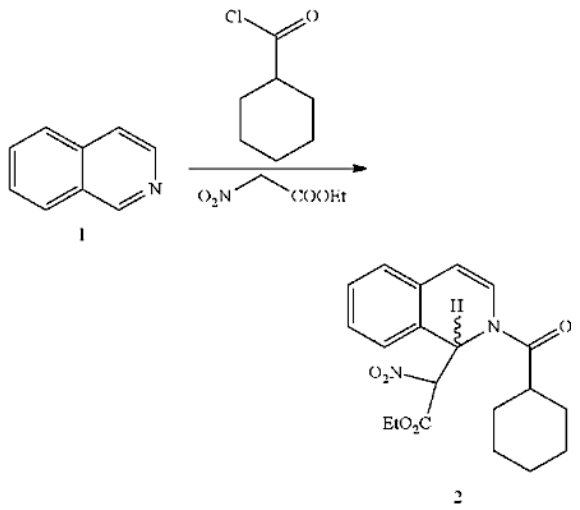

Figure 3.4: The schematic synthesis of racemic nitroester from nitroacetate in the presence of cyclohexanoyl chloride (U.S. Patent 9,175,321) [19]**.**

Although, the racemic nitroester (compound 2) as a precursor used in this the production of R-praziquantel is commercially available but can also be prepared manually by reacting nitroacetate (compound 1) and cyclohexanoyl chloride in the presence of solvent (figure 3.4). The production of R-praziquantel is based on lipase stereoselective ester-hydrolysis method in which, racemic nitroester (compound 2) is hydrolyzed by lipase to produce the R-nitroacid intermediate (compound 4), and S-nitroester intermediate (compound 3), which is separated via resolution as shown in figure 3.5. Subsequently, as shown in figure 3.6, the compound produced in 4 was decarboxylated in the organic solvent to produce compound 5, which later undergo catalytic hydrogenation to produce compound 6 in the presence of organic solvent. Afterward, the compound produced in 6 was allowed to react with chloroacetyl chloride to form compound 7, which is the R-praziquantel in the presence of organic solvent [23].

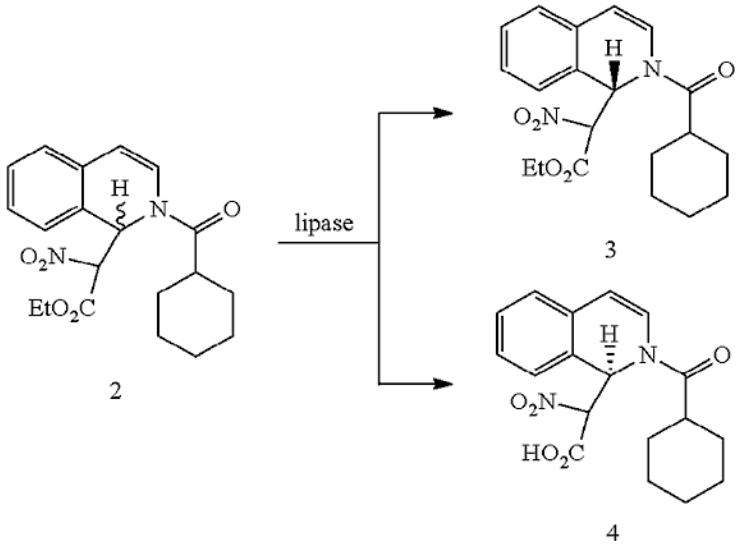

Figure 3.5: The formation of R-nitroacid intermediate through the hydrolysis of racemic nitroester by lipase (U.S. Patent 9,175,321) [19].

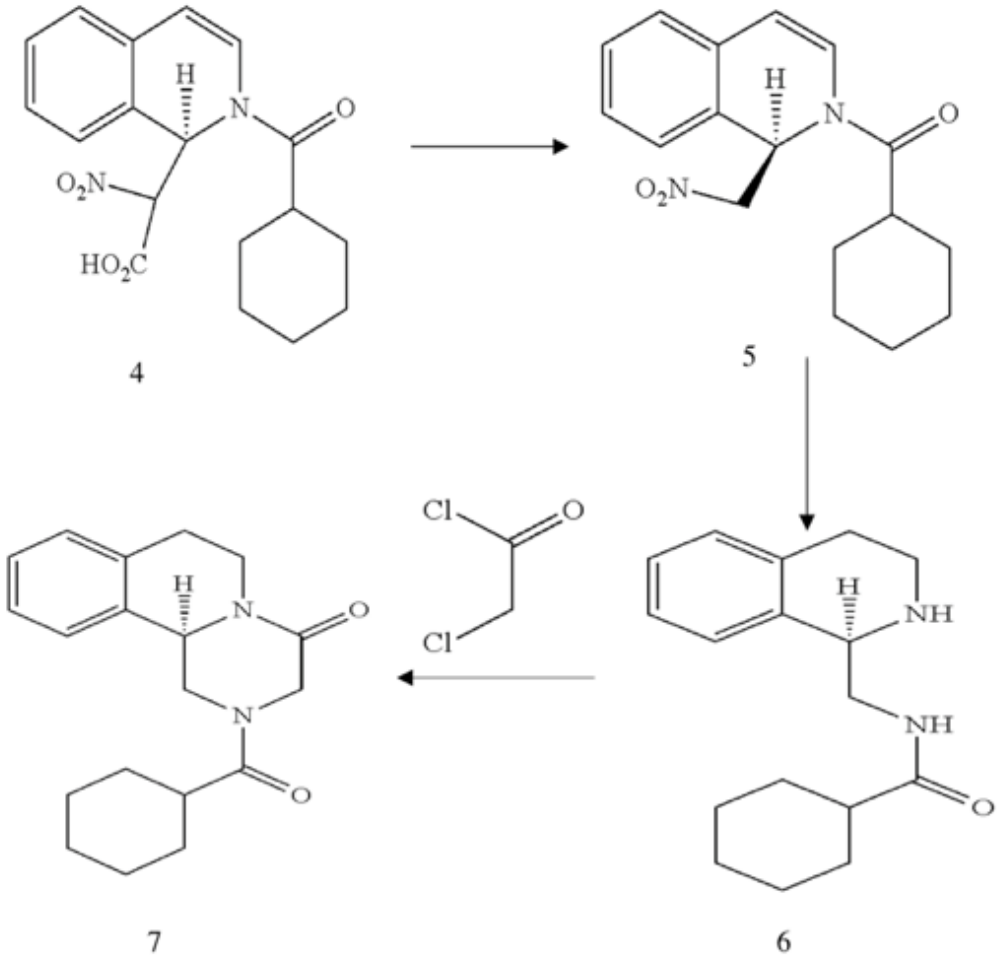

Figure 3.6: The formation of R-praziquantel from R-nitroacid through the decarboxylation and hydrogenation in the presence of chloroacetyl chloride (U.S. Patent 9,175,321) [19].

In like manner, Qian also used this enzymatic approach in patenting two other ways of preparing R-praziquantel in [24] using different precursors. In one of the patents (U.S. Patent 9,068,214), as shown in figure 3.7, (R)-tetrahydroisoquinoline formate (compound 3e) was stereo-selectively ammonolyzed by lipase and ammonia gas and/or ammonia source, which can decompose to generate ammonia gas in a solvent in the presence of ionic liquids to produce a pure optical (R)-tetrahydroisoquinoline formamide (compound 14). Thereafter, the compound 14 was added to triethlamine and dichloromethane in a reactor to produce compound 16, and an anhydrous methanol and a ruthenium catalyst (Ru/C) were added to compound 16 to obtain compound 17. Consequently, an organic solvent and a solution of a base was added to compound 17 in a reactor following a continuous stirring, and in a dropwise manner, chloroacetylchloride was added to the reaction in order to produce the reaction mixture of compound 18. This was later reacted to benzyl-triethyl ammonium chloride at 75 to 85 ^{o}C to generate compound 19, which was used to produce R-(−)-praziquantel amine; an intermediate of R-praziquantel in the presence of hydrochloric acid and phosphoric acid. The reaction of cyclohexane formyl chloride to R-(−)-praziquantel amine in the presence of triethylamine yield the R-praziquantel [24].

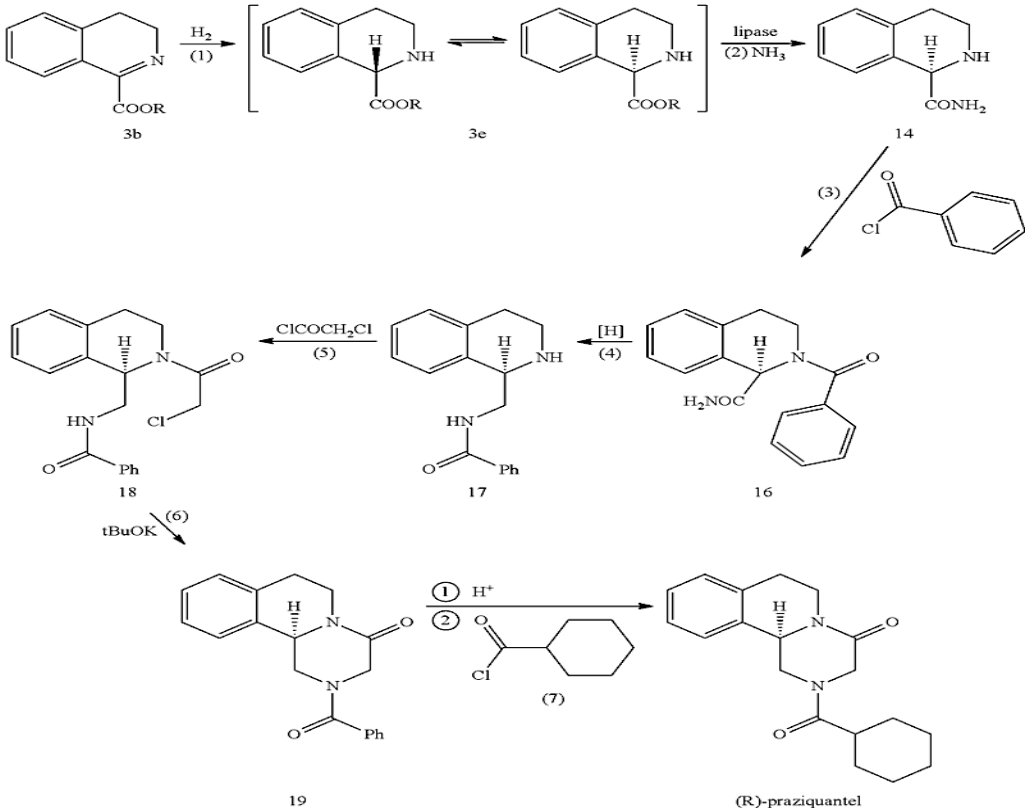

Figure 3.7: The production of R-praziquantel using (R)-tetrahydroisoquinoline formate as a precursor in the presence of lipase and ammonia gas (U.S. Patent 9,068,214) [20].

In the second patent (U.S. Patent 9,139,859) (figure 3.8), (R)-tetrahydroisoquinoline formate (compound 3e) was stereo-selectively hydrolyzed using lipase to produce a pure optical (R)-tetrahydroisoquinoline formic acid (compound 4). Afterward, the compound 4 that was previously converted to the free form of tetrahyrofuran or its hydrochloride form was suspended, and cooled to 0-5^{o}C, thereafter a solution of borane was added dropwise to tetrahyrofuran, or addition of sodium borohydride is followed by the addition of boron trifluoride etherate in a dropwise manner. After several reactions, the addition of tetrahyrofuran and compound 11 into a reactor and evenly stirred produced R-praziquantel [25].

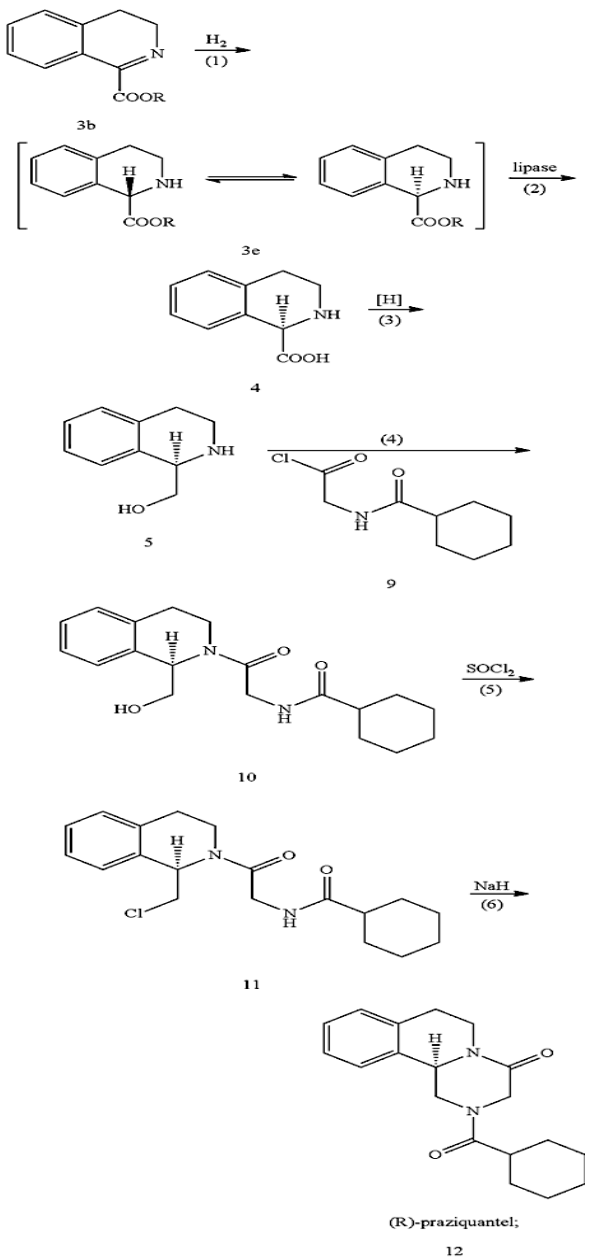

Figure 3.8: The synthesis of R-praziquantel from stereo-selective hydrolysis (R)-tetrahydroisoquinoline formate by lipase (U.S. Patent 9,139,859) [21].

Qian and Tongli Biomedical Co., LTD patented (U.S. Patent 9,802,934) an environmentally friendly and more cost-effective process of (R)-praziquantel synthesis (figure 3.9). In this patent, the higher optical purity of (R)-praziquantel produced was generated via four steps, involving the condensation-acylation of (1R)-2-[(tert-butyl) oxycarbonyl]-1,2,3,4-tetrahydroisoquinoline-1-carboxylic acid as the precursor compound (compound 1) to produce compound 2. Thereafter, compound undergoes reduction reaction to yield compound 3, which was later allowed to undergo an acylation process by reacting with a de-protective agent (such as hydrochloric acid and other acids) and cyclohexyl formyl chloride to form compound 4. Afterward, compound 5 was obtained from compound 4 through the ring-closing reaction with the help of chloroacetyl chloride [26].

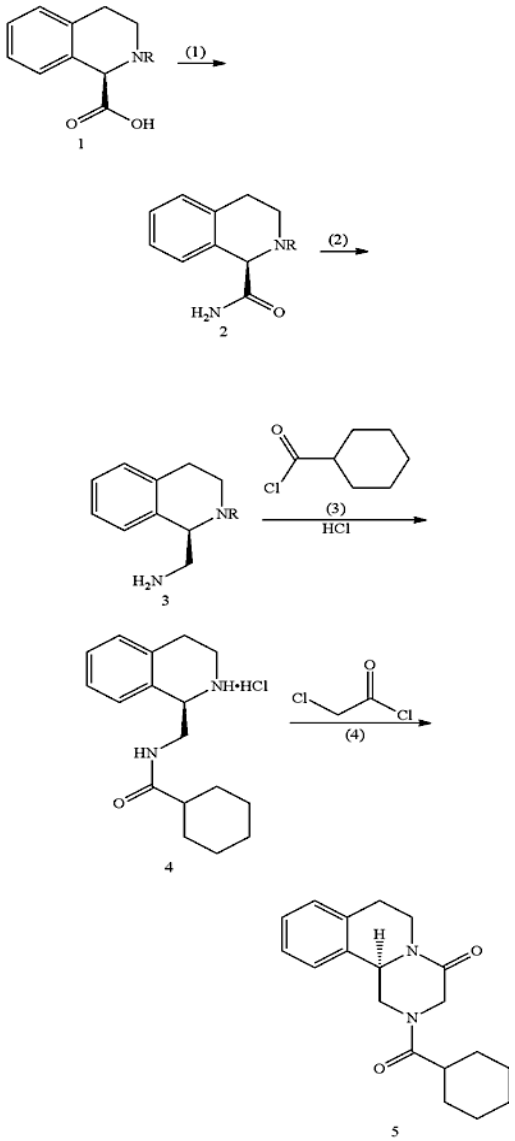

Figure 3.9: The synthesis of R-praziquantel via the condensation-acylation of (1R)-2-[(tert-butyl) oxycarbonyl]-1,2,3,4-tetrahydroisoquinoline-1-carboxylic acid as the precursor (U.S. Patent 9,802,934) [22].

Other patented methodological approaches which have described the novel methods for praziquantel synthesis includes, a preparation technique of synthesizing a crystal B sample of praziquantel by treating the substance of praziquantel crystal B as an active component, and its applications in the healthcare and disease control (CN102786519A and CN102786519B) [27]. Similar invention was also reported by the same inventor in another patent (U.S. Patent 9,657,017) [28]. A cost-effective, environmentally friendly, large-scale suitability, good reproducibility and a method that operates at a normal temperature and pressure in the crystal form of R-praziquantel preparation through an X-ray diffraction pattern. In [29,30], Zhang and co-workers patented (U.S. Patent 10035798) and (U.S. Patent. 20180030049A1) novels approaches of preparing praziquantel from β-phenethylamine as a precursor via a condensation reaction with chloroacetyl chloride, ethanolamine substitution and cyclohexanecarbonyl chloride acylation, which was later followed by oxidation and acylation reactions to form the pure desired products [29,30]. This patent approach was also reported in recently in a published patent (WO2016127350A1) [31].

Eberhardt et al patented a method of preparing a pure R-praziquantel and analogues thereof using a setereoselective approach, which involves the asymmetric hydrogenation and the cyclization process in (WO2017036577A1) and (U.S. Patent 10,273,213) [32,33]. In other related invention by Maillard and co-workers in [34,35], methods of preparing R-praziquantel using a mixture of the enantiomers (R)-(I) and (S)-(I) of a Praziquanamine; an enatioenriched or enantiopure praziquantel precursor were patented in (ES2706314T3) and (U.S. Patent 9,932,337). Waechtler and co-workers [36,37] patented (WO2016078758A1) the preparation of enantionmerically and enantiopure enriched form of praziquantel from the recycling of (S)-praziquantel using the racemization technique, which is easy to scale-up, cost-effective and reliable. The invention in (U.S. Patent. 20140370555) and (U.S. Patent. 20140370556), made use of readily available raw materials with low cost, environmentally friendly procedure and various conventionally and mature organic chemical reactions for large scale production of a purified R-praziquantel using the high stereo selectivity, site selectivity and region selectivity of an enzyme [38,39].

2.3.2. Patented Praziquantel pharmaceutical compositions

In recent times, a few pharmaceutical compositions of praziquantel have been patented such as reformulation of the drug to treat other diseases both in animals and human. Also, to address some limitations associated with the used of the drug, which includes the improvement in the dissolution and bioavailability of the drug, and improvement in the

palatability of the drug as well as a reduction in the dose for easier administration to ensure patient compliance.

In [2015], Malhotra and Raut patented (WO2015071668A1) an invention on the formulation of nanosized particles which is less than or equal to about 2000 nm of R-praziquantel using a more acceptable pharmaceutical excipients for the treatment of anthelmintic infections both in animal and/or human. It was stated that the invention was designed to reduce the dose of the drug, and to improve its bioavailability due to the enhancement in dissolution and solubility properties. It was further elucidated that the filed patent can overcome the repeatedly used (at regular interval of about 4 hours to 6 hours) of the drug, which may be something difficult for patients under self-treatment to keep a track administration of the drug. Whereas, the missing in the doses of this drug in one or two times can lead to the reduction in the therapeutic efficacy of the drug. More so, the improvement in the bioavailability of the drug is believed to enhance the therapeutic efficacy of the drug against the juvenile forms of the Schistosoma parasites [5].

Oral gel and paste have been reported to be the most suitable for ease administration, effective and efficient dosage, and cost-effective and practical use in the treatment of endoparasiticidal agents in animals and livestock. EP2662075A1 describes the oral formulation of praziquantel, which was substantially free from the bitter taste associated with the drug for the treatment and control of endoparasitic infestations in warm-blooded animals like horses, cats and dogs. This invention was achieved through the process of taste masking using a lipid or a mixture of lipids which are not water soluble. These lipids served as integral coating agent for the production of praziquantel particles which ranging between 1 to 300 μm in diameters. The lipids also help to mask the extreme bitter taste of the drug immediately after the oral administration, but dissolve and disperse on contact with GIT and this do not affect the bioavailability of the drug. This was observed in the *in vivo* bioavailability evaluation carried out on the lipids-coated and non-coated praziquantel. The statistical analysis of the appropriate pharmacokinetics parameters tested on the formulation reliably fulfil the requirements of bioequivalence. More so, the palatability testing of the formulation carried out in 129 male and female dogs of several breeds and age, as well as 34 cats showed positives results [40].

US8241669B2 described the preparation method for an endoparasiticidal gel composition from moxidectin and praziquantel for the effective treatment and control of external and internal parasites in homeothermic animals and livestock. This invention formulation was achieved using composition that contains the mixture of about 10% to 15% ($^{w}/_{w}$) of

praziquantel; approximately 1% to 3.5% ($^{w}/_{w}$) of moxidectin; about 1% to 20% ($^{w}/_{w}$) surfactant; about 1% to 34% ($^{w}/_{w}$) of ethanol; about 35% to 61% ($^{w}/_{w}$) of an oil; about 4% to 24% ($^{w}/_{w}$) of benzyl alcohol and about 2% to 15% ($^{w}/_{w}$) colloidal silicon dioxide. This veterinary gel composition possesses a wide spectrum of efficacy against endoparasites for a longer period of time and allows higher concentrations of parasiticidal agents mixture in a single application. This was noticed in the efficacy analysis that was carried out in 26 new forest cross male ponies of about 1 to 2 years of age which was infected with *Gasterophilus spp.* and *A. perfoliate* in South West England [41]. Another similar invention, which described the gel formulation of praziquantel for the treatment of endoparasitic infection in livestock animals was patented in U.S. Patent 6,893,652 [42].

EP2594258A1 illustrated the formulation of an oral hydrosuspension gel containing praziquantel, water and at least one gelifer in order to enhance the medicament palatable for oral treatment in camelids animal. In the invention, an oral hydrosuspension gel was formulated by using 15% ($^{w}/_{w}$) native praziquantel, at least 30% water and at the minimum one gelifer. The gelifer is a typical gelling agent, for example a hydrocolloid, which is selected from the group containing cellulose derivatives, for instance, water soluble cellulose ether (methyl hydroxyethyl cellulose, hydroxyl propyl cellulose, hydroxyl ethyl methyl cellulose among others); starches (hydroxyethyl starch); natural gums (xanthum gum) and synthetic polymers (polymers and copolymers of carbomeres, and polyvinylpyrrolidone). The acceptance (palatability) test was carried on 34 illamas naturally infected with *Dicrocoelium dentriticum,* and the efficacy of the formulation was calculated to be 88.2% when treated at a dose rate of 50 mg/kg bodyweight, and 82.3% efficacy was observed when 25mg/kg bodyweight was used [43].

Similar patent was described in US8541019B2 for the production of palatable ductile chewable oral composition for the treatment of ectoparasites and endoparasites, and capable of treating prophylactic or cure diseases in warm-blooded animal such as cattle, dogs, horses, sheep, cats or poultry. The palatability analysis of different chewables flavored was carried out in 100 female and male dogs of the same bodyweight, and an analogous evaluation was examined in 100 cats. In the dogs, the total acceptance was observed in all the formulations, also the analogues analysis carried out in cats showed absolutely similar range of results generated in the dog analysis. Subsequently, the stability analysis of the formulations was examined under stress conditions so as to simulate several temperatures and humidity conditions. A good stable result was observed, which is capable of improving the shelf life for at least 12 months when stored under normal conditions [44].

More so, the technology involved in the preparation of praziquantel emulsion injection was illustrated in CN103432074A, and the patent has a high bioavailability and strong stability; and has a high effective concentration in the blood and stay over 18 hours in an animal body. The preparation of the praziquantel emulsion contains hydroxypropyl methyl cellulose, sucrose palmitate and poloxamer 188, the emulsion also contains mixture of oil-phase ethyl oleate and glyceryl triacetate. In the application of the praziquantel emulsion injection in the treatment of coenurosis in a goat brain, a good treatment efficiency was obtained; and the recovery rate clinically can be up to 100%. Furthermore, the invention does not generate significant adverse effects such as general adaptation syndrome and irritative response in animals; the invention permeated hematoencephalic barrier significantly [45].

CN103381141A patented the preparation of praziquantel of long-circulating nanoparticle injection, which contains the use of a long-circulating modification material, for instance, distearoyl phosphatidyl ethanolamine-polyethylene glycol 2000 (DSPE-PED2000). It was reported in this patent that this preparation approach can enhance the slow discharge of praziquantel in vivo, decrease cytophagy, extend the persistent period of blood drug level, reduce the dose of the drug, improve patient's compliance, enhance the curative effect of medication. More so, solved the short problem of conventional praziquantel injection effective drug duration, have both the ability to prevent and treat schistosomiasis infection [46]. A freeze-drying method for the preparation of lyophilized lipid praziquantel was patented in CN102697729A where 0.5-1.5 wt% of praziquantel, 97-99 wt% of lecithin and 0.5-1.5 wt% of cholesterol, chloroform, anhydrous ethanol were used as starting materials. In this invention, the proportion of lecithin, cholesterol, praziquantel, and the amount of chloroform, dehydrated alcohol, as well as the time for freeze-drying and rehydration, and the rehydrating medium, and ultrasonication time to generate small unilamellar vesicle from milk shape multilamelar liposome suspension was patented [47].

In CN103316005A, the method for the preparation of praziquantel-mebendazole oral liquid nanoemulsion was patented in order to improve the bioavailability, prolong the in vivo metabolism time of medicament, reduction in the amount of auxiliary materials and to lower the production cost. In the this patent, the percentage of raw materials used in the preparation of the oral lipid nanoemulsion was reported to be 15.00-30.00% of a surfactant, 15.23-24.00% of a cosurfactant, 0.10-1.50% of praziquantel, 0.10-1.50% of mebendazole, 5.00-15.00% of ethyl acetate, 5.00-18.00% of N,N-dimethylacetamide and 5.80-53.40% of distilled water, and the total components are 100%. This invention was patented because an oral liquid nanoemulsion of praziquantel-mebendazole has a wide market prospect in the medicine field [48]. In another related patented invention in CN105816421A, the method for the preparation

of praziquantel nanoemulsion for in situ gel was documented. The prepared praziquantel nanoemulsion in situ gel was shown to have advantages in control-release character of praziquantel in an in vivo experiments, which in turn could improve and prolong the function of preventing and treating bilharziasis [49].

Other recently patented invention include, the method for the preparation of bi-continuous phase emulsion for compound ivermectin praziquantel CN106361758A. It was documented that the prepared emulsion by this invention is wide in insect-resistant spectrum and that the selection is flexible according to the clinical specific circumstances. More so, obvious in treatment effect and not only can be used for injection after being diluted with oil, but also can be drunk or used for injection after been diluted with water when in use [50]. Taking into consideration the aforementioned patents, some of the current assignees are Suzhou Tongli Biomedical Co., LTD, Merck Patent GmbH, Zhejiang Hisun Pharmaceutical Co Ltd and Sequent Scientific Ltd. Meanwhile, it was noticed that none of the patents are currently marketed by any pharmaceutical industries.

3.4. Closing the gap in praziquantel treatment for schistosomiasis in human host

The design and development of new drugs have been faced with one of these major shortcomings that is, poor financial support and motivation for pharmaceutical companies as well as, a huge cost associated with the process of new molecules or new chemical entities (NCEs) via the long drug discovery pipeline [4]. And unfortunately, it has been reported recently that over 40% of active pharmaceutical ingredients are less bioavailable and possess poor therapeutic effect as well as possessing adverse effects due to their water insoluble properties [51]. Hence, nanomedicine which uses the application of nanotechnology (advanced drug delivery systems (DDSs) and targeted approach) for monitoring, treatment, control and prevention of biological diseases has been a promising approach in improving pharmaceutical ingredients in the treatments of several diseases and disorders [52].

The application of nanomedicine in disease treatment uses a precise method to target specific cells and/or receptors using a suitable nanosystem as a carrier. The use of this target technique on the delivery of the drug in specific areas of the body is very important in order to reduce possible adverse effects associated with the active compounds, when enter non-targeted tissues and organs [4,53]. Additionally, DDSs has drawn attention in enhancing the bioavailability and therapeutic efficacy of drugs. DDSs is used to deliver a biologically active compound at predefined periods of time and predetermined rates that is, it can be used to deliver a drug in a controlled manner, but not only that, it can also be used to maintain the drug level in the body within the therapeutic window [53].

Thus, the integration of nanomedicine approach using the drug delivery systems in infectious diseases treatment has posed several advantageous effects such as, better disease targeting most especially intracellular pathogens [54-56]. Other includes longer time of drug action, the ability of the drug to cross membranes and enter cells, reduction of adverse effect, and cost-effectiveness from lower doses [54-56]. Recently, several studies have employed nanotechnology approach in improving the bioavailability and therapeutic efficacy of praziquantel for the treatment of schistosomiasis (Table 3.2). A study conducted by Amara and co-workers demonstrated that praziquantel-lipid nanocapsules (LNCs) with postabsorption targeting ability proved to be highly effective as oral nanocarriers for a large dose drug, PZQ. The study also showed that a single oral dose of PZQ-LNCs (250 mg/kg) significantly enhanced PZQ anti-schistosomal activity in *S. mansoni* infected mice [57]. In another related study by Frezza and co-worker [50], it was revealed that PZQ containing liposome improved the efficacy of treatment with liposomes-PZQ (lip.PZQ) at 300 mg/kg on *S. mansoni,* BH strain when administered 45 days following infection when compared with the untreated group and the groups treated with free PZQ. Their observation showed that the lip.PZQ has a greater bioavailability in the host organism; the preferred target of the lip.PZQ is the liver, and lip.PZQ is better absorbed by the tegument of *S. mansoni,* which has an affinity for phospholipids [58].

Mourao and co-workers formulated the PZQ-loaded liposome containing phosphatidylcholine in order to improve the anti-schistosomal activity of the drug [59]. The findings from this study revealed that the liposome enhanced the anti-schistosomal activity of the drug by reducing the amounts of eggs and parasite in the animal model [59]. In a similar study carried out by El Gendey el al [60] where the therapeutic efficacy effect of PZQ-loaded liposome against *S. mansoni* infection was studied in murine models. It was discovered that the incorporation of PZQ into the liposome causes an immense decrease in the number of eggs and worm count in the intestine and the liver. It was further noticed in the histopathological analysis that the delivery system causes a reduction in the diameter and number of hepatic granulomas [60].

Frezza and colleagues [61] studied the experimental treatment of schistosomiasis by examining the efficacy of hyperbaric oxygen (HBO) using both the free PZQ and liposomes incorporated PZQ. In the study, it was deduced that free PZQ and PZQ-loaded liposomes with HBO (100mg/kg) reduced both the worms and eggs/oograms in the feces by 48.0% and 83.3%, respectively, and the interruption in the oviposition in 100% of the mice due to the alteration of oograms. The findings of that study further revealed that the HBO has ability to stimulate the immune response, thereby depicting is adjuvant potency in infection treatment

[61]. Radwan et al. [62] formulated PZQ encapsulated labrasol solid lipid nanoparticles (SLNs) for the treatment of murine *S. mansoni* infection. It was shown that the formulation, improved the bioavailability and the anti-schistosomal effectiveness of the PZQ due to a significant decrease in the eggs load both in the intestinal and hepatic tissue. More so, the improvement in the anti-schistosomal activity of the drug was as a result of an extension in its release process due to the protection of the drug from enzymatic degradation by SLNs encapsulation. It was further revealed that formulation causes total disappearance in the deposition of the immature eggs [62].

The ameliorative effect of gold nanoparticles was examined on the renal tissue damage (nephrotoxicity) induced by *S. mansoni* infected mice by Dkhil at el [63]. It was discovered that the gold nanoparticles reduced the extent of renal oxidative damage and histological impartment caused by the schistosome in the mice and was able to regulate the expression of gene impaired by the *S. mansoni* infection. In all, it was showed that the gold nanoparticles were able to scavenge the radical generated due to the infection in the mice. In [64], Tawfeek and co-workers investigated the therapeutic efficiency of praziquantel loaded mesoporous silica nanoparticles on murine *S. mansoni*. The oral administration of the drug in the carrier showed a great impact on the level of oorgram pattern, tissue egg count, hepatic granuloma count, worm burden and the diameter. Also, there was a significant improvement in the level of immunomodulatory effect and the status liver oxidative stress of the infected mice, more so, reduction in the therapeutic dose of encapsulation of praziquantel was permitted when compared to non-encapsulation drug [64]. The in vivo therapeutic efficacy and the oral bioavailability of praziquantel incorporated into montmorillonite clay as a nanodelivery systems was examined by El-Feky et al [65]. In the study, it was showed that the formulation significantly reduced the total tissue egg load as well as enhanced the bioavailability and anti-schistosomal efficacy of the drug.

Table 3.2: Summary of the recent praziquantel lipid formulations in the literature

S/N	PZQ-lipid formulations	Types of delivery systems	Test *Schistosoma* species	References
1	LNCs-PZQ	Lipid nanocapsules	*S. mansoni*	[57]
2	PZQ-Liposomes	Liposomes	*S. mansoni*	[58, 59, 60]
3	PZQ-Liposomes combined with hyperbaric oxygen therapy (HBO)	Liposomes	*S. mansoni*	[61]
4	SLN-PZQ	Solid Lipid Nanoparticles	*S. mansoni*	[62]

3.5. Conclusion

This review described several patents related to the synthesis and formulation of praziquantel for the treatment of Schistosoma infections. We have reported several patented approaches which were employed to overcome several drawbacks associated with the synthesis of praziquantel such as toxicity, cost, time require, harsh environment conditions among others. We further documented several patented techniques which are involved in the reformulation of praziquantel in the treatment of different endoparasitic infestation both in animals and human. More so, we were able to report different patented document which deem it fit to improve the dissolution and bioavailability, as well as palatability and a reduction in the dose of praziquantel for the treatment of schistosomiasis. Thus, the evidence from all the different patents reviewed showed that a new approach is needed to optimize and improve the therapeutic efficacy of praziquantel against younger schistosome, improve the patient compliance by reducing the dose of the drug. In addition, the optimization is needed to hamper the reported cases of drug resistance in some part of the world. Conclusively, we suggested the design and development of a novel lipid-based nanoparticles as a carrier for PZQ, because we believe that this approach will improve the ability and the efficacy of the drug in order to cause spastic paralysis in the musculature of the worm as well as destroy the tegument of the schistosomes.

3.6. Expert opinion

In an extensive review of patents published from 2010 till date, it was discovered that there are limited numbers of patent regarding patent formulation in the area of praziquantel, which only covered and focused on praziquantel synthesis with a few patent on the optimization and reformulation on the drug. This may be due to poor financial supports and lack of motivations

from pharmaceutical companies in the area of neglected tropical diseases (NTDs) researches. Also, this may be as a result of non-lucrativeness of NTDs, when compared with cancer, diabetes, tuberculosis, malaria and other prominent diseases, because they are tagged poor people diseases, as well as lack of interest by the researchers. Meanwhile, schistosomiasis cause by Schistosoma parasites is the second most prevalent among the NTDs [66-69]. In recent times, a huge number of people lose their life yearly due to this group of diseases, and over 240 million people across the world bear the full impact of the disease which hold major influence on the health, social, financial and economic status of both the government and households [70].

Praziquantel, the drug of choice in the treatment of this disease due to characteristics associated with the drug, while some lapses related to the drug have also been documented in the introductory section, hence the need for therapeutic improvement in the drug. In order to improve the therapeutic efficacy, bioavailability and rapid metabolism of PZQ; the major cause of ineffectiveness of the drug against young schistosomes, drug delivery system using lipid-based nanosystems (LBNSs) formulations can be used to overcome these shortcomings.

LBNSs is a wide-ranging designation for formulations consisting of a dissolved or suspended drug in lipidic excipients, which comprises of SLNs, lipid nanocapsules (LNCs), liposomes, micelles, polymeric micelles among others. In recent time, LBNSs or submicron bilayer lipid vesicle technological products have gained more interest in pharmaceuticals, nutraceuticals and cosmetics industries in encapsulation and delivery of active agents. LBNSs are potential candidates in a vast range of fields, including nanotherapy (diagnosis, gene delivery cancer therapy), cosmetics, agriculture food technology, this is due to their several unique characteristics exhibited such as biocompatibility and biodegradability as well as their nanosized.

In pharmaceutical industries, LBNSs has drawn more attention in enhancing the bioavailability and therapeutic efficacy of drugs, reducing side effects, also preventing unwanted interactions with other molecules. Additionally, they are cell specific targeting, which is a perquisite to achieve drug concentrations required for optimum therapeutic efficacy in the target site whereas, minimising side effects on healthy cells and tissues. This nanodelivery systems has gained more interest in drug delivery approach due to their amphiphatic nature, which is the basic skeleton of biological membrane. Phospholipids produce fluid filled, closed spheres when reacted with water, because lipid molecules are polar, due to their hydrophilic ionizable head and hydrophobic tail, which consist of long fatty acid chains. Thus, when the sufficient molecules of phospholipid are in water, the tails naturally herd together excluding the water,

whilst the hydrophilic phosphate heads produce bonds with the water. The end-product is a bilayer in which the fatty acid tails facing the interior of the newly generated membrane with the polar heads facing the aqueous medium.

The polar heads at one surface of the membrane facing the aqueous interior layer of LBNSs and those at the other surface points at the aqueous exterior environment. This chemical tendency is the approach uses to form liquid filled spheres, which allows the LBNSs to be loaded with drugs or other bioactive compounds. The formation of LBNSs leads to the incorporation of water-soluble molecules into the aqueous interior, while the lipophilic molecules will tend to be incorporated into the lipid-bilayer. These attributes make them to play a crucial role in maintaining the cell membrane fluidity. Conversely, the developments of amphiphilic drug-lipid complex or pharmacosomes improve drug potential and make it easier to penetrate cell membrane without altering the cellular lipid bilayer. Thus, improving the absorption and therapeutic efficacy of poorly soluble drugs by enhancing the bioavailability, due to the solubility modification, and rate at which drugs are being release across biological barriers.

Hence, the incorporation of PZQ into a LBNSs could be a promising vehicle for the delivery of the drug, which in turn enhances the bioavailability, as well as reduce in the dose frequency and improve the patient compliance. This also could cause sustain release of PZQ and improve the rapid conversion of the drug into inactive metabolites due to rapid metabolism.

More so, the loading of PZQ into LBNSs will increase and improve the lipophilicity of the drug, which will make it easier to interact with the hydrophobic cores of the worm tegument thereby exposing the worm-antigen for the host immune response. The tegument of the schistosomes is covered by double outer membrane which enclosed the whole surface of the fluke, and this has been shown to have an association with immune evasion mechanism which makes them undetectable by the host antibodies [71].

The composition of novel LBNSs carrier for PZQ could also help to elicit worm-antigen and other molecular receptors. Since LBNSs can enhance the efficiency and specificity of drugs to tissues or cells by expressing surface molecular receptors for instance, unregulated selectin, antigens and serpin enzyme complex-receptor [4]. In addition, this approach could be cost-effective in the treatment of schistosomiasis by reducing the average dose recommendation of PZQ (20 mg/kg body weight; three times per day) requires in the disease treatment. This approach could also help in reducing the period of treatment of schistosomiasis as well as its co-infection with other diseases. For example, the incorporation

of amphotericin B (a drug used in the treatment of leishmaniasis) into a liposome increased penetration whilst reducing duration of treatment and drug toxicity [72]. Remarkedly, this liposomal amphotericin B achieved 90 % to 100 % curative rate within 7 days in visceral leishmaniasis patients unlike the free amphotericin B treatment regimens that goes for approximately 30days [73]. Indeed, the carrier system improved the pharmacokinetic and bioavailability profile of the drug. Due to the effectiveness of this lipid formulation, it has been recommended by the WHO as the first line drug for HIV-Leishmania co-infection because this co-infection model increases treatment failure, relapse rates, toxicity and mortality [74].

3.7. References

Papers of special note have been highlighted as either of interest (•) or of considerable interest (••) to readers.

1 Aruleba RT, Adekiya TA, Oyinloye BE, et al., PZQ therapy: how close are we in the development of effective alternative anti-schistosomal drugs?. Infect Disor Drug Targets *(*Formerly Curr Drug Targets Infect Disor). 2019;19(4):337-349.

2 Utzinger J, N'goran EK, N'dri A, et al., Efficacy of praziquantel against Schistosoma mansoni with particular consideration for intensity of infection. Trop Med Int Health. 2000;5(11):771-778.

3 Friis H, Byskov J, The effect of praziquantel against Schistosoma mansoni-infections in Botswana. Trop Geo Med. 1989;41(1):49-51.

4 Adekiya TA, Kondiah PP, Choonara YE, et al., 2020. A Review of Nanotechnology for Targeted Anti-schistosomal Therapy. Front Bioengine Biotechnol. 2020;8.

5 Malhotra G, Raut P, Pharmaceutical compositions. WO2015071668A1; 2015

6 Gryseels B, Nkulikyinka L, Coosemans MH, Field trials of praziquantel and oxamniquine for the treatment of schistosomiasis mansoni in Burundi. T Roy Soc Trop Med H. 1987;81(4):641-644.

7 Magnussen P, Treatment and re-treatment strategies for schistosomiasis control in different epidemiological settings: a review of 10 years' experiences. Acta Trop. 2003;86(2-3):243-254.

8 Cioli D, Pica-Mattoccia L, Basso A, et al., Schistosomiasis control: praziquantel forever?. Mol Biochem Parasitol. 2014;195(1):23-29.

9 Zingone G, Albertini B, Passerini N, et al., Praziquantel coground with mesoporous silica: solid state characterization and antihelmintic Activity. In *3rd European Conference on Pharmaceutics*. 3rd European Conference on Pharmaceutics. 2019.

10 Perissutti B, Passerini N, Trastullo R, et al., An explorative analysis of process and formulation variables affecting comilling in a vibrational mill: The case of praziquantel. Int J Pharmaceut. 2017;533(2):402-412.
11 Timóteo TRR, de Melo CG, de Alencar Danda LJ, et al., Layered double hydroxides of CaAl: a promising drug delivery system for increased dissolution rate and thermal stability of praziquantel. Appl Clay Sci. 2019;180:105197.
12 Trainor-Moss S, Mutapi F, Schistosomiasis therapeutics: whats in the pipeline?. 2016.
13 Lago EM, Xavier RP, Teixeira TR, et al., Antischistosomal agents: state of art and perspectives. Fut Med Chem. 2018;10(1):89-120.
14 Bergquist R, Utzinger J, Keiser J., Controlling schistosomiasis with praziquantel: How much longer without a viable alternative?. Infect Dis Poverty. 2017;6(1):1-10.
15 Mafud AC, Ferreira LG, Mascarenhas YP, et al., Discovery of novel antischistosomal agents by molecular modeling approaches. Trends Parasitol. 2016;32(11):874-886.
16 Pax R, Bennett JL, Fetterer R, A benzodiazepine derivative and praziquantel: effects on musculature of Schistosoma mansoni and Schistosoma japonicum. Naunyn-Schmiedebergs Arch Pharmacol 1987;304(3):309-315.
*Gives an insight to the mechanism of PZQ.
17 Kohn AB, Anderson PA, Roberts-Misterly JM et al., Schistosome calcium channel β subunits unusual modulatory effects and potential role in the action of the antischistosomal drug praziquantel. J Biol Chem. 2001;276(40):36873-36876.
*Gives an insight to the mechanism of PZQ.
18 Doenhoff MJ, Cioli D, Utzinger J, Praziquantel: mechanisms of action, resistance and new derivatives for schistosomiasis. Curr Opin Infect Dis. 2008;21(6):659-667.
*Gives an insight to the mechanism of PZQ in relation to parasite resistance.
19 Doenhoff MJ, Sabah AAA, Fletcher C, et al., Evidence for an immune-dependent action of praziquantel on Schistosoma mansoni in mice. T Roy Soc Tro Med H. 1978;81(6):947-951.
20 Harnett W, Kusel JR, Increased exposure of parasite antigens at the surface of adult male Schistosoma mansoni exposed to praziquantel in vitro. Parasitol. 1986;93(2):401-405.
21 Brindley PJ, Strand M, Norden AP, et al., Role of host antibody in the chemotherapeutic action of praziquantel against Schistosoma mansoni: identification of target antigens. Mol Biochem Parasitol. 1989;34(2):99-108.
22 Balaya L, Manjathuru M, Derambala Y, et al., Process for the preparation of praziquantel. U.S. Patent 8,754,215; 2014
23 Qian M, Tongli Biomedical Co., Ltd. R-praziquantel preparation method. U.S. Patent 9,175,321; 2015.

24 Qian M, Tongli Biomedical Co., Ltd. Method for preparing (R)-praziquantel. U.S. Patent 9,068,214; 2015.
25 Qian M, Tongli Biomedical Co., Ltd. Method for preparing (R)-praziquantel. U.S. Patent 9,139,859; 2015.
26 Qian M, Tongli Biomedical Co., Ltd. Process for the synthesis of (R)-praziquantel. U.S. Patent 9,802,934; 2017.
27 Qian M, Tongli Biomedical Co., LTD. Praziquantel crystal B substance, its preparation method and its applications in medicines and healthcare products. CN102786519A and CN102786519B; 2017
28 Qian M, Ho RJ, Qiao C et al., Crystal form of (R)-praziquantel and preparation method and application thereof. U.S. Patent 9,657,017; 2017.
29 Zhang F, Yang Z, Bao R, et al., Shanghai Institute of Pharmaceutical Industry and Zhejiang Hisun Pharmaceutical Co Ltd, Preparation method for praziquantel and intermediate compounds thereof. U.S. Patent 10,035,798; 2018.
30 Zhang F, Yang Z, Bao R, et al., Shanghai Institute of Pharmaceutical Industry and Zhejiang Hisun Pharmaceutical Co Ltd. Preparation method for praziquantel and intermediate compounds thereof. U.S. Patent 20180030049A1; 2018
31 Shanghai Institute of Pharmaceutical Industry Zhejiang Hisun Pharmaceutical Co Ltd. Preparation method for praziquantel and intermediate compounds thereof. WO2016127350A1; 2020
32 Eberhardt L, Waechtler A, Maillard D, et al., Method for the production of praziquantel and precursors thereof. WO2017036577A1; 2018
33 Eberhardt L, Waechtler A, Maillard D, et al., Method for the production of praziquantel and precursors thereof. U.S. Patent 10,273,213; 2019.
34 Maillard D, Waechtler A, Maurin J, et al., Method for the production of praziquantel and its precursors. ES2706314T3; 2019
35 Maillard D, Waechtler A, Maurin J, et al., Method for the production of Praziquantel and precursors thereof. U.S. Patent 9,932,337; 2018.
36 Waechtler A, Saleh-kassim H, Jasper C, et al., Method for the production of praziquantel. U.S. Patent 10,160,758; 2018.
37 Waechtler A, Saleh-kassim H, Jasper C, et al., Method for the production of praziquantel. WO2016078758A1; 2016
38 Qian M (Suzhou, CN). United States Suzhou Tongli Biomedical Co., Ltd. method for preparing (r)-praziquantel. 20140370555; 2014
39 Qian M (Suzhou, CN). United States Suzhou Tongli Biomedical Co., Ltd. method for preparing (r)-praziquantel. 20140370556; 2014

40 Lavet Gyogyszergyarto es Szolgaltato Kft. Taste masking compositions of praziquantel. EP2662075A1; 2013
41 Sabnis SS, Hayes J, Zupan JA, Endoparasiticidal gel composition. US8241669B2; 2012
42 Sabnis SS, Hayes J, Zupan JA, Wyeth LLC. Endoparasiticidal gel composition. U.S. Patent 6,893,652; 2005.
43 Dadak A, Franz S, Liebhart A, Oral gel comprising praziquantel. EP2594258A1; 2020
44 Ute Isele. Palatable ductile chewable veterinary composition. US8541019B2; 2013
45 Praziquantel emulsion injection and preparation technology thereof. CN103432074A; 2015
46 CN103381141A, Praziquantel long-circulating nanoparticle injection and preparation method thereof. CN103381141A; 2013
47 CN102697729A, Preparation method of praziquantel lipid lyophilized preparation. CN102697729A; 2012.
48 CN103316005A, Praziquantel-mebendazole nanoemulsion oral liquid and preparation method thereof. CN103316005A; 2013.
49 CN105816421A, Praziquantel nanoemulsion in situ gel for preventing and treating bilharziasis and preparation method and application thereof. CN105816421A; 2016.
50 CN106361758A, Compound ivermectin praziquantel bi-continuous phase emulsion and preparation method thereof. CN106361758A; 2016.
51 Qin L, Niu Y, Wang Y, et al., Combination of phospholipid complex and submicron emulsion techniques for improving Oral bioavailability and therapeutic efficacy of water-insoluble drug. Mol Pharmaceut. 2018;15(3):1238-1247.
52 Bell IR, Schwartz GE, Boyer NN, et al., Advances in integrative nanomedicine for improving infectious disease treatment in public health. Eur J Integr Med. 2013;5(2):126-140.
53 Coelho JF, Ferreira PC, Alves P, et al., Drug delivery systems: Advanced technologies potentially applicable in personalized treatments. EPMA J 2010;1(1):164-209.
54 Torres ES, Holban AM, Gestal MC, Applications of Nanodiamonds in the Detection and Therapy of Infectious Diseases. Materials (Basel, Switzerland). 2019;12(10).
55 Qasim M, Lim DJ, Park H, et al., Nanotechnology for diagnosis and treatment of infectious diseases. J Nanosci Nanotechnol. 2014;14(10):7374-7387.
56 Ranghar S, Sirohi P, Verma P, et al., Nanoparticle-based drug delivery systems: promising approaches against infections. Braz Arch Biol Technol. 2014;57(2):209-222.
57 Amara RO, Ramadan AA, El-Moslemany RM, et al., Praziquantel–lipid nanocapsules: an oral nanotherapeutic with potential Schistosoma mansoni tegumental targeting. Int J Nanomed. 2018;13:4493.

*Study where the activity of lipid based nanodelivery systems have been tested on human schistosomiasis in animal model.

58 Frezza TF, Gremião MPD, Zanotti-Magalhães EM, et al., Liposomal-praziquantel: efficacy against Schistosoma mansoni in a preclinical assay. Acta Trop. 2013;128(1):70-75.

*Study where the activity of lipid based nanodelivery systems have been tested on human schistosomiasis in animal model.

59 Mourão SC, Costa PI, Salgado HR, et al., Improvement of antischistosomal activity of praziquantel by incorporation into phosphatidylcholine-containing liposomes. Int J Pharm 2005;295(1-2):157-162.

60 El Gendy AEML, Mohammed FA, Abdel-Rahman SA, et al., Effect of nanoparticles on the therapeutic efficacy of praziquantel against Schistosoma mansoni infection in murine models. J Parasit Dis. 2019;43(3):416-425.

*Study where the activity of lipid based nanodelivery systems have been tested on human schistosomiasis in animal model.

61 Frezza TF, de Souza ALR, Prado CCR, et al., Effectiveness of hyperbaric oxygen for experimental treatment of schistosomiasis mansoni using praziquantel-free and encapsulated into liposomes: assay in adult worms and oviposition. Acta trop. 2015;150:182-189.

62 Radwan A, El-Lakkany NM, William S, et al., A novel praziquantel solid lipid nanoparticle formulation shows enhanced bioavailability and antischistosomal efficacy against murine S. mansoni infection. Parasite vector. 2019;12(1):304.

*Study where the activity of lipid based nanodelivery systems have been tested on human schistosomiasis in animal model.

63 Dkhil MA, Khalil MF, Bauomy AA, et al., Efficacy of gold nanoparticles against nephrotoxicity induced by Schistosoma mansoni Infection in mice. Biomed Environ Sci. 2016;29(11):773-781.

64 Tawfeek GM, Baki MHA, Ibrahim AN, et al., Enhancement of the therapeutic efficacy of praziquantel in murine Schistosomiasis mansoni using silica nanocarrier. Parasitol Res. 2019;118(12):3519-3533.

65 El-Feky GS, Mohamed WS, Nasr HE, et al., Praziquantel in a clay nanoformulation shows more bioavailability and higher efficacy against murine Schistosoma mansoni infection. Antimicrob Agents Chemother. 2015;59(6):3501-3508.

66 Adekiya TA, Aruleba RT, Oyinloye BE, et al., The effect of climate change and the snail-schistosome cycle in transmission and bio-control of schistosomiasis in sub-saharan Africa. Int J Environ Res Public Health. 2020;17(1):181.

67 Adekiya TA, Kappo AP., Okosun KO., Temperature and rainfall impact on schistosomiasis. Glob J Pure Appl Math. 2017;13:8453-8469.

68 Adekiya TA, Theoretical modelling of temperature and rainfall inuence on Schistosoma species population dynamics (Doctoral dissertation, University of Zululand). 2018.

69 Adekiya TA, Aruleba RT, Klein A., et al., In silico inhibition of SGTP4 as a therapeutic target for the treatment of schistosomiasis. J Biomol Struc Dyn. 2020;1-9.

70 WHO Fact Sheets, 2020. https://www.who.int/health-topics/schistosomiasis#tab=tab_1

71 Pearce EJ, Freitas TC., Reverse genetics and the study of the immune response to schistosomes. Parasite Immunol. 2008;30(4):215-221.

72 Aruleba RT, Carter KC, Brombacher F., et al., Can We Harness Immune Responses to Improve Drug Treatment in Leishmaniasis?. Microorganisms. 2020;8(7):1069.

73 Sundar S, Lockwood DN, Agrawal G, et al., Treatment of Indian visceral leishmaniasis with single or daily infusions of low dose liposomal amphotericin B: randomised trialCommentary: cost and resistance remain issues. Bmj. 2001;323(7310):419-422.

*A similar parasitic study where the approach proposed in this manuscript was reported for leishmaniasis with the use of liposomal amphotericin B

74 Van Griensven J, Carrillo E, Lopez-Velez R, et al., Leishmaniasis in immunosuppressed individuals. Clin Microbiol Infec. 2014;20(4):286-299.

CHAPTER FOUR

ANTI-CALPAIN ENGINEERED LIPOIDIAL NANOSYSTEMS: PREPARATION, CHARACTERIZATION AND APPLICATION IN PRAZIQUANTEL DELIVERY AS POTENTIAL FOR SCHISTOSOMIASIS TREATMENT

This chapter employed nanotechnological techniques to design and develop praziquantel nanoliposomal (NLP) nanosystem and surface-functionalized the NLP with anticalpain antibody (anticalpain-NLP) for targeted praziquantel (PZQ) delivery in the treatment of schistosomiasis. Anticalpain-NLP were prepared and validated for their physicochemical properties, *in vitro* and *in vivo* toxicity, drug loading capacity (DLC), drug entrapment efficiency (DEE), drug release and parasitological cure rate. The particle sizes for the formulated nanoliposomes ranged from 88.3 to 92.7 nm (PdI= 0.17-0.35), and zeta potential ranged from -20.2 to -31.9 mV. The DLC and DEE ranged from 9.03 to 14.16 and 92.07 to 94.63, respectively. The surface functionalization of the nanoliposomes was stable, uniform and spherical. Fourier transform infrared (FTIR), thermal behaviour and X-ray powder diffraction (XRPD) analysis confirmed that anticalpain antibody and PZQ were incorporated into the surface and inner core of the nanoliposomes, respectively. The sustained drug release was shown to be 93.2 and 91.1% within 24 h for NLP and anticalpain-NLP, respectively. In the *in vitro* analysis study, the nanoliposomes concentrations range of 30 to 120 μg/ml employed revealed acceptable levels of cell viability, with no significant cytotoxic effects on RAW 264.7 murine macrophage and 3T3 human fibroblast cells. Biochemical markers and histopathological analysis showed that the formulated nanoliposomes present no or minimal oxidative stress and confer hepatoprotective effects on the animals. The cure rate of the anticalpain-NLP and PZQ was assessed by parasitological analysis and it was discovered that treatment with 250 mg/kg anticalpain-NLP showed greater activity on the total worm burden, ova count in both the intestine and the liver of juvenile and adult schistosomes. The findings obtained support the ability of oral anticalpain-NLP to target young and adult schistosomes in the liver and portomesenteric locations, resulting in improved effectiveness of PZQ.

4.1. Introduction

Neglected tropical diseases (NTDs) are groups of disabling, chronic and disfiguring diseases that have been abandoned in favor of cancer, diabetes, tuberculosis, malaria, and other well-known diseases because they are most prevalent in poverty extreme areas, particularly among some disadvantaged urban and the rural poor populations. Meanwhile, schistosomiasis caused by *Schistosoma* parasites is the second most prevalent among the

NTDs (Adekiya *et al*., 2017; Adekiya *et al*., 2019). Approximately, 800 million people are currently living with this disease globally, with over 200,000 deaths yearly with sub-Sharan Africa with the highest proportion of this population (Elflein, 2021). The full impact of the disease holds a major influence on the health, social, financial and economic status of both the government and households. The design and development of new drugs for this disease has been faced with several shortcomings such as insufficient financial support and motivation for pharmaceutical companies, as well as a huge cost associated with the process of new chemical entities (NCEs) due to the long drug discovery pipeline and lack of interest by researchers in the area of NTDs (Adekiya *et al*., 2020; Adekiya *et al*., 2021). Hence, with the absence of vaccine, our current study uses a nanomedicine approach to optimize the existing anti-schistosomal gold standard drug; PZQ.

PZQ is the main drug and standard regimen used to treat schistosomiasis due to its efficacy against all adult forms of *Schistosoma* species and has been effective and well-tolerated by the affected populations, also reduces parasitic load and severity of symptoms (Aruleba *et al*., 2019). Thus, the use of PZQ has been encountered with some significant problems which are inefficient against the immature Schistosoma species, rapid uptake into the bloodstream after ingestion, extensive first-pass metabolism (Vale *et al*., 2017; Xiao *et al.*, 2018). Other include less bioavailability and solubility and tolerant multidrug resistance strains which has been reported in an endemic area as well as described in the laboratory (Doenhoff *et al.,* 2008; Adekiya *et al.*, 2020).

Nanomedicine which uses the application of nanotechnology for monitoring, treatment, control and prevention of biological diseases has been a promising approach in improving pharmaceutical ingredients in the treatments of several diseases and disorders (Adekiya *et al.*, 2020). Thus, nanoliposomes which are vesicles made up of concentric bilayer phospholipid-based membranes that may encapsulate or entrap hydrophobic or hydrophilic drugs and deliver them to specific locations in the body through a targeted drug delivery approach for diseases treatment (Mufamadi *et al*., 2013). Lipid-based formulations have gained a lot of attention for improving drug absorption and bioavailability, more importantly, reducing some of the adverse effects (Adekiya *et al.*, 2021). Furthermore, due to their amphipathic nature, nanoliposomes have attracted substantial attention in drug delivery, making them important for the enhancement and improvement in the absorption of drugs across biological barriers in the rate at which drugs may be released and in solubility modification (Cheng *et al*., 2017). Nanoliposomes, on the other hand, have the ability to reduce blood circulation times due to significant absorption by the reticuloendothelial system macrophage cells (RES). Several studies have revealed that PZQ-loaded liposomes

improved the anti-schistosomal activity of PZQ, and this can serve as a bases for alternative oral nanocarrier for the drug administration. Furthermore, the European Medicines Agency (EMA) and the Food and Drug Administration (FDA) of USA has endorsed numerous liposomal formulations for clinical usage.

Surface-modified liposomes containing polyethylene glycol (PEG), silk-fibroin, chitosan, or polyvinyl alcohol (PVA) have been found to increase liposome blood circulation half-life. Although, several studies have employed similar approach with positive outcomes such as; gold nanoparticles conjugated with antibody as tumour-targeting radiosensitizers for proton therapy; a potential strategy to improve cell killing (Li *et al*., 2019). The functionalization of multilayered particles with monoclonal antibodies for cancer cells targeting, which is capable of preserving the protein coronas; an essential protein that determines the surface charateristics of particles and their targeting capabilities (Dia *et al.*, 2015). Other includes the drug conjugated aptamer for the doxorubicin targeted delivery into HER3 cell for cardiotoxicity reduction in breast cancer treatment (Dou *et al.*, 2018), also, functionalization of polymeric nanoparticles with mannose for therapeutic anti-tumor immune responses and the induction of prophylactic in a melanoma model (Silva *et al.*, 2015).

Thus, this study would be first to design a nanoliposomes surface-engineered with an antibody (anticalpain) for the PZQ targeted delivery in schistosomiasis treatment. There are several target proteins and molecular receptors located on the schistosome tegument surface such as; schistosome cysteine protease calpain which belongs to calpain family that are expressed in the Schistosoma tegument (Siddiqui *et al.*, 1992; Wang *et al.*, 2017). Schistosome glucose transporter 1 (SGTP1) and 4 (SGTP4) which are found in all types of schistosomes (Skelly *et al.,* 1994; Skelly *et al.,* 1998), acetylcholinesterase (AChE) and a nicotinic form of acetylcholine receptor (nAChR) which are mostly present on the male schistosomes surface (MacDonald *et al.,* 2014; Mansour and Mansour, 2002). Other targeted protein found on the surface of the tegument is dynein (*Schistosoma mansoni*) (Mansour and Mansour, 2002). For the purpose of this study, cysteine protease calpain was the targeted protein on the schistosomes because, the activities of calpain occur at the sites of extracellular cell-cell adhesion and cell-substrate adhesion. In schistosomes, calpain are part of the tegumental proteases which are expressed at the host-parasite interface. They are located in the cytoplasmic extensions of microtubular bundles that connect the surface syncytial epithelium to the schistosomes cell bodies underlying muscle of both the juvenile and adult schistosomes (Siddiqui *et al*., 1992; Wang *et al*., 2017). In that location, they perform similar functions with other calpains such as the transportation and delivery of membrane precursors that is, as a mediator in the synthesis of surface membranes. They are also found across the syncytial

layer, where they function with the apical plasma membrane, causing membrane turnover (Siddiqui *et al*., 1992). Based on the function of calpains in calcium-mediated signaling processes, surface membrane biogenesis and immunological evasion, they have been proposed as a potential candidate for chemotherapy targets and/or for a define-molecular vaccine (Siddiqui *et al*., 1992; Wang *et al*., 2017).

Thus, this study employed nanotechnological techniques to design and develop praziquantel nanoliposomal (NLP) nanosystem and surface-functionalized the NLP with anticalpain antibody (anticalpain-NLP) for targeted praziquantel (PZQ) delivery in the treatment of schistosomiasis. The NLP designed in this study have a significant effect on targeting adult and the juvenile schistosomes and improve the specificity and efficacy in cells and tissues through overexpressed surface receptors (cysteine protease calpain). Also, the lipoidal nanosystem could clear all the traces of drug resistance and avert the reinfection of the disease by scavenging all the remnant of the parasite in the human host body

4.2. Materials and methods

4.2.1. Materials

Praziquantel, phospholipids (Asolectin from soybean), cholesterol (CHOL), phosphatidylethanolamine distearoyl methoxypolyethleneglycol conjugate (DSPE-mPEG^{2000}COOH), N-hydroxysulfosuccinimide (NHS), N,N′ -dicyclohexylcarbodiimide (DCC), 49409 Atto 488 Phalloidin and Biochemical assays (AST, ALT, ALP, bilirubin and creatinine) kits were purchased from Sigma-Aldrich. DAPI stain were purchased from Thermofisher. Monoclonal calpain antibody was purchased from Abcam (ab154167; Cambridge, UK) raised from rabbit, RAW 264.7 murine macrophage and 3T3 human fibroblast cell lines were procured from ATCC (Virginia, USA). All other chemicals were of analytical grade.

4.2.2. Methods

4.2.2.1. Nanoliposome Preparation

Nanoliposomes (NL) was formulated by adapting reverse-phase evaporation method formulated by Mufumadi *et al*. (2013). Briefly, asolectin, CHOL, and mPEG^{2000}COOH were dissolved in methanol and chloroform mixture (1:9$^{v}/_{v}$) and mixed with a probe sonicator at 60 rpm for 30 s in a round-bottom flask. The solvents were evaporated by a rotavap and maintained at 60 – 65 ^{o}C for 3 h, so as to get a thin lipid film on the flask wall. The adequate amount of phosphate buffered saline (PBS) (preheated at 60 ^{o}C) was added thereafter and the vessel was vigorously agitated on a rotary mixer so as to form multilamellar vesicles (MLVs).

To generate the PZQ-loaded nanoliposome (NLP), PZQ was dissolved in the NL-chloroform solution, in a PZQ/NL molar ratio of 1:6, and this was hydrated in 4 mL PBS buffer at pH 7.4 at 65 ^{o}C for 30 mins. Subsequently, the mixture was cooled to 4 ^{o}C and dialyzed against deionized water to eliminate the ammonia and residual drug. Unilameliar nanoliposomes was generated by a freeze-thawing method. Briefly, nanoliposome solutions was frozen at -80 ^{o}C by liquid nitrogen thereafter thaw on a water bath set at 37 ^{o}C (N = 6) (Song *et al.,* 2008). Moreover, samples were put on an ultrasonic bath at 50kHz for 5 mins before storing at 4 ^{o}C. Particle size was generated by slow and steady extrusion of the nanoliposome formulation via a polycarbonate membrane filter of μm pore size.

4.2.2.2. Surface-engineering of the nanoliposomes with anti-calpain

The monoclonal calpain antibody from Abcam (ab154167; Cambridge, UK) was purchased. The anticalpain-functionalized PZQ-loaded nanoliposomes was synthesized following the method described by Mufumadi *et al*. (2013) briefly by reacting native nanoliposomes with 87 mg of DCC after dissolving in 100 μL of DMSO in the presence of 46 mg of NHS in 4 mL of PBS (pH 7.2). 10 μL of 50 μg (0.68 mg/mL) of the anti-calpain was mixed with the treated nanoliposome suspension and allowed to mix for about 6 hrs at a room temperature. Subsequently, solvents was precipitated by rotary evaporator for 2-3h at 65 ^{o}C in water bath. This was followed by the dialysis of anti-calpain-functionalized PZQ-loaded nanoliposomes (anticalpain-NLP) using SnakeSkin Pleated dialysis tubing for about 24 h in order to eliminate excess NHS, DCC and uncoupled antibody in DDW. The anti-calpain-functionalized nanoliposome was stabilized by a freeze-thaw process and stored at 4 ^{o}C for future use.

4.2.2.3. Morphological analysis

Scanning Electron Microscopy

The morphological surface of the Anticalpain-NLP was determined by employing SEM analysis (SIGMA VP, Zeiss Electron Microscopy, Carl Zeiss Microscopy Ltd; Cambridge, UK). A drop of NLP suspensions were placed on a metallic sample stub and leave overnight to dry. Subsequently, the samples loaded on metallic sample stub were sputter-coated with both gold and palladium and covered with a carbon layer in order to reduce the surface charging. Thereafter, each samples was observed under different magnifications at an accelerated voltage of 20 kV.

Transmission Electron Microscopy

High Resolution Transmission Electron Microscopy (HRTEM) version TECNAIF3OST-TEM was employed in ascertaining the morphology of the Anticalpain-NLP and the elemental

distribution of the particles. Dispersions were concentrated to approximately 1:10 with PBS buffer at pH 7.4 and ultrasonicated for 5 mins at 37 ^{o}C. A drop of the concentrated sample was mounted on the carbon-coated copper grid for 5 mins following the excess removal of liquid, this was attained by blotting it with filter paper and air-dried at 25 ^{o}C. Subsequently, the films on the copper grid was visualized under an electron microscope at 10,000x magnifications.

4.2.2.4. Particle size distribution, zeta potential and polydispersity index (PDI) analysis

The polydispersity index (PdI), average particle size and zeta potential of native nanoliposomes, PZQ-NLP and PZQ-loaded anti-calpain-functionalized nanoliposomes was measured by a Malvern ZetaSizer Nano ZS (Malvern Instruments, Worcestershire, UK) at 25 ^{o}C. All nanoliposomes PdI , zeta potential and particle size measurements were done following the same method, that is, each sample was concentrated (1:10) with deionized water for each run by disposable cuvettes. Each test was carried out in triplicate, and the mean value in each case was documented accordingly.

4.2.2.5. Evaluation of the drug entrapment efficiency of the PZQ-loaded nanoliposomes

To determine the entrapment efficiency of PZQ inside the nanoliposomes, PZQ-nanoliposomes suspension (2 mL; *n* = 3), were centrifuged for 1 h at 5000 rpm. The concentration of the drug in the clear supernatant was analysed at a wavelength of λmax= 265 nm using UV-Vis spectroscopy (Specord40, Analytik Jena, AG, Germany) and computed using a standard linear curve of PZQ in concentrations range of 0 and 16 μg/mL in double-distilled water (R^2=0.99). Triplicate measurements were determined in order to ascertain the percentage value of EE and drug loading capacity of the nanoliposomes by the Equation (4.1) and (4.2) below, respectively;

$$\%EE = \frac{Total\ amount\ of\ PZQ\ loaded - Amount\ of\ PZQ\ in\ the\ supernatant}{Total\ amount\ of\ PZQ\ loaded} \times 100 \text{.....(Equation 4.1)}$$

$$\%LC = \frac{Amount\ of\ PZQ\ in\ nanoliposomes}{The\ weight\ of\ nanoliposomes} \times 100 \text{.....(Equation 4.2)}$$

4.2.2.6. Fourier transform infrared spectroscopy (FT-IR)

Fourier transform infrared (FTIR) analysis of the PZQ, NL, NLP, and Anticalpain-NLP was investigated in order to determine the characteristics of the possible interactions of the

molecular structural of the antibody and the nanoliposomes consisting of $mPEG^{2000}COOH$ on the nanoliposomes surface. The analysis was determined using Perkin-Elmer spectrum 2000 ATR-FTIR (PerkinElmer 100, Llantrisant, Wales, UK) via KBr pellets method in the region of 4000-650 cm^{-1} with a resolution of 4 cm^{-1}.

4.2.2.7. X-ray powder diffraction (XRPD) analysis

The degree of crystallinity transitions of the PZQ, NL, NLP, and Anticalpain-NLP in lyophilized form were investigated using x-ray powder diffraction (XRPD) spectra (Rigaku MiniFlex 600, Tokyo, Japan) sourced with CuKα radiation at 40 kV and 15 mA. The 2θ scan ranging from 3^o to 90 ^oC was chosen, and a scanning rate of 10^o per minute was used to achieved diffractograms of the samples.

4.2.2.8. Differential scanning calorimetry (DSC) analysis

Thermal behaviour of the PZQ, NL, NLP, and Anticalpain-NLP in lyophilized form were analysed on a DSC by a Mettler Stare system provided with STARe SW software. This physicochemical parameter was achieved by weighing 3 to 10 mg depending on each sample in a pin-hole alumina crucible and heated from 30°C to 300°C with a heating rate of 5°C/min under a nitrogen flow.

4.2.2.9. Thermogravimetric analyser (TGA) analysis

The range of thermal degradation of the PZQ, NL, NLP, and Anticalpain-NLP was evaluated by employing thermogravimetric analyser (PerkinElmer, TGA 4000, Llantrisant, Wales, UK). The samples were heated from 30 to 900°C with a 10°C/min heating rate under the continuous flow of nitrogen. Thermograms generated were given in percentage weight against temperature.

4.2.2.10. In vitro release of the drugs

PZQ release from PZQ-nanoliposomes dispersion was determined in dissolution medium containing 100 mL of PBS (pH 7.4) consisting of 0.002% Tween 80 through a dialysis technique in a thermostatically controlled orbital shaking incubator- horizontal (type LM-530, Yihder Technology Co., LTD.) set at 25 rpm for 24 h at 37 ± 1°C. The suspension of PZQ (25 mg/mL) was utilized as the control. At specified time intervals (1, 2, 4, 8, 12, and 24 hrs), 2 mL of the samples were drawn for analysis and an equivalent amount of pre-warmed fresh media was replaced into the samples in order to sustain sink conditions. The samples withdrawn were analysis for drug (PZQ) release using nanophotometer at 263 nm. The quantity of PZQ released was calculated from a standard linear curve (R^2 = 0.99) of PZQ in PBS (pH 7.4).

Each experiment was carried out in triplicate. The values of mean dissolution time (MDT) was calculated for each sample utilizing the Equation below;

$$MDT = \sum_{i=1}^{n} ti \left(\frac{M_t}{M_\infty}\right) \text{.....(Equation 4.3)}$$

Where the fraction of dose released in time *ti =(ti + ti – 1)*/2 denotes M_t and M_∞ represents the ejecting dose.

4.2.2.11. In vitro cytotoxicity assay (MTT Assay)

The *in vitro* cytotoxicity of the PZQ, NL, NLP, and Anticalpain-NLP in RAW 264.7 murine macrophage cell and 3T3 human fibroblast cell was investigated by an MTT cell viability assay. The cells were cultured in DMEM and RPMI, respectively, supplemented with 10% fetal bovine serum and 1% penicillin-streptomycin in a humidified incubator at 37°C and 5% CO_2 . After every two days, the growth medium was replaced with fresh medium until the cells reached about 80 to 90 % confluence. The cells were seeded at a density of 1 x 10^5 cells per well in a 96-well plate. After 24h, the adhered cells were treated with NL, NLP, and Anticalpain-NLP and PZQ at a range concentration range of 30 to 120 μg/mL, undertaken in triplicate. Subsequently, the cells were incubated for 24 h in a humidified incubator at 37°C and 5% CO_2 . After 24 h, 10 μl of MTT reagent (Merck, Darmstadt, Germany) was added to the wells and the cells were incubated at 37°C for 4 h. Thereafter, 110 μl of DMSO was added and the well plates were further incubated at 37°C for an hour to dissolve the formazan crystals. Thereafter, the absorbance was measured at 570 nm, with a reference wavelength of 690 nm using a multimode microplate reader (FilterMaxTM F5, Molecular Devices, CA, USA). The percentage of cell viability was calculated from the ratio of absorbance of the test samples to that of the untreated samples (control).

$$\text{Percentage cell viability} = \frac{(Absorbance\ of\ the\ test\ sample)\ x\ 100}{(Absorbance\ of\ untreated\ sample\ (control))} \text{ .....(Equation 4.4)}$$

4.2.2.12. Cell morphology analysis

As previous section (section 4.2.2.11), after RAW 264.7 murine macrophage cells cultured reached about 80 to 90 % confluence, cell density of 2.5 x 10^6 cells/mL were seeded and cultured on coverslips in 6-well plates containing 2 mL DMEM supplemented with 1.0%($^v/_v$) penicillin-streptomycin antibiotic and 10%($^v/_v$) FBS and incubated for 24 hours at 37°C under 5% CO_2. After 24h, the adhered cells were treated with 90 μg/ml concentration of NL, NLP, Anticalpain-NLP and PZQ as well as 10 μg/ml of 5- fluorouracil (5-FU) as a negative control in triplicates. Subsequently, the cells were further incubated for 24 h in a humidified incubator at 37°C and 5% CO_2. Upon 24 hours of treatment, the phase contrast morphology of the cells

were visualized under inverted compound light microscope (Olympus CKX53, Olympus Corporation, Tokyo, Japan). Thereafter, the cells were fixed by first spiking the media growth containing the cells with 500μL of 4% formaldehyde to avoid damaging the cells by the abrupt change between the fixation solution osmolarity and culture medium osmolarity. Then the media were aspirated and decanted after 2 mins, and subsequently covered the cells with fresh 1mL of 4% formaldehyde for about 20mins. After 20mins of fixation, the fixed cells were gently washed with 2mL of PBS for 4 times to remove any unbound fixation agent, thereafter, the cells were stained with 500μL of a 50μM fluorescent phalloidin solution for 40 mins at room temperature under dark condition. 40 mins after, the cells were washed 4 times with PBS to remove unbound phalloidin stain, subsequently, the cells were stained with 500μL of 500nM DAPI stain solution and incubate at room temperature for 5 mins in the absence of light. Afterward, the cells were rinsed thoroughly with PBS to remove the unbound DAPI stain solution. Then, the coverslips were mounted on glass slides and viewed under the compound fluorescent microscope (Olympus IX51, Olympus Corporation, Tokyo, Japan).

4.2.2.13. In vivo toxicity

The evaluation of in vivo toxicity was done in Sprague Dawley rats with weight range 250-300g, kept in a standard husbandry and housing condition at normal room temperature and fed with normal tap water and a normal rat chow. The animals were group into four (4) randomly, and each group was named as follow, Group I: control, Group II: PZQ, Group III: PZQ-NLP, and Group IV: PZQ-loaded anti-SGTP4-functionalized NLP. Equivalent amount of the dose (250mg/kg) in about 2 to 3mL of PZQ, PZQ-NLP and PZQ-loaded anti-SGTP4-functionalized NLP were administered into the animals via the once off oral gavage orally. 7 days after, all the animals were euthanized, and their blood were collected via cardiac puncture and stored in microcentrifuge heparin tubes and centrifuge for 5 min at 2500 rpm in 4°C to isolate plasma from red blood cells (RBCs). Thereafter, the plasma was examined for liver functioning test in order to assess the hepatotoxicity of the various formulations by the measurement of the plasma levels of aspartate aminotransferase (AST), alanine aminotransferase (ALT), creatinine and bilirubin using commercially available kits from Sigma Aldrich, South Africa. The activities of ALT, AST, creatinine and bilirubin was calculated for each assay using the Equations below;

$$\text{ALT activity} = \frac{B\ x\ Sample\ Dilution\ Factor}{(Final\ temperate - Initial\ temperature)\ x\ V} \quad \text{.....(Equation 4.5)}$$

Where B is the amount (nmole) of pyruvate generated between the initial temperature and final temperate and the final temperature is the time of first reading in minutes, while initial temperature is the time of penultimate reading in minutes, and V is the sample volume (mL) added to well.

$$\text{AST activity} = \frac{B\ x\ Sample\ Dilution\ Factor}{(Reaction\ Time)\ x\ V} \quad \text{.....(Equation 4.6)}$$

Where B is the amount (nmole) of of glutamate generated between the initial temperature and final temperate, and the reaction time is the final temperature minus the initial temperature in minutes and V is the sample volume (mL) added to well.

$$\text{Concentration of creatinine} = \frac{Sa}{Sv} \quad \text{.....(Equation 4.7)}$$

Where Sa is the amount of creatinine in unknown sample (nmole) from standard curve and Sv is the sample volume (μL) added into the wells, while C is the concentration of creatinine in sample and the creatinine molecular weight is taken as 113.12 g/mole.

$$\text{Bilirubin concentration} = \frac{(A_{530})sample - (A_{530})blank}{(A_{530})calibrator - (A_{530})water}\ x\ (5\ mg/dL) \quad \text{....(Equation 5.8)}$$

Where (A_{530}) sample is the value of the sample (total or direct) and (A_{530}) blank is the value of the sample blank, while (A_{530}) calibrator and (A_{530}) water are the value of the calibrator reading and the value of the water control reading, respectively. 5 mg/dL is the equivalent bilirubin concentration of the calibrator using a multimode microplate reader (FilterMaxTM F5, Molecular Devices, CA, USA).

4.2.2.14. Sample preparation for histopathological analysis

In order to determine the toxicity of the nanoliposome formulations to the organ, tissue samples (liver, lung, kidney and spleen) were obtained and placed in 10 % Neutral Buffered Formalin thereafter inserting them in paraffin for sectioning the tissues. Then the tissues were stained with eosin and haematoxylin for microscopic determination and spotted for toxicity markings according to IDEXX protocol (IDEXX-JB632262).

4.2.2.15. In vivo antischistosomal study

4.2.2.15.1. Infection of animals

The *in vivo* antischistosomal study was conducted in the Schistosome Biological Supply Centre (SBSC) of Theodor Bilharz Research Institute (TBRI), Giza, Egypt. Male Swiss albino mice (CD-1) were obtained from SBSC of TBRI, Giza, Egypt, weighing 18–20 g each, and housed in an environmentally controlled room temperature of 20–22 °C, a 12 h light/dark cycle and 50–60% humidity with access to food and water *ad libitum* throughout the acclimatization and experimental periods. The cercarial suspension (0.1 ml) was gently mixed, stained with picric acid solution and counted.

Subsequently, the mice were infected with *S. mansoni* cercariae (provided by SBSC) through subcutaneous (Liang *et al*., 1987) and exposure to 60 ± 10 cercariae/mouse. All the animal experiments were conducted in accordance with the Guide for Care and Use of Laboratory Animals by the Institutional Review Board of TBRI (appendix B).

4.2.2.15.2. Experimental design and animals grouping

Mice infection*: S. mansoni* cercariae were inoculated subcutaneously infected with 60±10 Egyptian strain of *S*. *mansoni* cercariae sheds from *Biomphalaria alexandrina* snail according to Liang *et al* (1987).

Animals were divided according to the time of drug administration:

Group 1: Infected control.

Group 2: Single dose 250 mg/kg of Anti-calpain**-**PZQ-loaded nanoliposomes was given two weeks post infection

Group 3: A drug (PZQ) 250 mg/kg single dose was given two weeks post infection

Group 4: Single dose 250 mg/kg of Anti-calpain**-**PZQ-loaded nanoliposomes was given four weeks post infection.

Group 5: A drug (PZQ) 250 mg/kg single dose was given four weeks post infection.

All animals were sacrificed six weeks post infection.

4.2.2.15.3. Assessment of parasitological criteria of cure

Worm recovery: Sacrificed mice were exposed to hepato-portomesentric perfusion technique to collect adult *S*. *mansoni*, detect sex (male/female/copula), determine worm burden, and then calculate the percentage of reduction of total worms (Christensen *et al.*, 1984).

Oogram pattern: The percentage of egg developmental stages (oogram pattern) was studied (Pelligrino *et al*., 1962). Identifying and counting the eggs at different stages of maturity in three fragments of the intestine, and the mean number of each stage was calculated.

Egg count in tissues: Small pieces of hepatic and intestinal tissues were weighted, digested overnight in 5 mL KOH 5% solution and three samples (each 50 µl) of the digested tissue were microscopically examined to determine the mean egg count (Pelligrino *et al*., 1962). Number of eggs/gram tissue and the percentage of reduction of total ova/gram tissue were calculated according to Kloetzel (1967).

4.2.3. Statistical Analysis

The results are expressed as mean values and standard deviation (±SD), and the significance of the difference observed was calculated using student's t-test (GraphPad Prism software). In all the tests, p-values <0.0001 are considered statistically significant.

Other data were coded and entered using the statistical packages Microsoft excel 2016. The percentage reduction of worm/egg burden in each treated group was calculated according to the following equation: % reduction = [(No. of worms/eggs in control group) – (No. of worms/eggs in treated group)] / (No. of worms/eggs in control group) × 100.

4.3. Results

4.3.1. Physicochemical characterization of the Nanoliposomes

4.3.1.1. Surface morphology and shape analysis of the formulated nanoliposomes

Surface electron microscopy (SEM) and Transmission Electron Microscope (TEM) were used to evaluate the surface morphology and the shape of the formulated nanoliposomes. The SEM and TEM images in Figure 4.1a-d revealed that the formulated nanoliposomes are uniformly spherical in shape with stable or intact structure, showing typical SEM and TEM images of the nanoliposomes. As further shown in Figure 4.1b, the SEM image of the anticalpain-functionalized nanoliposomes presented a uniform surface morphology different from the unfunctionalized nanoliposomes shown in Figure 4.1a. These results also confirmed that anticalpain antibody was surface-conjugated onto the nanoliposomes. Interestingly, the morphology profile showed in Figure 4.1c and d for anticalpain-NLP did not show aggregation after the entrapment of PZQ within the core and surface engineering of the antibody onto the surface of the nanoliposomes. Furthermore, the particle size distribution for anticalpain-NLP was within the nanoscale, which corroborated the data obtained by the Malvern ZetaSizer Nano ZS.

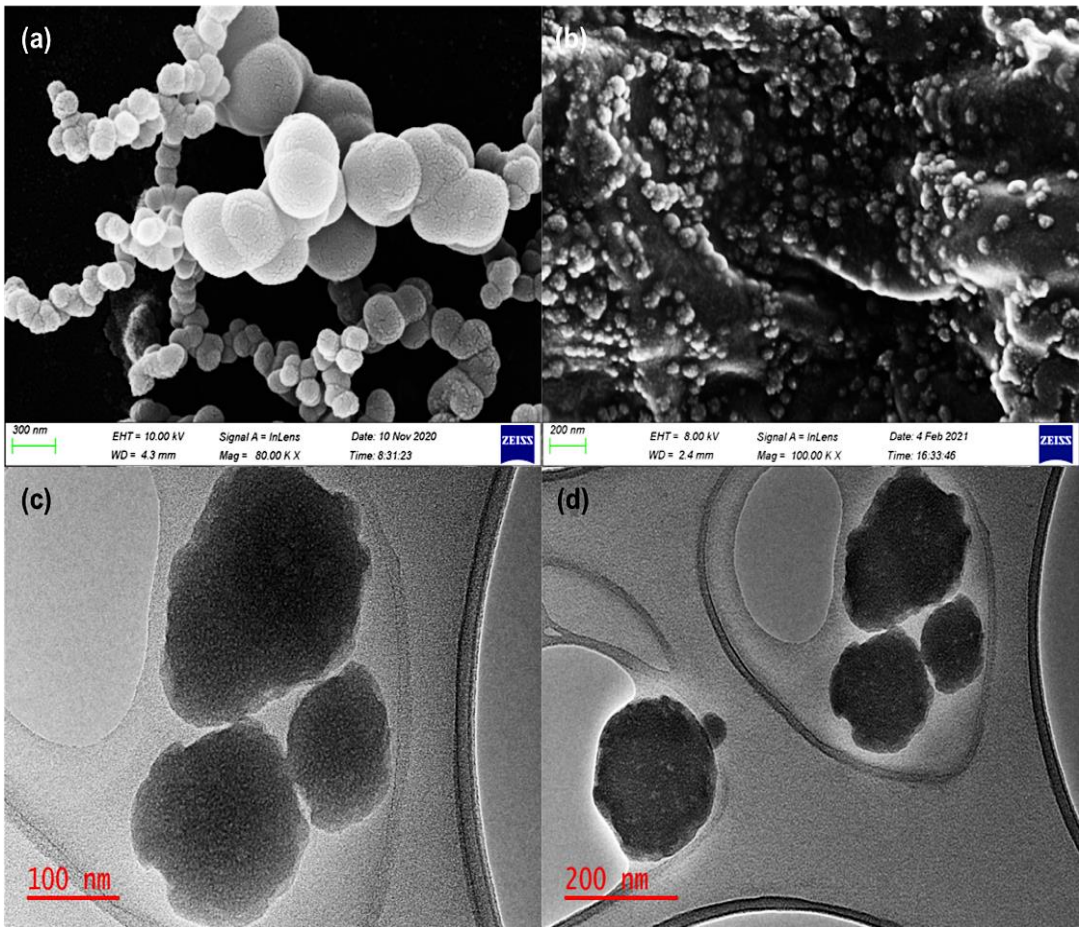

Figure 4.1: SEM images of NLP (a), and Anticalpain-NLP (b), TEM images of (c) Anticalpain-NLP at 100 nm (d) at 200 nm.

4.3.1.2. Particle size distribution, PDI, zeta potential, drug entrapment efficacy and drug loading capacity analysis

Table 4.1 shows the particle sizes of the NL, NLP and anticalpain-NLP to be 88.3 ± 0.75, 89.0 ± 0.66 and 92.7 ± 2.85 nm, respectively, which showed that the formulated nanoliposomes falls within the good particle size range. Furthermore, the PDI for the nanoliposomes formulated were observed to be 0.17 ± 0.011, 0.22 ± 0.010 and 0.35 ± 0.032 a.u for NL, NLP and anticalpain-NLP, respectively. This indicates that the nanoliposomes are stable regarding flocculation, aggregation, sedimentation, creaming and coagulation through a strong electrostatic repulsion, which keeps the charges of the particles from one and another. The zeta potential happens to be one of the significant parameters responsible for the stability of colloidal dispersions. Thus, the zeta potentials in this study are shown to be -31.9 ± 2.41, -29.2 ± 0.37 and -20.2 ± 2.28 mV for NL, NLP and anticalpain-NLP, respectively. These high zeta potential values displayed, confered stability to all the nanoliposomes formulated and resist aggregation of the particle dispersion.

Table 4.1 further shows the drug entrapment efficacy and drug-loading capacity for the NLP and anticalpain-NLP. This revealed that the nanoliposomes achieved high PZQ entrapment

efficacy of 94.63 ± 0.30 and 92.07 ± 0.23 %, respectively with drug-loading capacity of 14.16 ± 0.61 and 9.03 ± 0.42 %, respectively.

Table 4.1: Particle size, PDI, zeta potential of unloaded, PZQ-loaded and Anti-calpain-PZQ-loaded nanoliposomes and the drug entrapment efficacy and drug loading capacity

S/N	Sample	Size (nm)	PDI (a.u)	Zeta Potential (mV)	%DEE	%DLC
1	NL	88.3 ± 0.75	0.17 ± 0.011	-31.9 ± 2.41	-	-
2	NLP	89.0 ± 0.66	0.22 ± 0.010	-29.2 ± 0.37	94.63 ± 0.30	14.16 ± 0.61
3	AntiCal-NLP	92.7 ± 2.85	0.35 ± 0.032	-20.2 ± 2.28	92.07 ± 0.23	9.03 ± 0.42

Note: Values are expressed as mean ± SD (n = 3)

PDI means polydispersity index, NL represents unloaded nanoliposomes, NLP means PZQ-loaded nanoliposomes, and AntiCal-NLP represent the Anti-calpain engineered PZQ-loaded nanoliposomes. %DEE Drug entrapment efficacy, %DLC drug-loading capacity

4.3.1.3. Molecular vibrational transitions and X-ray powder diffraction of the formulated nanoliposomes evaluation

FTIR spectra of the PZQ, NL, NLP and anticalpain-NLP are illustrated in Figure 4.2a. The FTIR spectrum for the PZQ showed vibration peaks at the wavenumbers 2929.49 cm^{-1} and 2852.52 cm^{-1}, which indicated the presence of symmetric CH and CH_3 asymmetric stretching vibrations. The NL showed a broad FTIR spectrum band at wavenumber 3256 cm^{-1}, which could be ascribed to the absorption bands for the O-H, two bands were observed at wavenumbers 2924 cm^{-1} and 2853 cm^{-1} which could be attributed to -CH_2 and -CH_3 stretching vibrations. Furthermore, two bands were observed at 1739 cm^{-1} and 1640 cm^{-1} which are ascribed to the intensities of the carboxyl group vibration absorptions. After the entrapment of PZQ with the nanoliposomes, the absorption peaks corresponded to the peaks of PZQ disappeared, and the carboxyl group absorption at 1739 cm^{-1} stretched became weak and the peak absorption at 1640 cm^{-1} became stronger. This is an affirmation that there is an interaction between the PZQ and nanoliposomes during the drug entrapment process. Anti-calpain engineered PZQ-loaded nanoliposomes showed an absorption band at 1851 cm^{-1} and absorption at 1739 cm^{-1}, while there is a slight shift and a very high peak absorption at 1624 cm^{-1}. This indicates a formation of amide(-NH_2) bending vibrations during the covalent attachment of the anti-calpain antibody. These FTIR findings showed that there was an interaction between the -NH_2 group on the antibody and the -OH group of DSPE-mPEG2000COOH during the formulation of anticalpain engineered PZQ-loaded nanoliposomes.

The crystal nature of the PZQ, NL, NLP and anticalpain-NLP evaluated using powder X-ray diffraction technique are illustrated in Figure 4.2b. PZQ was observed to be crystallized in nature with major peaks at 2θ-4.2°, 7.6°, 16.6°, 17.8° and 20.3°; NL was shown to be crystalline with specific peaks at 2θ-5.2° and 20.1°. Following interaction of PZQ with NL, there is a slight shift in the peaks at 2θ-6.0° and 20.1°, and the NLP was shown to be crystallized. Importantly, the peaks that corresponded to the peaks of PZQ were not noticed, which is an indication that PZQ interacted with NL and was well embedded in NL. Anti-calpain engineered PZQ-loaded nanoliposomes were observed to be crystalline in nature with major peaks at 2(-9.2°, 29.5° and 42.6°, which could be another added advantage that there was a covalent attachment of the anticalpain with the -OH group of DSPE-mPEG^{2000}COOH during the formation of the anticalpain-NLP.

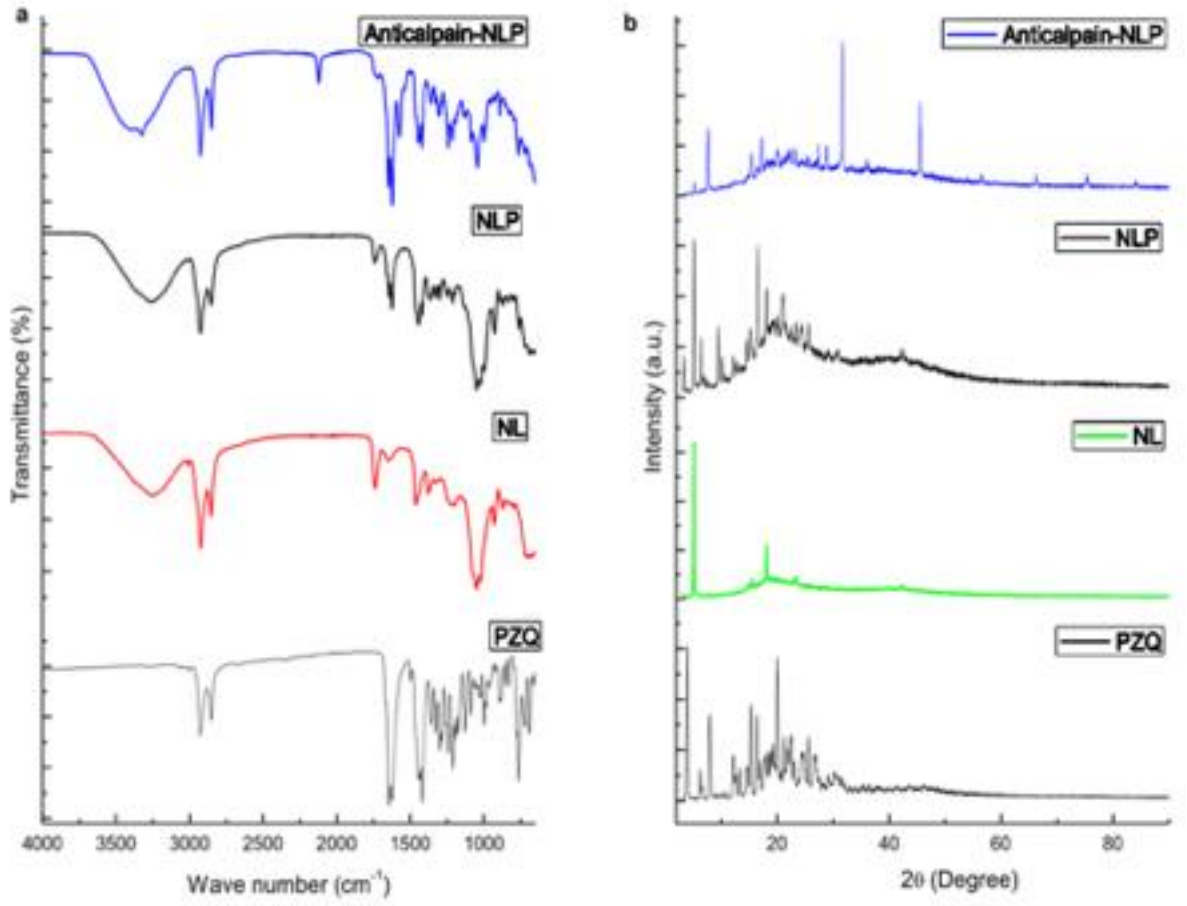

Figure 4.2: FTIR spectra of PZQ, NL, NLP and Anticalpain-NLP; (b) P-XRD images of PZQ, NL, NLP and Anticalpain-NLP

4.3.1.4. Thermal behaviour of the formulated nanoliposomes

Differential scanning calorimetry (DSC) analysis was used to examine the formulated nanoliposomes' thermal behaviour to determine the changes in exothermic and endothermic temperature that occurred during the nanoliposomes formulation. The data in Figure 4.3a showed the thermal curves of PZQ, NL, NLP and anticalpain-NLP. The endothermic peaks were observed at 137.99^{o} for PZQ. The endothermic peak for native nanoliposomes was observed at 111.09^{o}; 198.22^{o}, the NLP has endothermic peaks at 112.58^{o} and 198.21^{o}, and the endothermic peaks for the anticalpain-NLP were observed at 115.99^{o} and 198.27^{o}. The thermal behavior of the NLP showed that there was a strong hydrophobic interaction between PZQ and the phospholipids of the nanoliposomes during the entrapment of the drug. This was revealed by the lack of peak corresponding to the peak of the drug for both the NLP and anticalpain-NLP. The broadening endothermic peak and the disappearing glass transition in the anticalpain-NLP indicated strong hydrophobic interaction between PZQ and the antibody-functionalized nanoliposomes. Figure 4.3b demonstrated the thermal stability of the PZQ, NL, NLP and anticalpain-NLP using thermal gravimetric analysis. PZQ showed a major weight loss (95.4%), temperature range of 270-342°C, while both the native nanoliposomes and PZQ-loaded nanoliposomes and anticalpain functionalized PZQ-loaded nanoliposomes showed the same slow and steady weight loss pattern at similar temperature ranges. It can be deduced from this data that there is improvement in the drug's stability and showed the entrapment of the drug during the hydrophobic interaction between the PZQ and the phospholipids.

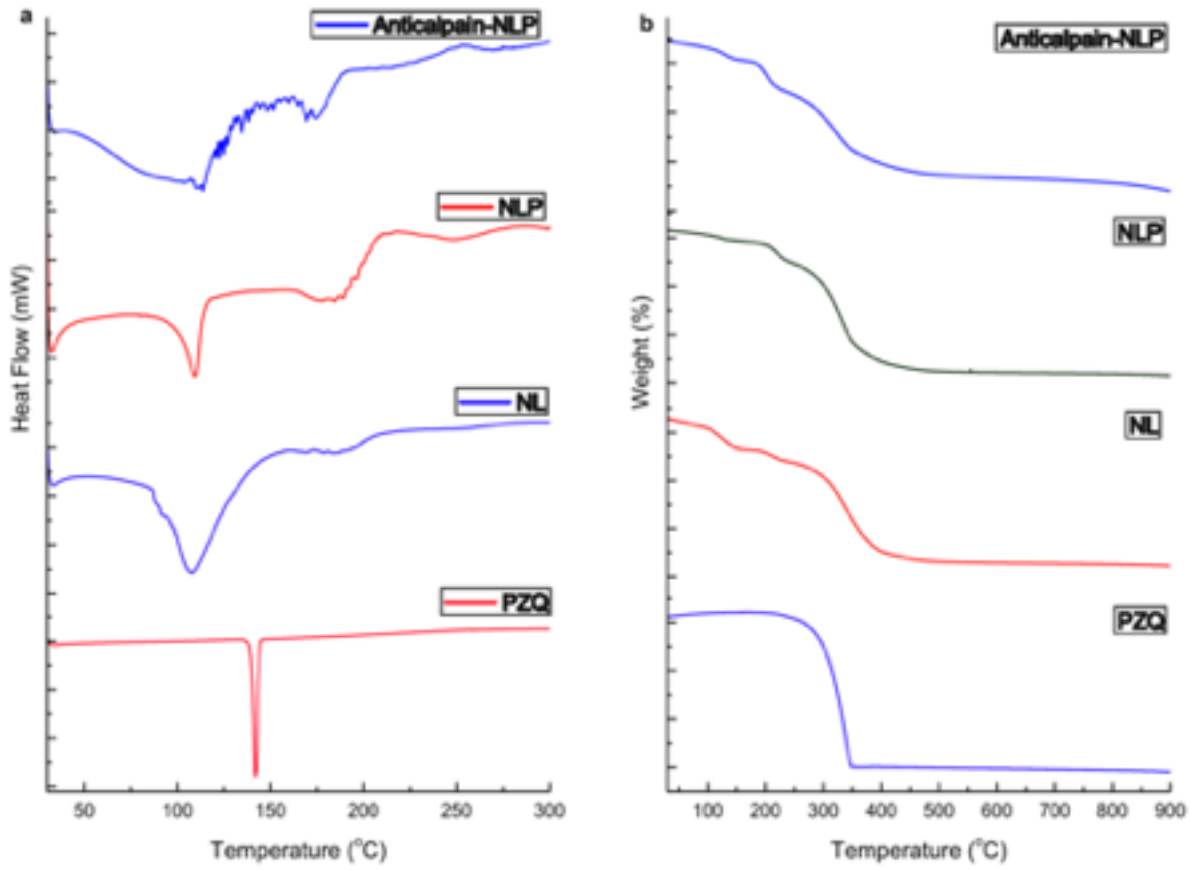

Figure 4.3: (a) DSC thermograms of PZQ, NL, NLP and Anticalpain-NLP; (b) Thermogravimetric analyses of PZQ, NL, NLP and Anticalpain-NLP

4.3.2. In vitro release behaviour of PZQ analysis

The *in vitro* release ability of the PZQ-loaded nanoliposomes and PZQ-loaded functionalized nanoliposomes was evaluated in PBS (pH 7.4 at 37 ^{o}C) over 24 h. PBS (pH 7.4) was used to create pH conditions pertinent to the human physiological pH conditions and increase the analytical method's sensitivity. Figure 4.4 demonstrates the percentage cumulative release profiles of PZQ, from the native PZQ (control), PZQ-loaded nanoliposomes and PZQ-loaded functionalized nanoliposomes. Free PZQ suspension released virtually all free PZQ in 2 hours at 37°C under sink conditions. On the other hand, the formulated nanoliposomes showed an initial burst release pattern at 4 hours followed by approximately 93.2 and 91.1 % of PZQ released within 24 h for PZQ-loaded nanoliposomes and PZQ-loaded functionalized nanoliposomes, respectively. Interestingly, both the PZQ-loaded nanoliposomes and PZQ-loaded functionalized nanoliposomes exhibited typical sustained release profiles. This sustained release profiles of PZQ exhibited by the formulated nanoliposomes may be attributed to the concentration of cholesterol, which is well-known to stabilize lipid bilayers through the reduction of membrane fluidity, whereby causing restriction in the movement of drug across the formulated nanoliposomes. It could also be deduced that the rapid release of

PZQ at the initial 4 hours burst phase could be as a result of the hydration process in the formulated nanoliposomes.

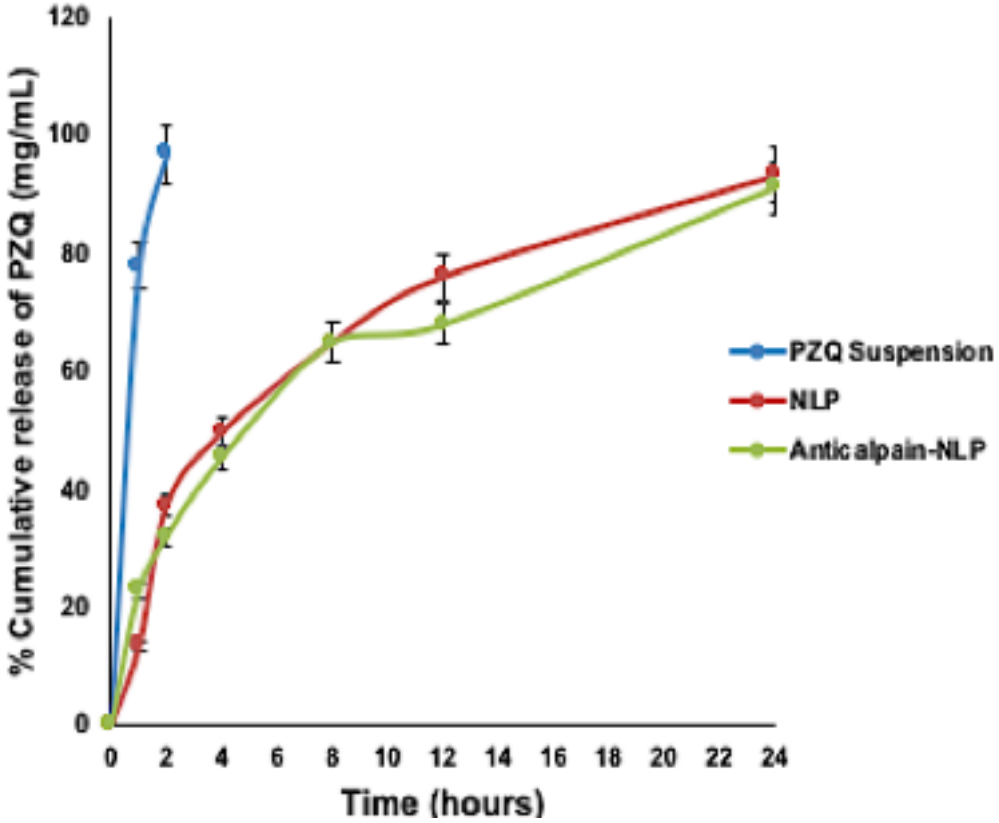

Figure 4.4: *In vitro* release profile of free PZQ, and NLP. Release medium = PBS, Temperature = 37 ± 1°C, pH = 7.4 (n = 3, mean ± SD)

4.3.3. In vitro toxicity analysis

The MTT (3- [4, 5-dimethylthiazol-2yl]-2, 5-diphenyl tetrazolium bromide) assay was used to investigate the cytotoxicity of the formulated nanoliposomes and PZQ on RAW 264.7 murine macrophage cells and 3T3 human fibroblast cells. This MTT assay was used to measure the viability of RAW 264.7 murine macrophage and 3T3 human fibroblast cells after 24-hour treatment with free PZQ, NL, NLP, and anticalpain-NLP at different concentrations ranging from 30 to 120 μg/ml. The results showed that the formulated nanoliposomes (NL, NLP and anticalpain-NLP) and PZQ showed acceptable levels of cell viability, with no cytotoxic effects on the RAW 264.7 cells after 24 hours and the viability are dose-dependent as shown in Figure 4.5. The opposite effect that was observed in PZQ group, that is, an increase in cell viability with increasing concentration prompted the use of 3T3 human fibroblast cells for MTT assay in order to ascertain the cytotoxicity of the formulated nanoliposomes and PZQ. Thus, Figure 4.6 further showed that the concentrations ranging (30 to 120 μg/mL) employed in this study revealed acceptable levels of cell viability, with no significant cytotoxic effects on 3T3 human

fibroblast cells. Interestingly, a significant increase ($p<0.0001$) in the percentage cell viability was observed in the PZQ tested group compared to the NLP and anti-NLP tested groups with higher viability. More so, it was revealed that the percentage of cell viability depends on the dose concentration of both the PZQ and the formulations.

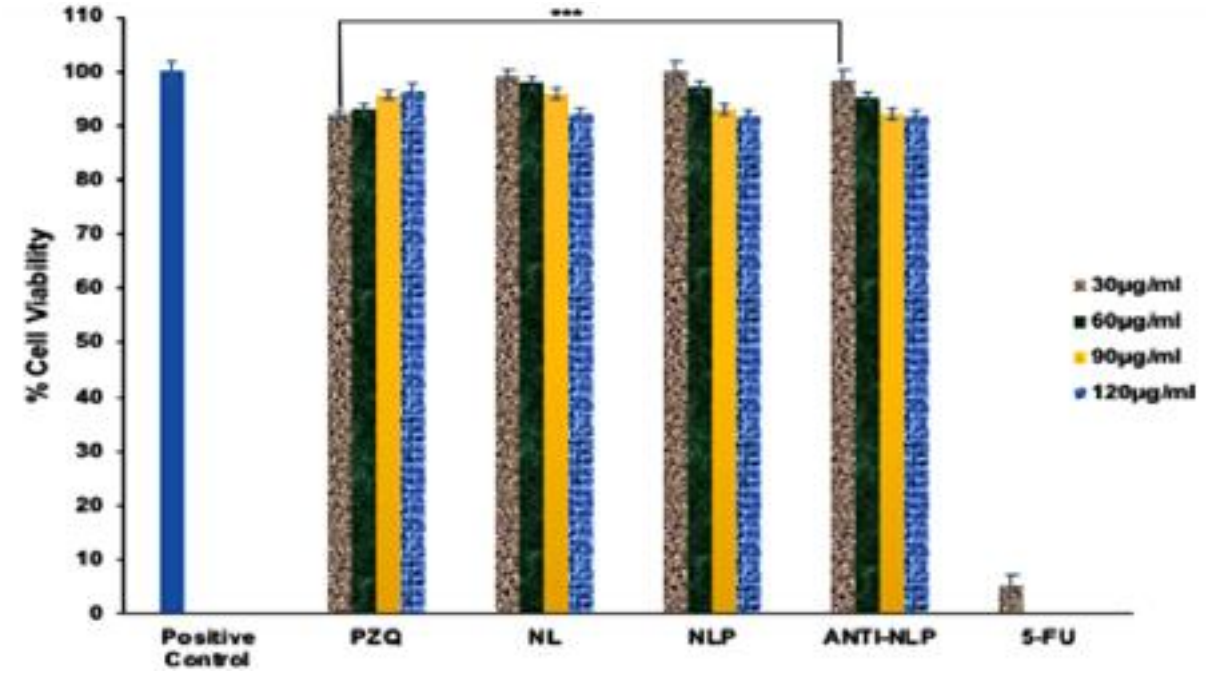

Figure 4.5: MTT assay measurement of the viability of RAW 264.7 murine macrophage cells after 24-hour treatment with free PZQ, NL, NLP, and Anticalpain-NLP at different concentrations (Data represent n = 3, mean ± SD). *** indicates $p<0.0001$ when compared to the NLP and Anticalpain-NLP groups to the same concentration of PZQ.

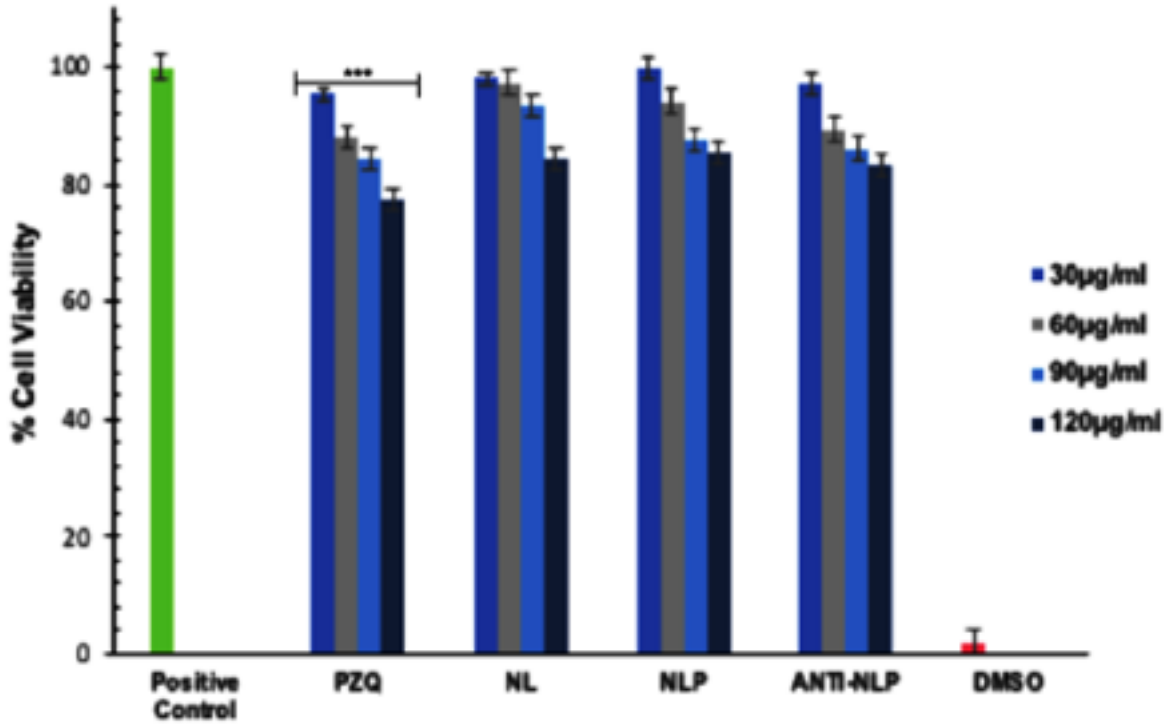

Figure 4.6: MTT assay measurement of the viability of 3T3 human fibroblast cells after 24-hours treatment with free PZQ, NL, NLP, and Anticalpain-NLP at different concentrations (Data represent n = 3, mean ± SD). *** indicates p<0.0001 when compared to the NLP and Anticalpain-NLP groups to the same concentration of PZQ.

4.3.4. Morphological studies on RAW 264.7

Figure 4.7a and b presented the morphology of the RAW 264.7 murine macrophage cells visualized by fluorescent microscopy and inverted microscopy after the cells were treated with 90 μg/ml of free PZQ, NL, NLP, and anticalpain-NLP and 5-FU (5-fluorouracil) (10 μg/ml) as a negative control, while using the untreated cells as the positive control. It was observed that all the cells treated with nanoliposomes and PZQ possess normal cell morphology of RAW 264.7 murine macrophage cells showed round and smooth shape by phase contrast images, while the cell treated with 10 μg/ml of 5-FU showed pseudopodia and cell shrinkage, which is the hallmark of apoptosis. Since DAPI staining can bind to DNA in the nucleus, while phalloidin binds to F actin cytoskeleton of the cell membrane of the cells, thus, they can be used to detect cells that have compromised membranes. From the Figure 4.7a and 4.7b, the blue (DAPI) showing the nucleus of the cells, while the green (phalloidin) represent the cytoskeleton of the cells. It can be deduced by fluorescence microscopy that phalloidin did not stain the nucleus as shown in the centre of phalloidin images; the position of the nucleus. Furthermore, from the superimposition of the blue and green, it was revealed that the nanoliposomes did not show any direct cytotoxic effect on both the nucleus and the cytoplasm membrane of the RAW 264.7 murine macrophage cells after 24 hours. Meanwhile, 10 μg/ml of 5-FU as a negative control ruptured the membrane and the cytoplasm of the cells, thereby exposing the nucleus.

Figure 4.8 presents the phase contrast morphology of the 3T3 human fibroblast cells visualized by inverted microscopy after the cells were treated with 30 μg/ml of free PZQ, NL, NLP, and anticalpain-NLP and 20 μL of DMSO as negative control while using the untreated as the positive control. It was observed that all the cells possess normal cell morphology of 3T3 human fibroblast cells and showed active structures due to the appearance of stellate and/or spindle shapes and centrally placed round nucleus or oval, as well as the abundant rough endoplasmic reticulum. Although, the cell treated with 20 μL of DMSO (negative control) showed cell shrinkage that result in apoptosis.

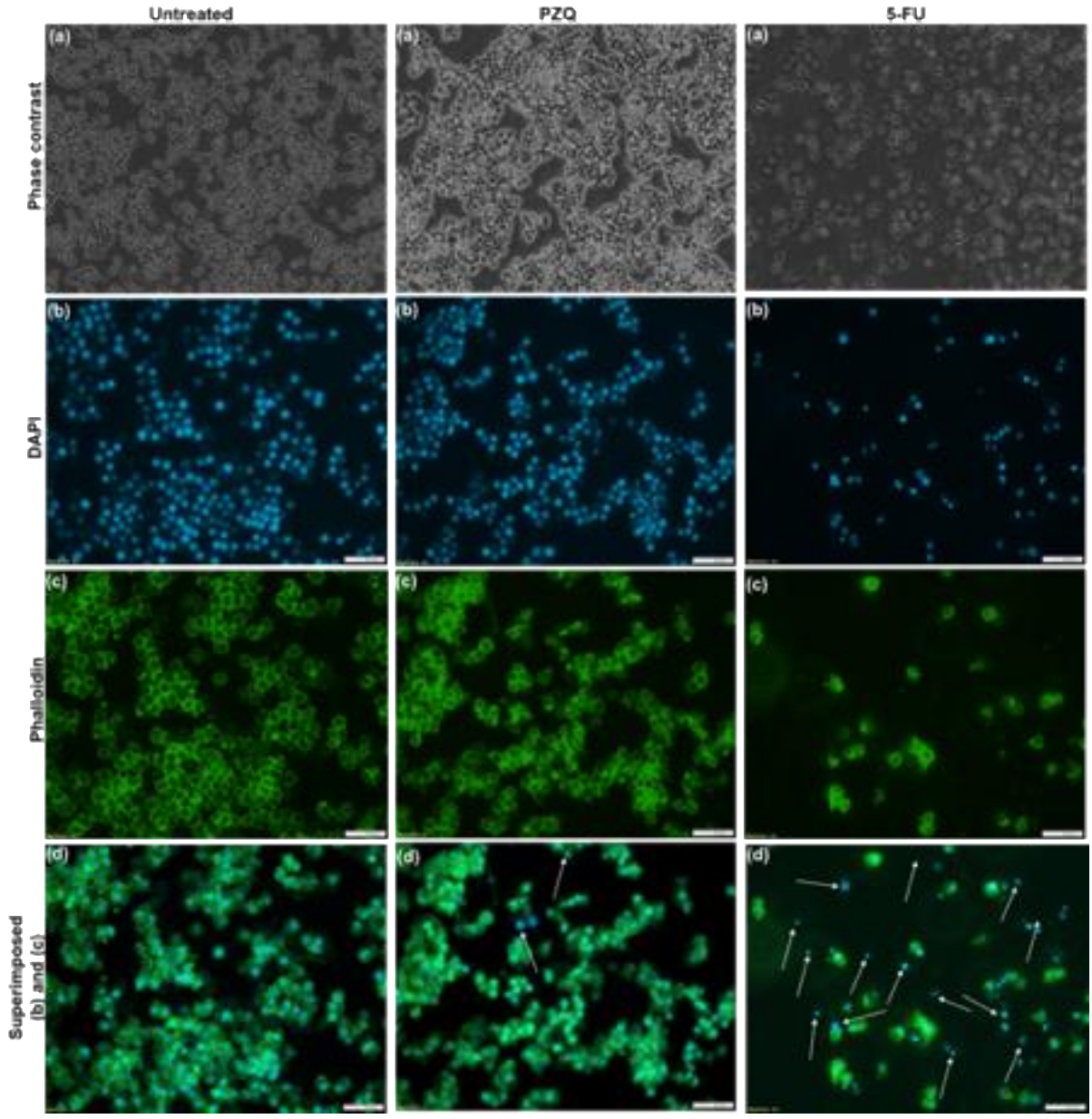

Figure 4.7a: Morphology analysis. Fluorescent microscopy images of RAW 264.7 macrophage cell (a) Phase constrat, (b) DAPI, (c) Phalloidin and (d) Superimposed of (b) and (c) for untreated (control), cell treated with 90 μg/ml of PZQ and 5-FU (10 μg/ml) (negative control). Scale bar: 100μm; (x20 magnification).

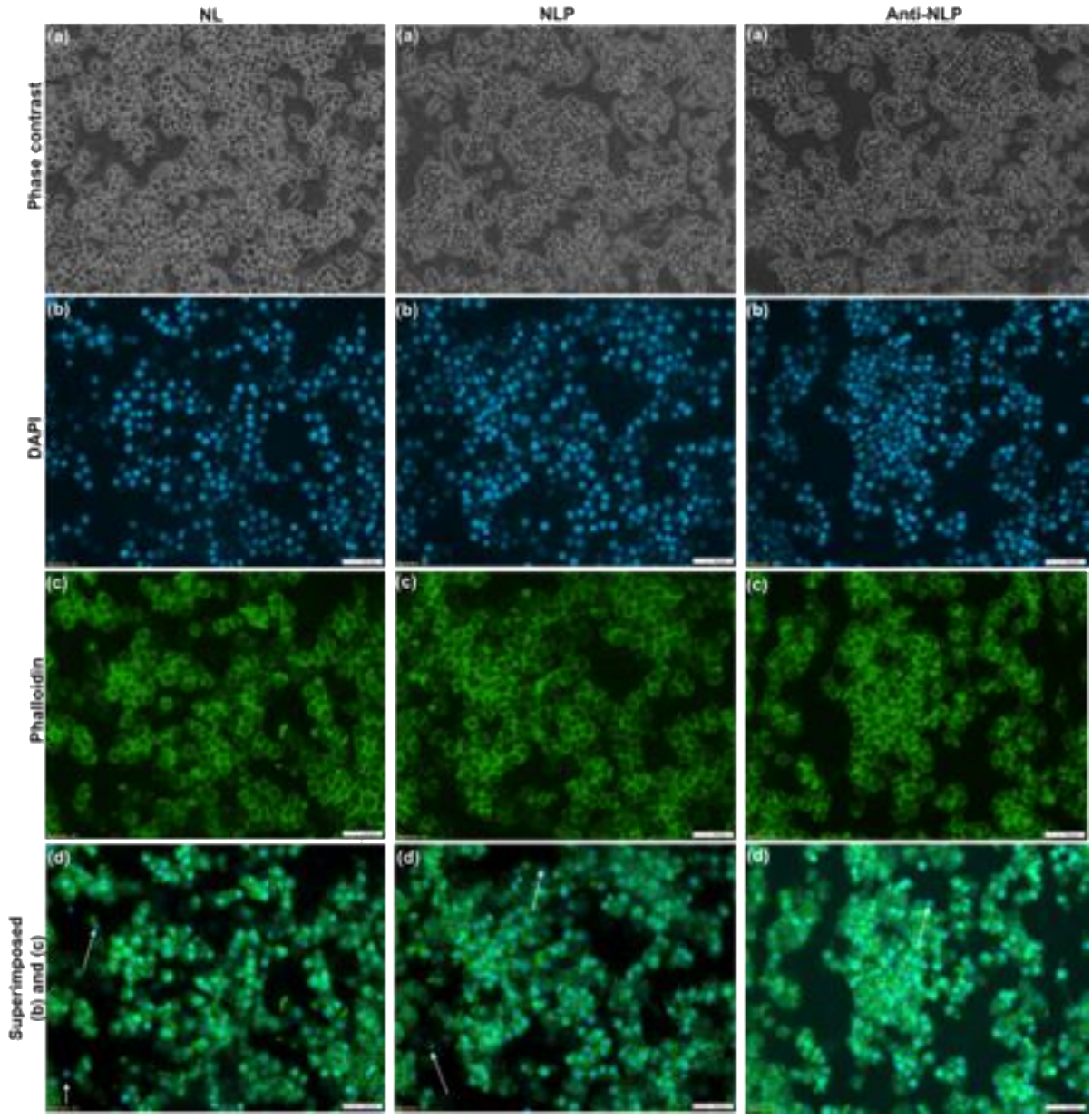

Figure 4.7b: Morphology analysis. Fluorescent microscopy images of RAW 264.7 macrophage cell (a) Phase constrat, (b) DAPI, (c) Phalloidin and (d) Superimposed of (b) and (c) with 90 μg/ml of NL, NLP and Anticalpain-NLP. Scale bar: 100μm; (x20 magnification).

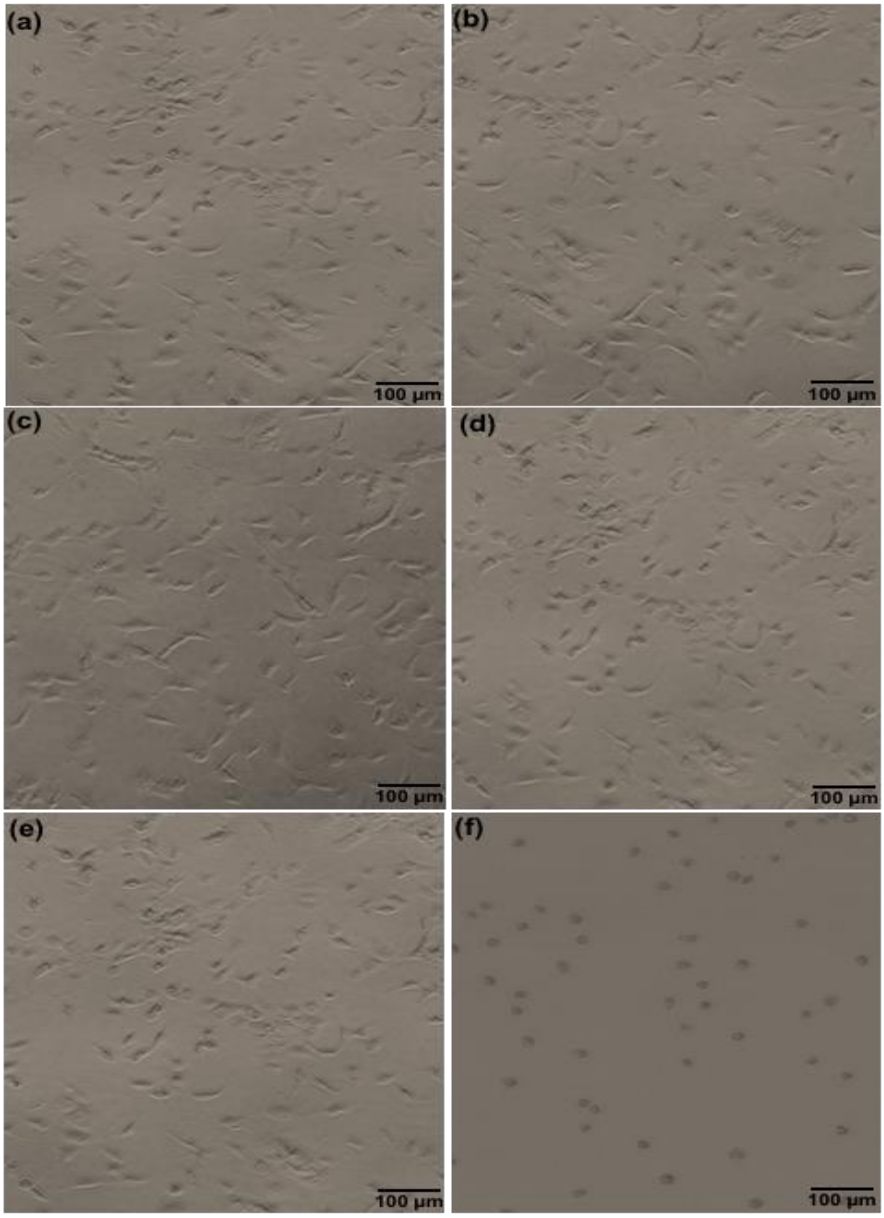

Figure 4.8: Phase contrast morphology of 3T3 human fibroblast cell visualized by inverted microscope (x10 magnification). The cells were treated with 30 µg/ml of Control (a), PZQ (b), NL (c), NLP (d), Anticalpain-NLP (e), and DMSO (f).

4.3.5. In vivo toxicity analysis

The evaluation of different biochemical markers was carried out to ascertain extent of potential damage to the kidney and liver. As shown in Figure 4.9, there is a significant increase ($p<0.0001$) in the levels of biochemical markers (ALT, AST, creatinine and bilirubin) in the plasma of the rats that received PZQ when compared to the control groups. It was further revealed that there is no significant increase in the biomarker levels of the groups that received the formulated nanoliposomes compared to the control. Interestingly, a significant decrease ($p<0.0001$) was observed in the biochemical markers of the animals that received the

formulated nanoliposomes compared with the PZQ groups. This indicates that the formulated nanoliposomes present no or minimal oxidative stress and confer hepatoprotective effects on the animals.

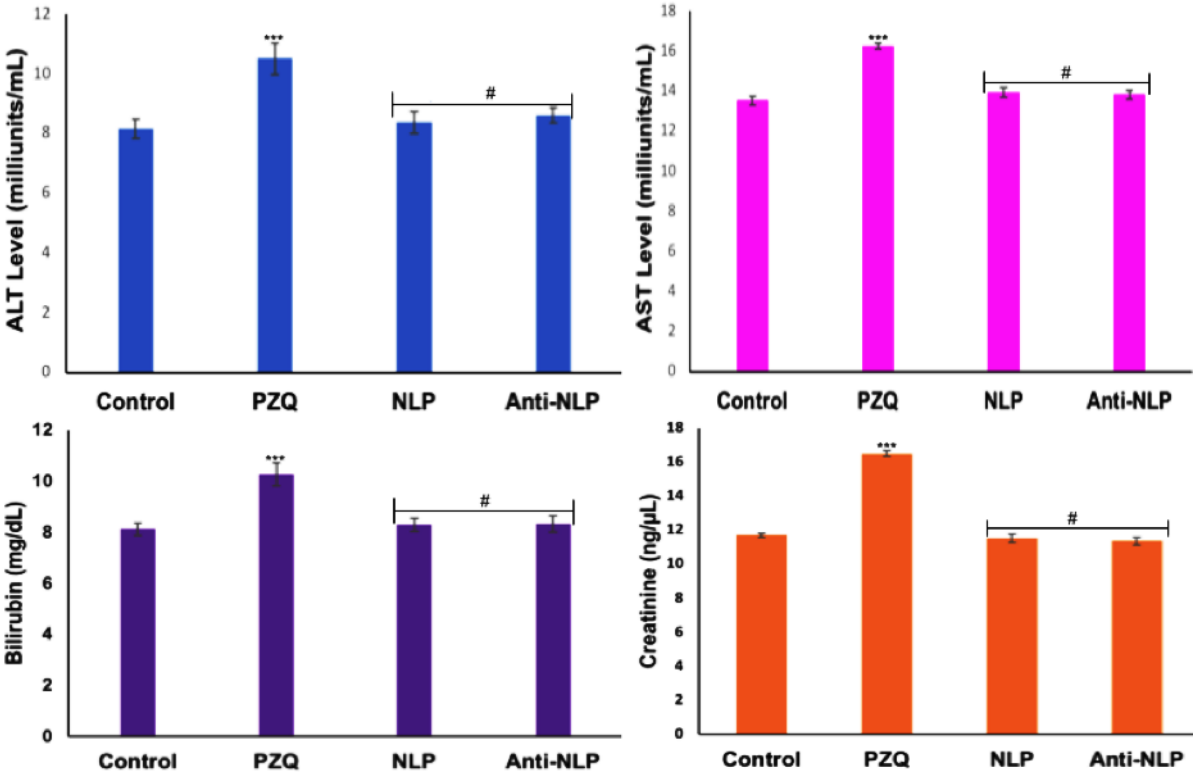

Figure 4.9: Biochemical markers (a) ALT (b) AST (c) Bilirubin and (d) creatinine levels in plasma. Values are expressed as mean ± standard deviation of five determinations (Data represent n = 3, mean ± SD). *** indicates $p<0.0001$ when compared to control group, and # indicates $p<0.0001$ when compared to PZQ group.

4.3.6. Histopathological analysis

Figure 4.10, depicts the histopathological examination images of untreated control, PZQ, NLP and anticalpain-NLP of the animal livers, kidneys, lungs and spleens. A similar toxicity pattern was observed in histopathology sections of the liver, kidney, lung and spleen. *Hepatocyte granularity:* This indicates active cellular function primarily due to swelling in cell organelles or increased cytoplasmic organelles. These organelles include smooth endoplasmic reticulum or peroxisomes, mitochondria. It is thus not a pathological lesion, only indicative of increased cellular activity, which was present throughout the samples. Hepatocellular swelling and vacuolar change: The vacuolar difference is a non-specific indication of degeneration, and it is often considered borderline between adaptation, resolution or inability to adapt. It can also be described as cytoplasmic alteration. In addition to degenerative changes developing due to hypoxic, toxic, metabolic or inflammatory conditions, it may also occur due to glycogen accumulation. The latter may be of metabolic origin. Glycogen retention may also be a treatment-induced metabolic perturbation. The mild vacuolar change was present, mainly in

the periportal regions. Renal tubular changes: The changes are minimal and only evident in few tubules. They are likely hypoxic in origin thus probably terminal primarily since the lesions are restricted to the deep cortical tissues where hypoxia would be first expected. Mild tubular epithelial cell swelling may develop due to disruption of ATP production, mitochondrial injury, free radical formation, peroxidation or perturbed cell signalling. Pulmonary alveolar atelectasis: This finding correlated with the handling procedures and experimental design as blood collection from the heart may have caused pulmonary atelectasis. Oedema may develop terminally following euthanasia. Active bronchial associated lymphoid tissue would be expected in animals exposed to respiratory pathogens and is an incidental finding. Normal active lymphoid tissue was shown in the spleen with no any observable abnormalities.

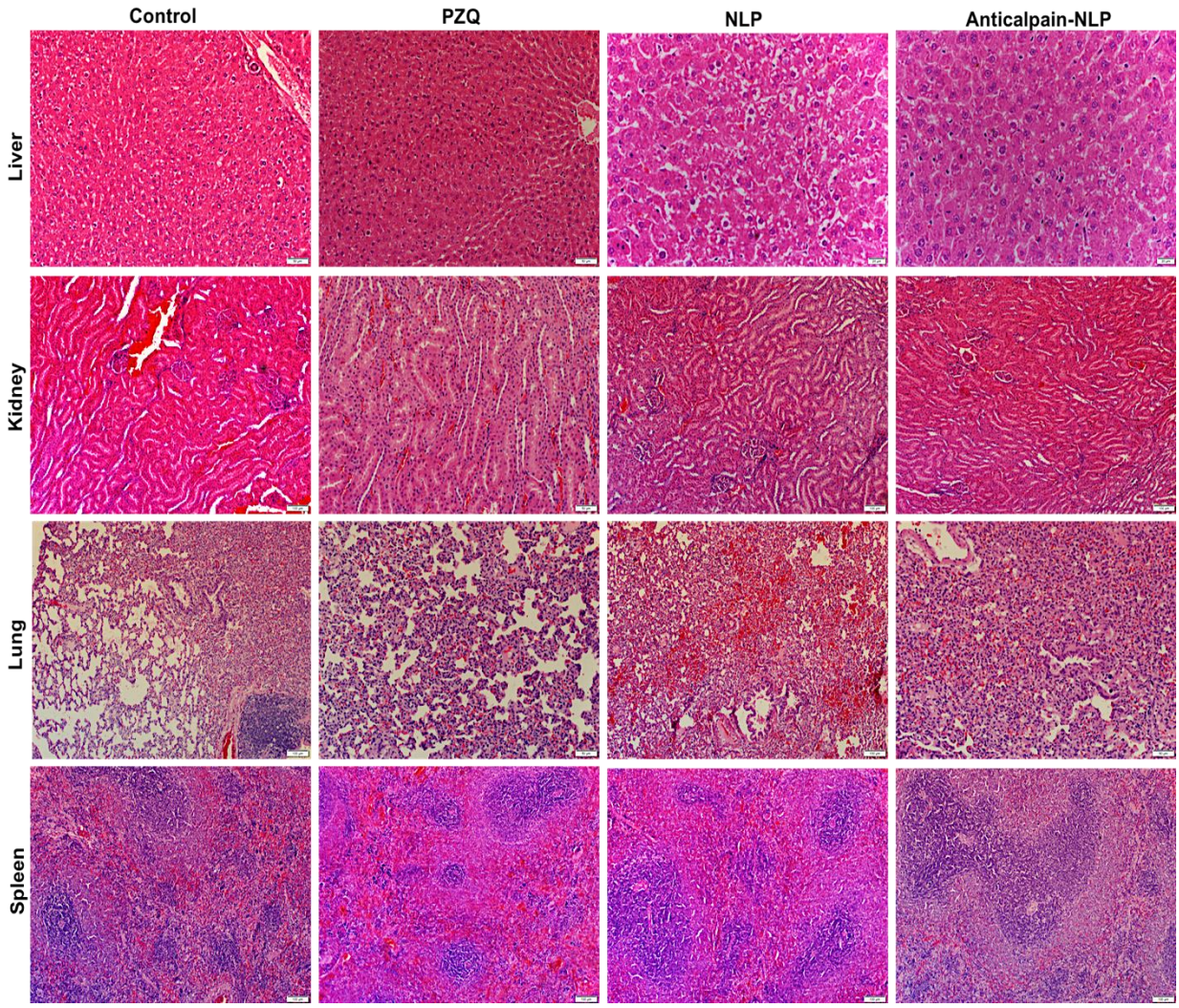

Figure 4.10: Histopathological sections of (A) liver, (B) kidney, (C) Lung and (C) spleen after treating uninfected rats with 250 mg/kg of PZQ, NLP and Anticalpain-NLP. Haematoxylin and eosin staining (x20 magnification).

4.3.7. Assessment of parasitological cure rate

As shown in the Figure 4.11, the imaging of how *S. mansoni* eggs were counted and the distribution and development of eggs according to their different maturity stage in the small intestine of infected mice are presented, which was similar to what has been reported previously in the literature by Mati and Melo, (2013). Two weeks post-infection treatment data for worm recovery, oogram pattern and egg count in tissues are shown in Tables 4.2, 4.3 and Figure 4.12. The oral administration of 250 mg/kg single dose of anticalpain-NLP on worm load and sex in *S. mansoni*-infected mice resulted in a statistically significant percentage reduction of the total worm burden (Table 4.2) compared to the PZQ-treated group. As shown in Figure 4.12, there were statistically significant reductions in the percentage of immature and mature ova and an increase in the percentage of dead ova in the anticalpain-NLP treated group compared to the control PZQ groups. Table 4.3 showed a statistically significant improvement in the percentage reduction of the ova count in the liver and intestine following the administration of 250 mg/kg single dose of PZQ equivalent in anticalpain-NLP two weeks post-infection compared to the PZQ and untreated control groups.

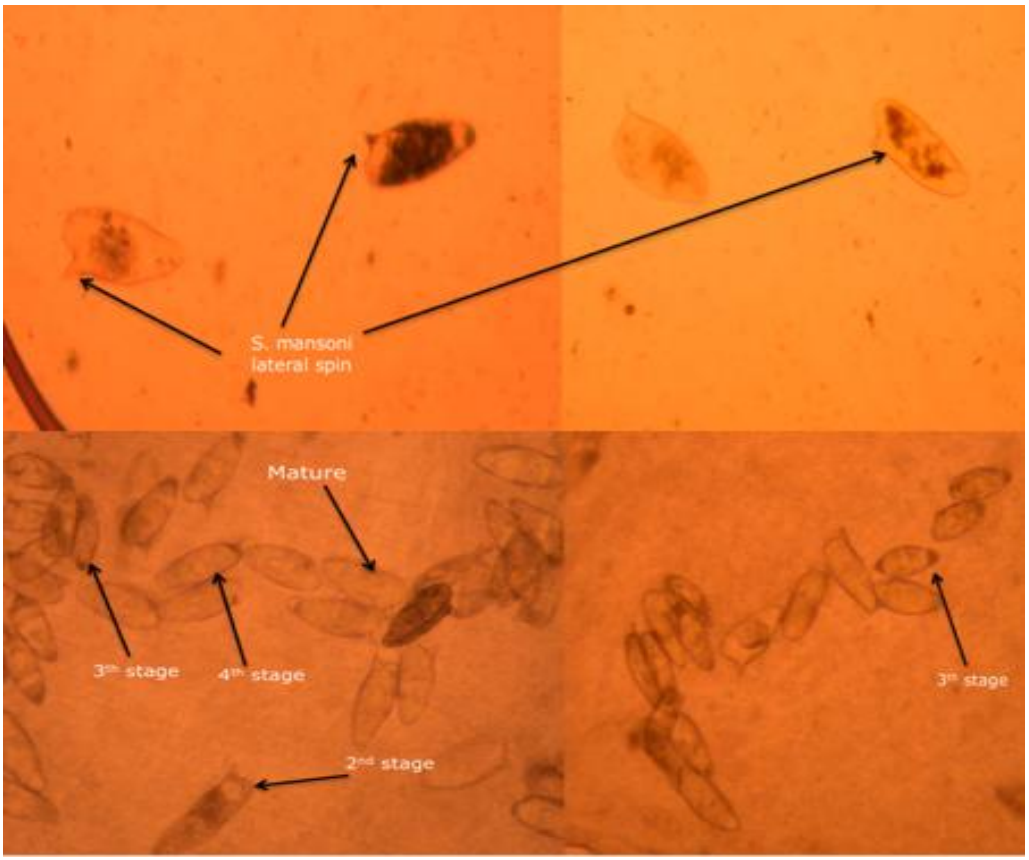

Figure 4.11: Typical imaging of S. mansoni eggs count at different stages of maturity in the small intestine of infected mice visualized with the aid of a light microscope (x40 magnification)

Table 4.2: Effect of PZQ and Anticalpain-NLP (single dose 250 mg/kg two weeks post-infection) on worm load and sex in S. mansoni-infected mice sacrificed six weeks post-infection

	Mean worm burden ±SD (liver and porto-mesenteric)				% reduction in total worm burden
	Male	Female	Couples	Total	
Control	2.33±0.81	0.33±0.52	6.17±0.75	15±0.89	
PZQ	1.33±1.21	0	4.33±0.82	10.0±1.41	33.3
Antical-NLP	1.10±0.52	0.17±0.41	3.67±1.37	6.83±2.4	54.5

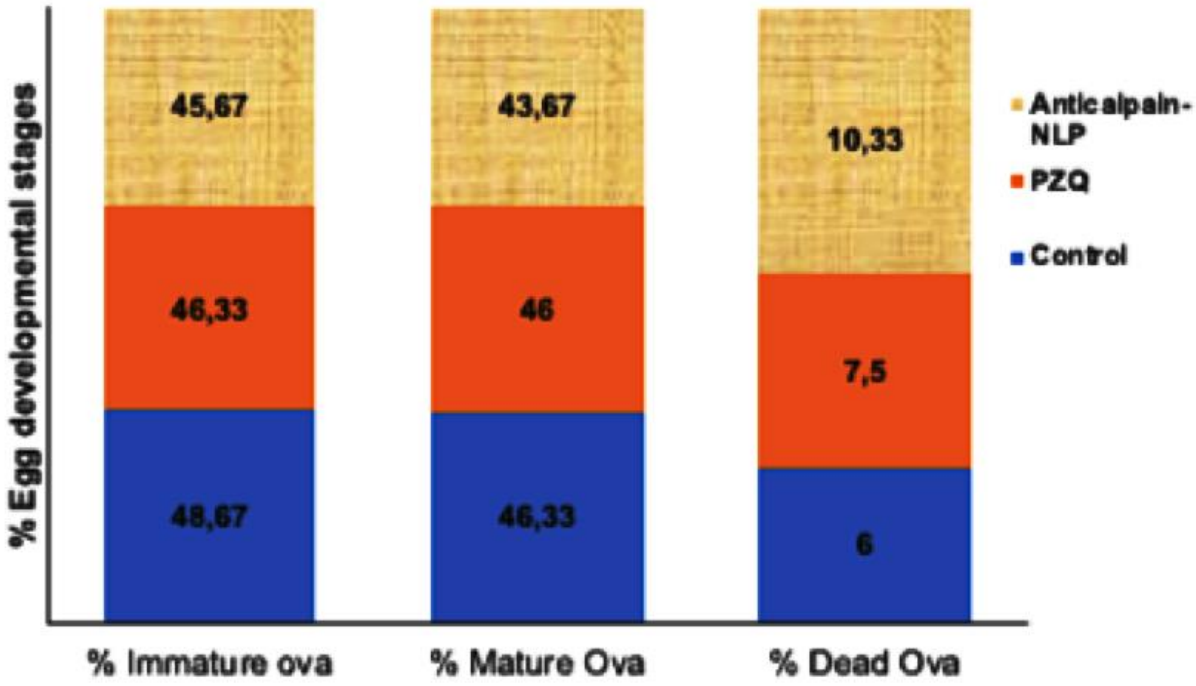

Figure 4.12: Effect of PZQ and Anticalpain-NLP (single dose 250 mg/kg two weeks post-infection) on % egg developmental stages in S. mansoni-infected mice sacrificed six weeks post infection

Table 4.3: Effect of PZQ and Anticalpain-NLP (single dose 250 mg/kg two weeks post-infection) on number of ova/gm tissues in *S. mansoni*-infected mice sacrificed six weeks post-infection

Mice group	Liver	% reduction in ova count in liver	Intestine	% reduction in ova count in intestine
Control	28202±4372		31902±4342	
PZQ	20303±2175	28.00	22702±5347	28.84
Antical-NLP	12387±2951	56.07	13436±2332	57.88

Four weeks post-infection treatment data for worm recovery, oogram pattern and egg count in tissues are shown in Table 4.4, 4.5 and Figure 4.13 for adult worms. As shown in table 4.4,

there was a statistically significant reduction in the percentage of the total worm burden in the liver and portomesenteric of the anticalpain-NLP compared to the PZQ-treated group. The oral administration of 250 mg/kg single dose of anticalpain-NLP resulted in statistically significant in the percentage of egg developmental stages in *S. mansoni*-infected mice compared to the infected untreated control and PZQ groups (Figure 4.13). However, improvement in the percentage reduction of the ova count in the intestine and liver was observed (Table 4.5) in anticalpain-NLP group compared to the PZQ and the infected untreated control groups.

Table 4.4: Effect of PZQ and Anticalpain-NLP (single dose 250 mg/kg four weeks post-infection) on worm load and sex in *S. mansoni*-infected mice sacrificed six weeks post-infection

	Mean worm burden ±SD (liver and porto-mesenteric)				% reduction in total worm burden
	Male	Female	Couples	Total	
Control	2.33±0.81	0.33±0.52	6.17±0.75	15.00±0.89	
PZQ	1.50±1.40	0	2.00±0.89	5.50±2.60	63.30
Antical-NLP	1.00±0.63	0	1.50±0.83	4.17±1.47	72.20

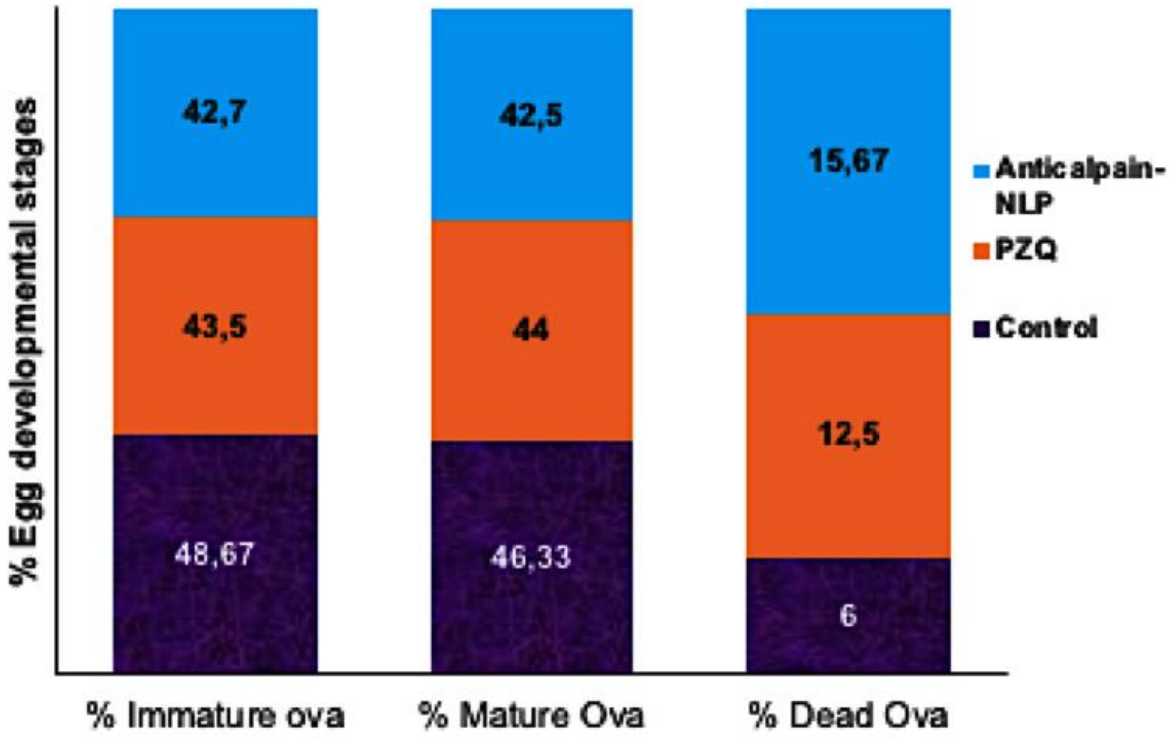

Figure 4.13: Effect of PZQ and Anticalpain-NLP (single dose 250 mg/kg four weeks post-infection) on % Egg developmental stages in S. mansoni-infected mice sacrificed six weeks post infection

Table 4.5: Effect of PZQ and Anticalpain-NLP (single dose 250 mg/kg four weeks post-infection) on number of ova/gm tissues in S. mansoni-infected mice sacrificed six weeks post- infection

Mice group	Liver	% reduction in ova count in liver	Intestine	% reduction in ova count in intestine
Control	28202±4372		31902±4342	
PZQ	13626±2936	51.68	14658±3699	54.05
Antical-NLP	10112±3745	64.14	9310±3789	70.81

4.4. Discussion

Praziquantel usage in the treatment of schistosome infections has been hampered by several issues, including low aqueous solubility, a shorter plasma half-life of roughly 1 to 2 hours, and significant hepatic first-pass metabolism (Vale *et al.*, 2017; Xiao *et al.*, 2018). Others include praziquantel ineffectiveness against young schistosome worms, as well as drug tolerance and resistance in some parts of the world, which can be attributed to poor treatment compliance, parasite mutation rates, overall parasite load, and co-infection with different Schistosoma parasite strains (Aruleba *et al.*, 2019; Adekiya *et al.*, 2020). Thus, this work used nanotechnological approaches to design and construct liposomal nanosystems (LNS) and surface-functionalize the LNS with anti-calpain antibodies for targeted PZQ administration in Schistosomiasis therapy.

Nanoliposomes have gotten a lot of interest in drug delivery because of their amphipathic nature, making them useful in enhancing and improving drug absorption across biological barriers, increasing the pace at which drugs may be released, and modifying drug solubility (Adekiya *et al.*, 2021; Aguilar-Pérez *et al.*, 2020). Due to considerable absorption by the reticuloendothelial system macrophage cells (RES), nanoliposomes, on the other hand, can decrease blood circulation times (Bozzuto and Molinari, 2015). PZQ-loaded liposomes have been shown in several studies to improve PZQ anti-schistosomal activity, and this might be the basis for new PZQ administration routes (Amara *et al*., 2018; Frezza *et al*., 2013). Oral use of liposomes increases drug activity and bioavailability (Daeihamed *et al*., 2017). The fact that the liposome is a suitable carrier of drugs with poor water solubility, which is a feature of PZQ, might help explain the increase in availability. *S. mansoni* also possesses a phospholipid affinity, which might make the encapsulated drug more easily absorbed by the worm. When taken orally, the liposomal drug may shield the entrapped PZQ from digestive enzymes in the stomach, allowing the drug to reach the eggs and parasites in the liver.

In this study, the nanoliposomes synthesized are in the nanoranges with excellent polydispersity index and zeta potential. The average particle size and the PDI are some of the indication of the quality of the size distribution of nanocarriers (Danaei *et al*., 2018; Clayton *et al*., 2016). The particle size distribution and PDI of lipid-based nanocarriers are essential physical properties to consider when dealing with pharmaceutical-grade products because the particle size affects encapsulation efficiency, stability, biodistribution, mucoadhesion, drug release profile and cellular uptake (Aguilar-Pérez *et al*., 2020; Danaei *et al.*, 2018; Clayton *et al.*, 2016; Bahari and Hamishehkar, 2016). It has been reported that particle size has a significant influence on drug delivery systems by influencing certain physiological processes such as tissue extravasation, tissue diffusion, hepatic uptake and accumulation (pharmacokinetics), and clearance through kidney excretion (Danaei *et al.*, 2018).

More so, the smaller the particle size nanocarriers (nanoliposomes), the larger the surface area and have more capability to increase solubility, improve bioavailability, enable accurate targeting of the encapsulated drug, enhance controlled release (Aguilar-Pérez *et al.*, 2020). Also, nanocarriers with smaller particle sizes range from 20 to 100 nm may be easily distributed to the spleen, liver sinusoids and bone marrow and may leave the bloodstream through the leaky capillaries of these organs to some extent (Danaei *et al*., 2018). Internal cellular binding and uptake of drug-loaded nanosystems are influenced by the nanoparticulate system shape and size (Patra *et al.*, 2018; Lombardo *et al*., 2019). Thus, the SEM and TEM images in this study revealed that the formulated nanoliposomes are in the nanosize range and uniformly spherical in shape with stable or intact structure, which showed a typical SEM and TEM images of the nanoliposomes (Mufamadi *et al*., 2013) and corroborated the particle size, PDI and zeta potential results. It can be deduced from the physicochemical parameters (FTIR, DSC, XPDR and TGA) data that there is improvement in the drug's stability and showed the entrapment of the drug during the hydrophobic interaction between the PZQ and the phospholipids.

Both the NLP and anticalpain-NLP showed high PZQ entrapment and loading capacity, revealing that the nanoliposomes achieved high PZQ entrapment efficacy of 94.63 ± 0.30 and 92.07 ± 0.23, respectively with a drug-loading capacity of 14.16 ± 0.61 and 9.03 ± 0.42, respectively. Other similar studies have reported the high encapsulation efficacy of lipophilic drugs in the lipid core of the lipid-based nanocarrier (Amara *et al*., 2018; Campani *et al*., 2018). More so, nanoparticles have been investigated for precise targeting of brain tissues due to their small particle size and high drug encapsulation efficacy (Ghasemiyeh and Mohammadi-Samani, 2018). This showed that the formulated nanoliposomes could be used for the

treatment of cerebral schistosomiasis. The formulated nanoliposomes showed an initial burst release pattern at 4 hours followed by approximately 93.2 and 91.1 % of PZQ released within 24 hours for PZQ-loaded nanoliposomes and PZQ-loaded functionalized nanoliposomes, respectively. Interestingly, both the PZQ-loaded nanoliposomes and PZQ-loaded functionalized nanoliposomes exhibited typical sustained release profiles. The concentration of cholesterol, which is well-known to stabilize lipid bilayers by reducing membrane fluidity, may be responsible for the prolonged release profiles of PZQ displayed by the formulated nanoliposomes, causing a restriction in the flow of drug across the formulated nanoliposomes (Mufamadi *et al*., 2013; Bozzuto and Molinari, 2015). It is also possible that the fast release of PZQ during the initial 4 hours burst phase was caused by the hydration process in the formulated nanoliposomes.

Safety assessment of these nanoformulations *in vitro* revealed that the concentrations ranging from 30 to 120 μg/ml employed in this study were in acceptable levels of cell viability, with no significant cytotoxic effects on RAW 264.7 murine macrophage cells and 3T3 human fibroblast cells. More so, it was revealed that the percentage of cell viability depends on the dose concentration of both the PZQ and the formulations. Interestingly, a significant increase ($p<0.0001$) in the percentage of cell viability was observed in the PZQ group compared to the NLP and anti-NLP groups. This *in vitro* cytotoxicity cell culture result was further supported by *in vivo* toxicity studies where the extent of PZQ, NLP and anticalpain-NLP were shown in the histopathological analysis of different organs and evaluation of biochemical markers. Based on these observations, the fabrication NLP and engineering of NLP with anticalpain antibody play an indispensable role in circumventing the traces of the toxic aspects associated with the drug.

Additionally, the extent of safety of the formulated nanoliposomes was shown, and the biochemical markers and histopathological examinations present no or minimal oxidative stress and confer hepatoprotective effects on the animals. Since in severe instances of intestinal schistosomiasis, liver enlargement is prevalent, and it is often accompanied by a buildup of fluid in the peritoneal cavity and abdominal blood vessel hypertension. Spleen hypertrophy is also possible in such circumstances (Elbaz *et al.*, 2013; McManus *et al*., 2018). More so, haematuria is the most common symptom of urogenital schistosomiasis (blood in urine) (McManus *et al*., 2018). In advanced cases, fibrosis of the bladder and ureter, as well as kidney impairment, may be discovered (McManus *et al*., 2018). Thus, the anticalpain-NLP would localize, recognize and bind to the schistosomes without posing any adverse effects on the organs or tissues.

The cure rate of the anticalpain-NLP and PZQ was assessed by parasitological analysis, and it was discovered that the treatment with 250 mg/kg of drug equivalent in anticalpain-NLP showed more significant activity on the total worm burden, ova count in both the intestine and the liver. Also, the anticalpain engineered lipoidial nanosysem when compared with the same dose of PZQ showed a greater effect on both the mature and immature ova, as well as caused ova dead during the egg developmental stages in both the young and adult worm represented by two weeks and four weeks post-infected mice, respectively. The calculation of the reduction in the total worm burden, egg developmental stages, and the number of eggs/gram tissue and the percentage of reduction of total ova/gram tissue is the criteria for parasitological cure rate (Christensen *et al.*, 1984; Pelligrino *et al*., 1962; Kloetzel, 1967). These enormous effects of the anticalpain engineered nanoliposomes on schistosomes eggs, and worms may be due to the target rate and greater absorption of the nanosystem by the worms and the eggs in the liver, porto-mesenteric and intestine. The effects of the anticalpain surface engineering of the lipoidal nanosystem could be due to the suppression of the calpain protein activity. This could lead to the blocking of cell-cell adhesion or cell-substrate adhesion, which occur via the host-parasite interfaces, impairs the schistosomes' capacity to conduct calcium-mediated signaling and stops surface membrane biogenesis, i.e. the surface membrane synthetic process. Since the calpain host-parasite is crucial for the schistosomes developmental activities, failure in the supply and transfer of membrane precursors might cause the tegument to rupture, disrupting the worm's capacity to maintain solute balance (Siddiqui *et al*., 1992; Wang *et al*., 2017).

4.5. Conclusion

The findings of this study revealed that anticalpain-functionalized nanoliposomes might be used to improve the transport of PZQ into the liver and intestines of both the young and adult schistosomes for schistosomiasis treatment**.** It was discovered that the nanoliposomes synthesized are in the nanoscale range with excellent polydispersity index and zeta potential. The SEM and TEM images in this study revealed that the formulated nanoliposomes are in the nanosize range and uniformly spherical with stable or intact structure, showing typical SEM and TEM images of the nanoliposomes and corroborated the particle size, PDI and zeta potential results. More so, the physicochemical parameters (FTIR, DSC, XPDR and TGA) data revealed that there is improvement in the stability of the drug and also showed the entrapment of the drug during the hydrophobic interaction between the PZQ and the phospholipids. It was shown that both the NLP and anticalpain-NLP showed high PZQ entrapment and loading capacity. Interestingly, both the PZQ-loaded nanoliposomes and PZQ-loaded functionalized nanoliposomes exhibited typical sustained release profiles. Safety assessment of these nanoformulations in an *in vitro* revealed that the concentrations ranging from 30 to 120 μg/ml employed in this study revealed acceptable levels of cell viability, with no significant cytotoxic

effects on RAW 264.7 murine macrophage and 3T3 human fibroblast cells. The extent of safety of the formulated nanoliposomes was shown and the biochemical markers and histopathological examinations present no or minimal oxidative stress and confer hepatoprotective effects on the animals. In *S. mansoni*-infected mice, a single 250 mg/kg oral dosage of drug equivalent in anticalpain-NLP significantly increased PZQ antischistosomal activity compared to free PZQ. The findings obtained support the ability of oral anticalpain-NLP to target young and adult schistosomes in the liver and portomesenteric locations, resulting in improved effectiveness of PZQ, hence, a promising therapeutic strategy against schistosomiasis.

4.6. References

1. Adekiya, T.A., Aruleba, R.T., Oyinloye, B.E., Okosun, K.O. and Kappo, A.P., 2020. The effect of climate change and the snail-schistosome cycle in transmission and bio-control of schistosomiasis in Sub-Saharan Africa. *International journal of environmental research and public health*, *17*(1), p.181.
2. Adekiya, T.A., Kappo, A.P. and Okosun, K.O., 2017. Temperature and rainfall impact on schistosomiasis. *Global Journal of Pure and Applied Mathematics*, *13*(12), pp.8453-8469.
3. Adekiya, T.A., Kondiah, P.P., Choonara, Y.E., Kumar, P. and Pillay, V., 2020. A review of nanotechnology for targeted anti-schistosomal therapy. *Frontiers in bioengineering and biotechnology*, *8*, p.32.
4. Adekiya, T.A., Kumar, P., Kondiah, P.P., Pillay, V. and Choonara, Y.E., 2021. Synthesis and therapeutic delivery approaches for praziquantel: a patent review (2010-present). *Expert Opinion on Therapeutic Patents*, pp.1-15.
5. Aguilar-Pérez, K.M., Avilés-Castrillo, J.I., Medina, D.I., Parra-Saldivar, R. and Iqbal, H., 2020. Insight into nanoliposomes as smart nanocarriers for greening the twenty-first century biomedical settings. *Frontiers in Bioengineering and Biotechnology*, *8*, p.1441.
6. Amara, R.O., Ramadan, A.A., El-Moslemany, R.M., Eissa, M.M., El-Azzouni, M.Z. and El-Khordagui, L.K., 2018. Praziquantel–lipid nanocapsules: an oral nanotherapeutic with potential *Schistosoma mansoni* tegumental targeting. *International journal of nanomedicine*, *13*, p.4493.
7. Aruleba, R.T., Adekiya, T.A., Oyinloye, B.E., Masamba, P., Mbatha, L.S., Pretorius, A. and Kappo, A.P., 2019. PZQ therapy: how close are we in the development of effective alternative anti-schistosomal drugs?. *Infectious Disorders-Drug Targets (Formerly Current Drug Targets-Infectious Disorders)*, *19*(4), pp.337-349.
8. Bahari, L.A.S. and Hamishehkar, H., 2016. The impact of variables on particle size of solid lipid nanoparticles and nanostructured lipid carriers; a comparative literature review. *Advanced pharmaceutical bulletin*, *6*(2), p.143.

9. Bozzuto, G. and Molinari, A., 2015. Liposomes as nanomedical devices. *International journal of nanomedicine*, *10*, p.975.
10. Campani, V., Giarra, S. and De Rosa, G., 2018. Lipid-based core-shell nanoparticles: Evolution and potentialities in drug delivery. *OpenNano*, *3*, pp.5-17.
11. Cheng, W., Li, X., Zhang, C., Chen, W., Yuan, H. and Xu, S., 2017. Preparation and *in vivo-in vitro* evaluation of polydatin-phospholipid complex with improved dissolution and bioavailability. *Int. J. Drug Dev. Res*, *9*, pp.39-43.
12. Christensen N, Gotsche G, Frandsen F. Parasitological technique for use in laboratory maintenance of schistosomes and for use in studies on the epidemiology of human and bovine schistosomiasis. Teaching note Danish Bilharziasis Laboratory. 1984.
13. Clayton, K.N., Salameh, J.W., Wereley, S.T. and Kinzer-Ursem, T.L., 2016. Physical characterization of nanoparticle size and surface modification using particle scattering diffusometry. *Biomicrofluidics*, *10*(5), p.054107.
14. Daeihamed, M., Dadashzadeh, S., Haeri, A. and Faghih Akhlaghi, M., 2017. Potential of liposomes for enhancement of oral drug absorption. *Current drug delivery*, *14*(2), pp.289-303.
15. Dai, Q., Yan, Y., Ang, C.S., Kempe, K., Kamphuis, M.M., Dodds, S.J. and Caruso, F., 2015. Monoclonal antibody-functionalized multilayered particles: targeting cancer cells in the presence of protein coronas. *ACS nano*, *9*(3), pp.2876-2885.
16. Danaei, M., Dehghankhold, M., Ataei, S., Hasanzadeh Davarani, F., Javanmard, R., Dokhani, A., Khorasani, S. and Mozafari, M.R., 2018. Impact of particle size and polydispersity index on the clinical applications of lipidic nanocarrier systems. *Pharmaceutics*, *10*(2), p.57.
17. Doenhoff MJ, Cioli D, Utzinger J. Praziquantel: mechanisms of action, resistance and new derivatives for schistosomiasis. Curr Opin Infect Dis. 2008;21(6):659–667.
18. Dou, X.Q., Wang, H., Zhang, J., Wang, F., Xu, G.L., Xu, C.C., Xu, H.H., Xiang, S.S., Fu, J. and Song, H.F., 2018. Aptamer–drug conjugate: Targeted delivery of doxorubicin in a HER3 aptamer-functionalized liposomal delivery system reduces cardiotoxicity. *International journal of nanomedicine*, *13*, p.763.
19. Elbaz, T. and Esmat, G., 2013. Hepatic and intestinal schistosomiasis. *Journal of advanced research*, *4*(5), pp.445-452.
20. Frezza, T.F., Gremião, M.P.D., Zanotti-Magalhães, E.M., Magalhães, L.A., de Souza, A.L.R. and Allegretti, S.M., 2013. Liposomal-praziquantel: efficacy against *Schistosoma mansoni* in a preclinical assay. *Acta tropica*, *128*(1), pp.70-75.
21. Ghasemiyeh, P. and Mohammadi-Samani, S., 2018. Solid lipid nanoparticles and nanostructured lipid carriers as novel drug delivery systems: applications, advantages and disadvantages. *Research in pharmaceutical sciences*, *13*(4), p.288.

22. John Elflein, Statista dossier on neglected tropical diseases. Jan 28, 2021. https://www.statista.com/study/55475/neglected-tropical-diseases/. Accessed on 19th July, 2021.
23. Kloetzel, K.U.R.T., 1967. A suggestion for the prevention of severe clinical forms of schistosomiasis *mansoni*. *Bulletin of the World Health Organization*, *37*(4), p.686.
24. Li, S., Bouchy, S., Penninckx, S., Marega, R., Fichera, O., Gallez, B., Feron, O., Martinive, P., Heuskin, A.C., Michiels, C. and Lucas, S., 2019. Antibody-functionalized gold nanoparticles as tumor-targeting radiosensitizers for proton therapy. *Nanomedicine*, *14*(3), pp.317-333.
25. Liang, Y.S., Bruce, J.I. and Boyd, D.A., 1987. Laboratory cultivation of schistosome vector snails and maintenance of schistosome life cycles. In *Proceeding of the 1st Sino-American symposium* (Vol. 1, pp. 34-48).
26. Lombardo, D., Kiselev, M.A. and Caccamo, M.T., 2019. Smart nanoparticles for drug delivery application: development of versatile nanocarrier platforms in biotechnology and nanomedicine. *Journal of Nanomaterials*, *2019*.
27. MacDonald, K.; Buxton, S.; Kimber, M.J.; Day, T.A.; Robertson, A.P.; Ribeiro, P. Functional characterization of a novel family of acetylcholine-gated chloride channels in *Schistosoma mansoni*. *PLoS Pathog.* 2014, *10*(6), e1004181.
28. Mansour, T. and Mansour, J. (2002). Targets in the Tegument of Flatworms. In *Chemotherapeutic Targets in Parasites: Contemporary Strategies* (pp. 189-214).
29. Mati, V.L.T. and Melo, A.L., 2013. Current applications of oogram methodology in experimental schistosomiasis; fecundity of female Schistosoma mansoni and egg release in the intestine of AKR/J mice following immunomodulatory treatment with pentoxifylline. *Journal of helminthology*, *87*(1), pp.115-124.
30. McManus, D.P., Dunne, D.W., Sacko, M. *et al.* Schistosomiasis. *Nat Rev Dis Primers* **4,** 13 (2018). https://doi.org/10.1038/s41572-018-0013-8
31. Mufamadi, M.S., Choonara, Y.E., Kumar, P., Modi, G., Naidoo, D., van Vuuren, S., Ndesendo, V.M., du Toit, L.C., Iyuke, S.E. and Pillay, V., 2013. Ligand-functionalized nanoliposomes for targeted delivery of galantamine. *International journal of pharmaceutics*, *448*(1), pp.267-281.
32. Patra, J.K., Das, G., Fraceto, L.F., Campos, E.V.R., del Pilar Rodriguez-Torres, M., Acosta-Torres, L.S., Diaz-Torres, L.A., Grillo, R., Swamy, M.K., Sharma, S. and Habtemariam, S., 2018. Nano based drug delivery systems: recent developments and future prospects. *Journal of nanobiotechnology*, *16*(1), pp.1-33.
33. Pellegrino, J., Oliveira, C.A., Faria, J. and Cunha, A.S., 1962. New approach to the screening of drugs in experimental schistosomiasis mansoni in mice. *American Journal of Tropical Medicine and Hygiene*, *11*(2), pp.201-215.

34. Siddiqui, A.A., Zhou, Y., Podesta, R.B., Karcz, S.R., Tognon, C.E., Strejan, G.H., Dekaban, G.A. and Clarke, M.W., 1993. Characterization of Ca2+-dependent neutral protease (calpain) from human blood flukes, *Schistosoma mansoni*. Biochimica et Biophysica Acta (BBA)-Molecular Basis of Disease, 1181(1), pp.37-44.
35. Silva, J.M., Zupancic, E., Vandermeulen, G., Oliveira, V.G., Salgado, A., Videira, M., Gaspar, M., Graca, L., Préat, V. and Florindo, H.F., 2015. *In vivo* delivery of peptides and Toll-like receptor ligands by mannose-functionalized polymeric nanoparticles induces prophylactic and therapeutic anti-tumor immune responses in a melanoma model. *Journal of Controlled Release*, *198*, pp.91-103.
36. Skelly, P.J.; Kim, J.W.; Cunningham, J.; Shoemaker, C.B. Cloning, characterization, and functional expression of cDNAs encoding glucose transporter proteins from the human parasite *Schistosoma mansoni*. *J. Biol. Chem.* 1994, *269*(6), 4247-4253.
37. Skelly, P.J.; Tielens, A.G.M.; Shoemaker, C.B. Glucose transport and metabolism in mammalian-stage schistosomes. *Parasitol. Today*, 1998, *14*(10), 402-406.
38. Song, S., Liu, D., Peng, J., Sun, Y., Li, Z., Gu, J.R. and Xu, Y., 2008. Peptide ligand-mediated liposome distribution and targeting to EGFR expressing tumor in vivo. *International journal of pharmaceutics*, *363*(1-2), pp.155-161.
39. Vale, N., Gouveia, M.J., Rinaldi, G., Brindley, P.J., Gärtner, F. and Correia da Costa, J.M., 2017. Praziquantel for schistosomiasis: single-drug metabolism revisited, mode of action, and resistance. *Antimicrobial agents and chemotherapy*, *61*(5), pp.e02582-16.
40. Wang, Q., Da'dara, A.A. and Skelly, P.J., 2017. The human blood parasite *Schistosoma mansoni* expresses extracellular tegumental calpains that cleave the blood clotting protein fibronectin. Scientific reports, 7(1), pp.1-13.
41. Xiao, S.H., Sun, J. and Chen, M.G., 2018. Pharmacological and immunological effects of praziquantel against *Schistosoma japonicum*: a scoping review of experimental studies. *Infectious diseases of poverty*, *7*(1), pp.1-15.

CHAPTER FIVE

SYNTHESIS AND EVALUATION OF PRAZIQUANTEL-LOADED COMPRITOL ATO 888-LECITHIN SOLID LIPID NANOPARTICLES AGAINST *S. mansoni* INFECTION IN PRECLINICAL MURINE MODELS

This chapter aimed to develop and evaluate the long-term stability of drug-loaded solid lipid nanoparticles (SLNs). The SLNs were designed to extend the release profile and overcome the problem of bioavailability and solubility, investigate its toxicity, and improve the anti-schistosomal efficacy of praziquantel. The aim was pursued using solvent injection-co-homogenization techniques to fabricate SLNs in which compritol ATO 888 and lecithin were used as lipids, and Pluronic F127 (PF127) was used as a stabilizer. The long-term stability effect of the PF127 as a stabilizer on the SLNs was evaluated. The particle size, stability and polydispersity were determined by a dynamic light scattering (DLS) technique. The morphological analysis of the SLNs was investigated by Transmission and Scanning Electron Microscopy (TEM) and (SEM). The chemical properties, mechanical, thermal, and crystal behaviours of SLNs were evaluated using FTIR, ElastoSens Bio2, XRPD, DSC and TGA, respectively. SLNs with PF127 depicted an encapsulation efficiency of 71.63% and a drug loading capacity of 11.46%. The *in vitro* drug release study for SLNs with PF127 showed a cumulative release of 48.08% for the PZQ within 24 h, with a similar release profile for SLNs suspension after 120 days. DLS, ELS, and optical characterization and stability profiling data indicate that the addition of PF127 as the surfactants provided long-term stability for SLNs. *In vitro* cell viability and *in vivo* toxicity evaluation signify the safety of SLNs stabilized with PF127. In conclusion, the parasitological data showed that a single (250 mg/kg) oral dose of CLPF-SLNs significantly improved the antischistosomal activity of PZQ in *S. mansoni*-infected mice in both two and four weeks post-infection. Thus, the fabricated CLPF-SLNs demonstrated significant efficiency toward the delivery of PZQ, hence, a promising therapeutic strategy against schistosomiasis.

5.1. Introduction

Praziquantel is an anthelmintic drug that is used for the treatment of parasitic worm diseases like schistosomiasis. Praziquantel (PZQ) is currently the only available drug against schistosomiasis. Praziquantel acts by producing severe muscle spasms and paralysis in the worms. This paralysis is accompanied by and most likely caused by a fast Ca^{2+} influx inside the schistosome (Kohn *et al*., 200). Even though PZQ is effective against adult worms, two major drawbacks associated with the use of the drug have been reported, which include. rapid metabolism that reduces the bioavailability of the drug in the circulation, and the minimal level

of the drug effectiveness against the juvenile and immature forms of Schistosoma worm (Vale *et al*., 2017). More so, multidrug resistance against PZQ has been reported in some parts of the world (Aruleba *et al.*, 2019).

However, no meaningful and considerable impetus has been placed on the discovery of new drugs for the treatments of schistosomiasis, which may be due to a lack of motivation and poor financial support for pharmaceutical researchers in that research area (Adekiya *et al*., 2020). Also, the huge cost associated with the process of new molecules via the long drug discovery pipeline (Adekiya *et al.*, 2020). Thus, pharmaceutical scientists have focused on improving the therapeutic efficacy of the gold-standard drug, PZQ, by developing more efficacious delivery systems through a nanomedicine approach. The approach uses nanotechnological-based techniques in the advanced drug delivery systems (DDS) and targeted strategies in the improvement of pharmaceutical ingredients for diseases and disorders treatments (Mourão *et al*., 2005; Frezza *et al*., 2013; El-Feky *et al*., 2015; Amara *et al*., 2018).

Hence, this chapter aims to improve the effectiveness of the drug by enhancing its bioavailability via reducing the release of PZQ over time and enhancing its effectiveness against the immature forms of the Schistosoma parasite. Moreover, this study aims to bypass the multidrug resistance mechanism using compritol ATO 888-lecithin solid lipid nanoparticles (SLN) formulation delivery approach. SLNs can overcome the problem of solubility and bioavailability faced by pharmaceutical ingredients with poor permeability (Kushwaha *et al.*, 2013; Mishra *et al*., 2018; Khan *et al*., 2015). SLNs have the potential to encapsulate drugs with different physiological and pharmacological characteristics (Kushwaha *et al*., 2013; Mishra *et al.*, 2018; Khan *et al.*, 2015). Also, its multidrug resistance mechanisms bypass activities have been reported (Bayón-Cordero *et al.*, 2019). Meanwhile, lipidic-based nanosystems have been shown to mimic the formation of chylomicrons, which gives this type of delivery system the ability to transport the entrapped or encapsulated bioactive molecules effectively when passing through the classical transcellular lipid absorption mechanism (Mourão *et al.*, 2005; Frezza *et al.*, 2013; El-Feky *et al*., 2015; Amara *et al*., 2018). More so, for the treatment of schistosomiasis, it is believed that a lipid-based nanosystem will improve the modification and target rate of PZQ, thereby enhancing and improving the absorption of the drug across the biological barrier (tegument) of the schistosomes in the human host.

The stability of pharmaceutical products influences the efficacy and safety of the product, as degradation impurities could result in loss of efficacy and possibly generate side effects. Given this, the attainment of physical and chemical stability of drugs is very important to ensure their

quality and safety (Garnero *et al*., 2018). The use of surfactants as a stabilizer for delivery systems have been hypothesized as one of the easiest and most effective approaches for sustaining the release profiles, improving the physical stability of the nano-delivery system, as well as enhancing the chemical stability of entrapped lipid-soluble drugs (Chuacharoen, T. and Sabliov, 2016). Several other studies that have explored the use of PF127 to improve the stability and solubility of drug molecules include the study carried out by Shaarani *et al* (2017) where it was discovered that the addition of PF127 to the nanodispersion system maintained the stability of lutein for days of storage. The preparation of gold nanoparticles (GNP) by reacting PF127 and chloroauric acid ($HAuCl_4$) was thoroughly studied by Sokolsky-Papkov and Kabanov (2019). It was reported in their study that the presence of PF127 improves the methods of preparing pure, stable and uniform GNP, that can be employed in nanomedicine. More so, the stability of the dispersion of nanocarriers in a colloidal system influences the efficacy of therapeutic formulation in terms of post-reconstitution in withdrawal of dose and before oral administration (Kumar and Yagnesh, 2016).

Thus, this study seeks to evaluate the long-term stability of PZQ-loaded compritol ATO 888-lecithin solid lipid nanoparticles solution stabilizer with pluronic F127 (PF127) surfactant using dynamic light scattering (DLS) and electrophoretic light scattering (ELS), Turbiscan and Transmission Electron Microscope (TEM). Furthermore, the study investigates the efficacy of the PZQ loaded compritol ATO 888-lecithin solid lipid nanoparticles solution stabilizer with PF127 surfactant nanoformulation. The *In vitro* cell viability and *in vivo* toxicity evaluation were carried out to ascertain the safety of the nanoformulations. Also the antischistosomal activities against *Schistosoma mansoni* infection in a pre-clinical model was conducted so as to determine the parasitological cure rate.

5.2. Materials and methods

5.2.1. Material and reagents

Glyceryl behenate (Compritol 888 ATO) was procured as a free sample from Gattefosse SAS (Saint-Priest, Cedex, France), praziquantel was purchased from LeapChem (Co. Ltd.,), L-α-lecithin soybean which is composed of less than 2% triglycerides and 94% phosphatidylcholine), PF127, phosphate-buffered, 49409 Atto 488 Phalloidin, were bought from Sigma-Aldrich (St. Louis, MO, USA). RAW 264.7 cell line was procured from ATCC (Virginia, USA), ethanol and chloroform were obtained from Merck (Pty Ltd., South Africa). DAPI stain were purchased from Thermofisher. All other components and chemicals utilized in this study were of analytical grade. For all the preparations in the study double deionized water (DDW) was employed. Biochemical assays (AST, ALT, ALP, bilirubin and creatinine)

kits were purchased from Sigma-Aldrich. All other components and reagents used in this study were of analytical grade. Double deionized water (DDW) was used for all the preparations in the study.

5.2.2. Preparation of Compritol-lecithin SLN-loaded praziquantel

SLN were synthesized by employing solvent injection-co-homogenization techniques described, as follows. Briefly, a compritol-lecithin solution was prepared by dissolving the compritol and lecithin in a ratio of 1:1 (100 mg) in 20 mL of chloroform. Thereafter, 40 mg of praziquantel was dissolved in 10 ml of ethanol solution (99%) and added dropwise to compritol-lecithin solution under mild stirring conditions. The mixture of drug-containing lipid layers was then injected into the aqueous phase containing 0.5 w/v of PF127 at 70°C as surfactant under hot mechanical stirring to properly homogenize the suspension. Subsequently, the traces of organic solvent in the suspension was completely evaporated by using a rotary evaporator (Rotavapor® RII, Büchi Labortechnik AG, Flawil, Switzerland) at 70°C. The resultants SLN suspension was dialyzed overnight to purify the generated products. In like manner, PZQ unloaded-compritol-lecithin emulsion was made following the same method and served as the controls. The schematic diagram showing the preparation procedure is shown in Figure 5.1. The suspension was collected and kept for further analysis at room temperature.

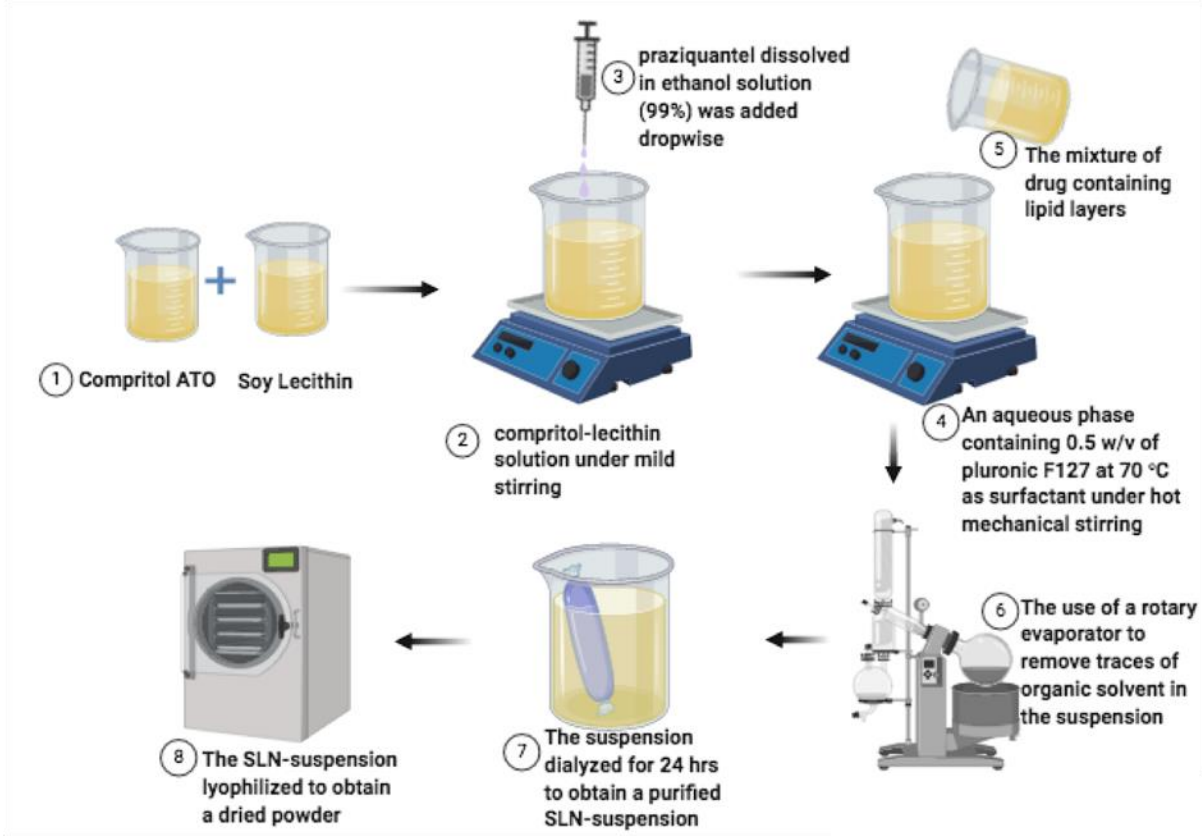

Figure 5.1: The schematic overview showing the preparation procedure praziquantel-loaded compritol-lecithin SLNs.

5.2.3. Determination of zeta potential, particle size distribution and polydispersity index (PDI)

The SLNs suspension kept at room temperature was used in ascertaining the zeta potential, average particle size and polydispersity index (PDI) of the SLN using Malvern ZetaSizer Nano ZS (Malvern Instruments, Worcestershire, UK) over 120 days. This was achieved by preparing samples of 0.1-0.2 mg/mL of final concentration from the SLNs suspension using distilled water and filtered (0.22 μm), and about 2 mL of the sample of SLN prepared was placed cuvettes measured. All measurements were carried out in triplicate.

5.2.4. Evaluation of the drug entrapment efficacy and drug loading capacity

The entrapment efficiency of PZQ trapped within the compritol-lecithin SLN was evaluated. Briefly, the lyophilized SLN sample was dissolved and ruptured in an adequate amount of chloroform. Thereafter, the concentration of the PZQ was calculated at a wavelength of λmax= 265 nm using ultraviolet-visible spectroscopy (UV-Vis Spec) (Specord40, Analytik Jena, AG, Germany) and computed using a standard linear curve of PZQ in concentrations between 0 and 16 μg/mL in double-distilled water (R^2=0.99). The percentage value of DEE (drug entrapment efficacy) and loading capacity (%LC) of the SLN was carried out in triplicate and computed using these Equations below:

$$\%DEE = \frac{A_q}{T_q} \times 100 \quad \text{.....(Equation 5.1)}$$

Where A_q represent the actual amount of PZQ measure by UV spectrophotometry and T_q denoted the theoretical amount of PZQ mixed with the compritol-lecithin SLN formulation.

$$\%LC = \frac{A_q}{W} \times 100 \quad \text{.....(Equation 5.2)}$$

Where A_q represent the actual amount of PZQ measure by UV spectrophotometry and W denoted the weight of compritol-lecithin SLN.

5.2.5. Evaluation of Fourier transform infrared spectroscopy (FTIR)

Native PZQ, lecithin, compritol, compritol-lecithin SLN-loaded and unloaded PZQ and compritol-lecithin SLN-loaded PZQ with surfactant in powdered form were analysed to determine possible structural interactions between the lipids and the PZQ. The formulations

were analysed using the Spectrum 2000 ATR-FTIR (PerkinElmer 100, Llantrisant, Wales, UK) with the wavelength ranging between 4000 cm^{-1} - 650 cm^{-1} with a 4 cm^{-1} resolution.

5.2.6. Mechanical properties analysis

The mechanical properties of the different SLNs formulations were investigated at physiological conditions using the non-destructive vibration of acoustic and laser determination of responses from rheology without the sample contact method previously described by (Ceccaldi *et al.,* 2017). 10 mg of the dried SLN was briefly dissolved in 5 mL of PBS (pH 7.4), thereafter, 3 ml of the suspension were loaded into the detachable sample holder designed specifically for ElastoSens^{TM} Bio2 (Rheolution, Montreal, Quebec, Canada). The real-time storage modulus for the complexation reaction of the suspension in the sample holder was performed for 2 h at 37°C using ElastoSens^{TM} Bio2. The device was used for each sample, the storage modulus was measured every 30 sec. The procedures for each sample at physiological conditions were done in triplicates.

5.2.7. X-ray powder diffraction (XRPD) evaluation

The degree of crystallinity natures of the native PZQ, lecithin, compritol, PF127, compritol-lecithin SLN loaded and unloaded PZQ and compritol-lecithin SLN loaded PZQ with surfactant in powdered form were evaluated by XRPD spectra (Rigaku Mini Flex 600, Tokyo, Japan) fortified with CuKα radiation at 15 mA and 40 kV. The 2θ scan ranged from 3^{o} to 90 ^{o}C was selected at a scanning rate of 10^{o} per minute was used to obtain diffractograms of the formulations.

5.2.8. Analysis of differential scanning calorimetry (DSC)

Thermal behaviour of native PZQ, PF127, lecithin, compritol, compritol-lecithin SLN loaded and unloaded PZQ and compritol-lecithin SLN loaded PZQ with surfactant in powdered form were analysed on a DSC by Mettler Stare system provided with STARe SW software. This task was achieved by weighing 3 to 6 mg depending on each sample in an alumina crucible of a pinhole and heated from 30°C - 300°C with a heating rate of 5°C/min under a nitrogen flow.

5.2.9. Colloidal system analysis of the formulated SLNs

The colloidal system of the SLNs dispersions was analysed under an inverted compound light microscope (Olympus CKX53, Olympus Corporation, Tokyo, Japan). The dispersion of the SLNs increased and the surface and the attractive component of the interparticle interaction of the formulated SLNs was observable. This colloidal dispersion was determined to ascertain how the SLNs can be prevented from aggregation or flocculation.

5.2.10. In vitro analysis of PZQ release from the formulated SLNs

To evaluate the *in vitro* release behaviour of PZQ in free PZQ, PZQ-loaded SLNs with surfactant. Thirty milligrams of free PZQ, PZQ-loaded SLNs were weighed and dispensed into specimen vessels containing 100 mL of pH 7.4 PBS (containing 0.002% Tween 80) and incubated at 37 ± 1°C in an orbital shaking incubator- horizontal (type LM-530, Yihder Technology Co., LTD.) set at 25 rpm for 24 h. A minute before sampling, agitation was stopped to allow the SLNs to settle and also to reduce the number of intact particles removed from the dissolution medium. Sampling was conducted at stipulated time periods (1, 2, 4, 8, 12, and 24 hrs) and all aliquots withdrawn were centrifuged and diluted appropriately before UV-Vis spectrophotometric analysis at 265 nm. The experiments were done in triplicate on all the formulated PZQ-loaded SLN and free PZQ.

To determine the *in vitro* release behaviour of PZQ from CLPF suspension after day 120 of the stability study, a similar method described above was used through a dialysis technique and 20 mg/mL of PZQ suspension as a control.

5.2.11. Optical characterization and stability profiling of the suspensions of SLNs formulation

The stability and optical interactions of the SLNs suspension at the first and last day of stability analysis was evaluated using the TurbiscanTM LAB (Formulaction, L'Union, France). Briefly, about 20 mL of CLF-SLN and CLPF-SLN suspensions were aliquot and introduced into specialized sample holders and evaluated at pre-determined intervals (6 mins) over 1 h duration at 25 ± 05^{o}C. The instrument was equipped with two detectors, the backscattering and transmission detectors, which are positioned at 54^{o} and 180^{o}, respectively. More so, the instrument was fixed with a pulsed near infra-red-light source, which travels vertically along the sample collecting data at 40 µm-intervals. The transmission detector revealed the light that was transmitted via the suspended SLNs formulation, while the backscattering detector exposed the light that was recovered/rebounded by the suspended SLNs formulation. The delineate SLNs formulation stability were obtained from Turbiscan^{TM} LAB through the measurements of the changes in backscatter (∆BS).

5.2.12. Scanning Electron Microscopy and Transmission Electron Microscopy and

The morphological analysis of the formulated SLNs was investigated by Scanning Electron Microscopy (SEM). The lyophilized SLNs samples were dissolved in distilled water and a drop was positioned on an aluminium specimen stub and leave overnight to dry. Subsequently, the samples loaded on the stub were sputter-coated with both gold and palladium and shielded with a double-coated carbon glue disc for 4 min at 20 KV. The SEM pictures of the formulated

unloaded and PZQ-loaded SLNs were generated with the help of SEM (Zeiss Electron Microscopy, SIGMA VP, Carl Zeiss Microscopy Ltd; Cambridge, UK).

High-Resolution Transmission Electron Microscopy (HRTEM) version TECNAIF3OST-TEM was employed in ascertaining the morphology of the CLPF after 120 days. The CLPF suspension was concentrated to about 1:10 with distilled water and filtered using 0.22 μm. A drop of the concentrated CLPF suspension was mounted on the carbon-coated copper grid for 5 mins followed by the excess removal of liquid, which was attained by blotting and thereafter air-dried at room temperature. Subsequently, the films on the copper grid were visualized under an electron microscope at 10,000x magnification.

5.2.13. In vitro cytotoxicity assay (MTT Assay)

The *in vitro* cytotoxicity of the SLNs on RAW 264.7 macrophages was investigated through an MTT cell viability study. DMEM supplemented with 1% penicillin-streptomycin and 10% fetal bovine serum was used to culture the cells at 37°C and 5% CO_2 (in a humidified incubator). After every two days, the spent growth medium was replenished with fresh growth medium was until the cells reached about 80 to 90 % confluence. The cells at a density of 1 x 10^5 cells per well were seeded in 96-well plates. After 24 h, the adhered cells were treated with SLNs and PZQ of 30 - 120 μg/ml concentration range in triplicates. Subsequently, the cells were incubated for 72 h in a humidified incubator at 37°C and 5% CO_2. After 72 h, 10 μl of MTT reagent (Merck, Darmstadt, Germany) was included in the wells and the cells were further incubated for 4 h at 37°C. Thereafter, 110 μl of DMSO was added to the well plates and incubated subsequently at 37°C for an hour so as dissolve the formed crystals formazan. Thereafter, the absorbance at 570 nm, with a reference wavelength of 690 nm was measured by a multimode microplate reader (Victor X3 Multimode Multilabel Microplate Reader 2030-0030, Perkin Elmer, MA, USA). The cell viability percentage was determined from the ratio of absorbance of the test samples to that of the untreated sample.

5.2.14. Evaluation of cell morphology

After RAW 264.7 murine macrophage cells had reached 80 to 90% confluence, 2.5 x 106 cells/mL were seeded and cultured on coverslips in 6-well plates containing 2 mL DMEM supplemented with 1.0% ($^v/_v$) penicillin-streptomycin antibiotic and 10% ($^v/_v$) FBS and incubated for 24 hours at 37 °C under 5% CO_2. After 24 hours, the adherent cells were treated in triplicates with 90 μg/ml of CLF, CLPF, and PZQ, as well as 10 μg/ml of 5-fluorouracil (5-FU) as a negative control. The cells were then cultured for another 24 hours in a humidified incubator at 37°C and 5% CO_2. The phase contrast morphology of the cells was observed under an inverted compound light microscope after 24 hours of treatment (Olympus CKX53,

Olympus Corporation, Tokyo, Japan). After that, the cells were fixed, this was done by first spiking the media growth containing the cells with 500μL of 4% formaldehyde to avoid harm from the rapid shift in osmolarity between the fixation solution and the culture medium osmolarity. After about 2 minutes, the medium was aspirated and decanted, and the cells were then fixed with pure 1mL of 4% formaldehyde for about 20 minutes. After 20 minutes of fixation, the fixed cells were gently washed four times with 2mL PBS to remove any unbound fixation agent, then stained with 500μL of a 50μM fluorescent phalloidin solution to bind F-actin cytoskeleton of the cell membrane for about 40 minutes at room temperature in the dark. After 40 minutes, the cells were washed four times with PBS to remove any unbound phalloidin stain, then stained with 500μL of 500nM DAPI stain solution to bind the nucleus of the cells, and incubated at room temperature for 5 minutes in the absence of light. After that, the cells were carefully washed with PBS to eliminate any remaining DAPI stain solution. The coverslips were then placed on glass slides and examined using a compound fluorescence (x20 magnification) microscope (Olympus IX51, Olympus Corporation, Tokyo, Japan).

5.2.15. In vivo toxicity evaluation

The evaluation of *in vivo* toxicity was done in Sprague Dawley rats with a weight range of 250-300 g, kept in a standard husbandry and housing condition at normal room temperature and provides with normal tap water and normal rat chow. The animals were grouped into 3 randomly, and each group was named as follows: Group I: control, Group II: PZQ, and Group III: CLPF. An equivalent amount of the dose (250 mg/kg) in about 2 to 3 mL of PZQ and CLPF were administered to the animals via a once-off oral gavage orally. Seven days after, all the animals were humanely decapitated, and their blood was collected via cardiac puncture and stored in microcentrifuge heparin tubes and centrifuge for 5 min at 2500 rpm in 4°C to isolate plasma from red blood cells (RBCs). Thereafter, the plasma was examined for a liver functioning test to assess the hepatotoxicity of the various formulations by the measurement of the plasma levels of aspartate aminotransferase (AST), alanine aminotransferase (ALT), creatinine and bilirubin using commercially available kits from Sigma Aldrich, South Africa. The activities of ALT, AST, creatinine and bilirubin were calculated for each assay using the Equations below;

$$\text{ALT activity} = \frac{B\ x\ Sample\ Dilution\ Factor}{(Final\ temperate - Initial\ temperature)\ x\ V} \quad \text{.....(Equation 5.3)}$$

Where B is the amount (nmole) of pyruvate generated between the initial temperature and final temperate and the final temperature is the time of first reading in minutes, while the initial temperature is the time of penultimate reading in minutes, and V is the sample volume (mL) added to well.

$$\text{AST activity} = \frac{B\ x\ Sample\ Dilution\ Factor}{(Reaction\ Time)\ x\ V} \quad \text{.....(Equation 5.4)}$$

Where B is the amount (nmole) of glutamate generated between the initial temperature and final temperate, and the reaction time is the final temperature minus the initial temperature in minutes and V is the sample volume (mL) added to the well.

$$\text{Concentration of creatinine} = \frac{Sa}{Sv} \quad \text{.....(Equation 5.5)}$$

Where Sa is the amount of creatinine in an unknown sample (nmole) from the standard curve and Sv is the sample volume (μL) added into the wells, while C is the concentration of creatinine in the sample and the creatinine molecular weight is taken as 113.12 g/mole.

$$\text{Bilirubin concentration} = \frac{(A_{530})sample - (A_{530})blank}{(A_{530})calibrator - (A_{530})water} \; x \; (5\ mg/dL) \quad \text{....(Equation 5.6)}$$

Where (A_{530}) sample is the value of the sample (total or direct) and (A_{530}) blank is the value of the sample blank, while (A_{530}) calibrator and (A_{530}) water are the value of the calibrator reading and the value of the water control reading, respectively. 5 mg/dL is the equivalent bilirubin concentration of the calibrator.

To determine the toxicity of the SLNs formulations to the organ, tissue samples (liver, lung, kidney and spleen) were obtained and placed in 10 % Neutral Buffered Formalin thereafter inserting them in paraffin for sectioning the tissues. The tissues were then stained with eosin and haematoxylin for microscopic determination and spotted for toxicity markings.

5.2.16. In vivo parasitological study

5.2.16.1. Infection of animals

The *in vivo* antischistosomal study was conducted in the Schistosome Biological Supply Centre (SBSC) of Theodor Bilharz Research Institute (TBRI), Giza, Egypt. Male Swiss albino mice (CD-1) weighing 18–20 g were obtained from SBSC of TBRI (Giza, Egypt), and housed in an environmentally controlled room temperature of 20–22 °C, a 12 h light/dark cycle, and 50–60% humidity throughout the acclimatization and experimental periods, with access to food and water *ad libitum*. A hundred microliters of cercarial suspension was gently mixed before being counted and stained with a picric acid solution.

The mice were then infected with *S. mansoni* cercariae (supplied by SBSC) by subcutaneous injection (Liang et al., 1987) and exposure to 60 ± 10 cercariae per animal. The TBRI Institutional Review Board authorized all of the animal studies, which were carried out in line with the Guide for the Care and Use of Laboratory Animals.

5.2.16.2. Experimental design

Mice infection: According to Liang *et al* (1987) *S. mansoni* cercariae were injected subcutaneously with 60 ± 10 Egyptian strain S. mansoni cercariae shedding from *Biomphalaria alexandrina* snails.

The animals were split into three groups based on the timing of drug administration:

Group 1: Infected control.

Group 2: Single dose 250 mg/kg (PZQ equivalent) CLPF was administered two weeks post-infection

Group 3: A single dosage of PZQ 250 mg/kg was administered two weeks post-infection

Group 4: A single dosage of 250 mg/kg of CLPF was administered four weeks post-infection.

Group 5: A single dosage of PZQ 250 mg/kg was administered four weeks post-infection.

After six weeks post-infection, all animals were sacrificed.

5.2.16.3. Assessment of parasitological cure rate

Worm recovery: Sacrificed mice were subjected to a hepato-portomesentric perfusion method to collect adult *S. mansoni*, assess sex (male/female/copula), estimate worm load, and then compute the percentage of overall worm reduction (Christensen *et al*., 1984).

Oogram pattern: The percentage of eggs at various stages of development (oogram pattern) was investigated (Pelligrino *et al*., 1962). The eggs were identified and counted at different stages of development in three intestinal segments, and the mean number of each stage was determined.

Egg count in tissues: Small pieces of intestinal and hepatic tissue were weighed, digested overnight in a 5 ml solution of KOH 5%, and three samples (each 50 µl) of the digested tissue were inspected microscopically to estimate the mean egg count (Pelligrino *et al.*, 1962). The method described by Kloetzel (1967) was used to determine the number of eggs per gram of tissue and the percentage decrease of total ova per gram of tissue.

5.2.17. Statistical Analysis

The significance of the difference observed was evaluated using a student's t-test, and the findings are presented as mean values and standard deviation (±SD) (GraphPad Prism software). *P*-values of less than 0.0001 are considered statistically significant in all tests.

Other data was coded and input using the Microsoft Excel 2010 statistical software. The following calculation was used to compute the % reduction in worm/egg load in each treatment group: [(Number of worms/eggs in control group) − (Number of worms/eggs in the treated group)] / (Number of worms/eggs in control group) × 100.

5.3. Results

5.3.1. Physical analysis of the nanoparticulate system

PZQ loaded compritol-lecithin-SLN (CLPF-SLN) and unloaded compritol-lecithin SLN (CLF-SLN), were characterized. Table 5.1 showed the average particle size distribution, zeta potential and PDI were determined after the suspension was dialyzed and washed using dialysis tubing with M.W 12000 Da. The generated average particle size distribution, as well

as zeta potential for the formulated SLNs, showed that there was uniformity in size and zeta potential of the formulations as showed in Figure 5.2. The statistical analysis showed no significant difference in the size of particle distribution, PDI as well as zeta potential of the SLNs. The particle size of CLPF-SLN and CLF-SLN was 112.9± 1.0 nm and 101.6± 0.7 nm, respectively. The size of particles is an essential factor that affects the stability, biodistribution and release of the drug (Üstündağ-Okur et al., 2016).

The polydispersity index of the formulations ranges between 0.23 to 0.27a.u which showed the phospholipid vesicles homogenous population of the SLN. The average zeta potential of the SLNs formulation ranged between -19.0 ± 0.26 and -23.6 ± 0.26 which indicates that the formulations are stable regarding aggregation, flocculation, sedimentation, coagulation and creaming via a strong electrostatic repulsion that keeps the particles charged from one another. Meanwhile, any dispersions with a lesser zeta potential value will undergo inter-particle attractions to aggregate through Van Der Waal. Herein, the %EE of PZQ was observed to be 71.63 % in the drug-loaded compritol-lecithin-SLNs prepared using PF127 as a surfactant and the %LC was 11.46 %.

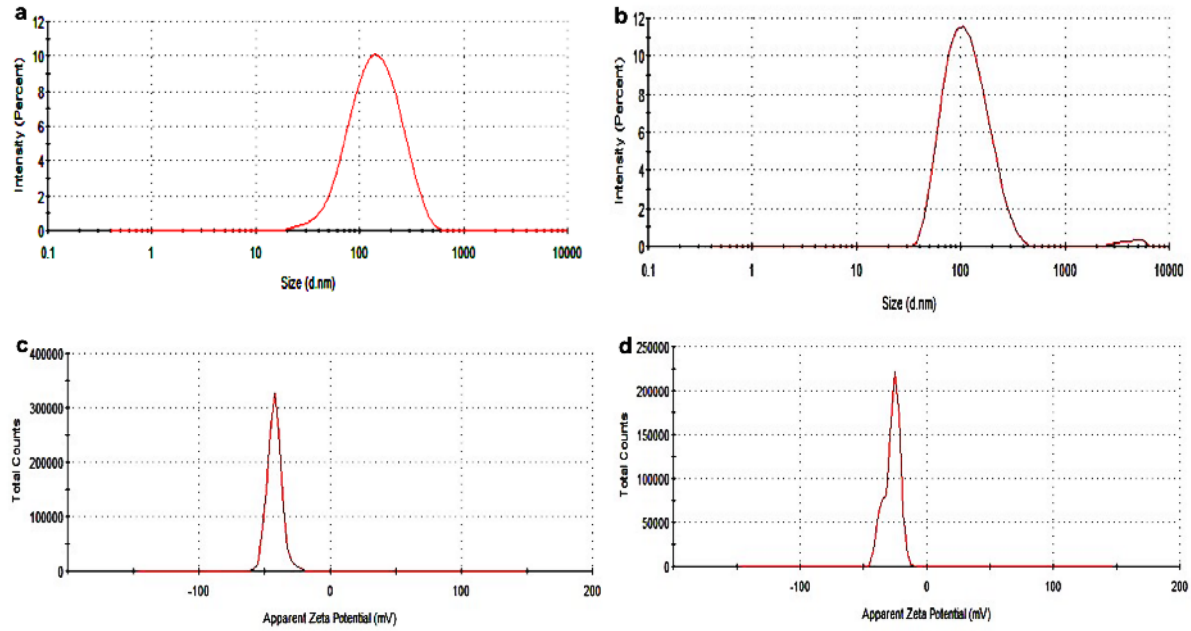

Figure 5.2: The generated particles size intensity profile for (a) CLF, (b) CLPF and particle Zeta potential measurement profile for (c) CLF (d) CLPF by Dynamic Light Scattering. Subsequently, the samples were suspended in distilled water before measurement.

CLF and CLPF represent the formulations of compritol-lecithin-solid lipid nanoparticles and PZQ-loaded compritol-lecithin- solid lipid nanoparticles with PF127 as a surfactant.

Table 5.1: Particle size, PDI, zeta potential of unloaded and PZQ-loaded compritol-lecithin solid lipid nanoparticles made with PF127 and the drug entrapment efficacy and drug loading capacity

S/N	Sample	Size (nm)	PDI (a.u)	Zeta Potential (mV)	%DEE	%LC
1	CLF-SLN	101.6 ± 0.7	0.27 ± 0.006	-23.6 ± 0.26	-	-
2	CLPF-SLN	112.9 ± 1.0	0.23 ± 0.010	-19.0 ± 0.26	71.63 ± 0.3	11.46 ± 0.61

Note: Values are expressed as mean ± SD (n = 3)

PDI means polydispersity index, CLF and CLPF represent the formulations of compritol-lecithin-SLN and PZQ-loaded compritol-lecithin-SLN with PF127 as a surfactant. %DEE Drug entrapment efficacy, %LC loading capacity

5.3.2. Evaluation of FTIR Spectroscopy

The chemical characteristic of PZQ, stabilizer (PF127), lipids (compritol 888 and lecithin), and the formulated SLNs were investigated by Fourier transform infrared (FTIR) spectroscopy. As shown in Figure 5.3a, compritol 888 showed characteristic peaks at wavenumbers 2955.89 cm^{-1} to 2849.07 cm^{-1}, 1736.42 cm^{-1}, 1465.14 cm^{-1} and 719.26 cm^{-1} which correlated to O-H and -C-H(CH_2), C=O and -C-H(CH_2) vibration respectively. All the FTIR stretching frequencies correspond to pure compritol 888, and the peaks are corroborated with other reported studies (Kumar *et al.*, 2019). In lecithin, the peaks found in wavenumbers 3385.24 cm^{-1}, 3011.09 to 2853.14 cm^{-1}, 1734.19 cm^{-1}, and 1466.14 cm^{-1} aligned with N-H, O-H, =-CH_3 and C-H, C=O and P=O respectively, and these peaks are similar to what is obtained in Sumaila et al (2019). Likewise, the vibration peaks found in PZQ at the wavenumbers 2929.49 cm^{-1} and 2852.52 cm^{-1} corresponded to the symmetric and asymmetric vibrations of CH and CH_3, respectively which are similar to other reported literature (Liu *et al*., 2004; Campos *et al*., 2013).

When comparing native lipids with the compritol-lecithin SLN (Figure 5.3b), a slight change was observed, and some peaks found in the native lecithin and compritol were not found in the formulated SLNs. Other vibrational peaks found in SLN similar to those found in native lipids may be due to electrostatic and hydrophobic interactions that occur between the two lipids and PF127 to form the SLN. Another possible interaction is hydrogen bonding which occurs between the amine group, the bonds between the oxygen atom of the phosphate group of phospholipids, as well as hydrogen bonding between carbonyl oxygens. The slight change in the peaks found in wavenumbers 2887.88 cm^{-1}, 2916.68 cm^{-1}, 2850.30 cm^{-1} of the SLNs may be a result of electrostatic repulsion which in turn enhances the stability of the particles. Interestingly, a comparison of the peaks found in unloaded and drug-loaded SLN showed that

the characteristic peaks corresponding to PZQ were not found in the PZQ-loaded CLPF-SLNs. This means that PZQ is not found on the surfaces of SLNs. It was surmised to say that PZQ was molecularly dispersed, well encapsulated and entrapped in the stable lipid matrix.

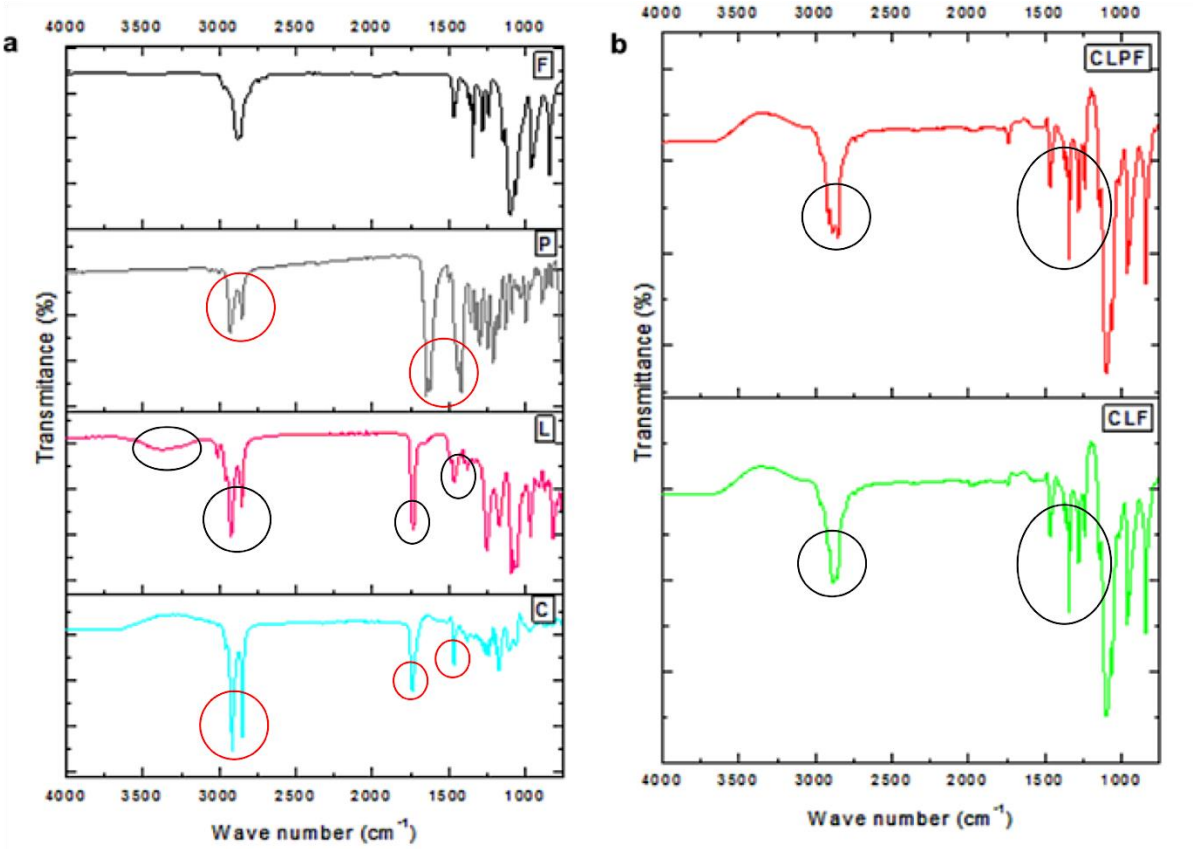

Figure 5.3: FTIR spectra of (a) all the excipients F- PF127, P-Praziquantel, L-Lecithin, C-Compritol (b) the formulated unloaded and PZQ-loaded SLNs.

6.3.3. Evaluation of mechanical properties under physiological conditions

The viscoelastic properties of the prepared SLNs were evaluated using ElastoSens™ Bio which uses a non-destructive real-time to determine the evolution of mechanical features of a formulation (Ceccaldi *et al*., 2017). As showed in Figures 5.4, the gelation time for CLF and CLPF samples were 322.2 and 207.8 sec respectively after the measurements were taken every 30 s at 37 °C. The gelation time for all four formulations ranges between 2 min 4 sec to 10 min 37 sec. It was observed that the onset gelation time for SLNs loaded PZQ had a relatively fast onset gelation time when compared with the SLNs unloaded with PZQ. As shown in Figure 5.4, the delay in the gelation time of the CLF-SLNs may be a result of several molecular interactions (electrostatic repulsion and hydrogen bonding) between the two lipids molecules to form a complex. It was shown that the addition of PZQ to produce CLPF increase the onset gelation in real-time of the SLNs loaded with PZQ, this may be as a result of quick

complexation interaction between the lipids-complex and the PZQ. More so, the result of that figure showed that the PZQ-loaded formulation has a rapid G′ and gelled after about an hour of the reaction. This may be attributed to the uninterrupted reaction between the molecules (amine and phosphate molecules) of the drug and lipids that facilitated the complexation process. At the end of the 2 hours of viscoelastic measurements, CLF and CLPF attained a G′ maximum of 286 Pa and 140 Pa, respectively. It was discovered that the drug-loaded formulation completed its gelation some minutes before the 2 hours reaction.

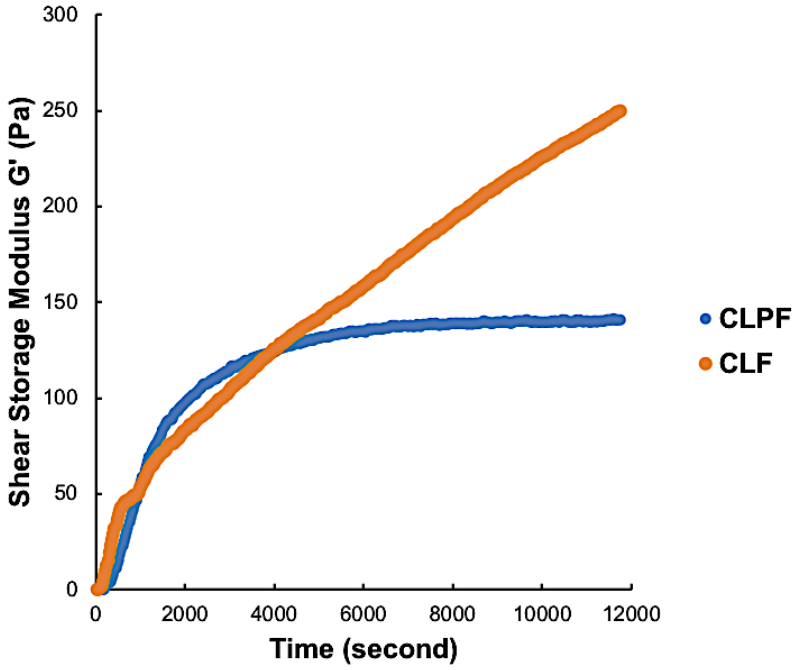

Figure 5.4: Kinetic gelation plots of (a) unloaded and (b) the PZQ-loaded SLNs showing the shear storage modulus (G′) (Pa) observed over the periods of 3 hours at 37 °C. CLF and CLPF represent the formulations of compritol-lecithin-solid lipid nanoparticles and PZQ-loaded compritol-lecithin- solid lipid nanoparticles with PF127 as a surfactant.

5.3.4. Evaluation of crystal nature of the formulated SLNs

The crystal characteristics of the samples were evaluated using the XRPD technique. This analysis was carried out for all the excipients (the lipids, drug and stabilizer) and the formulated SLNs for comparison. The patterns presented in Figure 5.5a and b depicted the patterns of all samples. It was shown that all the characteristic peaks of the excipient materials, that is, PZQ, compritol, Lecithin and PF127 in Figure 5.5a corresponded to the reported peaks in the literature (Kumar *et al*., 2019; Sumaila *et al*., 2019; Campos *et al*., 2013; Zanolla *et al*., 2020). In Figure 5.5a, the major characteristic peaks at 2θ-19.5^{o} and 23.8^{o} of the stabilizer (PF127) displayed the highly crystalline nature of the stabilizer, and for the lipids, compritol was shown to be highly crystalline with the diffraction peaks at 2θ-4.5^{o}, 20.1^{o} and 23.2^{o}. While lecithin

depicted semi-crystalline, amorphous properties with the major characteristic peak at 2θ-20.4°, broad amorphous peak at 2θ-40.8°, and other crystal peaks at 2θ-4.2°, 7.6° and 10.3°, and PZQ was shown to be highly crystalline in nature. As shown in Figure 5.5b, both the drug-loaded SLN and bare SLN with PF127 (that is, CLF and CLPF) shown to be highly crystalline in nature, which may be attributed to enough absorption of PF127 on the lipid matrix surface. Importantly, the corresponding diffraction peaks to pure PZQ were not found in both the PZQ-loaded SLNs with surfactant. This result further confirmed the encapsulation and the molecular presence of PZQ within the matrices of the lipid and correlated with FTIR and DSC.

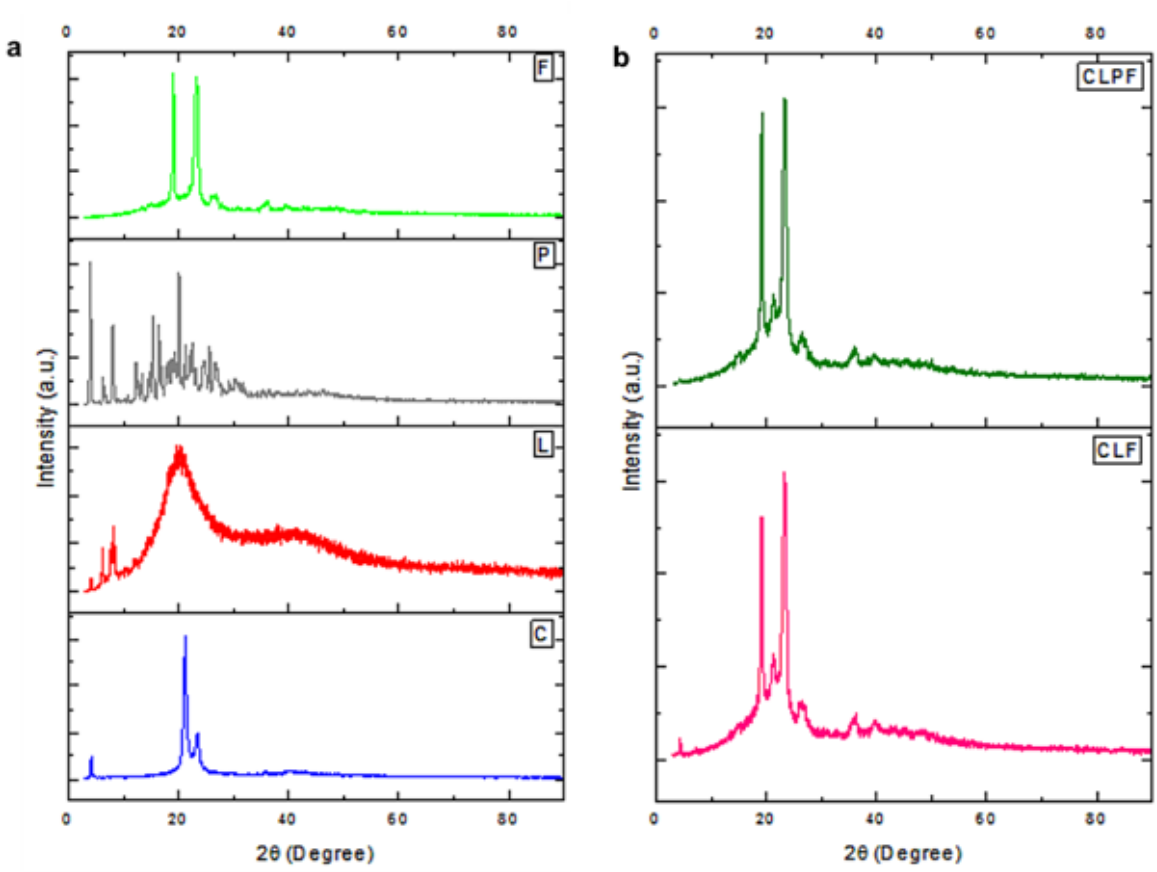

Figure 5.5: XRD diffractograms of (a) all the raw excipients F- PF127, P-Praziquantel, L-Lecithin, C- Compritol (b) the formulated unloaded and PZQ-loaded SLNs.

5.3.5. Evaluation of thermophysical properties of the formulated SLNs

The thermal behaviour of the formulated SLNs was examined by DSC analysis, this was done to ascertain any possible change in physical features of the components of the individual SLNs formulation and to determine the amorphous or crystalline attribute of the PZQ loaded SLNs. The data and resultant thermal bends are displayed in Table 5.2 and Figure 5.6, respectively. The melting point of the compritol, lecithin, drug PZQ, and stabilizer PF127 were shown to

have endothermic peaks at 71.83º, 223.08º, 137.99º and 55.06º respectively, which can be attributed to the fusion of their crystalline portions. All the raw excipients melting points were similar to results documented in the literature (Kumar *et al*., 2019; Sumaila *et al*., 2019; Campos *et al*., 2013; Zanolla *et al*., 2020). The DSC thermograms also displayed the endothermic melting peaks of the formulated native SLNs and PZQ loaded SLNs. For the SLNs made with PF127 as a stabilizer, minor endothermic melting peaks corresponding to the melting of the stabilizer was observed. The thermal response showed complete melting of the lipid matrix and a slight shift in the melting of the stabilizer. In the PZQ loaded SLNs (CLPF with melting peaks of 53.98), the endothermic melting peaks corresponding to the melting peaks of the native SLNs (CLF with the endothermic peaks of 53.53) was observed with the absence of the endothermic melting peaks corresponding to the drug, this is an indication that the drug PZQ is well properly dispersed or loaded within the core of lipid matrix.

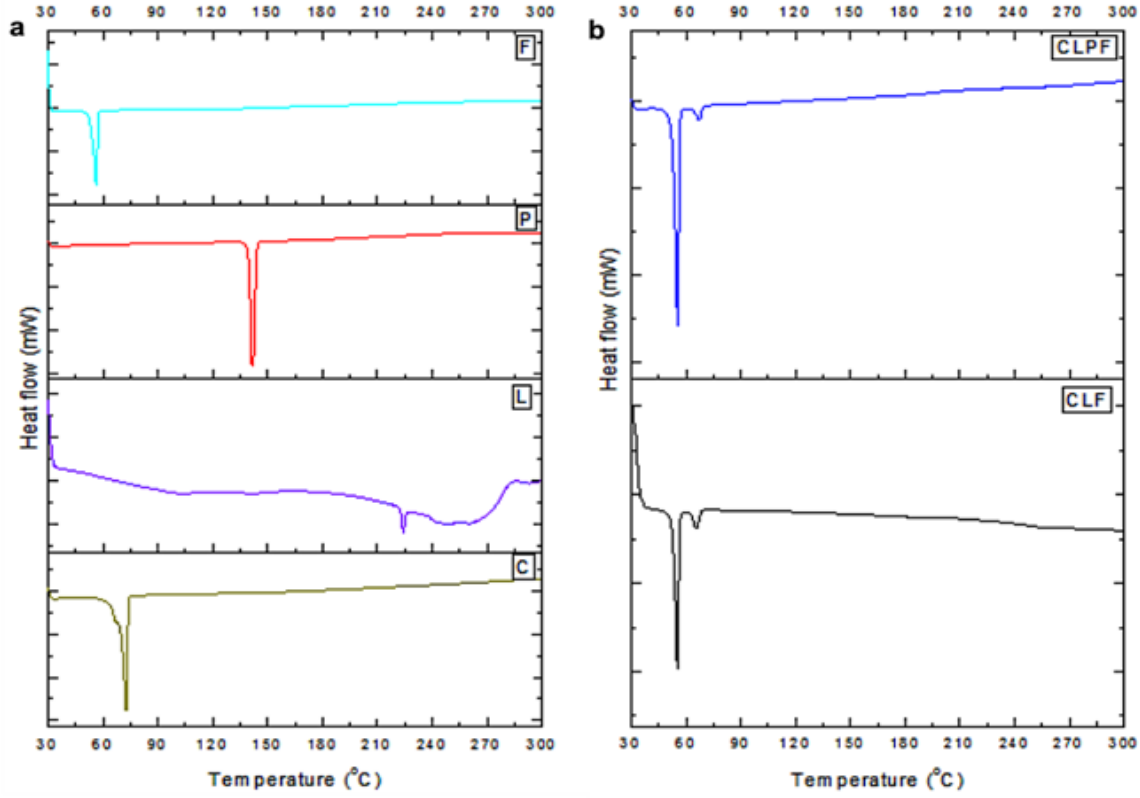

Figure 5.6: (a) DSC thermograms of all the raw excipients F- PF127, P-Praziquantel, L-Lecithin, C- Compritol (b) the formulated unloaded and PZQ-loaded SLNs

Table 5.2: The summary of the DSC thermograms data of all the excipients and the formulated unloaded and PZQ-loaded SLNs

S/N	Composition	T (onset)/ºC	T (peak)/ºC	ΔH (J/g)
1	PF127 (F)	54.02	55.84	-101.37
2	PZQ (P)	139.60	141.37	-115.10
3	Compritol (C)	69.08	72.29	-124.52
4	Lecithin (L)	222.85	223.99	-1.95
5	Comp-Lec-F127 (CLF)	52.64	55.22	-56.33

6	Comp-Lec-PZQ-F127(CLPF)	52.57	55.38	-65.05

5.3.6. Investigation of the colloidal system of the synthesized SLNs

The colloidal system of the formulated SLNs was investigated using an inverted light microscope (Olympus CKX53, Tokyo, Japan) using the X objective lens. The microscope images showed that the particles are uniformly suspended with well-defined shapes, sizes and form spherical surfaces as shown in Figure 5.7**.** Nanoparticles that are colloidal with size, composition, shapes, crystallinity or surface properties and structure, which are controllable can be fine-tuned based on the applications they are needed for through their properties and characterizations (Chhabra and Gurappa, 2019; Ashok *et al*., 2020). The dispersion of the colloidal system could also contribute to the stability, interparticle interactions, microstructure, thermodynamic aspects and transport properties of the nanoparticles. Since it has been reported that the dispersion of colloidal system enhances the stability, thermodynamic properties, interparticle interactions and microstructural aspect of particles that is if the dispersed particles remain as separate units and do not form a cluster or an aggregate (Chhabra and Gurappa, 2019; Ashok *et al*., 2020).

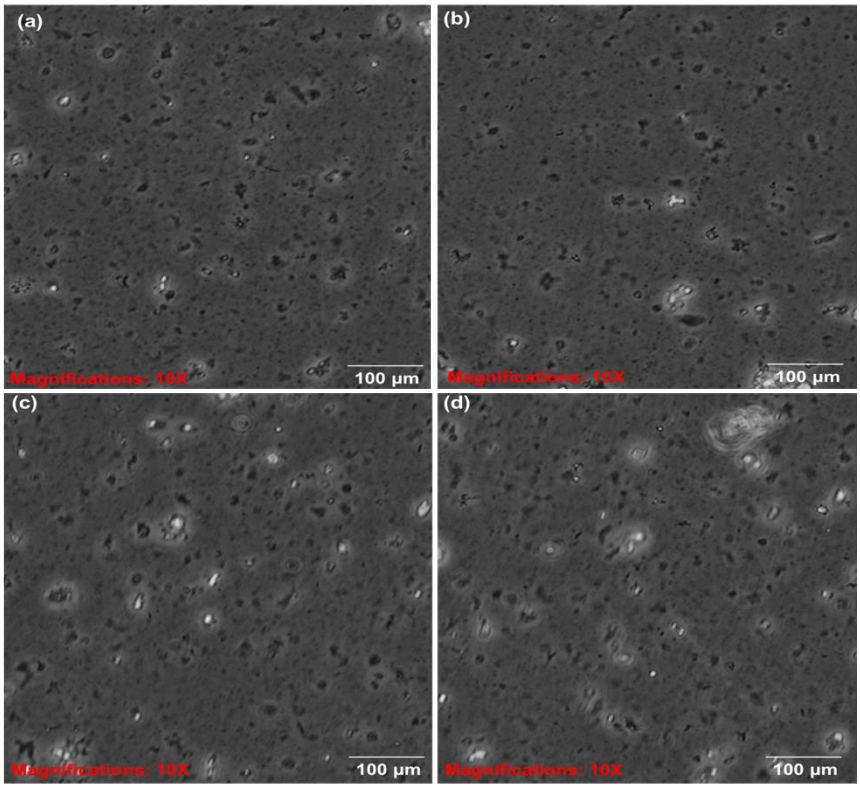

Figure 5.7: Inverted microscope images of colloidal aggregates of the (a and b) CLPF-SLNs and (c and d) CLF-SLNs (x10 magnification). CLF and CLPF represent the formulations of compritol-lecithin-solid lipid nanoparticles and PZQ-loaded compritol-lecithin- solid lipid nanoparticles with PF127 as a surfactant.

5.3.7. Analysis of the in vitro release behaviour of PZQ from the formulated CLPF-SLN

The *in vitro* release behaviour of PZQ from the CLPF-SLNs formulated was examined together with the free PZQ. As shown in Figure 5.8, there is a burst-release of PZQ in the initial stage (the first 2 hours) of the free PZQ with about 37.3 %, which was later followed by steady release over the remaining 24 h with a total release of approximately 95.8 %. This burst-release could account for the rapid metabolism and quick conversion of the drug to its inactive form. There was a slow and steady exponential release of PZQ from the formulated SLNs over the 24 h within the pH medium tested. Cumulative release of 48.08 % for CLPF was reached within 24 h at physiological pH of 7.4. As shown in Figure 5.9, the *in vitro* release profile of PZQ within the CLPF suspension after a 120-day stability study was determined, and the PZQ release profile obtained was similar to that observed in the normal CLPF, but with a slightly higher cumulative release of about 51.8% within 24 h. Meanwhile, the *in vitro* release profile of PZQ suspension released almost all free PZQ within 2 h at 37°C under sink conditions.

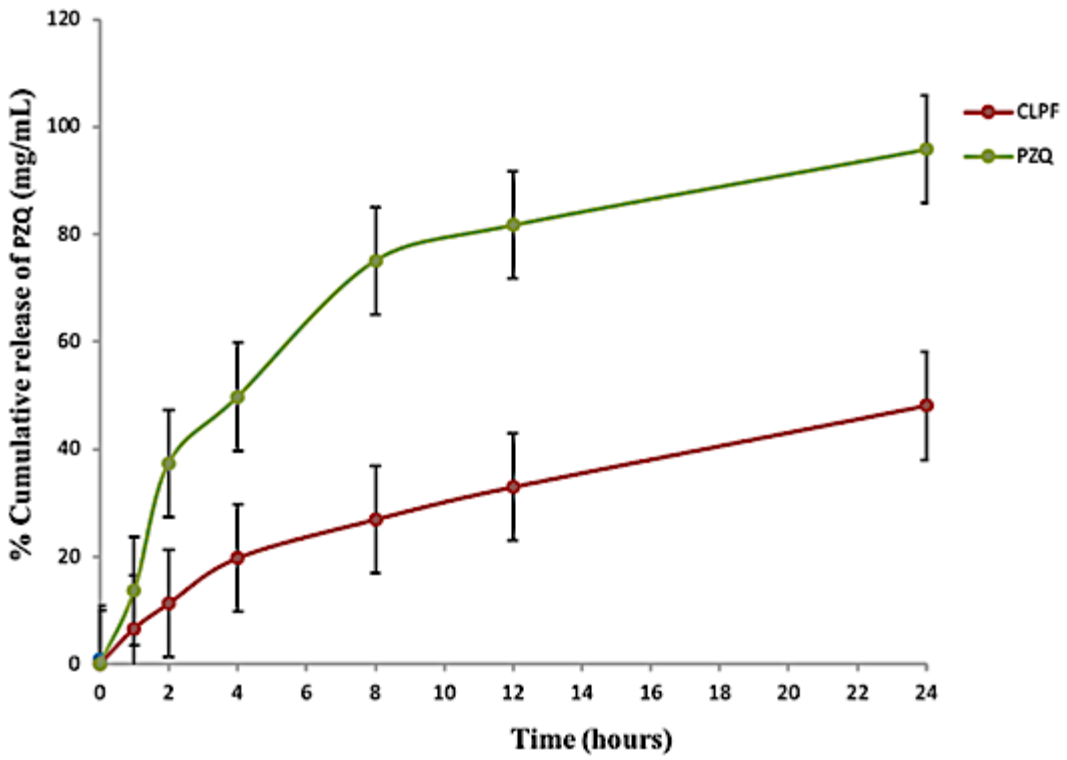

Figure 5.8: In vitro release profile of native PZQ, PZQ-loaded SLNs (CLPF). Temperature = 37±1°C, Release medium = PBS, pH = 7.4 (containing 0.002% Tween 80) (n = 3, mean ± SD).

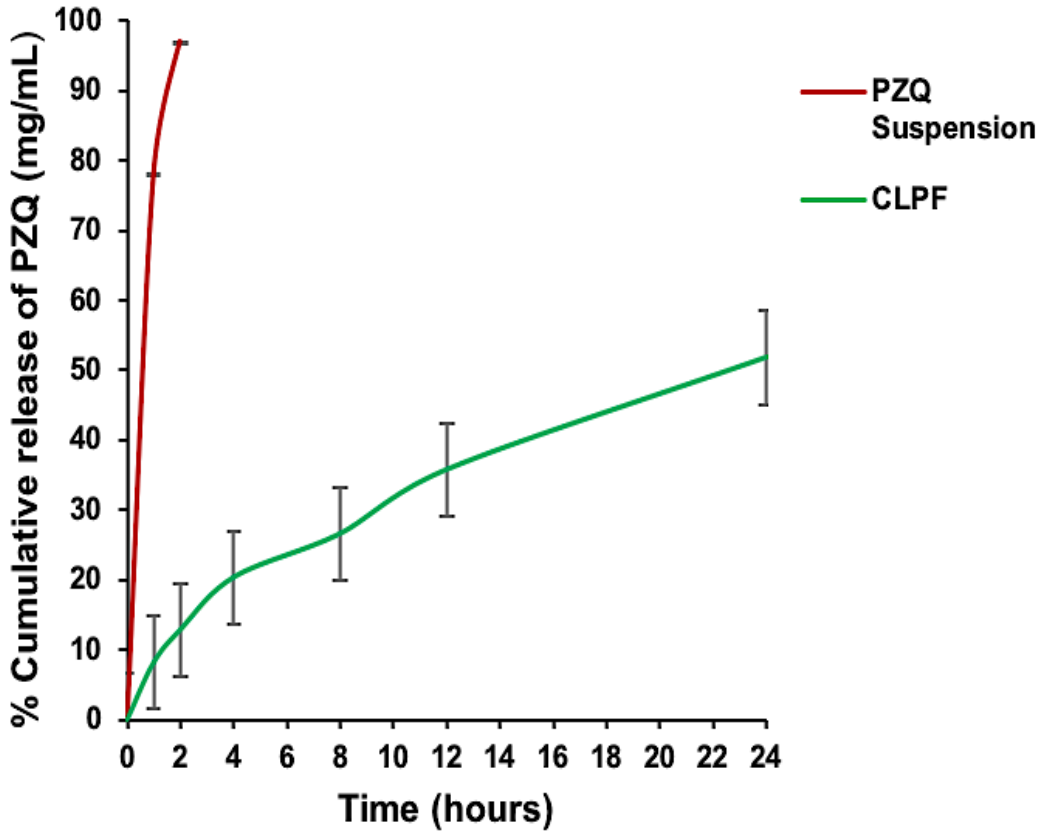

Figure 5.9: In vitro release profile of native PZQ suspension, PZQ-loaded SLNs (CLPF) after day 120. Temperature = 37±1°C, Release medium = PBS, pH = 7.4 (containing 0.002% Tween 80) (n = 3, mean ± SD).

5.3.8. Particle size distribution, PDI and zeta potential analysis of the SLNs as a function of time

The physical stability of both the unloaded and PZQ-loaded CLF-SLN was evaluated at room temperature over 120 days at 30 days intervals using dynamic light scattering (DLS) and electrophoretic light scattering (ELS), which measures the particle size, PDI, and zeta potential. Table 5.3 shows the average particle size for CLF to be 101.60 ± 0.70, 111.13 ± 0.65, 115.03 ± 0.11, 109.90 ± 1.80 and 102.23 ± 1.81 nm for day zero, days 30, days 60, days 90 and days 120, respectively. The polydispersity index and zeta potential for CLF from day zero to 120 days, ranges from 0.25 ± 0.008 to 0.28 ± 0.018 a.u and -20.58 ± 0.56 to -23.60 ± 0.26 mV, respectively. The average particle size in the range of 109.96 ± 3.17 - 116.06 ± 0.37 nm (PdI = 0.21 ± 0.003 - 0.23 ± 0.010; zeta potential = -18.21 ± 1.22 to -20.16 ± 0.44 mV) were observed for the PZQ-loaded CLF-SLN from the day zero to 120 days.

Table 5.3: Characteristics of unloaded and PZQ-loaded CLF-SLN at room storage temperatures over 120 days.

S/N	Sample	Time (days)	Size (nm)	PDI (a.u)	Zeta Potential (mV)
1	CLF-SLN	0	101.60 ± 0.70	0.27 ± 0.006	-23.60 ± 0.26
		30	111.13 ± 0.65	0.28 ± 0.018	-21.13 ± 0.19
		60	115.03 ± 0.11	0.26 ± 0.006	-20.58 ± 0.56
		90	109.90 ± 1.80	0.27 ± 0.019	-22.09 ± 1.22
		120	102.23 ± 1.81	0.25 ± 0.008	-22.88 ± 1.19
2	CLPF-SLN	0	112.9 1 ± 1.02	0.23 ± 0.010	-19.03 ± 0.26
		30	109.96 ± 3.17	0.21 ± 0.017	-20.16 ± 0.44
		60	114.30 ± 0.00	0.24 ± 0.005	-18.99 ± 0.15
		90	110.13 ± 0.30	0.22 ± 0.004	-19.14 ± 0.41
		120	116.06 ± 0.37	0.21 ± 0.003	-18.21 ± 1.22

Note: Values are expressed as mean ± standard deviation (n = 3).

5.3.9. Stability analysis of unloaded and PZQ-loaded CLF-SLN through Turbiscan technology as a function of time

The long-term stability of unloaded and PZQ-loaded CLF-SLN was investigated using a Turbiscan Lab Expert. The samples were scanned for 1h at 6 mins intervals for the dynamics of particle migration. As shown in the Figure 5.10, the ΔT and ΔBS profiles of unloaded and PZQ-loaded CLF-SLN showed that there were no significant modifications in the ΔT and ΔBS signals for both samples during the first day and the last day throughout the length of the stability analysis, indicating a good stability profile. The backscattering signals noticed at the upper portions of the samples in Figure 5.10 a-d was ignored since it also occurred at the same portions of the transmission signals, which suggests the impacts of secondary reflections on the glass.

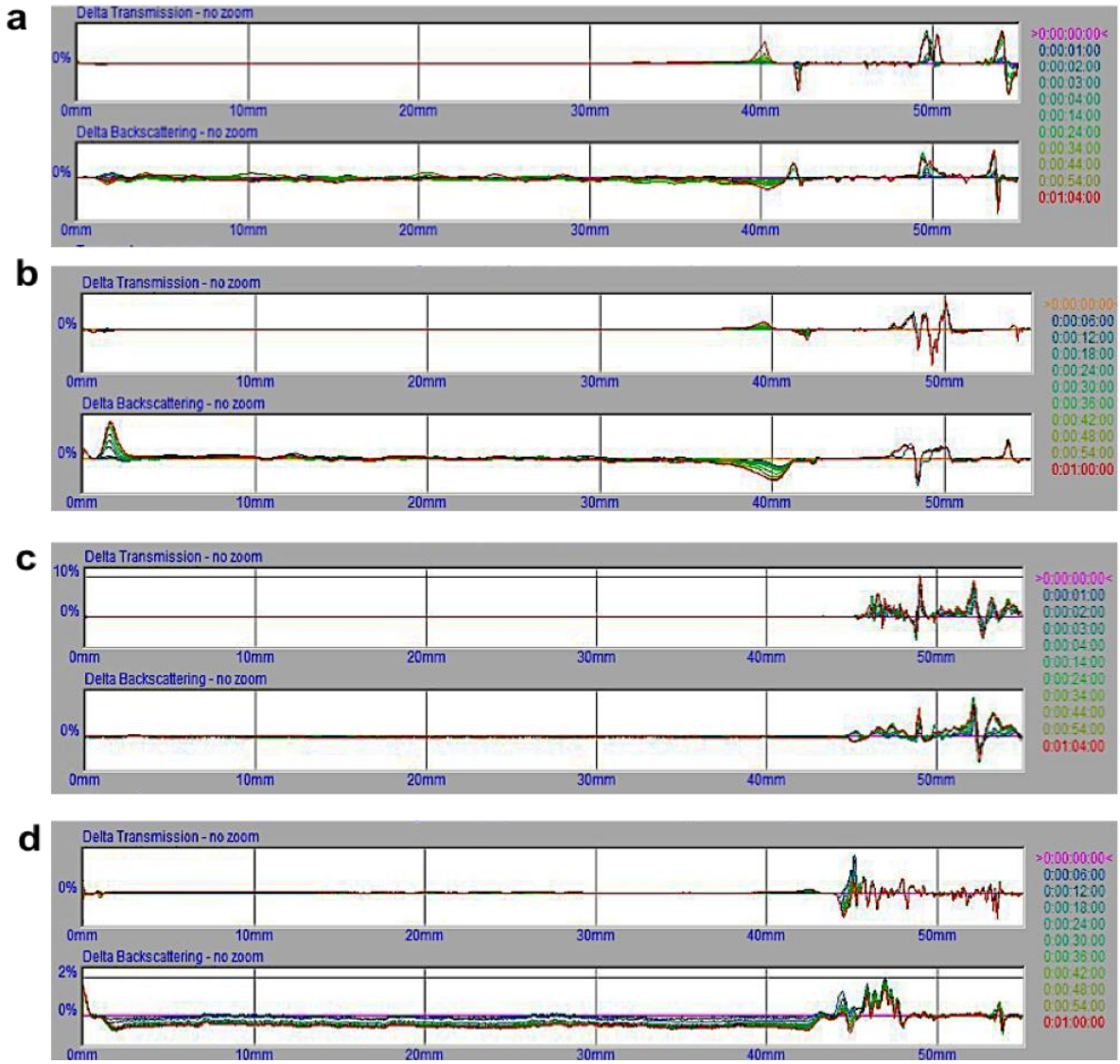

Figure 5.10: Representation of the destabilization kinetics of a) day 1 of CLF-SLN, b) day 120 of CLF-SLN, c) day 1 of CLPF-SLN and d) day 120 of CLPF-SLN suspension, indicating ΔBS and T measured at 25 ± 0.5 ^{O}C for 60 minutes duration.

5.3.10. Surface morphology characterization of the SLNs after 120 days

The morphological surface of the formulated SLNs was evaluated by SEM and TEM, and the SEM images showed the presence of discrete entities, smooth, slightly spherical and cubes-like morphological surface of the SLNs (Figure 5.11a-b). In Figure 5.11b, PZQ-loaded SLNs SEM images revealed the presence dark portion of the images of the matrix structure, which is an indication that the drug (PZQ) molecules are well and dispersed within the matrices of the lipid leading to the formulation of SLNs. A Transmission Electron Microscope (TEM) was also used to characterize the physical stability of the SLNs particle after 120 days. The TEM images in Figure 5.12 showed that the particles are spherical in morphology and shape.

Importantly, the morphology profile image for CLPF showed in Figure 5.12a revealed that the drug; PZQ molecules are still well completely dispersed within the lipid matrix of the nanoparticles, which could be presented as the chunk dark portion within the image of the matrix structure.

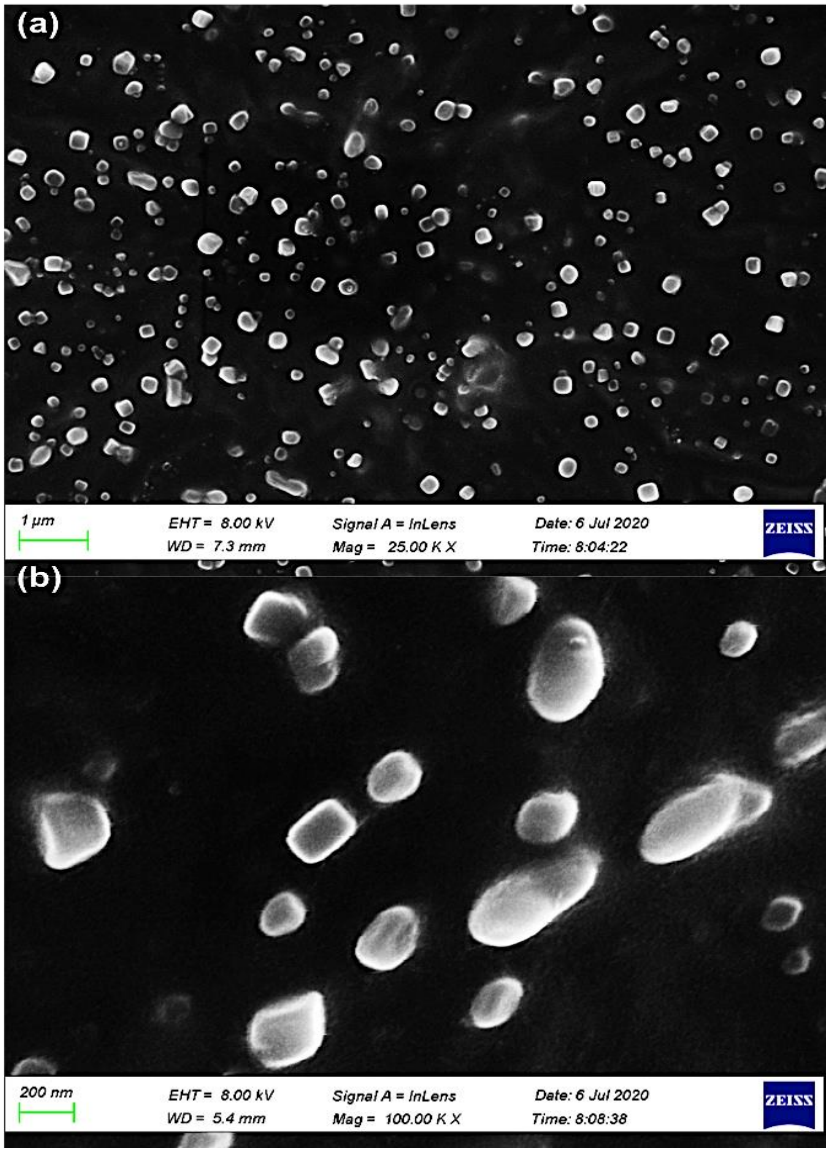

Figure 5.11: SEM images of the (a) SLNs (b) suspended drug molecules in the lipid matrices of the SLNs.

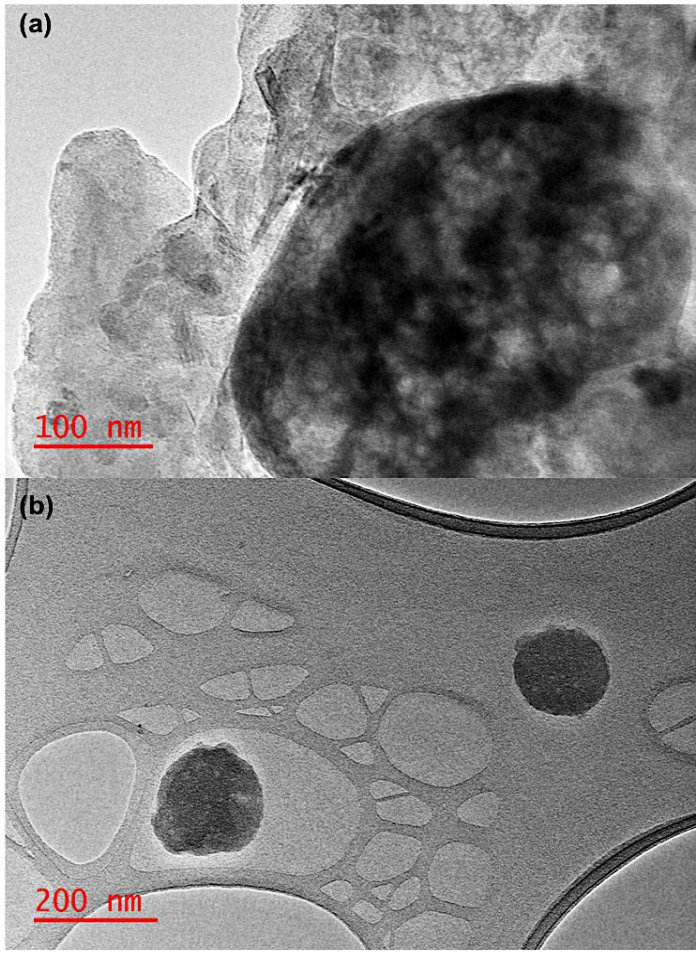

Figure 5.12: Transmission Electron Microscope (TEM) images of (a) SLNs at 100 nm (b) at 200 nm.

5.3.11. Analysis of in vitro cytotoxicity of SLNs

The 3- [4, 5-dimethylthiazol-2yl]-2, 5-diphenyl tetrazolium bromide (MTT) examination was carried out to investigate the cytotoxicity of SLNs and PZQ on RAW 264.7 murine macrophage cells. This assessment was carried out by testing all the formulated SLNs and PZQ on the macrophage cell line for 72 h within 30 to 120 μg/ml concentration. The results showed that the formulated SLNs showed acceptable levels of cell viability, with no substantial cytotoxic effects on the RAW 264.7 cells. The highest concentration of CLF (120 μg/ml), which is way beyond what was observed in drug release data, had about 66% viability: the lowest percentage viability (Figure 5.13).

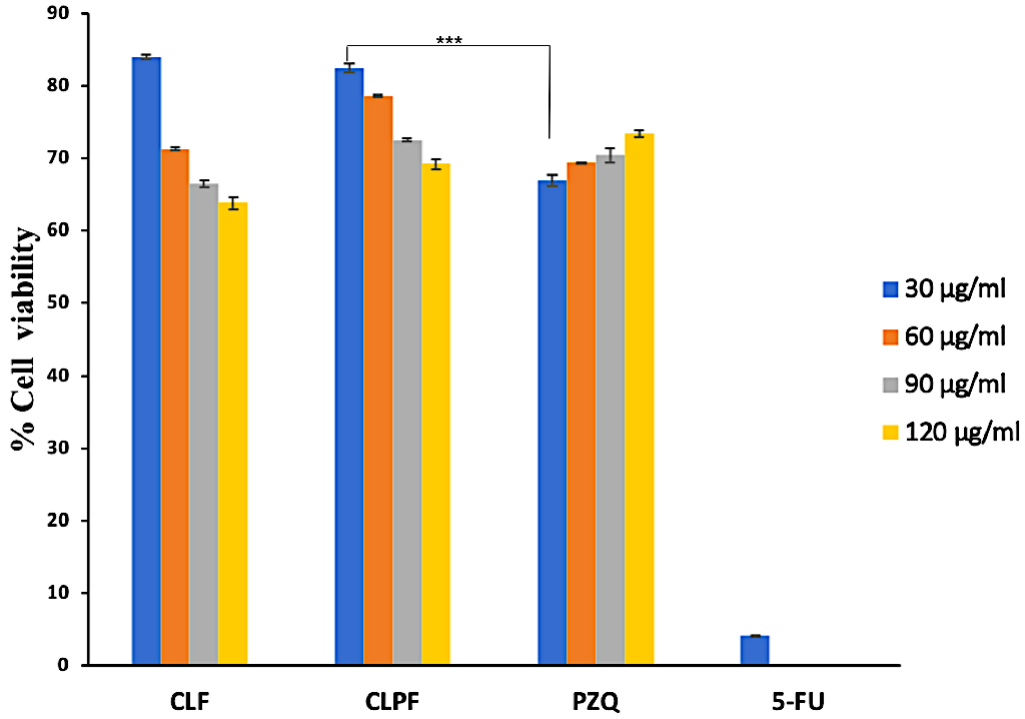

Figure 5.13: MTT assay measurement of the viability of RAW 264.7 murine macrophage cells after 72-hour treatment with free PZQ, the formulated unloaded and PZQ-loaded SLNs at different concentrations **(**Data represent n = 3, mean ± SD; ***indicates p-value ≤0.0001 when compared to the same concentration of PZQ. CLF: Compritol-Lecithin-F127; CLPF: Compritol-Lecithin-PZQ-F127; PZQ: Praziquantel; 5-FU: 5-fluorouracil (10 µg/ml)).

5.3.12. Analysis of RAW 264.7 murine macrophage cells morphology

Figure 5.14a and 5.14b presented the cell morphology of the RAW 264.7 macrophage cells after being treated with 90 µg/ml of the prepared SLNs, PZQ and 10 µg/ml of 5-fluorouracil (5-FU) as the positive control. The cells were visualized under an inverted microscope (Olympus CKX53) for phase contrast images and compound fluorescent microscope (Olympus IX51) for fluorescence images. It was revealed by the phase contrast images that all the treated cells showed normal RAW 264.7 cell morphology with round and smooth shape, whereas the cells treated with 5-FU as the negative control form pseudopodia, which resulted in the cell death. It was further shown by fluorescence microscopy analysis of the DAPI and phalloidin images that the prepared SLNs pose no cytotoxicity effect on the cellular morphology of RAW 264.7, because DAPI revealed the nucleus of the cells, while phalloidin showed the cytoplasm membrane of the cells. Additionally, the overlaid of DAPI and phalloidin images showed that the nuclei are well positioned within the cytoplasm of the untreated, PZQ and SLNs cells, while ruptures in the cytoplasm membrane and the exposure of the nucleus was observed in treated with 10 µg/ml of 5-FU as negative control.

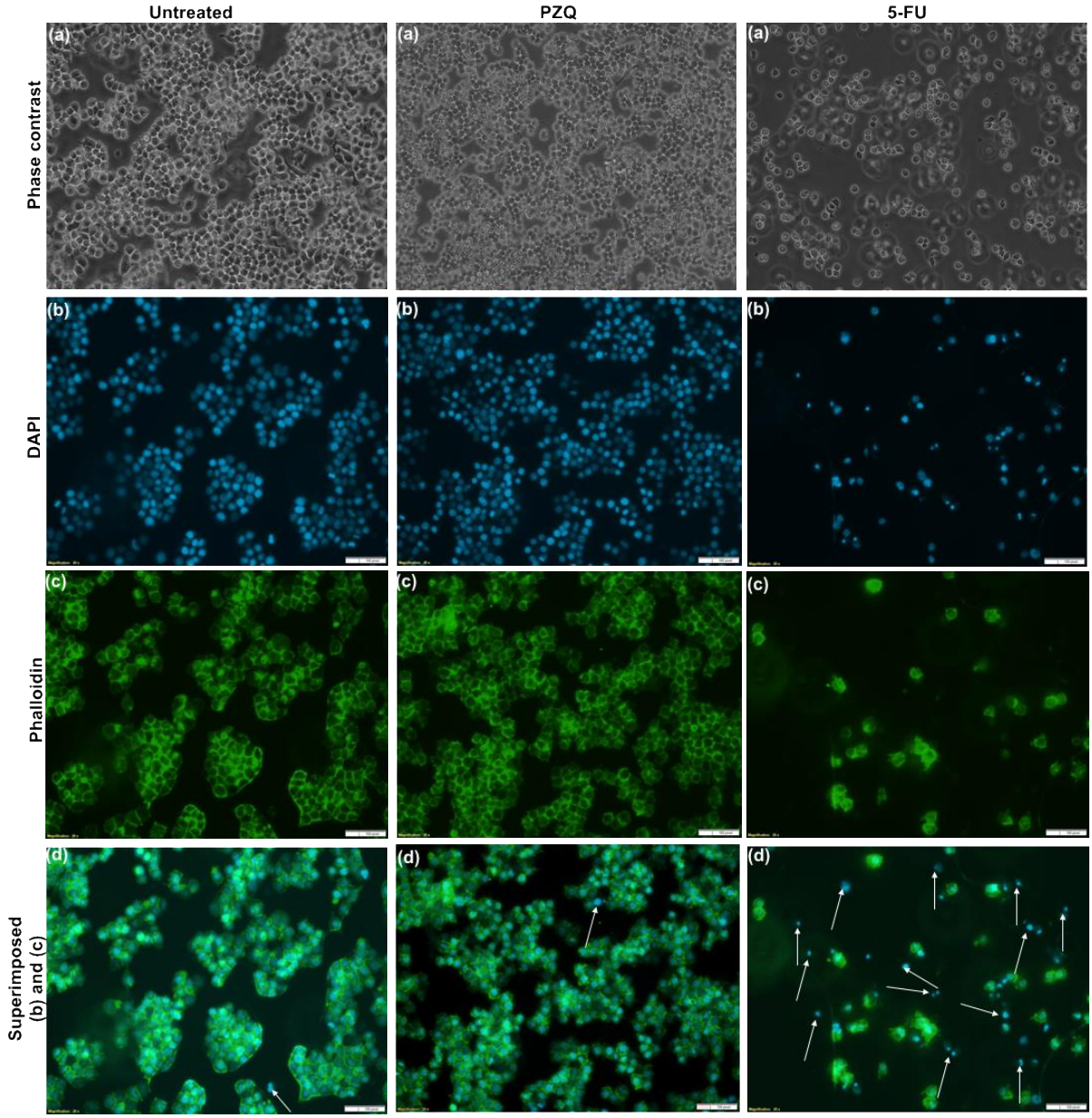

Figure 5.14a: Fluorescent microscopy images of RAW 264.7 macrophage cell morphology analysis (a) Phase constrat, (b) DAPI, (c) Phalloidin and (d) Superimposed of (b) and (c) for untreated (control), cell treated with 90 μg/ml of PZQ and 5-FU (10 μg/ml) (negative control). Scale bar: 100μm; (x20 magnification).

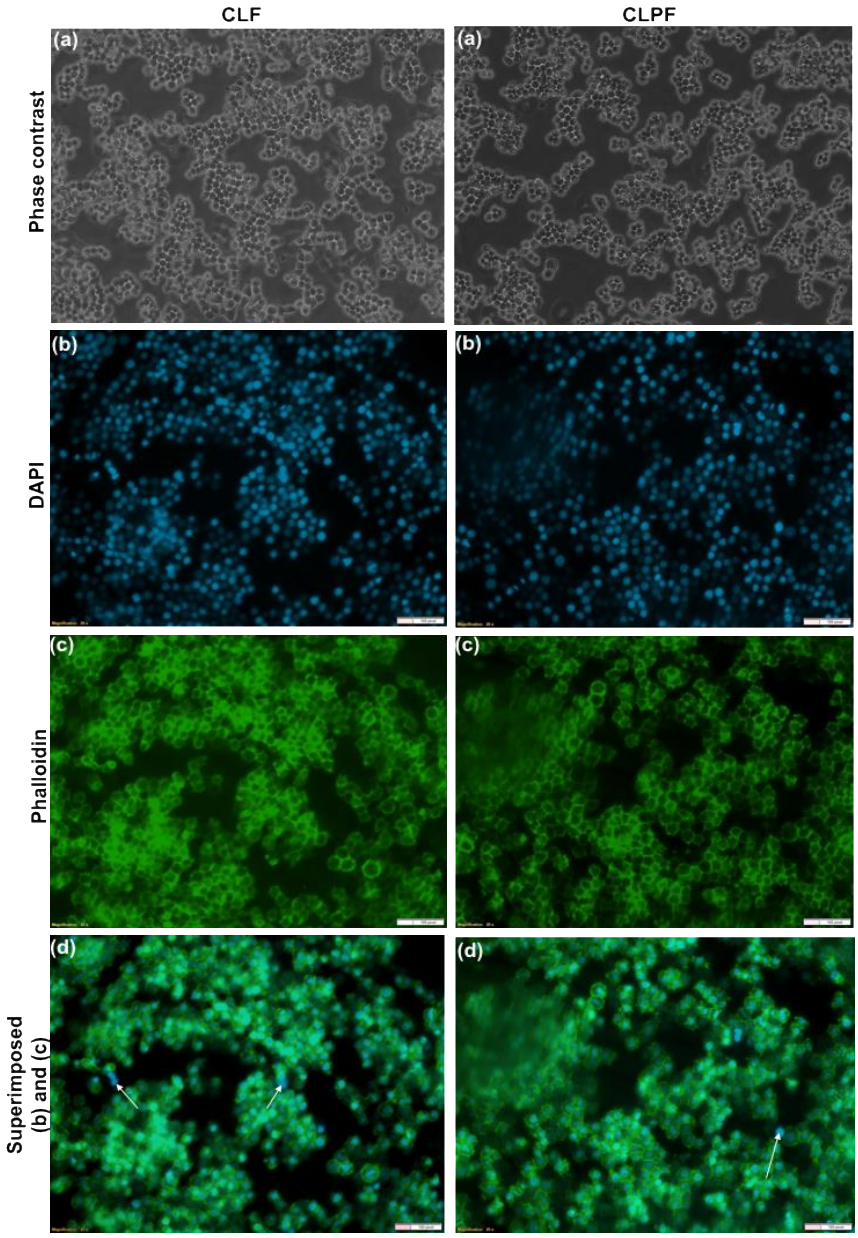

Figure 5.14b: Fluorescent microscopy images of RAW 264.7 macrophage cell morphology analysis (a) Phase constrat, (b) DAPI, (c) Phalloidin and (d) Superimposed of (b) and (c) with 90 μg/ml of CLF and CLPF. Scale bar: 100μm; (x20 magnification).

5.3.13. In vivo toxicity evaluation

The extent of liver and kidney damage of PZQ-loaded CLF-SLN and native PZQ was evaluated through the analysis of the different biochemical markers (Dora et al., 2017) (ALT, AST, bilirubin and creatinine) levels in the blood plasma in the rat model. As showed in Figure 5.15, the ALT level in the control group, PZQ group and CLPF group were observed to be 8.37, 10.05 and 8.7 milliunits/mL, respectively; 13.51, 15,70 and 13.93 7 milliunits/mL were observed for the AST level in the control, PZQ and CLPF groups, respectively. More so, both the bilirubin and creatinine levels were observed to be 8.09, 10.28 and 8.37 mg/dL, and 11.47,

15.32 and 11.09 ng/μL for the control groups, PZQ groups and CLPF groups, respectively. From the results, a significant increase ($p<0.0001$) in the levels of biochemical markers were observed in the plasma of the groups of rats that received PZQ as compared to the control. In addition, the plasma of the CLPF receiving group showed a significant decrease ($p<0.0001$) in the levels of all the biochemical markers when compared to the PZQ group. This showed that the PZQ-loaded CLF-SLN do not cause any oxidative stress damage to the rats (Ibrahim et al., 2008; Dora et al., 2017).

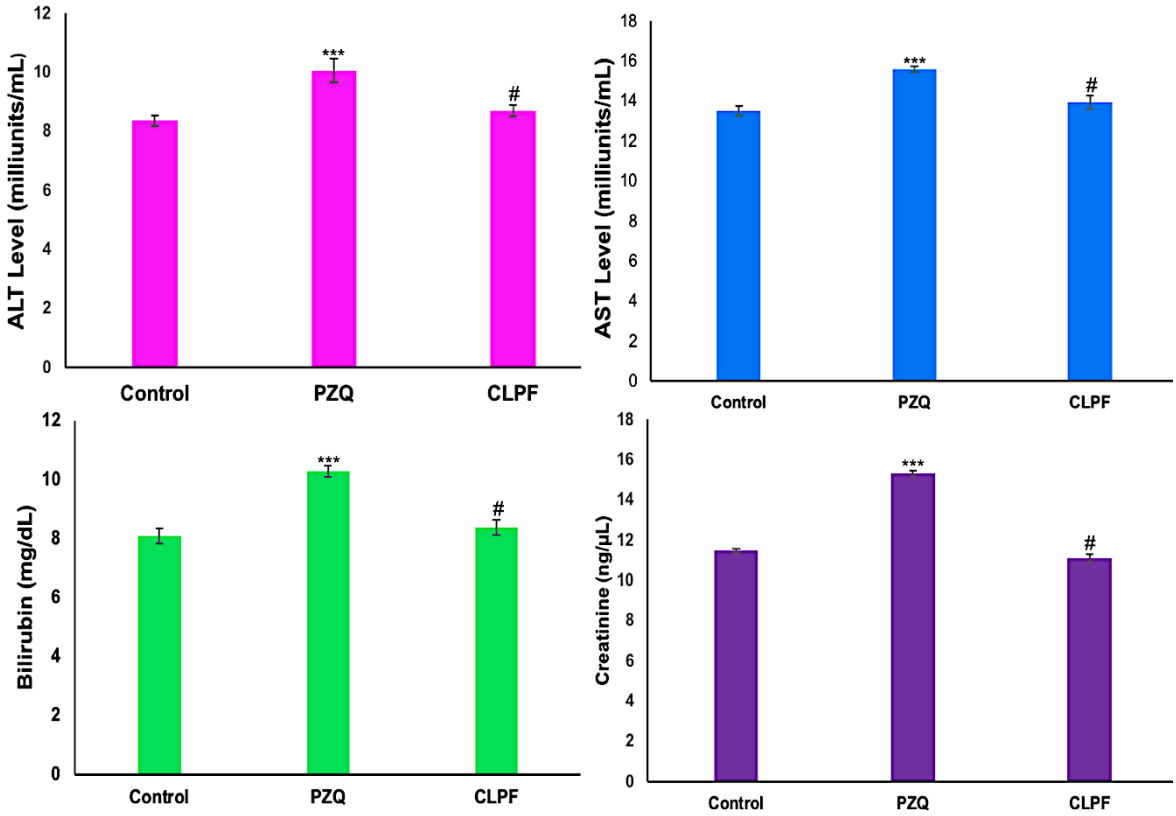

Figure 5.15: Biochemical markers (a) ALT (b) AST (c) Bilirubin and (d) creatinine levels in plasma. Values are expressed as mean ± standard deviation of five determinations (Data represent n = 3, mean ± SD). *** indicates $p<0.0001$ when compared to control group, and # indicates $p<0.0001$ when compared to PZQ group.

5.3.14. Histopathological analysis

As shown in Figure 5.16, the liver of an untreated control group showed moderate granularity in the hepatocyte cytoplasm, and the PZQ group depicts marked granularity in the hepatocyte cytoplasm. Hepatocytes show marked granularity of the cytoplasm in the CLPF group, with a few periportal hepatocytes in a few areas which appear mildly vacuolated with minimally swollen and a single blood vessel contains fibrin in the lumen. In the histopathological analysis of the kidneys, the untreated control group showed a normal histological appearance of the

kidneys, while, a few deep cortical tubular epithelial cells with a slightly granular cytoplasm were observed in the PZQ group, meanwhile, the kidneys in the CLPF group appear histologically normal.

The lung histological examination of an untreated control group depicts multifocal extensive alveolar atelectasis, and alveolar capillaries show multifocal moderate leukostasis of mononuclear cells and presence of few multifocal foamy macrophages in the alveolar walls. Also, few bronchial associated lymphoid tissue follicles (BALT) are visible and appear expanded. Moderate to severe diffuse alveolar atelectasis and alveolar capillaries were observed in the PZQ group, and show mild mononuclear leukostasis, with some active presence of BALT follicles. The CLPF group followed a similar pattern with a moderate diffuse alveolar atelectasis, and appearance of mildly active BALT. These lung histopathological results correlated with the experimental design and procedure because blood was collected from the heart, which may cause pulmonary atelectasis and oedema could also develop terminally following euthanasia. Normal active lymphoid tissue was shown in the spleen of all the groups, and the abnormalities are not clearly visible.

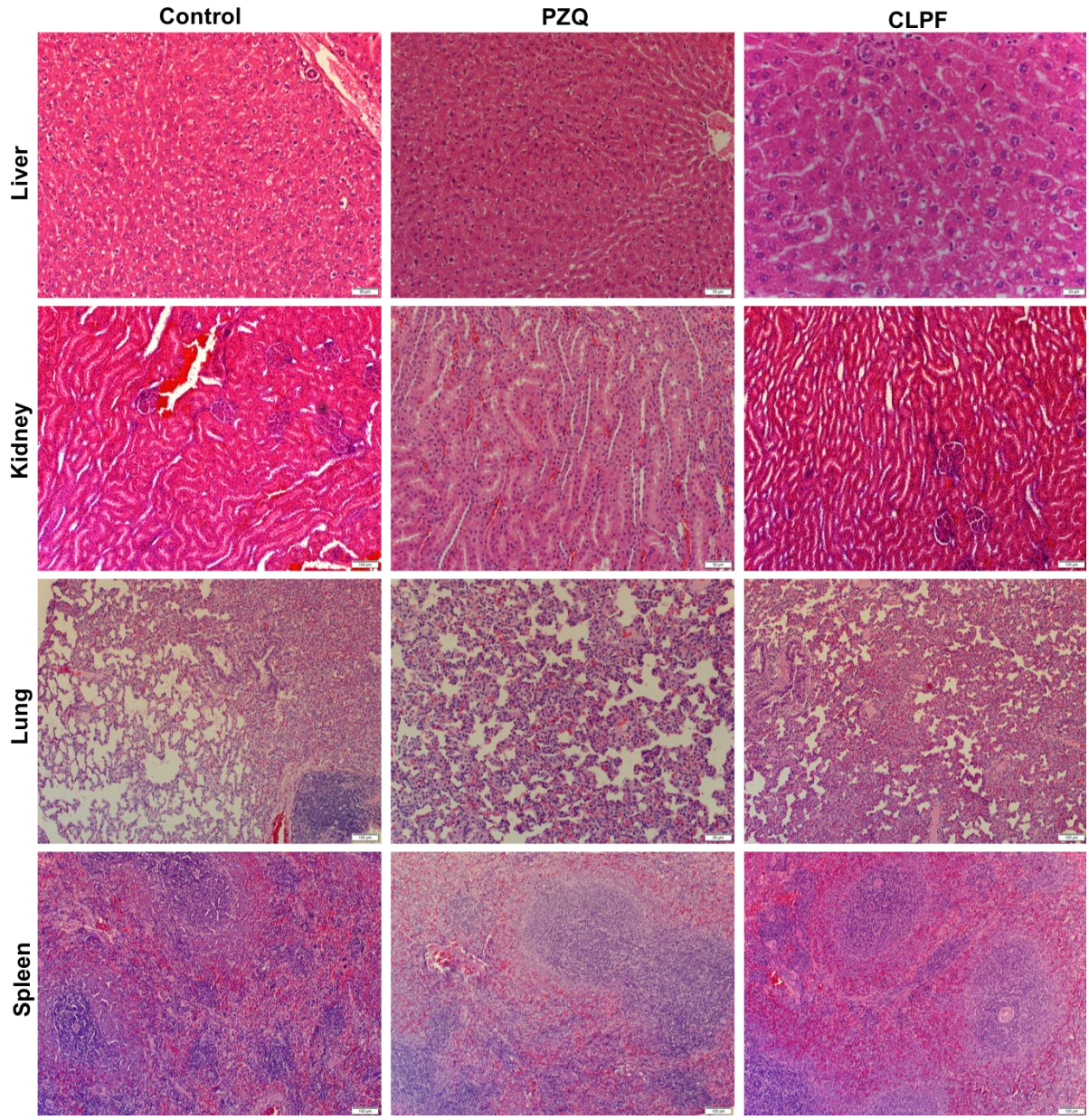

Figure 5.16: Histopathological images of (A) liver, (B) kidney, (C) Lung and (C) spleen after treating uninfected rats with 250 mg/kg of PZQ and CLPF (x20 magnification). CLPF: PZQ-loaded compritol-lecithin- solid lipid nanoparticles with PF127; PZQ: Praziquantel.

5.3.15. Evaluation of parasitological cure rate

Tables 5.4, 5.5 and Figure 5.17 showed the data for worm recovery, oogram pattern and egg count in tissues for two weeks post-infection treatment. As shown in Table 5.4, a statistically significant difference in the percentage reduction of the total worm burden was observed in the liver and portomesenteric following the oral administration of 250 mg/kg single dose of CLPF compared to the PZQ-treated group. The oral administration of CLPF (250 mg/kg single dose) shown a statistically significant reduction (enter p-value) in the percentage of mature and immature ova, as well as a percentage increase in the dead ova (Figure 5.17) when

compared to the infected untreated control and PZQ groups. The percentage reduction in the ova count in the liver and intestine depicted in Table 5.5 showed a statistically significant difference ($p<0.0001$) in the CLPF treated group when compared to the PZQ and the infected untreated control groups; two weeks post-infection.

Table 5.4: Effect of PZQ and CLPF (single dose 250 mg/kg two weeks post-infection) on worm load and sex in *S. mansoni*-infected mice sacrificed six weeks post-infection

	Mean worm burden ±SD (liver and porto-mesenteric)				% reduction in total worm burden
	Male	Female	Couples	Total	
Control	2.33±0.81	0.33±0.52	6.17±0.75	15.00±0.89	
PZQ	1.33±1.21	0	4.33±0.82	10.00±1.41	33.30
CLPF	1.50±0.55	0	3.67±1.21	8.83±2.64	41.13

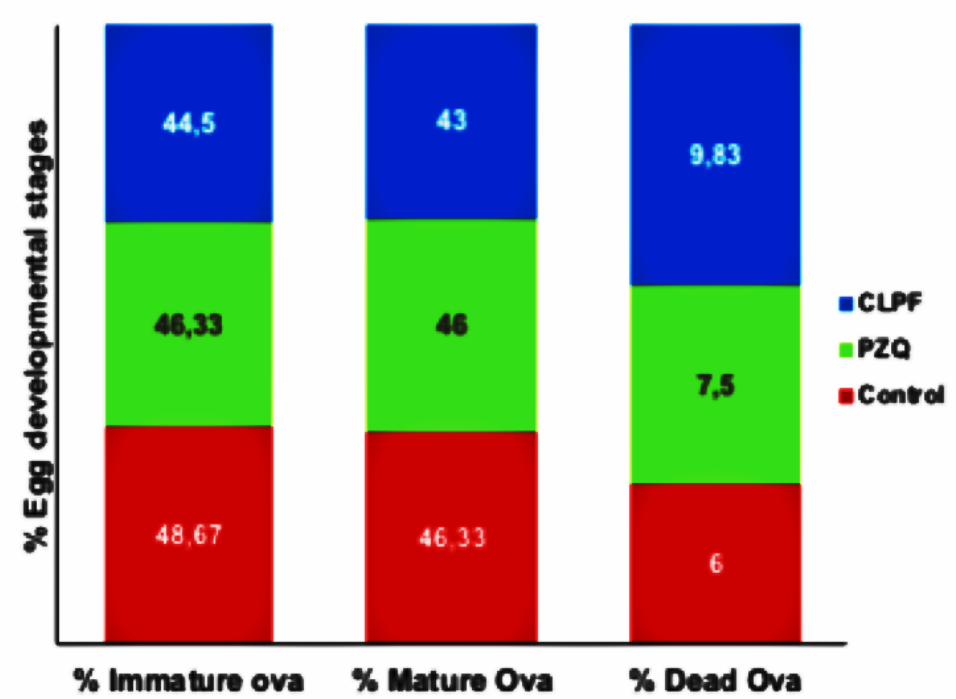

Figure 5.17: Effect of PZQ and CLPF (single dose 250 mg/kg two weeks post-infection) on % egg developmental stages in S. mansoni-infected mice sacrificed six weeks post-infection

Table 5.5: Effect of PZQ and CLPF (single dose 250 mg/kg two weeks post-infection) on number of ova/gm tissues in S. mansoni-infected mice sacrificed six weeks post-infection

Mice group	Liver	% reduction in ova count in liver	Intestine	% reduction in ova count in intestine
Control	28202±4372		31902±4342	
PZQ	20303±2175	28.00	22702±5347	28.84
CLPF	16548±6919	41.32	21120±6644	33.79

Data for worm recovery, egg count in tissues and oogram pattern for four weeks post-infection treatment are shown in Table 5.6, 5.7 and Figure 5.18. As demonstrated in table 5.6, the CLPF group had a statistically significant reduction in the percentage of total worm load in the liver and portomesenteric compared to the PZQ-treated group. When compared with the infected untreated control and PZQ groups, a single dosage of CLPF of 250 mg/kg resulted in a statistically significant increase ($p<0.0001$) in the percentage of dead ova and a decrease in mature and immature ova in *S. mansoni*-infected mice (Figure 5.18). Table 5.7 shows that when a single dosage of 250 mg/kg CLPF was given two weeks after infection, the percentage reduction in ova count in the liver and intestine was statistically significant ($p<0.0001$) when compared to the PZQ and the infected untreated control groups.

Table 5.6: Effect of PZQ and CLPF (single dose 250 mg/kg four weeks post-infection) on worm load and sex in *S. mansoni*-infected mice sacrificed six weeks post-infection

	Mean worm burden ±SD (liver and porto-mesenteric)				% reduction in total worm burden
	Male	Female	Couples	Total	
Control	2.33±0.81	0.33±0.52	6.17±0.75	15.00±0.89	
PZQ	1.50±1.40	0	2.00±0.89	5.50±2.60	63.30
CLPF	1.00±0.63	0	1.33±1.37	4.33±1.86	71.13

Figure 5.18: Effect of PZQ and CLPF (single dose 250 mg/kg four weeks post-infection) on % Egg developmental stages in S. mansoni-infected mice sacrificed six weeks post-infection

Table 5.7: Effect of PZQ and CLPF (single dose 250 mg/kg four weeks post-infection) on number of ova/gm tissues in *S. mansoni*-infected mice sacrificed six weeks post-infection

Mice group	Liver	% reduction in ova count in liver	Intestine	% reduction in ova count in Intestine
Control	28202±4372		31902±4342	
PZQ	13626±2936	51.68	14658±3699	54.05
CLPF	11384±4135	59.60	10310±1080	67.68

5.4. Discussion

Over the years, PZQ has been the main drug utilized for schistosomiasis treatment and the drug has been effective and well-tolerated by the affected populations, because of its ability to reduce the parasitic load of all species causing schistosomiasis. Also, PZQ reduces several symptoms of Schistosoma infection, and it is effective against adult schistosome worms (Adekiya *et al*., 2021; Vale *et al*., 2017).

PZQ has shortcomings, which include the inability to kill the juvenile schistosomes; a rapid metabolism that lowers the bioavailability of the drug molecules in the systemic circulation. More so, the development and increase in drug resistance, particularly since decreased susceptibility have frequently occurred both in the laboratory and in the field (Vale *et al*., 2017). Thus, there is an urgent need to improve some properties of PZQ such as, increasing its bioavailability and improving its release rate using drug delivery systems approach. These improvements could fight parasite resistance, increase the uptake of the drug into the bloodstream following ingestion as well as circumvent vast first-pass metabolism by extending the release rate of the drug over time.

SLNs synthesized from one and/or two or more blends of solid lipids have been approved for drug carriers for over two decades (Mishra *et al*., 2018; Khan *et al.*, 2015). This type of drug nanocarrier is more advantageous than others, such as polymeric nanoparticles, liposomes and emulsions, because the matrices of the solid lipid can protect the chemical instability of drugs. SLNs offer controlled release of drug patterns when likened to nanoemulsions, they also present nanosuspension that are more stable than liposomes. Additionally, the wide application of SLNs in oral, dermal, intravenous and pulmonary (Khan *et al*., 2015; Bayón-Cordero *et al*., 2019) when compared to polymeric nanoparticles is because they are made of excipients that are generally recognized as safe and physiologically well-tolerated with reduced cytotoxicity.

Thus, the formulation of SLNs using compritol and lecithin was demonstrated in this study through solvent injection-co-homogenization techniques for the delivery of PZQ to enhance the therapeutic effectiveness of PZQ in the treatment of schistosomiasis. The temporal stability was also studied. In this study, the particle size for the formulations are uniform and falls within the size range of a suitable nano-delivery system (Kushwaha *et al*., 2013; Mishra *et al*., 2018; Khan *et al*., 2015). Since the particles for a nanocarrier must be uniform and for many colloidal drug delivery systems designed from solid lipids, the size ranges between 50 and 1000 nm (Murthy and Shivakumar, 2010). The polydispersity index of the formulations showed the phospholipid vesicles homogenous population of the SLN. In the use of lipid-based carriers in the applications of drug delivery, a PdI equal to 0.3 or less is believed to be satisfactory and depicts phospholipid vesicles with a homogenous population (Danaei *et al*., 2018). The zeta potential data showed that the formulations are stable regarding aggregation, flocculation, sedimentation, coagulation and creaming via a strong electrostatic repulsion that keeps the particles charged from one another. The **%**EE of PZQ was observed to be 71.63 % in the drug-loaded compritol-lecithin-SLNs prepared using PF127 as a surfactant and the %LC was 11.46 %. This result corroborated all other physicochemical characterization results which showed that PZQ is not found on the surface of the SLNs and that PZQ molecules were well dispersed and encapsulated in the stable matrices of the lipids.

In this study, the slower or sustained PZQ release from SLNs could be attributed to the sustained-release property of SLNs, and this could further buttress other physicochemical results that PZQ is well dispersed and encapsulated within the lipid matrix. Thus, this slower and sustained release could be of importance in enhancing the therapeutic effect of the drug. Since it has been stated that the rapid metabolism and quick conversion of the drug to its inactive form could be the major reason while the drug fails to kill the juvenile worms (Aruleba *et al.*, 2019; Malhotra and Raut, 2015). This sustained release can also provide extended-release kinetics, which can lead to the reduction in the frequent administration of the drug, which will, in turn, enhance patient compliance most especially when treating infectious disease conditions (Sumaila *et al.*, 2019), in this case, schistosomiasis.

Drug stability has an impact on the efficacy and safety of the drug substance; degradation impurities could cause efficacy loss and potentially harmful consequences. As a result, attaining the physical and chemical stability of drugs is critical to ensuring their safety and quality (Garnero *et al.,* 2018). DLS and ELS measurements did not show any significant influence on the average particle size, PdI and zeta potential of both the unloaded and PZQ-loaded CLF-SLN from day zero to 120 days of the stability analysis at room temperature, which was also revealed in the surface morphology and *in vitro* drug release analysis. This

indicates that the addition of PF127 as the surfactants provided long-term stability for compritol ATO 888-lecithin solid lipid nanoparticles nanosuspension over 120 days at room temperature, and this corroborated with other studies that PF127 promote and enhance the stability of nanoparticles (Chuacharoen and Sabliov, 2016; Shaarani *et al.,* 2017; Sokolsky-Papkov and Kabanov, 2019). Furthermore, turbiscan data corroborated dynamic light scattering analysis, which showed that no significance in the variation of particle size of the sample solutions.

Interestingly, it can be further averred that the decrease in percentage viability of cells treated with the formulated SLNs is dose-dependent. Although RAW 264.7 cells showed acceptable cell viability levels following PZQ treatment, there was significantly lower cell viability (*P*-value <0.0001) following treatment with 30 μg/ml CLPF when compared with that of 30 μg/ml PZQ. In other words, even though a decrease in dose-dependent on cell viability was seen in SLNs, the opposite effect was observed in PZQ: an increase in cell viability with increasing concentration. Hence, the data suggest that macrophages may proliferate with increasing concentration of PZQ; an observation that was not made in formulated SLNs. In a similar vein, one research study indicated that concentrations less than 80 μM of the R enantiomer of PZQ could promote the proliferation of RAW 267.4 macrophages (Sun *et al.*, 2016). Thus, this dose-dependent increase in macrophage viability following PZQ treatment calls for further investigation, given that the mechanisms by which PZQ exhibits its antiparasitic effects and drug resistance are not fully understood.

The findings from *in vivo* toxicity examination corroborated the results obtained in *in vitro* cell viability study, which showed by histopathological and biochemical marker analysis that there are no toxicity or lesser oxidative stress, with the formulated CLPF have the ability to confer hepatoprotective effects on the animals. The histopathological and biochemical marker analysis data further suggested CLPF-SLNs possess the ability to circumvent traces of toxicity associated with bioactive molecules, because studies have reported the excipients used not to be toxic (Lippens *et al.*, 2013; Thornton *et al.*, 1988; Aburahma and Badr-Eldin, 2014). In a parasitological study, the cure rate of CLPF and PZQ was determined, and it was revealed that treatment with 250 mg/kg CLPF had stronger action on total worm load and ova count in both the intestine and the liver. In addition, when compared to the same dose of PZQ, the CLPF nanosystem had a greater effect on both mature and immature ova, as well as caused ova death during the egg developmental stages in both young and adult worms represented by two and four weeks post-infected mice, respectively. The higher rate and increased absorption of the CLPF nanosystem by the worms and eggs in the liver, porto-mesenteric, and intestine may be responsible for the huge impacts of the CLPF nanosystem on

schistosome eggs and worms. Since the study has shown in the indirect membrane immunofluorescence test (IF) that the incubation of *S. mansoni* lung-stage larvae in 90% corn oil for 6 hours exposed there, otherwise veiled apical membrane antigen interaction with anti-schistosome antibodies (Tallima *et al.,* 2005).

5.5. Conclusion

The development of new anti-schistosomal agents requires a lot of money and time. Nanoparticulate-based drug delivery systems can be promising to solve the problem of currently used antischistosomal drugs (PZQ) having poor solubility, chemical instability, and inadequate bioavailability profile and rapid metabolism. In this study, PZQ-loaded compritol lecithin SLNs stabilized with PF127 was successfully prepared using solvent injection-co-homogenization techniques. From the *in vitro* drug release behaviour, it can be deduced that the solvent injection-co-homogenization methods of preparing compritol and lecithin SLNs are suitable for drug delivery application with PF127 as a stabilizer, due to slow or sustained release of PZQ from SLNs. Furthermore, the addition of PF127 as the surfactants provided long-term stability of compritol ATO 888-lecithin solid lipid nanoparticles nanosuspension over 120 days at room temperature. RAW 264.7 macrophages showed acceptable, dose-dependent levels of viability following treatment with SLNs in an *in vitro* toxicity study. The findings from *in vivo* toxicity examination corroborated the results obtained in *in vitro* cell culture study, which showed that there are no toxicity or lesser oxidative stress, caused by the formulated CLPF-SLNs. The parasitological data showed that a single (250 mg/kg) oral dose of CLPF-SLNs significantly improved the antischistosomal activity of PZQ in *S. mansoni*-infected mice both two and four weeks post-infection. The fabricated CLPF-SLNs demonstrated significant efficiency toward the delivery of PZQ, hence, promising in drug delivery application toward the treatment of Schistosomiasis.

5.6. References

1. Aburahma, M.H. and Badr-Eldin, S.M., 2014. Compritol 888 ATO: a multifunctional lipid excipient in drug delivery systems and nanopharmaceuticals. *Expert opinion on drug delivery*, *11*(12), pp.1865-1883.
2. Adekiya, T.A., Kondiah, P.P., Choonara, Y.E., Kumar, P. and Pillay, V., 2020. A review of nanotechnology for targeted anti-schistosomal therapy. *Frontiers in bioengineering and biotechnology*, *8*, p.32.
3. Adekiya, T.A., Kumar, P., Kondiah, P.P., Pillay, V. and Choonara, Y.E., 2021. Synthesis and therapeutic delivery approaches for praziquantel: a patent review (2010-present). *Expert Opinion on Therapeutic Patents*, pp.1-15

4. Amara, R.O., Ramadan, A.A., El-Moslemany, R.M., Eissa, M.M., El-Azzouni, M.Z. and El-Khordagui, L.K., 2018. Praziquantel–lipid nanocapsules: an oral nanotherapeutic with potential Schistosoma mansoni tegumental targeting. *International journal of nanomedicine*, *13*, p.4493.
5. Aruleba, R.T., Adekiya, T.A., Oyinloye, B.E., Masamba, P., Mbatha, L.S., Pretorius, A. and Kappo, A.P., 2019. PZQ therapy: how close are we in the development of effective alternative anti-schistosomal drugs?. *Infectious Disorders-Drug Targets (Formerly Current Drug Targets-Infectious Disorders)*, *19*(4), pp.337-349.
6. Ashok, A., Kumar, A. and Tarlochan, F., 2020. Colloidal metal oxide nanocrystals in catalysis. In *Colloidal Metal Oxide Nanoparticles* (pp. 247-288). Elsevier.
7. Bayón-Cordero, L., Alkorta, I. and Arana, L., 2019. Application of solid lipid nanoparticles to improve the efficiency of anticancer drugs. *Nanomaterials*, *9*(3), p.474.
8. Campos, F.D.S., Cassimiro, D.L., Crespi, M.S., Almeida, A.E. and Gremião, M.P.D., 2013. Preparation and characterisation of Dextran-70 hydrogel for controlled release of praziquantel. *Brazilian Journal of Pharmaceutical Sciences*, *49*(1), pp.75-83.
9. Ceccaldi, C., Strandman, S., Hui, E., Montagnon, E., Schmitt, C., Hadj Henni, A. and Lerouge, S., 2017. Validation and application of a nondestructive and contactless method for rheological evaluation of biomaterials. *Journal of Biomedical Materials Research Part B: Applied Biomaterials*, *105*(8), pp.2565-2573.
10. Chhabra, R.P. and Gurappa, B. eds., 2019. *Coulson and Richardson's Chemical Engineering: Volume 2A: Particulate Systems and Particle Technology*. Butterworth-Heinemann.
11. Christensen N, Gotsche G, Frandsen F. Parasitological technique for use in laboratory maintenance of schistosomes and for use in studies on the epidemiology of human and bovine schistosomiasis. Teaching note Danish Bilharziasis Laboratory. 1984.
12. Chuacharoen, T. and Sabliov, C.M., 2016. Stability and controlled release of lutein loaded in zein nanoparticles with and without lecithin and pluronic F127 surfactants. *Colloids and surfaces A: Physicochemical and engineering aspects*, *503*, pp.11-18.
13. Danaei, M., Dehghankhold, M., Ataei, S., Hasanzadeh Davarani, F., Javanmard, R., Dokhani, A., Khorasani, S. and Mozafari, M.R., 2018. Impact of particle size and polydispersity index on the clinical applications of lipidic nanocarrier systems. *Pharmaceutics*, *10*(2), p.57.
14. Dora, C.P., Kushwah, V., Katiyar, S.S., Kumar, P., Pillay, V., Suresh, S. and Jain, S., 2017. Improved metabolic stability and therapeutic efficacy of a novel molecular gemcitabine phospholipid complex. *International journal of pharmaceutics*, *530*(1-2), pp.113-127

15. El-Feky, G.S., Mohamed, W.S., Nasr, H.E., El-Lakkany, N.M., Seif el-Din, S.H. and Botros, S.S., 2015. Praziquantel in a clay nanoformulation shows more bioavailability and higher efficacy against murine Schistosoma mansoni infection. *Antimicrobial agents and chemotherapy*, *59*(6), pp.3501-3508.
16. Frezza, T.F., Gremião, M.P.D., Zanotti-Magalhães, E.M., Magalhães, L.A., de Souza, A.L.R. and Allegretti, S.M., 2013. Liposomal-praziquantel: efficacy against Schistosoma mansoni in a preclinical assay. *Acta tropica*, *128*(1), pp.70-75.
17. Garnero, C., Chattah, A.K., Aloisio, C., Fabietti, L. and Longhi, M., 2018. Improving the stability and the pharmaceutical properties of norfloxacin form C through binary complexes with β-cyclodextrin. *AAPS PharmSciTech*, *19*(5), pp.2255-2263.
18. Ibrahim, W.H., Habib, H.M., Jarrar, A.H. and Al Baz, S.A., 2008. Effect of Ramadan fasting on markers of oxidative stress and serum biochemical markers of cellular damage in healthy subjects. *Annals of Nutrition and Metabolism*, *53*(3-4), pp.175-181.
19. Khan, S., Baboota, S., Ali, J., Khan, S., Narang, R.S. and Narang, J.K., 2015. Nanostructured lipid carriers: an emerging platform for improving oral bioavailability of lipophilic drugs. *International journal of pharmaceutical investigation*, *5*(4), p.182.
20. Kloetzel, K.U.R.T., 1967. A suggestion for the prevention of severe clinical forms of schistosomiasis *mansoni*. *Bulletin of the World Health Organization*, *37*(4), p.686.
21. Kohn, A.B., Anderson, P.A., Roberts-Misterly, J.M. and Greenberg, R.M., 2001. Schistosome calcium channel β subunits unusual modulatory effects and potential role in the action of the antischistosomal drug praziquantel. *Journal of Biological Chemistry*, *276*(40), pp.36873-36876.
22. Kumar, R., Singh, A. and Garg, N., 2019. Acoustic cavitation-assisted formulation of solid lipid nanoparticles using different stabilizers. *Acs Omega*, *4*(8), pp.13360-13370.
23. Kumar, R.S. and Yagnesh, T.N.S., 2016. Pharmaceutical suspensions: patient compliance oral dosage forms. *World Journal of Pharmacy and Pharmaceutical Sciences*, *5*(12), pp.1471-1537.
24. Kushwaha, A.K., Vuddanda, P.R., Karunanidhi, P., Singh, S.K. and Singh, S., 2013. Development and evaluation of solid lipid nanoparticles of raloxifene hydrochloride for enhanced bioavailability. *BioMed research international*, *2013*.
25. Liang, Y.S., Bruce, J.I. and Boyd, D.A., 1987. Laboratory cultivation of schistosome vector snails and maintenance of schistosome life cycles. In *Proceeding of the 1st Sino-American symposium* (Vol. 1, pp. 34-48).
26. Lippens, E., Swennen, I., Gironès, J., Declercq, H., Vertenten, G., Vlaminck, L., Gasthuys, F., Schacht, E. and Cornelissen, R., 2013. Cell survival and proliferation after

encapsulation in a chemically modified Pluronic® F127 hydrogel. *Journal of biomaterials applications*, *27*(7), pp.828-839.

27. Liu, Y., Wang, X., Wang, J.K. and Ching, C.B., 2004. Structural characterization and enantioseparation of the chiral compound praziquantel. *Journal of pharmaceutical sciences*, *93*(12), pp.3039-3046.
28. Malhotra, G., Raut, P., Pharmaceutical compositions. WO2015071668A1; 2015
29. Mishra, V., Bansal, K.K., Verma, A., Yadav, N., Thakur, S., Sudhakar, K. and Rosenholm, J.M., 2018. Solid lipid nanoparticles: Emerging colloidal nano drug delivery systems. *Pharmaceutics*, *10*(4), p.191.
30. Mourão, S.C., Costa, P.I., Salgado, H.R. and Gremião, M.P.D., 2005. Improvement of antischistosomal activity of praziquantel by incorporation into phosphatidylcholine-containing liposomes. *International journal of pharmaceutics*, *295*(1-2), pp.157-162.
31. Murthy, S.N. and Shivakumar, H.N., 2010. Topical and transdermal drug delivery. In *Handbook of non-invasive drug delivery systems* (pp. 1-36). William Andrew Publishing.
32. Pellegrino, J., Oliveira, C.A., Faria, J. and Cunha, A.S., 1962. New approach to the screening of drugs in experimental schistosomiasis mansoni in mice. *American Journal of Tropical Medicine and Hygiene*, *11*(2), pp.201-215.
33. Shaarani, S., Hamid, S.S. and Kaus, N.H.M., 2017. The Influence of pluronic F68 and F127 nanocarrier on physicochemical properties, in vitro release, and antiproliferative activity of thymoquinone drug. *Pharmacognosy research*, *9*(1), p.12.
34. Sokolsky-Papkov, M. and Kabanov, A., 2019. Synthesis of well-defined gold nanoparticles using pluronic: the role of radicals and surfactants in nanoparticles formation. *Polymers*, *11*(10), p.1553.
35. Sumaila, M., Ramburrun, P., Kumar, P., Choonara, Y.E. and Pillay, V., 2019. Lipopolysaccharide polyelectrolyte complex for oral delivery of an anti-tubercular drug. *AAPS PharmSciTech*, *20*(3), pp.1-16.
36. Sun, Q., Mao, R., Wang, D., Hu, C., Zheng, Y. and Sun, D., 2016. The cytotoxicity study of praziquantel enantiomers. *Drug design, development and therapy*, *10*, p.2061.
37. Tallima, H., Salah, M. and El Ridi, R., 2005. In vitro and in vivo effects of unsaturated fatty acids on Schistosoma mansoni and S. haematobium lung-stage larvae. *Journal of Parasitology*, *91*(5), pp.1094-1102.
38. Thornton, C.G., MacLellan, K.M., Brink Jr, T.L., Wolfe, D.M., Llorin, O.J. and Passen, S., 1998. Processing respiratory specimens with C18-carboxypropylbetaine: development of a sediment resuspension buffer that contains lytic enzymes to reduce the contamination rate and lecithin to alleviate toxicity. *Journal of Clinical Microbiology*, *36*(7), pp.2004-2013.

39. Üstündağ-Okur, N., Yurdasiper, A., Gündoğdu, E. and Homan Gökçe, E., 2016. Modification of solid lipid nanoparticles loaded with nebivolol hydrochloride for improvement of oral bioavailability in treatment of hypertension: polyethylene glycol versus chitosan oligosaccharide lactate. *Journal of microencapsulation*, *33*(1), pp.30-42.
40. Vale, N., Gouveia, M.J., Rinaldi, G., Brindley, P.J., Gärtner, F. and Correia da Costa, J.M., 2017. Praziquantel for schistosomiasis: single-drug metabolism revisited, mode of action, and resistance. *Antimicrobial agents and chemotherapy*, *61*(5), pp.e02582-16.
41. Zanolla, D., Hasa, D., Arhangelskis, M., Schneider-Rauber, G., Chierotti, M.R., Keiser, J., Voinovich, D., Jones, W. and Perissutti, B., 2020. Mechanochemical formation of racemic praziquantel hemihydrate with improved biopharmaceutical properties. *Pharmaceutics*, *12*(3), p.289.

CHAPTER SIX

CONCLUSIONS, RESEARCH LIMITATIONS RECOMMENDATIONS AND FUTURE PERSPECTIVES

6.1. CONCLUSIONS

Nanotechnology has been used to enhance drug solubility, bioavailability, absorption, and controlled-release. Nanodelivery systems and nanomedicine are a relatively new but quickly expanding discipline in which nanoscale materials are used to deliver therapeutic agents in a controlled manner to specific targeted sites or as diagnostic tools. The design as well as development of new-fangled drugs by pharmaceutical companies for the treatment and management of *Schistosoma* infection has been faced with some major setbacks. This includes the following: 1) the huge investment and complex procedure associated with the design of new drug molecules, 2) poor financial support and motivation to develop New Chemical Entities (NCEs) in the area of schistosomiasis, 3) in addition, the disease's non-lucrativeness among pharmaceutical companies, so to speak. Hence, the development of drug delivery systems capable of improving the pharmacokinetics of existing Schistosomiasis therapeutics could be a more logical way toward 'fighting' the disease. Biomedical engineering and nano-delivery systems has been promising tools in meeting the modern healthcare demands in regards to the development of targeted therapy, improvement in biopharmaceutical performance of bioactive compounds, enhancement of bioavailability, and ease of drug transport across biological barriers. Additionally, nanotechnology-inspired drug delivery could help minimise drug-associated adverse effects, reduce dosage frequency and facilitate the delivery of bioactive molecules to specific organs or tissues. The use of lipidic-based nanoparticles is gaining much interest in the treatment of parasitic infections, and this can be a potential approach in schistosomiasis treatment, due to the high affinity of schistosomes tegument to phospholipid bilayer. More so, the amphipathic nature of lipidic-based nanoparticles can also enact an essential role in modifying the solubility and the target rate of PZQ to enhance transport across the biological barriers (tegument).

In this study two nanodelivery systems; CLPF-SLNs and anticalpain-functionalized nanoliposomes were prepared. It was showed from this study that anticalpain-functionalized nanoliposomes could be utilized to enhance PZQ transport into the liver and intestines of both young and adult schistosomes for schistosomiasis treatment. The nanoliposomes and the SLNs prepared have a good polydispersity index and zeta potential, according to the findings. The SEM and TEM images in this study indicated that the formed nanoliposomes and SLNs are in the nanosize range and uniformly spherical in shape with stable or intact structure, confirming the particle size, PDI, and zeta potential results. Furthermore, the physicochemical

parameters (FTIR, DSC, XPDR, and TGA) data demonstrated an improvement in the drug stability, as well as drug entrapment during the hydrophobic interaction between the PZQ and the phospholipids of both the nanoliposomes and SLNs. This also confirmed that anticalpain antibody are incorporated into the surface of nanoliposomes. High PZQ entrapment and loading capacity was obtained in both the nanoliposomes and SLNs, as well exhibited sustained release profiles, meanwhile SLNs showed a slower and more sustained release behaviour. For the SLNs nanodelivery system, it was discovered that the use of PF127 as a surfactant enhanced long-term stability of compritol ATO 888-lecithin SLNs nanosuspension at room temperature during a 120-day stability testing.

In an *in vitro* cytotoxicity investigation, cell viability was shown to be acceptable at doses ranging from 30 to 120 g/ml, with no notable cytotoxic effects on cell lines for both the nanoliposomes and SLNs. This extent of safety was further corroborated by an *in vivo* toxicity study, which showed that the nanoliposomes and SLNs prepared in the study present no or minimal oxidative stress and confer hepatoprotective effects on the animals as revealed through the biochemical markers and histopathological examinations. Interestingly, the parasitological data obtained from this study showed that a single (250 mg/kg) oral dose of CLPF-SLNs and anticalpain-NLPs significantly improved the antischistosomal activity of PZQ in *S. mansoni*-infected mice both in two- and four-weeks post-infection, that is, juvenile and adult schistosomes, respectively. Overall, the fabricated CLPF-SLNs and anticalpain-NLPs demonstrated significant efficiency toward the targeted delivery of PZQ, hence, promising in drug delivery application toward the treatment of Schistosomiasis. However, further pharmacokinetic and pharmacodynamic studies are needed to substantiate the effectiveness of the nanosystems in regards to biopharmaceutical improvement of PZQ.

6.2. RESEARCH LIMITATIONS

In this study, there are several limitations encountered, but a few major ones are; the procurement of the antibody, which took several months for us to get. Meanwhile, anticalpain was not the proposed targeted molecular receptor, but due to the inability the antibody that can target this receptor, we opted and switched to calpain, which was purchased from ABCAM.

During the *in vivo* parasitological study, the transportation of the nanoformulated samples from South Africa to Egypt was very challenging, due to several factors such as the COVID-19 pandemic, the declaring of the samples to the DHL courier service in South Africa before accepting to transport the samples. Also, the clearing of the samples by the Egyptian custom, the acceptance of clearance from the health department as well as the delivery of the

nanoformulated samples to the SBSC of TBRI. In all, some of the major limitations encountered during this study were overcome.

6.3. RECOMMENDATIONS AND FUTURE PERSPECTIVES

The developed anticalpain engineered lipoidal nanosystem and the stable compritol ATO 888 lecithin solid lipid nanoparticles resulted to be nanocarrier systems that fulfilled the aims and objectives of this study. The physicochemical parameters, *in vitro* and *in vivo* evaluations of the developed nanoliposomes and SLNs nanocarrier systems produced outstanding results; nevertheless, more research may have improved the data output.

- *In vivo* toxicity evaluation of an increase dose concentration of anticalpain-NLP and CLPF (400 and/or 600 mg/kg) so as to ascertain any toxicity that an increase concentration of the lipoidal nanosysms could pose on animals.
- Parasitological analysis – increase in the dose concentration (to 400 and/or 600 mg/kg) of anticalpain-NLP and CLPF and assess the efficacy on the total worm burden, ova count in both the intestine and the liver of juvenile and adult schistosomes.
- Based on the exceptional surface properties and submicron particle size of the prepared lipoidal nanosystems, which can improve the diffusion of anti-schistosomal drug molecules through the blood brain barrier (BBB). Thus, further *in vivo* investigation could be carried out to ascertain whether the lipoidal nanosystems can be employed to treat cerebral schistosomiasis.
- Pilot and human clinical bio-studies trial is advised, and based on the outcomes of the findings, Wits enterprise will market the nanosystems to pharmaceutical companies leading to commercializing the product.

ANIMALS RESEARCH ETHICS COMMITTEE (AREC)

UNIVERSITY OF THE WITWATERSRAND JOHANNESBURG

STRICTLY CONFIDENTIAL

CLEARANCE CERTIFICATE NUMBER: 2021/02/02/B

APPLICANT: Dr T Adekiya
School: School of Therapeutic Sciences; Department: Pharmacy and Pharmacology; Location: WRAF
PROJECT TITLE: *In vivo* toxicity evaluation of targeted, praziquantel lipoidal nanosystem in Sprague Dawley rats model
Category: B; Species and Numbers involved: *18X 6 - 8 weeks/250 +/- 10g, male or female Albino, Sprague Dawley Rats*

Approval is hereby given for the use of animals for the research project named above and described in the application reviewed by a quorate meeting of the AREC held on 23 Feb 2021. This approval remains valid until 29 Mar 2023 and is conditional to the following (if blank there are no special conditions):

Condition 1	Condition 2	Condition 3	Condition 4
A pilot study (n=1) needs to be done to attest the non-toxicity of praziquantel 250 mg/kg	The other 17 rats will be provided once the pilot study report has proven the non-toxicity of praziquantel 250 mg/Kg		

All material changes to the approved research must be reported to the AREC before they are implemented. Failure to do so will invalidate this clearance certificate.

An annual progress report must be provided to the AREC.

The use of these animals is subject to AREC guidelines on the use and care of laboratory animals, is limited to the procedures described in the application and is subject to additional conditions listed below:

I, the Chair of the AREC (or my designated representative) am satisfied that the proposed research is ethical as judged by local law, international standards and University policy.

Signed: _____ _____ Date: ___30/03/2021___

(Chairperson of the AREC)

I am satisfied that the persons listed in this application are competent to perform the procedures described in the application, in the context of Section 23 (1) (c) of the veterinary and Para-veterinary Professions Act (19 of 1982).

CC: Student supervisor: «Title1» «Initials1» «Supervisor_surname»
Director Wits Research Animal Facility (WRAF): Dr Kim Jardine

SBSP
Schistosome Biological Supply Program
Theodor Bilharz Research Institute
Scientific Director : Fouad Yousif, Ph.D.

In Collaboration with
Center for Tropical Diseases
University of Massachusetts - Lowell, USA
Supported by
U.S. Agency for International Development

Theodor Bilharz Research Institute
Schistosome Biological Supply Center

Certificate

This is to certify that the Schistosome Biological Supply Centre (SBSC) breed and host laboratory animals (mice and hamsters) in its husbandry area according to the international ethics. The animals are also infected with Schistosoma parasite, as needed, according to the standard techniques that follow the international ethics for this purpose.

Scientific Director

(Prof. Fatem Ramzy Gerges)

Fatem Ramzy

El Nil Road, Warrak El Hadar , Imbaba
P . O . Box 30 Imbaba , Guiza 12411 , Egypt
Tel . & Fax : (202) 3121167

EXPERT OPINION ON THERAPEUTIC PATENTS
https://doi.org/10.1080/13543776.2021.1915292

Taylor & Francis
Taylor & Francis Group

REVIEW

Check for updates

Synthesis and therapeutic delivery approaches for praziquantel: a patent review (2010-present)

Tayo A. Adekiya, Pradeep Kumar, Pierre P.D. Kondiah, Viness Pillay and Yahya E. Choonara

Wits Advanced Drug Delivery Platform Research Unit, Department of Pharmacy and Pharmacology, School of Therapeutic Science, Faculty of Health Sciences, University of the Witwatersrand, Johannesburg, South Africa

ABSTRACT

Introduction: : Among all the anti-schistosomal drugs, praziquantel has been the most widely used. However, some major challenges have been faced using the drug in the treatment of schistosome infections.

Areas covered: : Several approaches used in the synthesis of praziquantel aimed at reducing the time and cost of production, the toxicity and experimental harsh conditions are discussed. Also, patented methods involved in the pharmaceutical reformulation of praziquantel in the treatment of diverse endoparasitic infestations are reported. Additionally, future perspectives in terms of nanomedicine approach in the formulation of praziquantel are highlighted.

Expert Opinion: : Lipid-based nanosystems (LBNSs) formulations can be used to overcome the shortcomings associated with the use of praziquantel in the schistosomiasis treatment due to their amphipathic nature. This could be a promising vehicle for the delivery of praziquantel, which could in turn improve the bioavailability, as well as reduce the frequent dose of the drug and improve patient compliance. This may sustain the release of the drug and improve the rapid conversion of the drug into inactive metabolite due to rapid metabolism. Additionally, LBNSs approach could increase and improve the lipophilicity of the drug, which could make it easier to interact with the hydrophobic cores of the worm tegument.

ARTICLE HISTORY
Received 18 November 2020
Accepted 7 April 2021

KEYWORDS
Praziquantel; schistosomiasis; drug delivery; lipid-based nanosystems; patent; synthesis

1. Introduction

Praziquantel (PZQ) happens to be a compound which belongs to the class of organic compounds derived from tetrahydrogenated isoquinoline, otherwise known as tetrahydroisoquinoline. Chemically, praziquantel is known as 2-cyclohexanecarbonyl-1,2,3,4,6,7,11b-piperazino[2,1-a]isoquinolin-4-one (Figure 1) with average molecular mass of 312.4061 g/mol. In biopharmaceutical classification system (BCS), PZQ is classified into group II, and the drug is easily

rates against the three major schistosomes are; 63–85% cure rates for *S. mansoni*, 75–85% for *S. haematobium* and for the co–infections with *S. haematobium* and *S. mansoni* are 60–80% at the recommended dose of 40 mg/kg while the cure rates for *S. japonicum* are 80–90% for a higher dose of 60 mg/kg [1,3]. Although, several limitations associated with the use of this drug for the treatment of schistosomiasis have been reported, which includes the resistance that has been described in the strains developed in the laboratory. Also, the resistance in an endemic region, due to failures that

frontiers in Bioengineering and Biotechnology

REVIEW
published: 31 January 2020
doi: 10.3389/fbioe.2020.00032

A Review of Nanotechnology for Targeted Anti-schistosomal Therapy

*Tayo Alex Adekiya, Pierre P. D. Kondiah, Yahya E. Choonara, Pradeep Kumar and Viness Pillay**

Wits Advanced Drug Delivery Platform Research Unit, Department of Pharmacy and Pharmacology, School of Therapeutic Science, Faculty of Health Sciences, University of the Witwatersrand, Johannesburg, South Africa

Schistosomiasis is one of the major parasitic diseases and second most prevalent among the group of neglected diseases. The prevalence of schistosomiasis may be due to environmental and socio-economic factors, as well as the unavailability of vaccines for schistosomiasis. To date, current treatment; mainly the drug praziquantel (PZQ), has not been effective in treating the early forms of schistosome species. The development of drug resistance has been documented in several regions globally, due to the overuse of PZQ, rate of parasitic mutation, poor treatment compliance, co-infection with different strains of schistosomes and the overall parasite load. Hence, exploring the schistosome tegument may be a potential focus for the design and development of targeted anti-schistosomal therapy, with higher bioavailability as molecular targets using nanotechnology. This review aims to provide a concise incursion on the use of various advance approaches to achieve targeted anti-schistosomal therapy, mainly through the use of nano-enabled drug delivery systems. It also assimilates the molecular structure and function of the schistosome tegument and highlights the potential molecular targets found on the tegument, for effective specific interaction with receptors for more efficacious anti-schistosomal therapy.

Keywords: schistosomiasis, nanoparticles, drug delivery, targeted agents, molecular receptors, antibody, aptamers

OPEN ACCESS

Edited by:
Olga Borges,
University of Coimbra, Portugal

Reviewed by:
Pradipta Ranjan Rauta,
University of Texas MD Anderson Cancer Center, United States
Stefano Leporatti,
Institute of Nanotechnology (NANOTEC), Italy

***Correspondence:**
Viness Pillay
viness.pillay@wits.ac.za

Specialty section:

INTRODUCTION

Schistosomiasis is recognized as the second most prevalent among the group of NTDs in

Nano-enabled treatments for Tropical Diseases affecting the CNS

Tayo Alex Adekiya[1], Pierre P D Kondiah[1], Pradeep Kumar[1]and Yahya E. Choonara[1]*

***Corresponding Author:** Yahya.Choonara@wits.ac.za

Wits Advanced Drug Delivery Platform Research Unit, Department of Pharmacy and Pharmacology, School of Therapeutic Science, Faculty of Health Sciences, University of the Witwatersrand, Johannesburg, 7 York Road, Parktown, 2193, South Africa.

Several tropical diseases have been associated with severe neurological disability or symptoms due to the impact of these diseases on the central nervous system (CNS). Thus, the treatment of these cerebral tropical diseases has been faced with low bioavailability of drugs due to their inability to cross the blood brain barrier (BBB) as well as the blood cerebrospinal fluid barrier (BCSFB). These two barriers lead to the blockade of therapeutic agents from penetrating or gaining access to the CNS. Based on the aforementioned limitation(s), there is an urgent need to enhance the delivery of bioactive molecules using nanocarriers system to achieve targeted delivery in the brain and enhance the bioavailability of drugs. This chapter gives an insight of cerebral tropical diseases, highlighted several current conventional drug delivery strategies into the CNS. More so, highlighting several potential nano-delivery systems that can be employed to bypass the BBB so as to deliver bioactive molecules effectively to the brain with great and improved bioavailability.

Keywords: Tropical diseases; drug delivery systems; central nervous system; cerebral tropical diseases; Nanocarriers; blood brain barrier

1. Introduction

Tropical diseases (TDs) are groups of diseases that are prevalent or indigenous to tropical or

Development and evaluation of praziquantel loaded lecithin-compritol nanoparticles with and without pluronic F127 surfactant

Clinical Science & Therapeutics for Health

October 15, 2020

10:48 am - 11:00 am

Speaker

- **Mr Adekiya** (Speaker) Postgraduate Student, University of the Witwatersrand

Description

Praziquantel (PZQ) remain the major drug use in the treatment of schistosomiasis. Although, the inability to kill the juvenile schistosome (worms) as a result of low bioavailability of the drug due to rapid metabolism to inactive form or less potent compound and low water solubility. Also, resistance to the drug has been reported in different part of the world. Hence, the needs to develop novel drugs or improve the existing active drug, PZQ. The present work aimed at improving the efficacy of PZQ by developing a novel lipid-based nanosystem as carrier for the treatment of Schistosoma infection. In this study, PZQ-loaded solid lipid nanoparticles (SLNs) were successfully formulated using liquid-liquid dispersion method in order to improve the efficacy of the drug. The average particle size distribution, zeta potential and PDI were determined, and the %EE of PZQ was observed to be 71.63% and 70.07% in the drug-loaded compritol-lecithin-SLNs prepared using pluronic F127 as surfactant and without surfactant respectively. The chemical characteristic of PZQ, lipids (compritol 888 and lecithin), and the formulated SLNs were investigated by fourier transform infrared spectroscopy. The viscoelastic properties of the prepared SLNs were evaluated using ElastoSensTM Bio, which uses a non-destructive real-time to determine the evolution of the mechanical features of a formulation. TEM imaging was used to provide information about the structure of the nanocarrier, and the TEM micrographs images of the all nanocarriers both made with surfactant and without surfactant are all spherical in shape. In all, it has been shown in this present study that this approach can be used in making a promising drug delivery

APPENDIX G

Anti-calpain engineered lipoidial nanosystems: preparation, characterization and application in PZQ delivery for schistosomiasis treatment

Tayo A. Adekiya, Pradeep Kumar, Pierre P.D. Kondiah, Yahya E. Choonara*

Wits Advanced Drug Delivery Platform Research Unit, Department of Pharmacy and Pharmacology, School of Therapeutic Sciences, Faculty of Health Sciences, University of the Witwatersrand, Johannesburg, 2193, South Africa

***Corresponding Author:**
Professor Yahya E. Choonara
Tel:+27-11-717-2052
Fax: +27-11-642-4355
Email: yahya.choonara@wits.ac.za

Abstract
This study employed nanotechnological techniques to design and develop praziquantel nanoliposomal (NLP) nanosystem and surface-functionalized the NLP with anticalpain antibody (anticalpain-NLP) for targeted praziquantel (PZQ) delivery in the treatment of schistosomiasis. Anticalpain-NLP were prepared and validated for their physicochemical properties, *in vitro* and *in vivo* toxicity, drug loading capacity (DLC), drug entrapment efficiency (DEE), drug release and parasitological cure rate. The particle sizes for the formulated nanoliposomes ranged from 88.3 to 92.7 nm (PdI= 0.17-0.35), and zeta potential ranged from -20.2 to -31.9 mV. The DLC and DEE ranged from 9.03 to 14.16 and 92.07 to 94.63, respectively. The surface functionalization of the nanoliposomes was stable, uniform and spherical. Fourier transform infrared (FTIR), thermal behaviour and X-ray powder diffraction (XRPD) analysis confirmed that anticalpain antibody and PZQ were incorporated into the surface and inner core of the nanoliposomes, respectively. The sustained drug release was shown to be 93.2 and 91.1% within 24 h for NLP and anticalpain-NLP, respectively. In the *in vitro* analysis study, the nanoliposomes concentrations range of 30 to 120 μg/ml employed revealed acceptable levels of cell viability, with no significant cytotoxic effects on 3T3 human fibroblast cells. Biochemical markers and histopathological analysis showed that the formulated nanoliposomes present no or minimal oxidative stress and confer hepatoprotective effects on the animals. The cure rate of the anticalpain-NLP and PZQ was assessed by parasitological analysis and it was discovered that treatment with 250 mg/kg anticalpain-NLP showed greater activity on the total worm burden, ova count in both the intestine and the liver of juvenile and adult schistosomes. The findings obtained support the ability of oral anticalpain-NLP to target young and adult schistosomes in the liver and portomesenteric locations, resulting in improved effectiveness of PZQ.

Keywords: Praziquantel; *Schistosoma mansoni;* nanoliposomes; anticalpain; antibody; surface-functionalization

APPENDIX H

Synthesis and evaluation of Praziquantel-loaded compritol ATO 888-lecithin solid lipid nanoparticles against *S. mansoni* infection in preclinical murine models

Tayo A. Adekiya[1], Pradeep Kumar[1], Pierre P.D. Kondiah[1], Philemon Ubanako[1], Yahya E. Choonara[1]*

[1]Wits Advanced Drug Delivery Platform Research Unit, Department of Pharmacy and Pharmacology, School of Therapeutic Sciences, Faculty of Health Sciences, University of the Witwatersrand, Johannesburg, 2193, South Africa

***Corresponding Author:**
Professor Yahya E. Choonara
Tel:+27-11-717-2052
Fax: +27-11-642-4355
Email: yahya.choonara@wits.ac.za

Abstract

This study aimed to develop and evaluate the long-term stability of drug-loaded solid lipid nanoparticles (SLNs). The SLNs were designed to extend the release profile and overcome the problem of bioavailability and solubility, investigate its toxicity, and improve the anti-schistosomal efficacy of praziquantel. The aim was pursued using solvent injection-co-homogenization techniques to fabricate SLNs in which compritol ATO 888 and lecithin were used as lipids, and Pluronic F127 (PF127) was used as a stabilizer. The long-term stability effect of the PF127 as a stabilizer on the SLNs was evaluated. The particle size, stability and polydispersity were determined by a dynamic light scattering (DLS) technique. The morphological analysis of the SLNs was investigated by Transmission and Scanning Electron Microscopy (TEM) and (SEM). The chemical properties, mechanical, thermal, and crystal behaviours of SLNs were evaluated using FTIR, ElastoSens Bio2, XRPD, DSC and TGA, respectively. SLNs with PF127 depicted an encapsulation efficiency of 71.63% and a drug loading capacity of 11.46%. The *in vitro* drug release study for SLNs with PF127 showed a cumulative release of 48.08% for the PZQ within 24 h, with a similar release profile for SLNs suspension after 120 days. DLS, ELS and Turbiscan data indicate that the addition of PF127 as the surfactants provided long-term stability for SLNs. *In vitro* cell viability and *in vivo* toxicity evaluation signify the safety of SLNs stabilized with PF127. In conclusion, the parasitological data showed that a single (250 mg/kg) oral dose of CLPF-SLNs significantly improved the antischistosomal activity of PZQ in *S. mansoni*-infected mice in both two and four weeks post-infection. The fabricated CLPF-SLNs demonstrated significant efficiency toward the delivery of PZQ, hence, a promising therapeutic strategy against schistosomiasis.

Keywords: Praziquantel; solid lipid nanoparticles; Compritol ATO 888; soy lecithin; *S. mansoni*; schistosomiasis; stability.

APPEDIX I

Table (1): Effect of PZQ and drug A&B (single dose 250 mg/kg two weeks post-infection) on worm load and sex in *S. mansoni*-infected mice sacrificed six weeks post infection

	Mean worm burden ±SD (liver and porto-mesenteric)				% total worm burden reduction
	Male	Female	Couples	Total	
Control infected	2	0	6	14	
	3	0	6	15	
	2	0	7	16	
	1	1	7	16	
	3	1	5	14	
	3	0	6	15	
Mean±SD	2.33±0.81	0.33±0.52	6.17±0.75	15±0.89	
PZQ	0	0	5	10	
	0	0	4	8	
	3	0	3	9	
	1	0	5	11	
	2	0	4	10	
	2	0	5	12	
Mean±SD	1.33±1.21	0	4.33±0.82	10.0±1.41	33.3
Drug (A)	2	0	4	7	
	2	0	3	5	
	3	1	3	6	
	2	0	5	9	
	2	0	3	6	
	3	0	4	8	
Mean±SD	1.10±0.52	0.17±0.41	3.67±1.37	11.83±2.4	54.5
Drug (B)	1	0	2	5	
	2	0	3	8	
	1	0	5	11	
	1	0	3	7	
	2	0	5	12	
	2	0	4	10	
Mean±SD	1.5±0.55	0	3.67±1.21	8.83±2.64	41.13

Table (2): Effect of PZQ and drug A&B (single dose 250 mg/kg two weeks post-infection) on % Egg developmental stages in *S. mansoni*-infected mice sacrificed six weeks post infection

	% Egg developmental stages		
	% Immature ova	% Mature ova	% Dead ova
Control	48	45	7
	47	49	4
	48	46	6
	47	46	7
	50	44	6
	52	42	6
Mean±SD	48.67±1.97	46.33±2.34	6±1.09
PZQ	45	48	7
	50	42	8
	47	44	9
	45	48	7
	43	49	8
	48	45	6
Mean±SD	46.33±2.50	46±2.76	7.5±1.05
Drug (A)	44	45	10
	47	42	11
	43	47	9
	45	40	12
	48	45	9
	47	43	11
Mean±SD	45.67±1.96	43.67±2.50	10.33±1.21
Drug (B)	47	44	12
	43	45	10
	44	42	9
	46	40	8
	44	42	11
	43	45	9
Mean±SD	44.50±1.64	43±2.00	9.83±1.47

Table (3): Effect of PZQ and drug A&B (single dose 250 mg/kg two weeks post-infection) on number of ova/gm tissues in *S. mansoni*-infected mice sacrificed six weeks post- infection

Mice group	**Liver**	**% Ova count in liver reduction**	**Intestine**	**% Ova count in Intestine reduction**
Control	25352		28729	
	32387		36251	
	33154		37854	
	30447		32387	
	22524		28651	
	25349		27537	
Mean±SD	28202±4372		31902±4342	
PZQ	17561		12500	
	22862		23974	
	19248		23542	
	18483		27495	
	22325		22334	
	21342		26371	
Mean±SD	20303±2175	28	22702±5347	28.84
Drug (A)	12784		11096	
	13888		13107	
	16464		18345	
	12969		13608	
	7948		12131	
	10269		12333	
Mean±SD	12387±2951	56.07	13436±2332	57.88
Drug (B)	15868		20814	
	10541		17559	
	20842		24218	
	27835		30988	
	17818		23772	
	6384		9369	
Mean±SD	16548±6919	41.32	21120±6644	33.79

Table (4): Effect of PZQ and drug A&B (single dose 250 mg/kg four weeks post-infection) on worm load and sex in *S. mansoni*-infected mice sacrificed six weeks post infection

	Mean worm burden ±SD (liver and porto-mesenteric)				% total worm burden reduction
	Male	Female	Couples	Total	
Control infected	2	0	6	14	
	3	0	6	15	
	2	0	7	16	
	1	1	7	16	
	3	1	5	14	
	3	0	6	15	
Mean±SD	2.33±0.81	0.33±0.52	6.17±0.75	15±0.89	
PZQ	0	0	2	4	
	1	0	2	5	
	1	0	1	3	
	1	0	3	7	
	4	0	3	10	
	2	0	1	4	
Mean±SD	1.5±1.4	0	2±0.89	5.5±2.6	63.3
Drug (A)	1	0	1	4	
	2	0	1	5	
	1	0	3	6	
	0	0	1	2	
	1	0	2	5	
	1	0	1	3	
Mean±SD	1.00±0.63	0	1.5±0.83	4.17±1.47	72.2
Drug (B)	1	0	4	7	
	1	0	1	4	
	0	0	2	6	
	1	0	0	2	
	1	0	0	3	
	2	0	1	4	
Mean±SD	1.00±0.63	0	1.33±1.37	4.33±1.86	71.33

Table (5): Effect of PZQ and drug A&B (single dose 250 mg/kg four weeks post-infection) on % Egg developmental stages in *S. mansoni*-infected mice sacrificed six weeks post infection

	% Egg developmental stages		
	% Immature ova	% Mature ova	% Dead ova
Control	48	45	7
	47	49	6
	48	46	6
	47	46	7
	50	44	6
	52	42	6
Mean±SD	48.67±1.97	46.33±2.34	6±1.09
PZQ	43	46	11
	47	42	11
	44	42	14
	42	45	13
	40	45	16
	45	44	10
Mean±SD	43.5±2.43	44±1.76	12.5±2.26
Drug (A)	42	45	14
	43	42	16
	41	45	17
	43	37	19
	42	43	16
	45	43	12
Mean±SD	42.7±1.36	42.5±2.95	15.67±2.42
Drug (B)	43	40	15
	40	44	13
	38	41	19
	44	40	12
	39	45	15
	42	47	10
Mean±SD	41±2.37	42.83±2.93	14±3.09

Table (6): Effect of PZQ and drug A&B (single dose 250 mg/kg four weeks post-infection) on number of ova/gm tissues in *S. mansoni*-infected mice sacrificed six weeks post- infection

Mice group	Liver	% Ova count in liver reduction	Intestine	% Ova count in Intestine reduction
Control	25352		28729	
	32387		36251	
	33154		37854	
	30447		32387	
	22524		28651	
	25349		27537	
Mean±SD	28202±4372		31902±4342	
PZQ	14752		12500	
	12346		12397	
	13241		21357	
	18848		12744	
	12232		12233	
	10334		16717	
Mean±SD	13626±2936	51.68	14658±3699	54.05
Drug (A)	9135		10069	
	18261		15993	
	8523		6517	
	8162		6046	
	9692		11899	
	6904		5339	
Mean±SD	10112±3745	64.14	9310±3789	70.81
Drug (B)	14226		10214	
	14782		10194	
	13792		10849	
	5552		9529	
	5550		8810	
	14406		12269	
Mean±SD	11384±4135	59.60	1031±1080	67.68

APPEDIX J

UNIVERSITY OF THE WITWATERSRAND JOHANNESBURG

FACULTY OF HEALTH SCIENCES

PLAGIARISM DECLARATION TO BE SIGNED BY ALL HIGHER DEGREE STUDENTS

SENATE PLAGIARISM POLICY: APPENDIX ONE

I TAYO ALEX ADEKIYA (Student number: 2272680) am a student registered for the degree of PhD in the academic year 2021.

I hereby declare the following:

- I am aware that plagiarism (the use of someone else's work without their permission and/or without acknowledging the original source) is wrong.
- I confirm that the work submitted for assessment for the above degree is my own unaided work except where I have explicitly indicated otherwise.
- I have followed the required conventions in referencing the thoughts and ideas of others.
- I understand that the University of the Witwatersrand may take disciplinary action against me if there is a belief that this is not my own unaided work or that I have failed to acknowledge the source of the ideas or words in my writing.
- I have included as an appendix a report from "Turnitin" (or other approved plagiarism detection) software indicating the level of plagiarism in my research document.

Signature: _____ Date: 16/08/2021

1

TARGETED, LIPOIDAL NANOSYSTEM FOR THE TREATMENT OF SCHISTOSOMIASIS

by Tayo Alex Adekiya

Submission date: 16-Aug-2021 02:17PM (UTC+0200)
Submission ID: 1632037170
File name: Tayo_Alex_Adekiya_PhD_Thesis.docx (81.51M)
Word count: 70695
Character count: 415674

TARGETED, LIPOIDAL NANOSYSTEM FOR THE TREATMENT OF SCHISTOSOMIASIS

ORIGINALITY REPORT

8%	4%	3%	2%
SIMILARITY INDEX	INTERNET SOURCES	PUBLICATIONS	STUDENT PAPERS

PRIMARY SOURCES

1	www.frontiersin.org Internet Source	1%
2	Sandra Gemma, Stefano Federico, Simone Brogi, Margherita Brindisi, Stefania Butini, Giuseppe Campiani. "Dealing with schistosomiasis: Current drug discovery strategies", Elsevier BV, 2019 Publication	<1%
3	"Systemic Delivery Technologies in Anti-Aging Medicine: Methods and Applications", Springer Science and Business Media LLC, 2020 Publication	<1%
4	Mohamed, Azza H., Gamalat Y. Osman, Tarek A. Salem, and Alshimaa M. Elmalawany. "The hepatoprotective activity of blue green algae in Schistosoma mansoni infected mice", Experimental Parasitology, 2014. Publication	<1%